

**Hypersingular Integrodifferential Equations and  
Applications to Fracture Mechanics of Homogeneous and  
Functionally Graded Materials with Strain-Gradient Effects**

By

**YOUN-SHA CHAN**

**DISSERTATION**

Submitted in partial satisfaction of the requirements for the degree of

**DOCTOR OF PHILOSOPHY**

in

**Applied Mathematics**

in the

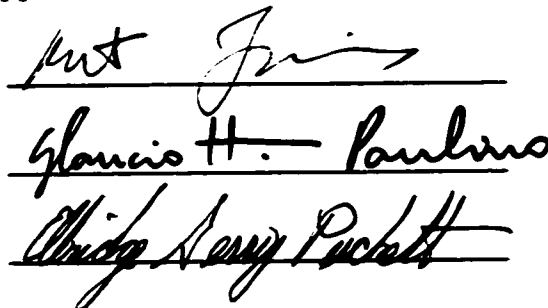
**OFFICE OF GRADUATE STUDIES**

of the

**UNIVERSITY OF CALIFORNIA**

**DAVIS**

Approved:

  
The image shows three handwritten signatures in black ink, each written over a horizontal line. The signatures are: 1. 'M. J. ...' (partially obscured), 2. 'Glanis H. Paulino', and 3. 'Chris S. Puckett'.

Committee in Charge

2001

UMI Number: 3051518

**UMI<sup>®</sup>**

---

UMI Microform 3051518

Copyright 2002 by ProQuest Information and Learning Company.  
All rights reserved. This microform edition is protected against  
unauthorized copying under Title 17, United States Code.

---

ProQuest Information and Learning Company  
300 North Zeeb Road  
P.O. Box 1346  
Ann Arbor, MI 48106-1346

# Contents

|          |   |           |
|----------|---|-----------|
| <b>1</b> | <b>Introduction</b>   | <b>1</b>  |
| 1.1      | Strain-Gradient Theories . . . . .  | 2         |
| 1.2      | Functionally Graded Materials . . . . .                                     | 3         |
| 1.3      | Functionally Graded Materials with Strain-Gradient Effect . . . . .         | 4         |
| 1.4      | Mathematical Aspects . . . . .  | 5         |
| 1.4.1    | Singular Integral Equation Method . . . . .                                 | 5         |
| 1.4.2    | Solution to the Crack Problems with Strain-Gradient Effect . . . . .        | 7         |
| 1.4.3    | Hypersingular Integral Equation Method . . . . .                            | 7         |
| 1.5      | Outline of Contents . . . . .   | 8         |
| <b>2</b> | <b>Singular Integral Equations in Classical Linear Elastic Fracture Me-</b> |           |
|          | <b>chanics</b>  | <b>10</b> |
| 2.1      | Introduction . . . . .  | 10        |
| 2.2      | Governing Partial Differential Equations and Boundary Conditions . . . . .  | 11        |
| 2.3      | Fourier Transform . . . . .   | 13        |
| 2.4      | Asymptotic Analysis and Kernel Decomposition . . . . .                      | 15        |
| 2.5      | Hypersingular Integral Equation . . . . .                                   | 17        |
| 2.6      | Displacement versus Slope Formulations . . . . .                            | 18        |
| 2.7      | Numerical Results . . . . .   | 21        |
| 2.7.1    | Stress Intensity Factors (SIFs) . . . . .                                   | 21        |

|          |  |           |
|----------|--|-----------|
| 2.7.2    | Displacement Profiles . . . . .  | 24        |
| 2.8      | Concluding Remark . . . . .  | 27        |
| <b>3</b> | <b>Constitutive Equations of Strain-Gradient Elasticity Theory for Functionally Graded Materials</b>   | <b>28</b> |
| 3.1      | Strain-Energy Density Function . . . . .   | 29        |
| 3.1.1    | Elasticity . . . . .   | 29        |
| 3.1.2    | Gradient Elasticity . . . . .  | 29        |
| 3.1.3    | Some Observation . . . . .   | 31        |
| 3.2      | Anti-Plane Shear . . . . .   | 32        |
| 3.2.1    | Constitutive Equations . . . . .   | 32        |
| 3.2.2    | Governing PDE . . . . .  | 34        |
| 3.3      | General State of Stresses . . . . .  | 36        |
| 3.3.1    | Constitutive Equations . . . . .   | 37        |
| 3.3.2    | Governing System of PDEs . . . . .   | 37        |
| 3.3.3    | Perturbation Pointview . . . . .   | 39        |
| 3.4      | Concluding Remark . . . . .  | 39        |
| <b>4</b> | <b>Hypersingular Integral Equations for Mode III Fracture in Functionally Graded Materials with Strain-Gradient Effect (Crack Perpendicular to the Material Gradation)</b> | <b>41</b> |
| 4.1      | Constitutive Equations of Gradient Elasticity . . . . .  | 42        |
| 4.2      | Governing Partial Differential Equation . . . . .  | 43        |
| 4.3      | Boundary Conditions . . . . .  | 45        |
| 4.4      | Fourier Transform . . . . .  | 45        |
| 4.5      | Hypersingular Integrodifferential Equation . . . . .   | 48        |
| 4.6      | Numerical Results . . . . .  | 54        |
| 4.7      | Summary . . . . .  | 63        |

|          |  |           |
|----------|--|-----------|
| <b>5</b> | <b>Finite Part Integrals and Hypersingular Kernels</b>             | <b>65</b> |
| 5.1      | Finite Part integrals . . . . .                                    | 65        |
| 5.1.1    | Cauchy Principal Value Integrals . . . . .                         | 66        |
| 5.1.2    | Definition of Finite Part Integrals . . . . .                      | 67        |
| 5.1.3    | Remark on Finite Part Integrals . . . . .                          | 70        |
| 5.2      | Plemelj Formulas . . . . .   | 71        |
| 5.3      | Hypersingular Kernels . . . . .                                    | 72        |
| <b>6</b> | <b>Asymptotics of Crack-tip Behavior by Using Mellin Transform</b> | <b>74</b> |
| 6.1      | Mellin Transform . . . . .   | 74        |
| 6.2      | Three Prototypes of Asymptotics . . . . .                          | 76        |
| 6.3      | Main Theorems . . . . .  | 78        |
| 6.4      | Crack-tip Asymptotics by the Mellin Transform . . . . .            | 79        |
| 6.4.1    | Cauchy Singular Integral Equations . . . . .                       | 80        |
| 6.4.2    | Quadratic Hypersingular Integral Equations . . . . .               | 82        |
| 6.4.3    | Cubic Hypersingular Integral Equations . . . . .                   | 83        |
| <b>7</b> | <b>Evaluation of Hypersingular Integrals</b>                       | <b>85</b> |
| 7.1      | Theoretical Aspects . . . . .                                      | 85        |
| 7.1.1    | Integration and Approximation . . . . .                            | 86        |
| 7.1.2    | Selection of Density Function . . . . .                            | 89        |
| 7.1.3    | Properties of the Chebyshev Polynomials . . . . .                  | 90        |
| 7.2      | Cauchy Singular Integral Formulas ( $\alpha = 1$ ) . . . . .       | 92        |
| 7.2.1    | $I_1(T_n, m, r)$ , $m = 0, 1, 2, 3$ . . . . .                      | 92        |
| 7.2.2    | $I_1(U_n, m, r)$ , $m = 1, 2, 3$ . . . . .                         | 93        |
| 7.2.3    | $I_1(T_n, m, r)$ and $I_1(U_n, m, r)$ . . . . .                    | 94        |
| 7.2.4    | Alternative Approach . . . . .                                     | 95        |
| 7.3      | Hypersingular Integral Formulas ( $\alpha \geq 2$ ) . . . . .      | 96        |

|          |   |            |
|----------|---|------------|
| 7.3.1    | $I_2(T_n, m, r)$  | 96         |
| 7.3.2    | $I_2(U_n, m, r)$  | 97         |
| 7.3.3    | $I_3(T_n, m, r)$  | 98         |
| 7.3.4    | $I_3(U_n, m, r)$  | 99         |
| 7.3.5    | $I_4(T_n, m, r)$  | 100        |
| 7.3.6    | $I_4(U_n, m, r)$ :  | 102        |
| 7.4      | <b>Evaluation of Stress Intensity Factors (SIFs)</b>        | 103        |
| 7.4.1    | $S_1(T_n, m, r)$ and $S_1(U_n, m, r)$                       | 104        |
| 7.4.2    | $S_2(T_n, m, r)$ and $S_2(U_n, m, r)$                       | 106        |
| 7.4.3    | $S_3(T_n, m, r)$ and $S_3(U_n, m, r)$                       | 106        |
| 7.5      | <b>Integrals associated with lower order <math>n</math></b> | 107        |
| 7.5.1    | $I_1(T_n, 1, r)$ , $n = 0, 1$                               | 107        |
| 7.5.2    | $I_1(T_n, 2, r)$ , $n = 0 \cdots 5$ , $ r  < 1$             | 108        |
| 7.5.3    | $I_1(T_n, 3, r)$ , $n = 0 \cdots 5$ , $ r  < 1$             | 108        |
| 7.5.4    | $I_1(U_n, 3, r)$ , $n = 0 \cdots 5$ , $ r  < 1$             | 109        |
| 7.5.5    | $I_2(T_n, 3, r)$ , $n = 0 \cdots 6$ , $ r  < 1$             | 109        |
| 7.5.6    | $I_2(U_n, 3, r)$ , $n = 0 \cdots 6$ , $ r  < 1$             | 110        |
| 7.5.7    | $I_3(T_n, 2, r)$ , $n = 0 \cdots 4$ , $ r  < 1$             | 111        |
| 7.5.8    | $I_3(T_n, 3, r)$ , $n = 0 \cdots 7$ , $ r  < 1$             | 111        |
| 7.5.9    | $I_3(U_n, 3, r)$ , $n = 0 \cdots 6$ , $ r  < 1$             | 112        |
| 7.5.10   | $I_4(T_n, 3, r)$ , $n = 0 \cdots 8$ , $ r  < 1$             | 113        |
| 7.5.11   | $I_4(U_n, 3, r)$ , $n = 0 \cdots 6$ , $ r  < 1$             | 113        |
| 7.5.12   | Others  | 114        |
| <b>8</b> | <b>Numerical Approximation Procedures</b>                   | <b>115</b> |
| 8.1      | Normalization   | 116        |
| 8.2      | Representation of Density Function                          | 117        |

|           |   |            |
|-----------|---|------------|
| 8.3       | Chebyshev Polynomial Expansion . . . . .  | 117        |
| 8.4       | Evaluation of the Derivative of Density Function . . . . .  | 118        |
| 8.5       | Formation of Linear System of Equations . . . . .   | 118        |
| 8.6       | Evaluation of Singular and Hypersingular Integrals . . . . .  | 119        |
| 8.7       | Evaluation of Non-singular Integral . . . . .   | 120        |
| 8.8       | Stress Intensity Factors . . . . .  | 121        |
| 8.9       | $T_n$ vs. $U_n$ . . . . .   | 123        |
| <b>9</b>  | <b>Mode III Crack Problems with Strain-Gradient Effect — A Case<br/>with Closed Form Solution</b>   | <b>129</b> |
| 9.1       | Hypersingular Integrodifferential Equations . . . . .   | 130        |
| 9.2       | Solutions of the Integral Equations . . . . .   | 131        |
| 9.2.1     | Case $\ell' = 0$ : Closed Form Solution . . . . .   | 132        |
| 9.2.2     | Case $\ell' \neq 0$ : Regular Perturbation . . . . .  | 135        |
| 9.3       | Crack-Tips Asymptotics for the Unknown Density Function $\phi(x)$ . .   | 136        |
| 9.4       | More General Form of Strain Energy Density Function . . . . .   | 138        |
| <b>10</b> | <b>Hypersingular Integral Equations for Mode III Fracture in Function-<br/>ally Graded Materials with Strain-Gradient Effect (Crack Parallel<br/>to the Material Gradation)</b> | <b>140</b> |
| 10.1      | Constitutive Equations of Gradient Elasticity . . . . .   | 142        |
| 10.2      | Governing Partial Differential Equation and Boundary Conditions . .   | 143        |
| 10.3      | Solutions of the ODE . . . . .  | 146        |
| 10.4      | Hypersingular Integrodifferential Equation . . . . .  | 148        |
| 10.5      | Numerical Solution and Results . . . . .  | 152        |
| 10.5.1    | Numerical Solution . . . . .  | 152        |
| 10.5.2    | Crack Surface Displacements . . . . .   | 153        |
| 10.5.3    | Strains . . . . .   | 156        |

|           |   |            |
|-----------|---|------------|
| 10.5.4    | Stresses . . . . .  | 158        |
| 10.5.5    | Stress Intensity Factors (SIFs) . . . . .                             | 159        |
| <b>11</b> | <b>Gradient Elasticity Theory for Mode I Fracture in Homogeneous</b>  |            |
|           | <b>Materials</b>  | <b>163</b> |
| 11.1      | Formulation of the Crack Problem . . . . .                            | 164        |
| 11.1.1    | Constitutive Equations . . . . .                                      | 164        |
| 11.1.2    | Governing System of PDEs and Boundary Conditions . . . . .            | 165        |
| 11.2      | Derivation for the System of Integral Equations . . . . .             | 165        |
| 11.2.1    | System of Fredholm Integral Equations . . . . .                       | 167        |
| 11.3      | Numerical Results . . . . .   | 170        |
| <b>12</b> | <b>Gradient Elasticity Theory for Mode I Fracture in Functionally</b> |            |
|           | <b>Graded Materials</b>   | <b>172</b> |
| 12.1      | Formulation of the Crack Problem . . . . .                            | 173        |
| 12.1.1    | Constitutive Equations . . . . .                                      | 173        |
| 12.1.2    | Governing System of PDEs and Boundary Conditions . . . . .            | 175        |
| 12.2      | Derivation for the System of Integral Equations . . . . .             | 175        |
| 12.2.1    | Finding Roots of System of ODEs . . . . .                             | 176        |
| 12.2.2    | Representation of the Solution . . . . .                              | 178        |
| 12.2.3    | System of Fredholm Integral Equations . . . . .                       | 179        |
| 12.3      | Numerical Results . . . . .   | 182        |
| 12.3.1    | Stress Intensity Factors . . . . .                                    | 183        |
| 12.3.2    | Crack Opening Displacement Profiles . . . . .                         | 185        |
| <b>13</b> | <b>Conclusions and Future Work</b>                                    | <b>188</b> |
| 13.1      | Hypersingular Integrodifferential Equation Method . . . . .           | 188        |
| 13.2      | Applicability of the Method . . . . .                                 | 189        |



**13.3 Future Work . . . . . 190**

# List of Figures

|     |  |    |
|-----|--|----|
| 1.1 | An illustration of a functionally graded material. . . . .   | 3  |
| 2.1 | Antiplane shear problem for a nonhomogeneous material. Shear modulus $G(x) = G_0e^{\beta x}$ ; $c$ and $d$ represent the left and right crack tip, respectively; $a$ is the half crack length. . . . .   | 12 |
| 2.2 | Normalized stress intensity factors for an infinite nonhomogeneous plane subjected to uniform crack surface traction $\sigma_{yz}(x, 0) = -p_0$ . The shear modulus is $G(x) = G_0e^{-\beta x}$ . . . . .  | 23 |
| 2.3 | Crack surface displacement in an infinite nonhomogeneous plane under uniform crack surface shear loading $\sigma_{yz}(x, 0) = -p_0$ and shear modulus $G(x) = G_0e^{\beta x}$ . Here $a = (d - c)/2$ denotes the half crack length. . . . .  | 24 |
| 2.4 | Crack surface displacement in an infinite nonhomogeneous plane under uniform crack surface shear loading $\sigma_{yz}(x, 0) = -p_0$ and shear modulus $G(x) = G_0e^{\beta x}$ . Here $a = (d - c)/2$ denotes the half crack length. . . . .  | 25 |
| 4.1 | FGM with continuously graded microstructure. . . . .   | 43 |
| 4.2 | Geometry for the mode III crack problem . . . . .  | 46 |
| 4.3 | Plot of the the integrand in equation (4.54) for $\ell = 0.05$ , $\ell' = 0.005$ , $\gamma = 0.1$ , $r = \sqrt{3}/7$ , and $s = \sqrt{2}/3$ . (a) $\xi \in [0, 5000]$ ; (b) Zoom for the range $\xi \in [0, 500]$ . Moreover, As $\xi \rightarrow 0$ , the limit of $N(\xi) \sin[\xi(s - r)]$ is about $22.4 \times 10^{-3}$ . . . . . | 53 |

|     |  |     |
|-----|--|-----|
| 4.4 | Full crack displacement profile in an infinite medium of homogeneous material ( $\tilde{\gamma} = 0$ ) under uniform crack surface shear loading $\sigma_{yz}(x, 0) = -p_0$ with choice of (normalized) $\tilde{\ell} = 0.2$ and $\tilde{\ell}' = 0$ . . . . .   | 56  |
| 4.5 | Crack surface displacement under uniform crack surface shear loading $\sigma_{yz}(x, 0) = -p_0$ and shear modulus $G(y) = G_0 e^{\gamma y}$ with choice of (normalized) $\tilde{\ell} = 0.05$ , $\tilde{\ell}' = 0$ , and various $\tilde{\gamma}$ . The dashed line stands for the homogeneous material case ( $\tilde{\gamma} = 0$ ). . . . .  | 57  |
| 4.6 | Crack surface displacement under uniform crack surface shear loading $\sigma_{yz}(x, 0) = -p_0$ and shear modulus $G(y) = G_0 e^{\gamma y}$ with choice of (normalized) $\tilde{\ell} = 0.2$ , $\tilde{\ell}' = 0.04$ , and various $\tilde{\gamma}$ . The dashed line stands for the homogeneous material ( $\tilde{\gamma} = 0$ ) in a gradient elastic medium. . . . .  | 58  |
| 4.7 | Crack surface displacement profiles under uniform crack surface shear loading $\sigma_{yz}(x, 0) = -p_0$ and shear modulus $G(y) = G_0 e^{\gamma y}$ with choice of (normalized) $\tilde{\ell}' = 0.05$ , $\tilde{\gamma} = 0.1$ , and various $\tilde{\ell}$ . The values of $\tilde{\ell}$ are listed in the same order as the solid-line curves. . . . .  | 59  |
| 4.8 | Crack surface displacement profiles under uniform crack surface shear loading $\sigma_{yz}(x, 0) = -p_0$ and shear modulus $G(y) = G_0 e^{\gamma y}$ with choice of (normalized) $\tilde{\ell} = 0.05$ , $\tilde{\gamma} = 0.1$ , and various $\tilde{\ell}'$ . The values of $\tilde{\ell}'$ (and $\rho$ ) are listed in the same order as the solid-line and dashed-line ( $\rho = 0$ ) curves representing the strain gradient results. . . . . | 60  |
| 4.9 | Crack surface displacement profiles under discontinuous loading $p(x/a) = -1 + 0.5 \text{sgn}(x/a)$ and shear modulus $G(y) = G_0 e^{\gamma y}$ with choice of (normalized) $\tilde{\ell} = 0.05$ , $\tilde{\gamma} = 0.2$ , and various $\rho$ . The values of $\rho$ are listed in the same order as the solid-line and dashed-line ( $\rho = 0$ ) curves representing the strain gradient results. . . . .                                      | 61  |
| 8.1 | A mode I crack in an infinite strip. . . . .   | 124 |

|      |   |     |
|------|---|-----|
| 8.2  | Displacement profiles for a mode I crack in an infinite strip obtained by means of $U_n$ and $T_n$ representations ( $N + 1 = 15$ ). Here $c = 0.1$ , $d = 20.1$ , $2a = 20$ , and $(c + d)/(d - c) = 1.01$ . The crack is tilted to the left because of the “edge effect” . . . . .                                      | 126 |
| 8.3  | Displacement profiles for a mode I crack in an infinite strip obtained by means of $U_n$ and $T_n$ representations ( $N + 1 = 8$ ). Here $c = 1$ , $d = 3$ , $2a = 2$ , and $(c + d)/(d - c) = 2$ . . . . .   | 128 |
| 9.1  | Numerical solution vs. closed form solution (9.15) . . . . .  | 137 |
| 10.1 | A geometric comparison of the material gradation with respect the crack location. . . . .   | 141 |
| 10.2 | Geometry of the crack problem. . . . .  | 144 |
| 10.3 | Full crack displacement profile for homogeneous material ( $\tilde{\beta} = 0$ ) under uniform crack surface shear loading $\sigma_{yz}(x, 0) = -p_0$ with choice of (normalized) $\tilde{\ell} = 0.2$ and $\tilde{\ell}' = 0$ . . . . .  | 153 |
| 10.4 | Classical LEFM, <i>i.e.</i> $\tilde{\ell} = \tilde{\ell}' \rightarrow 0$ . Crack surface displacement in an infinite nonhomogeneous plane under uniform crack surface shear loading $\sigma_{yz}(x, 0) = -p_0$ and shear modulus $G(x) = G_0 e^{\beta x}$ . Here $a = (d - c)/2$ denotes the half crack length. . . . .   | 154 |
| 10.5 | Classical LEFM, <i>i.e.</i> $\tilde{\ell} = \tilde{\ell}' \rightarrow 0$ . Crack surface displacement in an infinite nonhomogeneous plane under uniform crack surface shear loading $\sigma_{yz}(x, 0) = -p_0$ and shear modulus $G(x) = G_0 e^{\beta x}$ . Here $a = (d - c)/2$ denotes the half crack length. . . . .   | 155 |
| 10.6 | Crack surface displacement in an infinite nonhomogeneous plane under uniform crack surface shear loading $\sigma_{yz}(x, 0) = -p_0$ and shear modulus $G(x) = G_0 e^{\beta x}$ with choice of (normalized) $\tilde{\ell} = 0.10$ and $\tilde{\ell}' = 0.01$ . Here $a = (d - c)/2$ denotes the half crack length. . . . . | 156 |

|      |   |     |
|------|---|-----|
| 10.7 | Crack surface displacement in an infinite nonhomogeneous plane under uniform crack surface shear loading $\sigma_{yz}(x, 0) = -p_0$ and shear modulus $G(x) = G_0 e^{\beta x}$ with choice of (normalized) $\bar{\ell} = 0.10$ and $\bar{\ell}' = 0.01$ . Here $a = (d - c)/2$ denotes the half crack length. . . . .   | 157 |
| 10.8 | Strain $\phi(x/a)$ along the crack surface $(c, d) = (0, 2)$ for $\bar{\beta} = 0.5$ , $\bar{\ell}' = 0$ , and various $\bar{\ell}$ in an infinite nonhomogeneous plane under uniform crack surface shear loading $\sigma_{yz}(x, 0) = -p_0$ and shear modulus $G(x) = G_0 e^{\beta x}$ . Here $a = (d - c)/2$ denotes the half crack length. . . . .   | 158 |
| 10.9 | Stress $\sigma_{yz}(x/a, 0)/G_0$ along the ligament for $\bar{\beta} = 0.5$ , $\bar{\ell}' = 0$ , and various $\bar{\ell}$ . Crack surface $(c, d) = (0, 2)$ located in an infinite nonhomogeneous plane is assumed to be under uniform crack surface shear loading $\sigma_{yz}(x, 0) = -p_0$ and shear modulus $G(x) = G_0 e^{\beta x}$ . Here $a = (d - c)/2$ denotes the half crack length. . . . . | 159 |
| 11.1 | Mode I normalized crack profiles for homogeneous materials at $\bar{\ell} = 0.05, 0.1$ , $\bar{\ell}' = 0.0$ , and $\nu = 0.25$ . . . . .   | 171 |
| 12.1 | Geometry of the problem. . . . .  | 174 |
| 12.2 | Normalized crack profiles at $\beta a > 0$ , $\bar{\ell} = 0.10$ , $\bar{\ell}' = 0.01$ ; $\nu = 0.3$ . . .   | 184 |
| 12.3 | Normalized crack profiles at $\beta a < 0$ , $\bar{\ell} = 0.10$ , $\bar{\ell}' = 0.01$ ; $\nu = 0.3$ . . .   | 185 |
| 12.4 | Normalized crack profiles at $\beta a = 0.25$ , $\bar{\ell} = 0.05, 0.1, 0.2$ , $\bar{\ell}' = 0.01$ ; $\nu = 0.3$ . . . . .  | 186 |
| 12.5 | Normalized crack profiles at $\beta a = 0.5$ , $\bar{\ell} = 0.1$ , $\bar{\ell}' = 0.075, 0, -0.075$ ; $\nu = 0.3$ . . . . .  | 187 |

# List of Tables

|      |   |     |
|------|---|-----|
| 2.1  | Normalized stress intensity factors (SIFs) for mode III crack problem   | 26  |
| 3.1  | Governing PDEs in antiplane shear problems. . . . .   | 36  |
| 4.1  | Roots $\lambda_i$ together with corresponding mechanics theory and type of material. . . . .  | 48  |
| 4.2  | Variation of classical (normalized) SIFs with material gradation parameter $\tilde{\gamma} = \gamma/a$ . . . . .                                    | 55  |
| 4.3  | Convergence of (normalized) generalized SIFs for a mode III crack. . . . .  | 62  |
| 4.4  | Normalized generalized SIFs for a mode III crack at various values of $\tilde{\ell}$ , $\tilde{\ell}'$ , and $\tilde{\gamma}$ . . . . .             | 63  |
| 8.1  | Normalized stress intensity factors (SIFs) for an internal crack in a half-plane. $N + 1$ terms are used in approximating the primary variable.     | 127 |
| 10.1 | Roots $\lambda_i$ together with corresponding mechanics theory and type of material. . . . .  | 148 |
| 10.2 | Normalized SIFs for mode III crack problem in an FGM. ( $\ell = \ell' \rightarrow 0$ )  | 161 |
| 10.3 | Normalized generalized SIFs for a mode III crack at $\tilde{\ell} = 0.1$ , $\tilde{\ell}' = 0.01$ , and various values of $\tilde{\beta}$ . . . . . | 162 |

**12.1 Normalized SIFs for a mode I crack under uniform loading,  $p(x) = -p_0$ .**

**$(\ell/a = 0.1, \ell'/a = 0.01, \nu = 0.3)$  . . . . . 183**

## **ACKNOWLEDGEMENTS**

I am grateful to my advisors, Professor A. Fannjiang and Professor G. Paulino, for their invaluable advice and consistent supports in research.

I thank my parents who have devoted most of their time to their children.

This degree would not have been possible without my beloved wife, Yiuchun, her continuous encouragement. My two loving boys, Andrew and Timothy, have brought me a great deal of happiness and make my research an enjoyable one.

I have benefitted from many professors at UC Davis by taking or sitting in their classes, listening to their talks, chatting with them. Among them are Profs. A. Cheer, Y. F. Dafalias, T. R. Ginn, J. Gravner, J. Hunter, B. Jeremic, A. Mogilner, M. Mulase, E. G. Puckett, M. M. Rashid, N. Saito, N. Sukumar, and B. Temple. I am grateful to all of them.

My special thanks goes to graduate coordinators Kathy La Giusa and Celia Davis whose helps during my years of graduate study are simply indispensable.

Finally, I thank God for His love, forgiveness, and gracious providence.



## Abstract

The focus of this work is to solve crack problems in functionally graded materials (FGMs) with strain-gradient effect. The method used and developed is called hypersingular integral equation method in which the integral is interpreted as a finite part integral, and it can be considered as a generalization of the well-known singular integral equation method. In developing the method, we have derived the exact formulas for evaluating the hypersingular integrals and used Mellin transform to study the crack-tip asymptotics; we have detailed the numerical approximation procedures; also, we have generalized the definition of stress intensity factors (SIFs) under strain-gradient theory and provided formulas for computing SIFs.

Different types of crack problems have been solved: Conventional classical linear elastic fracture mechanics (LEFM) vs. strain-gradient theory; scalar problems (Mode III fracture) vs. vector ones (Mode I fracture); homogeneous materials vs. FGMs; different geometric setting of crack location and material gradation. In particular, we obtain a closed form solution for the crack profile in one simple case – Mode III crack problems in homogeneous materials with the characteristic length  $\ell'$  responsible for surface strain-gradient term being zero.

# Chapter 1

## Introduction

Displacement-equations of equilibrium in the absence of body force of conventional linear elasticity [1, 33] are

$$\mu \nabla^2 \mathbf{u} + (\lambda + \mu) \nabla \nabla \cdot \mathbf{u} = 0, \quad (1.1)$$

where  $\lambda$  and  $\mu$  are the Lamé constants,  $\mathbf{u}$  is the displacement vector,  $\nabla$ ,  $\nabla \cdot$ , and  $\nabla^2$  are the gradient, divergence, and Laplacian operators, respectively. Clearly, as shown in equation (1.1), the classical continuum theories possess no intrinsic length scale. Sometimes conventional continuum theories are referred as *local* theories because of the assumption that stress at a material point is a function of strain at the same point, and typical dimensions of length are generally associated with the overall geometry of the domain under consideration. Thus classical elasticity (and plasticity) are scale-free continuum theories in which there is no microstructure associated with material points [31], and it has been quite an adequate model when the length scale of a deformation field is much larger than the microstructural length scale of the material. However, if the two length scales are of comparable order, the adequacy of the local assumption may no longer stands as the material behavior at a point will be also under influence by the deformation of the neighboring points. In order to cope with this physical reality, conventional continuum theories are generalized so that stress is

not only a function of strain at one point, but also a function of the gradient of the strain. This leads to the so called *non-local*, higher order strain-gradient theories.

## 1.1 Strain-Gradient Theories

As a generalization of the conventional classical continuum theories, strain-gradient theories enrich the classical continuum with additional material characteristic lengths in order to describe the size (or scale) effects resulting from the underlining microstructure. For instance, the equilibrium displacement-equation without body force by using an anisotropic gradient elasticity theory with surface energy are [34, 35]

$$(1 - \ell^2 \nabla^2) [\mu \nabla^2 \mathbf{u} + (\lambda + \mu) \nabla \nabla \cdot \mathbf{u}] = 0. \quad (1.2)$$

There is a length parameter  $\ell$  appearing in (1.2), also the order of the governing partial differential equation(s) is higher than (1.1).

Higher order continua belong to a general class of constitutive models which account for the material microstructure. Starting from the earliest Cosserat couple stress theory [18], various non-local or strain-gradient continuum theories have been proposed. For instance, Toupin [90] and Mindlin [65, 66] proposed a theory that includes micro-curvature and gradients of normal strain. Casal [8, 9, 10] established the connection between surface tension effects and the anisotropic gradient elasticity theory. Recent work on strain gradient theories to account for size (or scale) effects in materials can be found in the articles by Fleck and Hutchinson 1997 [37], Lakes 1983, 1986 [55, 56], Smyshlyaev and Fleck 1996 [83], Van Vliet and Van Mier [94], and Wu 1992 [99]. Recent applications of gradient elasticity to fracture mechanics include the work by Aifantis 1992 [2], Exadaktylos *et al.* 1996 [35], Fannjiang *et al.* 2001 [36], Hutchinson & Evans 2000 [44], Hwang *et al.* 1998 [45], Paulino *et al.* 1998 [73], Vardoulakis *et al.* 1996 [92], and Zhang *et al.* 1998 [100]. Reference [37] is an excellent

review article providing a summary of the experimental evidence.

## 1.2 Functionally Graded Materials

Another interest that we are looking for in this thesis is the so called functionally graded materials (FGMs). In terms of mathematical description, the Lamé moduli  $\lambda$  and  $\mu$  in (1.1) are no longer constants, but functions that represent material gradation.

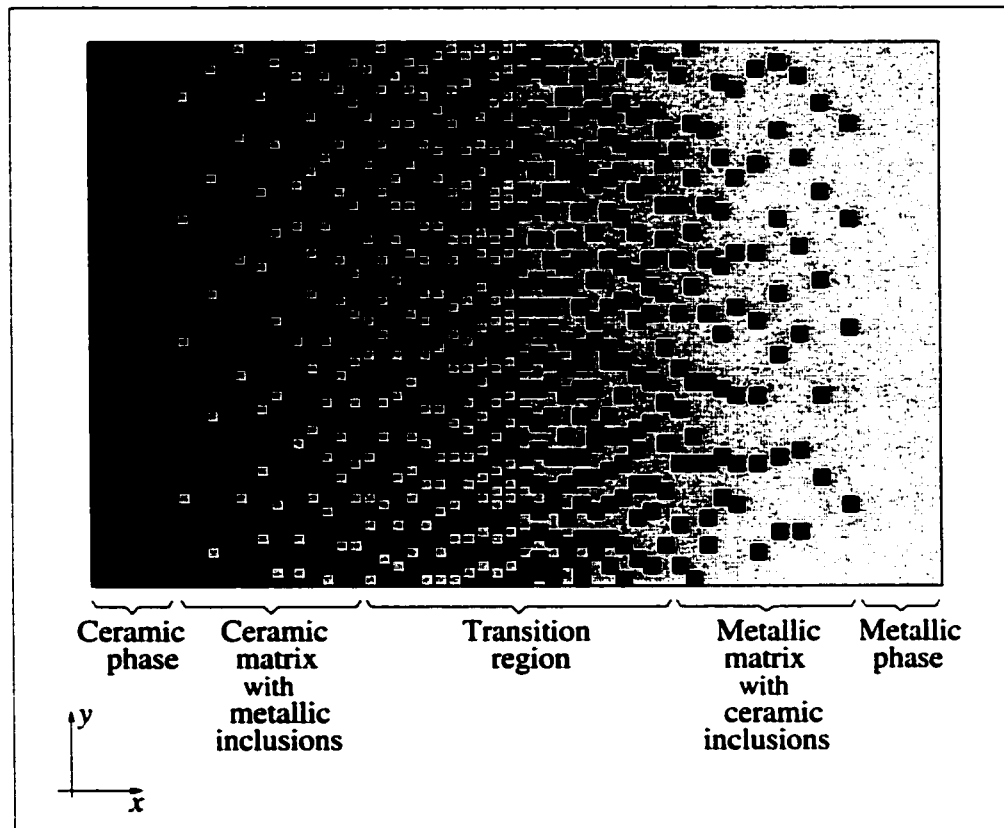


Figure 1.1: An illustration of a functionally graded material.

Thus, in the absence of body force, the equilibrium equations become (see Chapter 3 for the discussion of the derivation)

$$\mu(\mathbf{x})\nabla^2\mathbf{u} + [\lambda(\mathbf{x}) + \mu(\mathbf{x})]\nabla\nabla\cdot\mathbf{u} = 0, \quad (1.3)$$

where we have used  $\lambda(\mathbf{x})$  and  $\mu(\mathbf{x})$  to denote that  $\lambda$  and  $\mu$  are functions of position  $\mathbf{x} \equiv (x_1, x_2, x_3) \equiv (x, y, z)$ . It is worth to point out that equation (1.3) has the same order as in (1.1), it is just a replacement of the Lamé constants  $\lambda$  and  $\mu$  with functions  $\lambda(\mathbf{x})$  and  $\mu(\mathbf{x})$ , respectively.

The emergence of FGMs is the outcome of the need to accommodate material exposure to non-uniform service requirements. These multiphased materials feature gradual transition in composition and/or microstructure for the specific purpose of controlling variations in thermal, structural or functional properties. The spatial variation of microstructure is accomplished through nonuniform distribution of the reinforcement phase with different properties, sizes and shapes, as well as by interchanging the roles of reinforcement and matrix (base) materials in a continuous manner. This concept is illustrated by Figure 1.1, which shows an FGM with a continuously graded microstructure. Typical examples of FGMs include ceramic/ceramic, e.g.  $\text{MoSi}_2/\text{SiC}$  [7], and metal/ceramic, e.g.  $\text{Ti}/\text{TiB}$  [6], systems. Comprehensive reviews on several aspects of FGMs can be found in the articles by Erdogan 1995 [26], Hirai 1996 [41], Markworth *et al.* 1995 [59], and the book by Suresh & Mortensen 1998 [88].

### 1.3 Functionally Graded Materials with Strain-Gradient Effect

In this thesis we investigate the fracture problems in FGMs with strain-gradient effect. Thus, the problem is a combination of higher order strain-gradient theory and FGMs. The governing equilibrium equations become much more complicated than the corresponding equations (1.1) – (1.3) due to the interaction of the material gradation and the strain-gradient effect. For instance, instead of just replacing the Lamé moduli  $\lambda$  and  $\mu$  to be some function reflecting material gradation in (1.2), the

equilibrium equations become (see Chapter 3 for the detail of the derivation)

$$\begin{aligned}
& G(x, y) \nabla^2 (1 - \ell^2 \nabla^2) \mathbf{u} + [\lambda(x, y) + G(x, y)] \nabla (1 - \ell^2 \nabla^2) \nabla \cdot \mathbf{u} \\
& + [(1 - \ell^2 \nabla^2) (\nabla \mathbf{u} + \nabla \mathbf{u}^T)] \nabla G(x, y) + [(1 - \ell^2 \nabla^2) \nabla \cdot \mathbf{u}] \nabla \lambda(x, y) \quad (1.4) \\
& - \ell^2 \left\{ \left( \nabla \frac{\partial}{\partial x} \mathbf{u} \right) \nabla \frac{\partial G(x, y)}{\partial x} + \left( \nabla \frac{\partial}{\partial y} \mathbf{u} \right) \nabla \frac{\partial G(x, y)}{\partial y} - \nabla [\nabla \lambda(x, y) \cdot \nabla \nabla \cdot \mathbf{u}] \right\} \\
& - \ell^2 \left\{ \frac{\partial}{\partial x} [(\nabla \nabla u) \nabla G(x, y)] + \frac{\partial}{\partial y} [(\nabla \nabla v) \nabla G(x, y)] + (\nabla \nabla^2 \mathbf{u}) \nabla G(x, y) \right\} = 0,
\end{aligned}$$

if a two-dimensional plane problem is considered and the boldface  $\mathbf{u}$  denotes the displacement vector  $(u, v)$ .

Equation (1.4) seems to be a bit out of hand, and how to solve it becomes a pure mathematical task. It is the focus of this thesis to solve (1.4) both analytically and numerically.

## 1.4 Mathematical Aspects

Essentially, there are two types of mathematical methods being used very often in the field of fracture mechanics: integral transforms [88, 101] and complex function theories [71, 72]. Depending on the geometry and the coordinate system of the crack, the most often used integral transforms include Fourier, Mellin, and Hankel transforms. The techniques in complex analysis include Weiner-Hopf method, conformal mapping, Laurent series expansion, and boundary collocation method. Reference [27] by Erdogan is a good review paper on this aspect.

### 1.4.1 Singular Integral Equation Method

The system of equations in (1.1) is a second order elliptic type partial differential equations (PDEs), and it is often formulated as a mixed boundary value problems in fracture mechanics. The method of singular integral equations has been well known

and often used to solve such crack problems in the classical theory of elasticity [68, 69, 84, 86]. For example, a Mode III crack problem with crack surface sitting in the middle of an infinite homogeneous medium is just a Laplace equation for the displacement component  $w(x, y)$  with mixed boundary conditions (see the details in Chapter 2):

$$\begin{cases} \nabla^2 w(x, y) = 0, & -\infty < x < \infty, \quad y > 0, \\ w(x, 0) = 0, & x \notin [c, d], \\ \sigma_{yz}(x, 0^+) = p(x), & x \in (c, d). \end{cases} \quad (1.5)$$

By using integral transform, one can make (1.5) to be a Cauchy singular integral equation (see [86, 85] or Chapter 2 for detail)

$$\frac{G_0}{\pi} \int_c^d \frac{\phi(t, 0^+)}{t-x} dt = p(x), \quad c < x < d; \quad \text{with} \quad \phi(x) = \frac{\partial w(x, 0)}{\partial x}. \quad (1.6)$$

Of course, there is a closed form solution [79] to (1.6).

When the material gradation is included in the problems, equation (1.3) is still a second order elliptic type PDE. Crack problems in FGMs can be considered as a regular perturbation to the ones in homogeneous materials. For example, if the shear modulus  $G$  takes gradation function to be  $G = G_0 e^{\beta x}$ , then the corresponding PDE to (1.5) becomes (see Chapter 2 for detail)

$$\nabla^2 w(x, y) + \beta \frac{\partial w(x, y)}{\partial x} = 0. \quad (1.7)$$

As we know that Laplacian operator has rigid motion invariance, equation (1.7) says that the material gradation brings in the perturbation and ruins this invariance, and the consequence of it is that it will often ruin the solvability for closed form solution. However, the method to solve crack problems for FGMs in the classical theory of elasticity is very much the same as in the homogeneous materials in terms of deriving the governing singular integral equation [17, 24, 25, 26, 30, 46]. For the case that

closed form solution is not available, numerical solution procedures have been widely used and well addressed [24, 28, 29].

### 1.4.2 Solution to the Crack Problems with Strain-Gradient Effect

So far, not very much work has been done to the crack problems with strain-gradient effect, and most of them are pretty recent [34, 35, 36, 45, 73, 100]. Zhang *et al.* [100] used Weiner-Hopf method to obtain a Mode III full-field solution in elastic materials with strain-gradient effect; Shi *et al.* [82] used the same technique to solve both Mode I and Mode II problems. Vardoulakis *et al.* [92] used integral transform method to solve a Mode III crack problem for a gradient elasticity with a surface energy term, and Exadaktylos [34] solved the corresponding one for Mode I crack problem.

All work mentioned above is for homogeneous materials . For nonhomogeneous materials, *e.g.* FGMs, Paulino *et al.* [72] have solved a Mode III crack problem in FGMs with strain-gradient effect by using the hypersingular integral equation method.

### 1.4.3 Hypersingular Integral Equation Method

In this thesis we use the hypersingular integral equation method to solve main PDE (1.4). Kaya and Erdogan [50] have used hypersingular (finite part) integral to formulate crack problems in classical linear elastic fracture mechanics (LEFM). However, the finite part integral approach in LEFM is an alternative formulation; while in gradient elasticity, hypersingularity arises naturally in the formulation of the integral equation. For example, a simplest case, the governing PDE for a Mode III fracture in homogeneous material with strain-energy is

$$(1 - \ell^2 \nabla^2) \nabla^2 w = 0 ,$$

and it gives rise to (see details in Chapter 9)



$$\begin{aligned}
 & -\frac{2\ell^2}{\pi} \int_{-a}^a \frac{\phi(t)}{(t-x)^3} dt + \frac{1-\rho^2/4}{\pi} \int_{-a}^a \frac{\phi(t)}{t-x} dt \\
 & + \frac{1}{\pi} \int_{-a}^a K_0(t-x)\phi(t)dt - \frac{\ell'}{2}\phi'(x) = \frac{p(x)}{G}, \quad |x| < a,
 \end{aligned}$$

an integral equation with cubic singularity. Some concerns arise immediately. For instance, the exact evaluation of the hypersingular integrals (see details in Chapter 7)

$$\int_{-1}^1 \frac{T_n(s)\sqrt{1-s^2}}{(s-r)^3} ds, \quad |r| < 1 \quad \text{and} \quad \int_{-1}^1 \frac{U_n(s)\sqrt{1-s^2}}{(s-r)^3} ds, \quad |r| < 1$$

becomes an important issue in the numerical solution.

## 1.5 Outline of Contents

Several chapters in this thesis have been published in joint papers with my advisors Professor A. C. Fannjiang and Professor G. H. Paulino. Essential part of Chapter 2 is reported in [14]; Chapter 3 is under preparation [13]; Chapter 4 has appeared in both [72] and [73]; Chapter 7 consists of the major part of [11]; Chapter 9 is a part of [36]; Chapter 10 has been presented in *Third SIAM Conference on Mathematical Aspects of Materials Science* and submitted for publication [16]; a preliminary version of Chapter 11 has been submitted to *The 20th Int. Congress of the Int. Union of Theoretical and Applied Mechanics (IUTAM)* and collected as a proceeding paper [12]; a simplified version of Chapter 12 appeared in [15].

The remainder of the thesis is organized as follows.

In Chapters 2 and 4, we lay out how the hypersingular integral equations are formulated. Chapter 2 focuses on the case of classical LEFM, and Chapter 4 is devoted to the case of strain-gradient elasticity; both chapters are for the case of FGMs.

It is important to study the constitutive equations of the strain-gradient elasticity for FGMs, for the governing PDE depend on them. Thus we treat the constitutive

equations of the strain-gradient elasticity for FGMs in Chapter 3. Also, we use Chapter 3 to serve a common ground on which we introduce the consistent notations, strain energy function, PDEs.

Chapter 5 gives definitions of the finite part integrals and show how the hypersingular integrals arise in the formulation.

Chapter 6 is devoted to the analysis of the crack-tip asymptotics by using Mellin transform. Different order of singularity are examined under Mellin transform.

Chapter 7 provides the details of the derivation of the exact evaluation of the hypersingular integrals. Also, useful formulas needed for computing SIFs are addressed.

Chapter 8 details the numerical approximation procedures and provides the computation of SIFs. Also, at the end of Chapter 8 we demonstrate two sets of Chebyshev polynomials expansion by giving a Mode I crack problem in classical LEFM.

In Chapter 9, we find a closed form solution for a case of homogeneous materials with the surface energy term  $\ell' = 0$  for a Mode III crack problem. A plot of numerical solution vs. the closed form solution is provided. A discussion of a more general strain energy density function is provided at the end of the chapter.

Chapter 10 can be considered as a continuation of Chapter 4, with a different geometrical location of the crack to the material gradation. In Chapter 4, the crack is perpendicular to the material gradation; while in Chapter 10, the crack is parallel to the material gradation.

In Chapters 11 and 12, we deal with Mode I crack problems for homogeneous and FGMs, respectively. They are of type of vector problems, thus systems of hypersingular integral equations are derived.

Chapter 13 gives a brief remark and summary of the paper with some future work listed.

## Chapter 2

# Singular Integral Equations in Classical Linear Elastic Fracture Mechanics

In this chapter and Chapter 4, we develop a comprehensive presentation and lay out the details about how the hypersingular integral equations arise in solving crack problems. The formulation of hypersingular integral equations in the present chapter deals with the problems in classical linear elastic fracture mechanics (LEFM); while in Chapter 4, we address the crack problems in the higher order theory (elasticity with strain-gradient effects). In both chapters, we assume that the material is non-homogeneous, which in the field of functionally graded materials (FGMs) has gained renewed importance.

### 2.1 Introduction

In general, the solution to the crack problems in the classical LEFM often leads to a system of Cauchy type singular integral equations [28, 29, 46, 47, 51, 53, 68]

$$\frac{a_i}{\pi} \int_c^d \frac{\phi_i(t)}{t-x} dt + \sum_{j=1}^J \int_c^d k_{ij}(x,t) \phi_i(t) dt + b_i \phi_i(x) = p_i(x), \quad c < x < d,$$

where  $a_i, b_i$  ( $i = 1, 2, \dots, I$ ) are real constants, and the kernels  $k_{ij}(x, t)$  are bounded in the closed domain  $(x, t) \in [c, d] \times [c, d]$ . Each function  $p_i(x)$  is known and given by the boundary condition(s). Functions  $\phi_i(x)$  are the unknowns of the problems, also called by the density functions which often are the derivatives of the displacements. However, if the unknown density function is chosen to be the displacement, say  $D_i(x)$ , then the order of singularity increases. Thus, a formulation of (a system of) hypersingular integral equations is made. The choice of different unknown density function in the formulation of the integral equation leads to different order of singularity (of the integral equation) will be demonstrated in the following by means of a mode III problem (see also Reference [14] by Chan *et al.*).

## 2.2 Governing Partial Differential Equations and Boundary Conditions

Consider a mode III crack problem in a nonhomogeneous elastic medium with the shear modulus variation illustrated in Figure 2.1. The nontrivial equilibrium condition is

$$\frac{\partial \sigma_{xz}}{\partial x} + \frac{\partial \sigma_{yz}}{\partial y} = 0. \quad (2.1)$$

If the shear modulus  $G$  is a function of  $x$  and takes the exponential form

$$G(x) = G_0 e^{\beta x}, \quad (2.2)$$

where  $G_0$  and  $\beta$  are material constants (see Figure 2.1), then the equilibrium condition (2.1) can be rewritten as a partial differential equation (PDE) in terms of the  $z$  component of the displacement vector,  $w(x, y)$ , *i.e.*

$$\nabla^2 w(x, y) + \beta \frac{\partial w(x, y)}{\partial x} = 0. \quad (2.3)$$

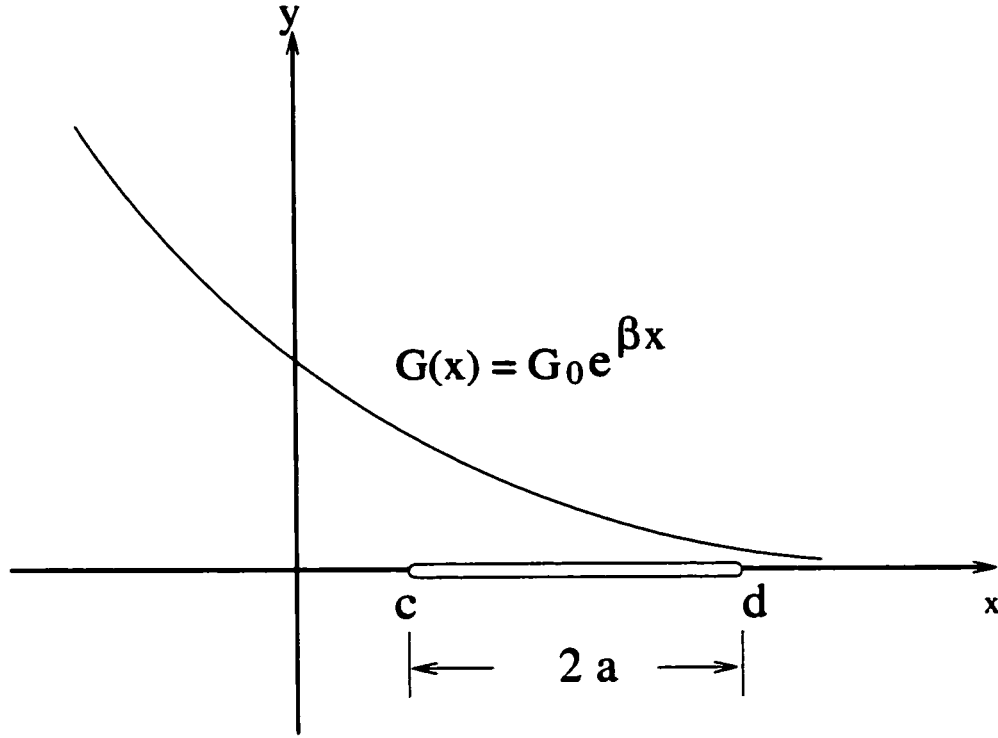


Figure 2.1: Antiplane shear problem for a nonhomogeneous material. Shear modulus  $G(x) = G_0 e^{\beta x}$ ;  $c$  and  $d$  represent the left and right crack tip, respectively;  $a$  is the half crack length.

Furthermore, the governing PDE (2.3) is solved under the following mixed boundary conditions:

$$\begin{aligned} w(x, 0) &= 0, & x \notin [c, d], \\ \sigma_{yz}(x, 0^+) &= p(x), & x \in (c, d), \end{aligned} \quad (2.4)$$

where  $p(x)$  is the traction function along the crack surfaces  $(c, d)$ . Due to symmetry, one can only consider the upper half plane  $y > 0$  for this problem. Thus the governing differential equation and boundary conditions can be summarized by:

|   |       |
|---|-------|
| $\begin{aligned} \nabla^2 w(x, y) + \beta \partial w(x, y) / \partial x &= 0, & -\infty < x < \infty, & y > 0, \\ w(x, 0) &= 0, & x \notin [c, d], \\ \sigma_{yz}(x, 0^+) &= p(x), & x \in (c, d). \end{aligned}$ | (2.5) |
|---|-------|

### 2.3 Fourier Transform

Let  $W(\xi, y)$  be the Fourier transform of  $w(x, y)$  defined by

$$\mathcal{F}\{w\}(\xi, y) = W(\xi, y) = \frac{1}{\sqrt{2\pi}} \int_{-\infty}^{\infty} w(x, y) e^{ix\xi} dx, \quad (2.6)$$

so that  $w(x, y)$  is the inverse Fourier transform of the function  $W(\xi, y)$ , *i.e.*

$$w(x, y) = \frac{1}{\sqrt{2\pi}} \int_{-\infty}^{\infty} W(\xi, y) e^{-ix\xi} d\xi. \quad (2.7)$$

With this approach, one transforms the PDE (2.3) for  $w(x, y)$  into an ordinary differential equation (ODE) for  $W(\xi, y)$ , *i.e.*

$$\frac{\partial^2 W(\xi, y)}{\partial y^2} - (\xi^2 + i\beta\xi)W = 0. \quad (2.8)$$

The corresponding characteristic equation to the ODE (2.8) above is

$$[\lambda(\xi)]^2 = \xi^2 + i\beta\xi. \quad (2.9)$$

To satisfy the far field boundary condition,  $\lim_{y \rightarrow \infty} w(x, y) = 0$ , we choose the root  $\lambda(\xi)$  with non-positive real part:

$$\lambda(\xi) = \frac{-1}{\sqrt{2}} \sqrt{\sqrt{\xi^4 + \beta^2 \xi^2} + \xi^2} - \frac{i}{\sqrt{2}} \text{sgn}(\beta\xi) \sqrt{\sqrt{\xi^4 + \beta^2 \xi^2} - \xi^2}, \quad (2.10)$$

where the signum function  $\text{sgn}(\cdot)$  is defined as

$$\text{sgn}(\eta) = \begin{cases} 1, & \eta > 0 \\ 0, & \eta = 0 \\ -1, & \eta < 0. \end{cases} \quad (2.11)$$

Thus  $W(\xi, y)$  is found to be

$$W(\xi, y) = A(\xi) e^{\lambda(\xi)y} \quad (2.12)$$

and, by equation (2.7),  $w(x, y)$  can be expressed as

$$w(x, y) = \frac{1}{\sqrt{2\pi}} \int_{-\infty}^{\infty} [A(\xi) e^{\lambda(\xi)y}] e^{-ix\xi} d\xi, \quad (2.13)$$

where  $A(\xi)$  is to be determined by the boundary conditions (2.4).

As the limit of  $y \rightarrow 0^+$  is taken,

$$w(x, 0^+) = \lim_{y \rightarrow 0^+} \frac{1}{\sqrt{2\pi}} \int_{-\infty}^{\infty} [A(\xi)e^{\lambda(\xi)y}] e^{-ix\xi} d\xi = \frac{1}{\sqrt{2\pi}} \int_{-\infty}^{\infty} A(\xi)e^{-ix\xi} d\xi, \quad (2.14)$$

that is,  $w(x, 0^+)$  is the inverse Fourier transform of  $A(\xi)$ . By inverting the Fourier transform, one obtains

$$A(\xi) = \frac{1}{\sqrt{2\pi}} \int_{-\infty}^{\infty} w(x, 0^+) e^{ix\xi} dx = \frac{1}{\sqrt{2\pi}} \int_c^d w(t, 0^+) e^{it\xi} dt, \quad (2.15)$$

where the first boundary condition in (2.4) and a change of dummy variable ( $x \leftrightarrow t$ ) have been applied.

On the other hand, the stress  $\sigma_{yz}$  is given by

$$\sigma_{yz}(x, y) = G(x) \frac{\partial w(x, y)}{\partial y} = \frac{G(x)}{\sqrt{2\pi}} \int_{-\infty}^{\infty} [A(\xi)\lambda(\xi)e^{\lambda(\xi)y}] e^{-ix\xi} d\xi. \quad (2.16)$$

Replacing  $A(\xi)$  in equation (2.16) above by the expression in equation (2.15), one gets

$$\begin{aligned} \sigma_{yz}(x, y) &= \frac{G(x)}{\sqrt{2\pi}} \int_{-\infty}^{\infty} \left[ \frac{1}{\sqrt{2\pi}} \int_c^d w(t, 0^+) e^{it\xi} dt \right] \lambda(\xi) e^{\lambda(\xi)y} e^{-ix\xi} d\xi \\ &= \frac{G(x)}{2\pi} \int_c^d w(t, 0^+) \int_{-\infty}^{\infty} \lambda(\xi) e^{\lambda(\xi)y} e^{i(t-x)\xi} d\xi dt. \end{aligned} \quad (2.17)$$

Defining

$$K(\xi, y) = \lambda(\xi) e^{\lambda(\xi)y}, \quad (2.18)$$

and using the second boundary condition in (2.4), one reaches

$$\begin{aligned} \sigma_{yz}(x, 0^+) &= \lim_{y \rightarrow 0^+} \sigma_{yz}(x, y), \quad c < x < d, \\ &= \lim_{y \rightarrow 0^+} \frac{G(x)}{2\pi} \int_c^d w(t, 0^+) \int_{-\infty}^{\infty} K(\xi, y) e^{i(t-x)\xi} d\xi dt \\ &= \frac{G(x)}{\pi} \int_c^d w(t, 0^+) \text{kernel}(x-t) dt \\ &= p(x), \end{aligned} \quad (2.19)$$

with

$$2 \times \text{kernel}(x - t) = \lim_{y \rightarrow 0^+} \int_{-\infty}^{\infty} K(\xi, y) e^{i(t-x)\xi} d\xi, \quad (2.20)$$

where equation (2.19) and the above kernel are interpreted in a limit sense.

## 2.4 Asymptotic Analysis and Kernel Decomposition

In order to make the kernel explicit (see (2.20)) and separate its singular and regular parts; we need to investigate the asymptotic behavior,  $|\xi| \rightarrow +\infty$ , of

$$K(\xi) \equiv K(\xi, 0^+) = \lambda(\xi). \quad (2.21)$$

A simple asymptotic analysis gives the following results:

$$\mathcal{R}(\lambda(\xi)) = \frac{-1}{\sqrt{2}} \sqrt{\sqrt{\xi^4 + \beta^2 \xi^2} + \xi^2} \quad |\xi| \rightarrow \infty \sim -|\xi|, \quad (2.22)$$

$$i \times \mathcal{I}(\lambda(\xi)) = \frac{-i}{\sqrt{2}} \text{sgn}(\beta \xi) \sqrt{\sqrt{\xi^4 + \beta^2 \xi^2} - \xi^2} \quad |\xi| \rightarrow \infty \sim -\frac{i\beta}{2} \frac{|\xi|}{\xi}, \quad (2.23)$$

where  $\mathcal{R}(\cdot)$  and  $\mathcal{I}(\cdot)$  denote the real part and the imaginary part of the argument, respectively. Thus we have the decomposition

$$K(\xi) = [K(\xi) - K_{\infty}(\xi)] + K_{\infty}(\xi), \quad (2.24)$$

with closed form expressions given by

$$K_{\infty}(\xi) = -|\xi| - \frac{i\beta}{2} \frac{|\xi|}{\xi}, \quad (2.25)$$

which gives rise to the quadratic hypersingular and Cauchy singular kernels (see Chapter 3.3).

The other part,  $K(\xi) - K_{\infty}(\xi)$ , called by the regular kernel takes the following form:



$$\begin{aligned}
 K(\xi) - K_\infty(\xi) &= \lambda(\xi) - \left( -|\xi| - \frac{i\beta|\xi|}{2\xi} \right) \\
 &= \left( |\xi| - \frac{1}{\sqrt{2}} \sqrt{\sqrt{\xi^4 + \beta^2\xi^2} + \xi^2} \right) + \frac{i|\xi|}{2\xi} \left( \beta - \sqrt{2} \operatorname{sgn}(\beta) \sqrt{\sqrt{\xi^4 + \beta^2\xi^2} - \xi^2} \right) \\
 &= \frac{\frac{1}{2}\xi^2 - \frac{1}{2}\sqrt{\xi^4 + \beta^2\xi^2}}{|\xi| + \frac{1}{\sqrt{2}}\sqrt{\sqrt{\xi^4 + \beta^2\xi^2} + \xi^2}} + \frac{i|\xi|}{2\xi} \frac{2\xi^2 + \beta^2 - 2\sqrt{\xi^4 + \beta^2\xi^2}}{\beta + \sqrt{2} \operatorname{sgn}(\beta) \sqrt{\sqrt{\xi^4 + \beta^2\xi^2} - \xi^2}} \\
 &= \frac{-\frac{1}{4}\beta^2\xi^2}{\left( |\xi| + \frac{1}{\sqrt{2}}\sqrt{\sqrt{\xi^4 + \beta^2\xi^2} + \xi^2} \right) \left( \frac{1}{2}\xi^2 + \frac{1}{2}\sqrt{\xi^4 + \beta^2\xi^2} \right)} + \frac{i|\xi|}{2\xi} \frac{\beta^4}{\left( \beta + \sqrt{2} \operatorname{sgn}(\beta) \sqrt{\sqrt{\xi^4 + \beta^2\xi^2} - \xi^2} \right) \left( 2\xi^2 + \beta^2 + 2\sqrt{\xi^4 + \beta^2\xi^2} \right)}. \quad (2.26)
 \end{aligned}$$

After dividing the first fraction in the equality numbered as (2.26) by  $|\xi|\sqrt{|\xi|}$ , one obtains

$$\begin{aligned}
 K(\xi) - K_\infty(\xi) &= \frac{-\beta^2\sqrt{|\xi|}}{2 \left( \sqrt{|\xi|} + \frac{1}{\sqrt{2}}\sqrt{\sqrt{\xi^2 + \beta^2} + |\xi|} \right) \left( |\xi| + \sqrt{\xi^2 + \beta^2} \right)} + \\
 &\quad \frac{i\beta^4|\xi|/\xi}{2 \left( \beta + \sqrt{2} \operatorname{sgn}(\beta) \sqrt{\sqrt{\xi^4 + \beta^2\xi^2} - \xi^2} \right) \left( 2\xi^2 + \beta^2 + 2\sqrt{\xi^4 + \beta^2\xi^2} \right)}. \quad (2.27)
 \end{aligned}$$

In general, the function  $K(\xi)$  may be complicated [51] and so is the corresponding asymptotic analysis. In any case, the singular part, such as (2.25), can be separated by using a symbolic calculation software such as MAPLE [96, 97] and the regular kernel can be dealt with numerically.

Thus, equation (2.20) becomes

$$\begin{aligned}
 2 \times \text{kernel}(x, t) &= \lim_{y \rightarrow 0^+} \int_{-\infty}^{\infty} K(\xi, y) e^{i(t-x)\xi} d\xi = \\
 &\underbrace{\lim_{y \rightarrow 0^+} \int_{-\infty}^{\infty} [K(\xi, y) - K_\infty(\xi, y)] e^{i(t-x)\xi} d\xi}_{\text{nonsingular part}} + \underbrace{\lim_{y \rightarrow 0^+} \int_{-\infty}^{\infty} K_\infty(\xi, y) e^{i(t-x)\xi} d\xi}_{\text{singular part}}, \quad (2.28)
 \end{aligned}$$

where

$$K_{\infty}(\xi, y) = \left( -|\xi| - \frac{i\beta |\xi|}{2\xi} \right) e^{-|\xi|y}. \quad (2.29)$$

Therefore, the decomposition of the kernel  $(x, t)$  (see (2.20)) into nonsingular and singular parts has been achieved.

## 2.5 Hypersingular Integral Equation

The singular part in equation (2.28) can be shown to converge in the sense of distribution (see Chapter 5.3 and Reference [36]):

$$\begin{aligned} \lim_{y \rightarrow 0^+} \int_{-\infty}^{\infty} K_{\infty}(\xi, y) e^{i(t-x)\xi} d\xi &= \lim_{y \rightarrow 0^+} \int_{-\infty}^{\infty} \left( -|\xi| - \frac{i\beta |\xi|}{2\xi} \right) e^{i(t-x)\xi} d\xi \\ &= \frac{2}{(t-x)^2} + \frac{\beta}{t-x}. \end{aligned} \quad (2.30)$$

The expression on the right side of equation (2.30) is a distribution (or generalized function) defined via Hadamard finite part integral (including Cauchy principal value). The nonsingular part in equation (2.28) can be obtained by means of equation (2.27), which leads to

$$\begin{aligned} N(x, t) &= \frac{1}{2} \lim_{y \rightarrow 0^+} \int_{-\infty}^{\infty} [K(\xi, y) - K_{\infty}(\xi, y)] e^{i(t-x)\xi} d\xi \\ &= \frac{1}{2} \int_{-\infty}^{\infty} [K(\xi) - K_{\infty}(\xi)] e^{i(t-x)\xi} d\xi \\ &= - \int_0^{\infty} \frac{\beta^2 \sqrt{\xi} \cos[(t-x)\xi]}{\left( 2\sqrt{\xi} + \sqrt{2} \sqrt{\sqrt{\xi^2 + \beta^2} + \xi} \right) \left( \xi + \sqrt{\xi^2 + \beta^2} \right)} d\xi - \\ &\quad \int_0^{\infty} \frac{\beta^3 \sqrt{\sqrt{\xi^4 + \beta^2 \xi^2} - \xi^2} \sin[(t-x)\xi]/2}{\left( \sqrt{\sqrt{\xi^4 + \beta^2 \xi^2} + \xi^2} + \sqrt{2}|\xi| \right) \left( 2\xi^2 + \beta^2 + 2\sqrt{\xi^4 + \beta^2 \xi^2} \right)} d\xi, \end{aligned} \quad (2.31)$$

where we have used the fact that the real part of  $[K(\xi) - K_{\infty}(\xi)]$  is an even function of  $\xi$ , and the imaginary part is an odd function of  $\xi$ . Also note that if  $\beta = 0$ , then  $N(x, t) = 0$ . If  $\beta \neq 0$ , then the denominators in the two integrands of equation (2.31) never vanish for  $\xi \in [0, \infty)$ .

Throughout this chapter, the notation  $\mathcal{F}$  is used for Hadamard's finite part integral (see Chapter 3), and the notation  $\mathcal{P}$  is used for the Cauchy principal value (Kutt, 1975 [54]). Thus using equations (2.28) to (2.31) together with equation (2.19), one obtains a hypersingular integral equation:

$$\boxed{\frac{G_0 e^{\beta x}}{\pi} \mathcal{F}_c^d \left[ \frac{1}{(t-x)^2} + \frac{\beta}{2(t-x)} + N(x, t) \right] w(t, 0^+) dt = p(x)}, \quad (2.32)$$

where  $c < x < d$  and the highest order singularity defines the notation adopted, and  $N(x, t)$  is given in equation (2.31). In order to have a unique solution of (2.32), we must impose the crack-tip conditions on  $w(t, 0^+)$  (Martin 1991 [60]; Fan-jiang *et al.*, 2001 [36]):

$$w(c, 0^+) = w(d, 0^+) = 0. \quad (2.33)$$

In case of homogeneous materials,  $\beta = 0$ , equation (2.32) becomes

$$\frac{G_0}{\pi} \mathcal{F}_c^d \frac{w(t, 0^+)}{(t-x)^2} dt = p(x), \quad c < x < d. \quad (2.34)$$

Therefore one may consider the hypersingular integral equation (2.32) as a perturbation of equation (2.34). Also note that the expressions for  $\sigma_{yz}(x, 0)$ , equations (2.19) and (2.32), are valid for  $c < x < d$  as well as for  $x$  is outside of  $[c, d]$ . That is,

$$\sigma_{yz}(x, 0) = \frac{G_0 e^{\beta x}}{\pi} \int_c^d \left[ \frac{1}{(t-x)^2} + \frac{\beta}{2(t-x)} + N(x, t) \right] w(t, 0^+) dt, \quad (2.35)$$

where  $x < c$  or  $x > d$ . Note that the integrals in equation (2.35) above are ordinary integrals, not evaluated as Hadamard finite part integral or the Cauchy principal value integral.

## 2.6 Displacement versus Slope Formulations

Erdogan [25] has studied the mode III crack problem in order to investigate the singular nature of the crack-tip stress field when the shear modulus is not smooth

(continuous but not differentiable). Erdogan uses the slope function, *i.e.*

$$\phi(x) = \frac{\partial}{\partial x} w(x, 0) \quad (2.36)$$

as the density function in formulating the governing integral equation. The resultant Cauchy singular integral equation is then solved together with the single-valuedness condition (see equations (15), (20), (21), and (22) in Erdogan [25])

$$\int_c^d \phi(x) dx = 0 . \quad (2.37)$$

Instead of the slope formulation, the displacement formulation is employed in this paper. Kaya [49] has pointed out three advantages for choosing displacement over slope as the density function:

- More direct, without an extra step of integration to recover the displacement.
- The displacement function  $w(x, 0)$  is bounded everywhere, but in classical LEFM the slope function is unbounded at the crack tips.
- Displacement would be a more natural candidate if a three-dimensional problem is considered.

Here, we point out another advantage by choosing displacement as the density function:

- *Alternative asymptotics.*

This point is important especially for the method of integral equation because the accuracy of the method relies on the exact cancellation of singularity (*i.e.* finite-part integrals), and a key step for achieving such cancellation is the asymptotic analysis of the kernel.

The demonstration of *alternative*, and in the present case, *simpler asymptotics* can be seen if one recalls the derivation regarding the decomposition of the kernel  $K(\xi)$

described in equations (2.24), (2.25), and (2.27). In terms of the notation adopted in this paper, we have:

$$\tilde{K}(\xi) = \lim_{y \rightarrow 0^+} \frac{\lambda(\xi)}{-i\xi} e^{\lambda(\xi)y} = \frac{\lambda(\xi)}{-i\xi}, \quad \text{if slope formulation is used;} \quad (2.38)$$

$$K(\xi) = \lim_{y \rightarrow 0^+} \lambda(\xi) e^{\lambda(\xi)y} = \lambda(\xi), \quad \text{if displacement formulation is taken.} \quad (2.39)$$

The decomposition of  $\tilde{K}(\xi)$  in (2.38) is less straightforward. Because of the term  $(-i\xi)$  in the denominator in (2.38), one needs to consider the asymptotics of  $\xi \rightarrow 0$  as well as  $\xi \rightarrow \infty$ . On the other hand, the decomposition of  $K(\xi)$  in (2.39) can be achieved by considering only the asymptotics of  $\xi \rightarrow \infty$ :

$$\begin{aligned} \mathcal{R}(\lambda(\xi)) &= \frac{-1}{\sqrt{2}} \sqrt{\sqrt{\xi^4 + \beta^2 \xi^2} + \xi^2} \stackrel{|\xi| \rightarrow \infty}{\sim} -|\xi| \\ i \times \mathcal{I}(\lambda(\xi)) &= \frac{-i}{\sqrt{2}} \operatorname{sgn}(\beta \xi) \sqrt{\sqrt{\xi^4 + \beta^2 \xi^2} - \xi^2} \stackrel{|\xi| \rightarrow \infty}{\sim} -\frac{i\beta}{2} \frac{|\xi|}{\xi} \end{aligned}$$

The resulting singular integral equations for the two formulations are as follows:

- Using slope  $(\partial/\partial x)w(x, 0) = \phi(x)$  as density function, one obtains

$$\frac{G(x)}{\pi} \int_c^d \left[ \frac{1}{t-x} + \frac{\beta}{2} \log|t-x| + \tilde{N}(x, t) \right] \phi(t) dt = p(x) \quad (2.40)$$

for  $c < x < d$ , where  $\phi(x)$  satisfies condition (2.37), and  $\tilde{N}(x, t)$  is a regular kernel and can be found as (Erdogan [25], p. 824, equations (24)–(27)):

$$\begin{aligned} \tilde{N}(x, t) &= \int_0^\infty \frac{-\beta^4 \{ \cos[(t-x)\xi] - 1 \} d\xi}{2\xi \left( \beta + \sqrt{2} \operatorname{sgn}(\beta) \sqrt{\sqrt{F(\xi, \beta)} - \xi^2} \right) \left( 2\xi^2 + \beta^2 + 2\sqrt{F(\xi, \beta)} \right)} \\ &+ \int_0^\infty \frac{\beta^2 \sin[(t-x)\xi] d\xi}{\left( 2\xi + \sqrt{2} \sqrt{\sqrt{F(\xi, \beta)} + \xi^2} \right) \left( \xi + \sqrt{\xi^2 + \beta^2} \right)}, \quad (2.41) \end{aligned}$$

with  $F(\xi, \beta) = \xi^4 + \beta^2 \xi^2$ . Three comments are made here. First, the two integrals in (2.41) are convergent. Second, the sine integral is exactly the same as the sine integral given by Erdogan (1985, equations (26) on p. 824). Moreover, although the cosine integral is different from Erdogan's (1985, p. 824, equations

(25)–(29)), they are equivalent due to condition (2.37). Third, the derivative (with respect of  $x$ ) of  $\tilde{N}(x, t)$  is the regular kernel in displacement formulation. This last remark indicates the equivalence between the slope and displacement formulations.

- Using displacement  $w(x, 0)$  as density function, one obtains

$$\frac{G(x)}{\pi} \int_c^d \left[ \frac{1}{(t-x)^2} + \frac{\beta}{2(t-x)} + N(x, t) \right] w(t, 0^+) dt = p(x), \quad c < x < d, \quad (2.42)$$

where  $N$  is given by (2.31) and  $w(t, 0^+)$  satisfies crack-tip conditions (2.33).

Equations (2.40) and (2.42) are equivalent integral equation formulations of the same boundary value problem. It is interesting to observe the similarities and difference between the displacement  $N(x, t)$  and the slope  $\tilde{N}(x, t)$  kernels (*cf.* equations (2.31) and (2.41), respectively).

## 2.7 Numerical Results

In this section we present some numerical results including stress intensity factors (SIFs) and crack surface displacements. The numerical solution procedures will be postponed until Chapter 8 in which we systematically address the numerical approximation in depth.

### 2.7.1 Stress Intensity Factors (SIFs)

The SIFs at the right and left crack tips are defined by

$$K_{III}(d) = \lim_{x \rightarrow d^+} \sqrt{2\pi(x-d)} \sigma_{yz}(x, 0) \quad (2.43)$$

and

$$K_{III}(c) = \lim_{x \rightarrow c^-} \sqrt{2\pi(c-x)} \sigma_{yz}(x, 0), \quad (2.44)$$

respectively (see Figure 2.1). It is worth pointing out that the limit is taken from outside of the crack surfaces, thus the integrals that involve  $1/(t-x)^2$  and  $1/(t-x)$  are not singular anymore. They will be just regular integrals. The derivation of SIFs are provided below.

$$\begin{aligned}
 K_{III}(d) &= \lim_{x \rightarrow d^+} \sqrt{2\pi(x-d)} \sigma_{yz}(x, 0) \\
 &= \lim_{x \rightarrow d^+} \sqrt{2\pi(x-d)} \left\{ \frac{G_0 e^{\beta x}}{2\pi} \int_c^d \left[ \frac{2}{(t-x)^2} + \frac{\beta}{t-x} + N(x, t) \right] D(t) dt \right\} \\
 &= \lim_{x \rightarrow d^+} \sqrt{2\pi(x-d)} \frac{G_0 e^{\beta x}}{\pi} \int_c^d \frac{D(t)}{(t-x)^2} dt \\
 &= \lim_{r \rightarrow 1^+} \sqrt{2\pi \left( \frac{d-c}{2} \right)} (r-1) G_0 e^{\beta \left[ \left( \frac{d-c}{2} \right) r + \left( \frac{d+c}{2} \right) \right]} \frac{1}{\pi} \int_{-1}^1 \frac{\mathcal{D}(s)}{(s-r)^2} ds \\
 &= \lim_{r \rightarrow 1^+} \sqrt{\pi \left( \frac{d-c}{2} \right)} \sqrt{2(r-1)} G_0 e^{\beta \left( \frac{d-c}{2} \right) r} e^{\beta \left( \frac{d+c}{2} \right)} \frac{1}{\pi} \int_{-1}^1 \frac{\mathcal{D}(s)}{(s-r)^2} ds. \quad (2.45)
 \end{aligned}$$

The  $T_n$  expansion leads to

$$\begin{aligned}
 K_{III}(d) &= \sqrt{\pi \left( \frac{d-c}{2} \right)} G_0 e^{\beta \left( \frac{d-c}{2} \right)} e^{\beta \left( \frac{d+c}{2} \right)} \sum_0^N a_n \\
 &= \sqrt{\pi \left( \frac{d-c}{2} \right)} G_0 e^{\beta d} \sum_0^N a_n, \quad (2.46)
 \end{aligned}$$

and the  $U_n$  expansion leads to

$$\begin{aligned}
 K_{III}(d) &= \sqrt{\pi \left( \frac{d-c}{2} \right)} G_0 e^{\beta \left( \frac{d-c}{2} \right)} e^{\beta \left( \frac{d+c}{2} \right)} \sum_0^N (n+1) b_n \\
 &= \sqrt{\pi \left( \frac{d-c}{2} \right)} G_0 e^{\beta d} \sum_0^N (n+1) b_n. \quad (2.47)
 \end{aligned}$$

Similarly, one may show that with  $T_n$  expansion

$$\begin{aligned}
 K_{III}(c) &= \sqrt{\pi \left( \frac{d-c}{2} \right)} G_0 e^{-\beta \left( \frac{d-c}{2} \right)} e^{\beta \left( \frac{d+c}{2} \right)} \sum_0^N (-1)^n a_n \\
 &= \sqrt{\pi \left( \frac{d-c}{2} \right)} G_0 e^{\beta c} \sum_0^N (-1)^n a_n, \quad (2.48)
 \end{aligned}$$

and with  $U_n$  expansion

$$\begin{aligned}
 K_{III}(c) &= \sqrt{\pi \left( \frac{d-c}{2} \right)} G_0 e^{-\beta \left( \frac{d-c}{2} \right)} e^{\beta \left( \frac{d+c}{2} \right)} \sum_0^N (-1)^n (n+1) b_n \\
 &= \sqrt{\pi \left( \frac{d-c}{2} \right)} G_0 e^{\beta c} \sum_0^N (-1)^n (n+1) b_n .
 \end{aligned} \tag{2.49}$$

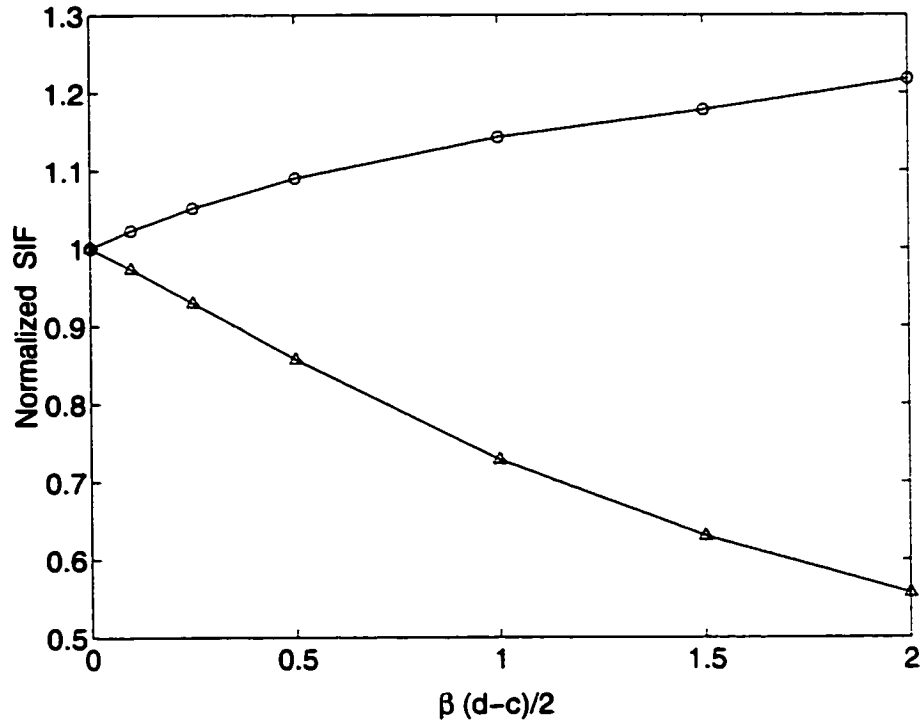


Figure 2.2: Normalized stress intensity factors for an infinite nonhomogeneous plane subjected to uniform crack surface traction  $\sigma_{yz}(x, 0) = -p_0$ . The shear modulus is  $G(x) = G_0 e^{-\beta x}$ .

Figure 2.2 shows the normalized SIFs for a crack in an infinite plane with shear modulus  $G = G(x) = G_0 e^{-\beta x}$  subjected to uniform shear traction  $\sigma_{yz}(x, 0) = -p_0$ . The symbol “o” stands for  $K_{III}(c)/(p_0 \sqrt{\pi(d-c)/2})$ , and the symbol “ $\Delta$ ” stands for  $K_{III}(d)/(p_0 \sqrt{\pi(d-c)/2})$ . The results obtained are consistent with those of Erdogan [25] (1985, p.826, Fig. 2). Note that the SIFs at the tip  $x = c$  (stiffer side) are higher than at the tip  $x = d$  (softer side). This result is surprising, however, it can be explained by considering the crack surface displacements (see Fig-



ures 2.3 and 2.4). For an homogeneous plane, the SIF is independent of  $G$ , *i.e.*  $K_{III}(c) = K_{III}(d) = p_0 \sqrt{\pi(d-c)}/2$ . Nevertheless, for a nonhomogeneous plane the crack surface displacement is inversely proportional to the material parameter  $G$  [25].

### 2.7.2 Displacement Profiles

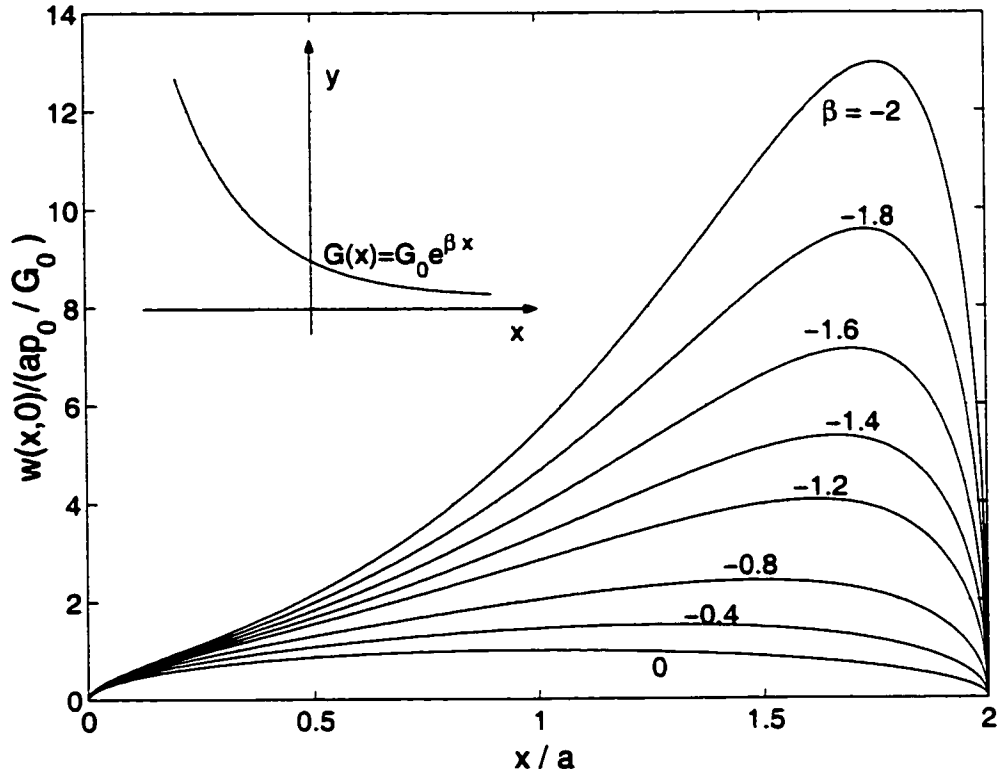


Figure 2.3: Crack surface displacement in an infinite nonhomogeneous plane under uniform crack surface shear loading  $\sigma_{yz}(x, 0) = -p_0$  and shear modulus  $G(x) = G_0 e^{\beta x}$ . Here  $a = (d - c)/2$  denotes the half crack length.

Figures 2.3 and 2.4 show numerical results for displacement profiles considering a crack with uniformly applied shear traction  $\sigma_{yz}(x, 0) = -p_0$ , ( $c < x < d$ ), and various values of the material parameter  $\beta$ . In Figure 2.3, the cracks are tilted to the right because  $\beta < 0$ , and the case  $\beta = 0$  corresponds to the crack surface displacement in an infinite homogeneous plane. In Figure 2.4, the cracks are tilted to the left

because  $\beta > 0$ . Figures 2.3 and 2.4 reveal the influence of the material parameter  $\beta$  in the range  $[-2, 2]$  on the crack profile. It can be observed that as  $\beta \rightarrow 0$ , the displacement profiles converge to the classical LEFM result. This numerical evidence shows that this antiplane shear problem can be considered as a perturbation of the classical antiplane shear problem for homogeneous material.

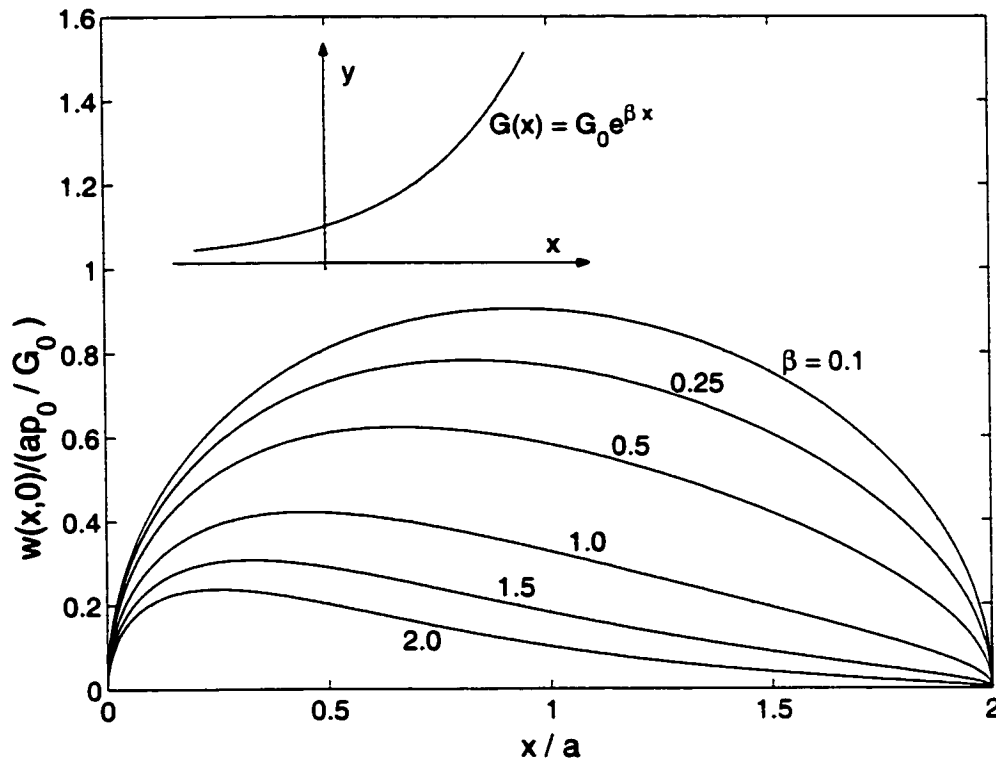


Figure 2.4: Crack surface displacement in an infinite nonhomogeneous plane under uniform crack surface shear loading  $\sigma_{yz}(x, 0) = -p_0$  and shear modulus  $G(x) = G_0 e^{\beta x}$ . Here  $a = (d - c)/2$  denotes the half crack length.

Table 2.1 presents stress intensity factors (SIFs) at both tips of the crack. Note that, from a numerical point of view, essentially the same results are obtained either by the  $U_n$  or  $T_n$  representations. In Table 2.1, 10 decimal digits are used for the SIFs just to allow verification of this statement, otherwise, less digits should be used in reporting these results.

Table 2.1: Normalized stress intensity factors (SIFs) for mode III crack problem

| $\beta(\frac{d-c}{2})$ | $U_n$ Representation                      |   | $T_n$ Representation                      |   |
|------------------------|---|---|---|---|
|                        | $\frac{K_{III}(c)}{p_0\sqrt{\pi(d-c)}/2}$ | $\frac{K_{III}(d)}{p_0\sqrt{\pi(d-c)}/2}$ | $\frac{K_{III}(c)}{p_0\sqrt{\pi(d-c)}/2}$ | $\frac{K_{III}(d)}{p_0\sqrt{\pi(d-c)}/2}$ |
| -2.00                  | 1.2177863137                              | 0.5567159837                              | 1.2177861733                              | 0.5567159865                              |
| -1.50                  | 1.1780106524                              | 0.6300690840                              | 1.1780106809                              | 0.6300690822                              |
| -1.00                  | 1.1430698167                              | 0.7284534442                              | 1.1430698277                              | 0.7284534422                              |
| -0.50                  | 1.0903639520                              | 0.8567631803                              | 1.0903639753                              | 0.8567631880                              |
| -0.25                  | 1.0518781405                              | 0.9296196207                              | 1.0518781461                              | 0.9296196340                              |
| -0.10                  | 1.0228896477                              | 0.9731176917                              | 1.0228896001                              | 0.9731176549                              |
| 0.00                   | 1.0000000000                              | 1.0000000000                              | 1.0000000000                              | 1.0000000000                              |
| 0.10                   | 0.9731176840                              | 1.0228896371                              | 0.9731176869                              | 1.0228896411                              |
| 0.25                   | 0.9296196372                              | 1.0518781831                              | 0.9296196411                              | 1.0518781724                              |
| 0.50                   | 0.8567631965                              | 1.0903639632                              | 0.8567631878                              | 1.0903639710                              |
| 1.00                   | 0.7284534446                              | 1.1430698429                              | 0.7284534433                              | 1.1430696546                              |
| 1.50                   | 0.6300690801                              | 1.1780108066                              | 0.6300690749                              | 1.1780105468                              |
| 2.00                   | 0.5567159815                              | 1.2177864998                              | 0.5567159896                              | 1.2177865939                              |

## 2.8 Concluding Remark

In this chapter, we have laid out the method of singular integral equation in classical LEFM by choosing displacement to be the unknown density function. Comparing this formulation with a slope-based formulation, one verifies that the former leads to a simpler asymptotics while the latter is much more involved (Erdogan [25], 1985, p. 824, equations (24)–(29)). Further, the displacement formulation leads to a hypersingular kernel of the type  $1/(t-x)^2$ , while the slope formulation leads to a simpler singular kernel of the Cauchy type, *i.e.*  $1/(t-x)$  and a weakly singular kernel of the logarithmic type, *i.e.*  $\log|t-x|$ . Both approaches lead to the same solution of the boundary value problem.

Another source for hypersingular integral equations to arise is attributed to the underlying higher order continuum theory, and it will be addressed in Chapter 4.

## Chapter 3

# Constitutive Equations of Strain-Gradient Elasticity Theory for Functionally Graded Materials

Before solving the crack problems in both homogeneous materials and FGMs with strain-gradient effect, we use the present chapter as a common ground to lay out some elementary ingredients which include notations, strain energy density function, constitutive equations, and the governing PDEs. Surprisingly, the investigation of the constitutive equations for strain-gradient elasticity leads us to find out that there are extra terms in the constitutive equations for FGMs due to the interaction of the gradation of the materials and the strain-gradient effect, while in the conventional classical elasticity, the constitutive equations have the same form for both homogeneous and nonhomogeneous materials. Thus, in solving crack problems for FGMs with strain-gradient effect, it is NOT correct to just change the material constants to be some function at the level of constitutive equations. One should start off with a more fundamental level – the strain-energy density function.

### 3.1 Strain-Energy Density Function

#### 3.1.1 Elasticity

In classical elasticity, the strain-energy density function has the well known form

$$\mathcal{W} = \frac{1}{2} \lambda(\mathbf{x}) \epsilon_{ii} \epsilon_{jj} + G(\mathbf{x}) \epsilon_{ij} \epsilon_{ji} , \quad (3.1)$$

where  $\lambda(\mathbf{x})$  and  $G(\mathbf{x})$  are the material parameters which are functions of position  $\mathbf{x} \equiv (x_1, x_2, x_3) \equiv (x, y, z)$ , and  $\epsilon$  is the small deformation tensor

$$\epsilon_{ij} = \frac{1}{2} (u_{i,j} + u_{j,i}) \quad (3.2)$$

with  $\mathbf{u}$  denoting the displacement vector. The Cauchy stresses are given by

$$\tau_{ij} = \frac{\partial \mathcal{W}}{\partial \epsilon_{ij}} = \lambda(\mathbf{x}) \epsilon_{kk} \delta_{ij} + 2G(\mathbf{x}) \epsilon_{ij} , \quad (3.3)$$

where  $\delta_{ij}$  is the Kronecker-delta. In the case of homogeneous materials,  $\lambda$  and  $G$  are constants (Lamé constants) and the Cauchy stresses, derived from (3.1), is

$$\tau_{ij} = \frac{\partial \mathcal{W}}{\partial \epsilon_{ij}} = \lambda \epsilon_{kk} \delta_{ij} + 2G \epsilon_{ij} . \quad (3.4)$$

Notice that equations (3.3) and (3.4) have the same form. Thus, in the conventional classical elasticity, one can simply replace the Lamé constants by some function that portrays the material gradation.

#### 3.1.2 Gradient Elasticity

However, for gradient elasticity such is not the case. The three-dimensional generalization of Casal's gradient dependent anisotropic elasticity with volumetric and surface energy for nonhomogeneous materials leads to the following expression for the strain-energy density function

$$\begin{aligned} \mathcal{W} = & \frac{1}{2} \lambda(\mathbf{x}) \epsilon_{ii} \epsilon_{jj} + G(\mathbf{x}) \epsilon_{ij} \epsilon_{ji} + \frac{1}{2} \lambda(\mathbf{x}) \ell^2 (\partial_k \epsilon_{ii}) (\partial_k \epsilon_{jj}) + \frac{1}{2} \ell' \nu_k \partial_k (\lambda(\mathbf{x}) \epsilon_{ii} \epsilon_{jj}) \\ & + G(\mathbf{x}) \ell^2 (\partial_k \epsilon_{ij}) (\partial_k \epsilon_{ji}) + \ell' \nu_k \partial_k (G(\mathbf{x}) \epsilon_{ij} \epsilon_{ji}) , \quad \ell > 0 , \end{aligned} \quad (3.5)$$

where  $\ell$  is a material characteristic length associated with volumetric energy gradient term,  $\ell'$  is another material characteristic length associated with surfaces energy gradient term,  $\partial_k = \partial/\partial x_k$  is a differential operator, and  $\nu_k$ ,  $\partial_k \nu_k = 0$ , is a director field. The terms associated with  $\ell'$  have the meaning of surface energy. It is easy to see that, after integrating  $\mathcal{W}$  over the material domain  $\Omega$  and applying the divergence theorem, the terms associated with  $\ell'$  become surface integrals, *i.e.*

$$\int_{\Omega} \left[ \frac{1}{2} \ell' \nu_k \partial_k (\lambda(\mathbf{x}) \epsilon_{ii} \epsilon_{jj}) + \ell' \nu_k \partial_k (G(\mathbf{x}) \epsilon_{ij} \epsilon_{ji}) \right] dV = \ell' \int_{\partial\Omega} \left[ \frac{1}{2} \lambda(\mathbf{x}) (\epsilon_{ii} \epsilon_{jj}) (\nu_k n_k) + G(\mathbf{x}) (\epsilon_{ij} \epsilon_{ij}) (\nu_k n_k) \right] dS, \quad (3.6)$$

where  $n_k$  is the outward unit normal to the boundary. By considering the particular case  $\nu_k \equiv n_k$ , which physically corresponds to surface-parallel micro-cracks, the surface integral becomes

$$\ell' \int_{\partial\Omega} \left[ \frac{1}{2} \lambda(\mathbf{x}) (\epsilon_{ii} \epsilon_{jj}) + G(\mathbf{x}) (\epsilon_{ij} \epsilon_{ij}) \right] dS. \quad (3.7)$$

By definition, the Cauchy stresses  $\tau_{ij}$ , couple stresses  $\mu_{kij}$ , and the total stresses  $\sigma_{ij}$ , are

$$\begin{aligned} \tau_{ij} &= \partial \mathcal{W} / \partial \epsilon_{ij} \\ \mu_{kij} &= \partial \mathcal{W} / \partial \epsilon_{ij,k} \\ \sigma_{ij} &= \tau_{ij} - \partial_k \mu_{kij}. \end{aligned} \quad (3.8)$$

Using equations (3.8) and (3.5), the constitutive equations for functionally graded materials are

$$\begin{aligned} \tau_{ij} &= \lambda(\mathbf{x}) \epsilon_{kk} \delta_{ij} + 2G(\mathbf{x}) \epsilon_{ij} + \ell' \nu_k [\epsilon_{ll} \partial_k \lambda(\mathbf{x}) + \lambda(\mathbf{x}) \partial_k \epsilon_{ll}] \delta_{ij} \\ &\quad + 2\ell' \nu_k [\epsilon_{ij} \partial_k G(\mathbf{x}) + G(\mathbf{x}) \partial_k \epsilon_{ij}] \end{aligned} \quad (3.9)$$

$$\mu_{kij} = \ell' \nu_k \lambda(\mathbf{x}) \epsilon_{ll} \delta_{ij} + \ell^2 \lambda(\mathbf{x}) \partial_k \epsilon_{ll} \delta_{ij} + 2\ell' \nu_k G(\mathbf{x}) \epsilon_{ij} + 2\ell^2 G(\mathbf{x}) \partial_k \epsilon_{ij} \quad (3.10)$$

$$\begin{aligned} \sigma_{ij} &= \lambda(\mathbf{x}) (\epsilon_{kk} - \ell^2 \nabla^2 \epsilon_{kk}) \delta_{ij} + 2G(\mathbf{x}) (\epsilon_{ij} - \ell^2 \nabla^2 \epsilon_{ij}) \\ &\quad - \ell^2 [\partial_k \lambda(\mathbf{x})] (\partial_k \epsilon_{ll}) \delta_{ij} - 2\ell^2 [\partial_k G(\mathbf{x})] (\partial_k \epsilon_{ij}) \end{aligned} \quad (3.11)$$

### 3.1.3 Some Observation

One may observe that the Lamé constants  $\lambda$  and  $G$  in equation (3.5) can be placed either before or after the differential operator  $\partial_k = \partial/\partial x_k$ , if it is the homogeneous material that the strain-energy density is corresponding to. However, if the material is nonhomogeneous, then different positions of  $\lambda$  and  $G$  in equation (3.5) would lead to different strain-energy density function. For instance, in functionally graded materials (FGMs),  $\lambda$  and  $G$  are functions of material point  $\mathbf{x} = (x, y, z)$ , *i.e.*  $\lambda \equiv \lambda(\mathbf{x})$  and  $G \equiv G(\mathbf{x})$ . Thus if one express the strain-energy density as

$$\begin{aligned} \mathcal{W}_A \equiv & \frac{1}{2} \lambda(\mathbf{x}) \epsilon_{ii} \epsilon_{jj} + G(\mathbf{x}) \epsilon_{ij} \epsilon_{ji} + \frac{1}{2} \ell^2 \partial_k [\lambda(\mathbf{x}) \epsilon_{ii}] (\partial_k \epsilon_{jj}) + \frac{1}{2} \ell' \nu_k \partial_k [\lambda(\mathbf{x}) \epsilon_{ii} \epsilon_{jj}] \\ & + \ell^2 \partial_k [G(\mathbf{x}) \epsilon_{ij}] (\partial_k \epsilon_{ji}) + \ell' \nu_k \partial_k [G(\mathbf{x}) \epsilon_{ij} \epsilon_{ji}], \end{aligned} \quad (3.12)$$

then it is clear that by the product rule of derivative,  $\mathcal{W}_A$  and  $\mathcal{W}$  are different. The other two expressions for the strain-energy density can be

$$\begin{aligned} \mathcal{W}_B \equiv & \frac{1}{2} \lambda(\mathbf{x}) \epsilon_{ii} \epsilon_{jj} + G(\mathbf{x}) \epsilon_{ij} \epsilon_{ji} + \frac{1}{2} \ell^2 \lambda(\mathbf{x}) (\partial_k \epsilon_{ii}) (\partial_k \epsilon_{jj}) + \frac{1}{2} \ell' \nu_k \lambda(\mathbf{x}) \partial_k (\epsilon_{ii} \epsilon_{jj}) \\ & + \ell^2 G(\mathbf{x}) \partial_k \epsilon_{ij} (\partial_k \epsilon_{ji}) + \ell' \nu_k G(\mathbf{x}) \partial_k (\epsilon_{ij} \epsilon_{ji}), \end{aligned} \quad (3.13)$$

and

$$\begin{aligned} \mathcal{W}_C \equiv & \frac{1}{2} \lambda(\mathbf{x}) \epsilon_{ii} \epsilon_{jj} + G(\mathbf{x}) \epsilon_{ij} \epsilon_{ji} + \frac{1}{2} \ell^2 \partial_k [\lambda(\mathbf{x}) \epsilon_{ii}] (\partial_k \epsilon_{jj}) + \frac{1}{2} \ell' \nu_k \lambda(\mathbf{x}) \partial_k (\epsilon_{ii} \epsilon_{jj}) \\ & + \ell^2 \partial_k [G(\mathbf{x}) \epsilon_{ij}] (\partial_k \epsilon_{ji}) + \ell' \nu_k G(\mathbf{x}) \partial_k (\epsilon_{ij} \epsilon_{ji}). \end{aligned} \quad (3.14)$$

In  $\mathcal{W}_B$ , both  $\lambda(\mathbf{x})$  and  $G(\mathbf{x})$  are placed before the differential operator  $\partial_k$ . In  $\mathcal{W}_C$ ,  $\lambda(\mathbf{x})$  and  $G(\mathbf{x})$  are placed after  $\partial_k$  for the volumetric ( $\ell^2$ -associated) terms, and located before  $\partial_k$  for the surface ( $\ell'$ -associated) terms.

However, not all of them are admissible. One condition for admissibility depends on if the surface terms can be reduced to a surface integral by applying the divergence theorem. Form  $\mathcal{W}_A$ , like  $\mathcal{W}$ , can be evaluated as a surface integral by using



the divergence theorem, but not for forms  $\mathcal{W}_B$  and  $\mathcal{W}_C$ . Thus in regarding to the surface energy term to be reduced to a surface integral, only the strain-energy density functions  $\mathcal{W}$  and  $\mathcal{W}_A$  are admissible. In this paper, we use expression  $\mathcal{W}$  for deriving the constitutive equations and the corresponding PDEs

## 3.2 Anti-Plane Shear

In this section we derive the governing PDE of gradient elasticity for an anti-plane shear problem in functionally graded materials from the first principle.

### 3.2.1 Constitutive Equations

In three-dimensional space, the displacement components are defined as:

$$u_x \equiv u, \quad u_y \equiv v, \quad u_z \equiv w. \quad (3.15)$$

Like equation (3.2), strains are defined as:

$$\epsilon_{ij} = \frac{1}{2} \left( \frac{\partial u_i}{\partial x_j} + \frac{\partial u_j}{\partial x_i} \right), \quad (3.16)$$

where both the indices  $i$  and  $j$  run through  $x$ ,  $y$ , and  $z$ . The strain-energy density function (for Mode III) is

$$\mathcal{W} = \frac{1}{2} \lambda \epsilon_{ii} \epsilon_{jj} + G \epsilon_{ij} \epsilon_{ji} + \ell^2 G (\partial_k \epsilon_{ij})(\partial_k \epsilon_{ji}) + \ell' \nu_k \partial_k (G \epsilon_{ij} \epsilon_{ji}). \quad (3.17)$$

We define the Cauchy stresses  $\tau_{ij}$ , the couple stresses  $\mu_{kij}$  and the total stresses  $\sigma_{ij}$  according to equations in (3.8). Thus, the constitutive equations of gradient elasticity in anti-plane problems for homogeneous materials can be directly derived as (Vardoulakis *et al.* [92], Exadaktylos *et al.* [35]):

$$\tau_{ij} = \lambda \epsilon_{kk} \delta_{ij} + 2G \epsilon_{ij} + 2G \ell' \nu_k \partial_k \epsilon_{ij} \quad (3.18)$$

$$\mu_{kij} = 2G \ell' \nu_k \epsilon_{ij} + 2G \ell^2 \partial_k \epsilon_{ij} \quad (3.19)$$

$$\sigma_{ij} = \lambda \epsilon_{kk} \delta_{ij} + 2G (\epsilon_{ij} - \ell^2 \nabla^2 \epsilon_{ij}). \quad (3.20)$$

For functionally graded materials the corresponding constitutive equations are:

$$\tau_{ij} = \lambda(\mathbf{x})\epsilon_{kk}\delta_{ij} + 2G(\mathbf{x})\epsilon_{ij} + 2\ell'\nu_k[\epsilon_{ij}\partial_k G(\mathbf{x}) + G(\mathbf{x})\partial_k\epsilon_{ij}] \quad (3.21)$$

$$\mu_{kij} = 2\ell'\nu_k G(\mathbf{x})\epsilon_{ij} + 2\ell^2 G(\mathbf{x})\partial_k\epsilon_{ij} \quad (3.22)$$

$$\sigma_{ij} = \lambda(\mathbf{x})\epsilon_{kk}\delta_{ij} + 2G(\mathbf{x})(\epsilon_{ij} - \ell^2\nabla^2\epsilon_{ij}) - 2\ell^2[\partial_k G(\mathbf{x})](\partial_k\epsilon_{ij}). \quad (3.23)$$

As it has been pointed out that in each of (3.21) and (3.23), there is an extra term compared with (3.18) and (3.20), respectively. The extra terms will disappear if there is no material gradation. Thus, for homogeneous materials, equations (3.21)-(3.23) will become same as (3.18)-(3.20).

According to the relations in (3.18)-(3.20), each component of the stress fields for the homogeneous materials can be written as (Vardoulakis *et al.* [92]):

$$\begin{aligned} \sigma_{xx} = \sigma_{yy} = \sigma_{zz} = 0, \quad \sigma_{xy} = 0 \\ \sigma_{xz} = 2G(\epsilon_{xz} - \ell^2\nabla^2\epsilon_{xz}) \neq 0 \\ \sigma_{yz} = 2G(\epsilon_{yz} - \ell^2\nabla^2\epsilon_{yz}) \neq 0 \end{aligned} \quad (3.24)$$

$$\begin{aligned} \mu_{xxz} &= 2G\ell^2\partial_x\epsilon_{xz} \\ \mu_{xyz} &= 2G\ell^2\partial_x\epsilon_{yz} \\ \mu_{yxz} &= 2G(\ell^2\partial_y\epsilon_{xz} - \ell'\epsilon_{xz}) \\ \mu_{yyz} &= 2G(\ell^2\partial_y\epsilon_{yz} - \ell'\epsilon_{yz}). \end{aligned} \quad (3.25)$$

For FGMs, from the relations in (3.21)-(3.23), each component of the stress fields is found to be

$$\begin{aligned} \sigma_{xx} &= \sigma_{yy} = \sigma_{zz} = 0, \quad \sigma_{xy} = 0 \\ \sigma_{xz} &= 2G(x, y)(\epsilon_{xz} - \ell^2\nabla^2\epsilon_{xz}) \\ &\quad - 2\ell^2\{[\partial_x G(x, y)](\partial_x\epsilon_{xz}) + [\partial_y G(x, y)](\partial_y\epsilon_{xz})\} \neq 0 \\ \sigma_{yz} &= 2G(x, y)(\epsilon_{yz} - \ell^2\nabla^2\epsilon_{yz}) \\ &\quad - 2\ell^2\{[\partial_x G(x, y)](\partial_x\epsilon_{yz}) + [\partial_y G(x, y)](\partial_y\epsilon_{yz})\} \neq 0 \end{aligned} \quad (3.26)$$

$$\begin{aligned}
 \mu_{xxz} &= 2G(x, y)\ell^2\partial_x\epsilon_{xz} \\
 \mu_{xyz} &= 2G(x, y)\ell^2\partial_x\epsilon_{yz} \\
 \mu_{yxx} &= 2G(x, y)(\ell^2\partial_y\epsilon_{xz} - \ell'\epsilon_{xz}) \\
 \mu_{yyz} &= 2G(x, y)(\ell^2\partial_y\epsilon_{yz} - \ell'\epsilon_{yz}).
 \end{aligned} \tag{3.27}$$

Again, comparing equations (3.24)-(3.25) and (3.26)-(3.27), one notices that there are extra terms in the total stresses  $\sigma_{ij}$  of (3.26) due to the interaction of material gradation and the nonlocal effect of strain gradient. Because of the equilibrium equation only involves  $\sigma_{ij}$  (see equation (3.30)), the extra terms will ravel the governing PDE(s) a bit more. The couple stresses  $\mu_{kij}$  in (3.25) and (3.27) assume the same form, except that  $G$  in (3.27) is not a constant, but a function reflecting the gradation of the material.

### 3.2.2 Governing PDE

For an anti-plane problem, the following relations hold:

$$u = 0, \quad v = 0, \quad w = w(x, y). \tag{3.28}$$

The non-trivial strains are:

$$\epsilon_{xz} = \frac{1}{2}\frac{\partial w}{\partial x}, \quad \epsilon_{yz} = \frac{1}{2}\frac{\partial w}{\partial y}. \tag{3.29}$$

By imposing the equilibrium equation

$$\frac{\partial\sigma_{xz}}{\partial x} + \frac{\partial\sigma_{yz}}{\partial y} = 0 \tag{3.30}$$

with the expressions  $\sigma_{xz}$  and  $\sigma_{yz}$  in (3.26), one obtains the the following PDE

$$\begin{aligned}
 &\nabla G(x, y) \cdot (1 - \ell^2\nabla^2) \nabla w + G(x, y) (1 - \ell^2\nabla^2) \nabla^2 w \\
 &- \ell^2 \left[ \nabla \frac{\partial G(x, y)}{\partial x} \cdot \nabla \frac{\partial w}{\partial x} + \nabla \frac{\partial G(x, y)}{\partial y} \cdot \nabla \frac{\partial w}{\partial y} + \nabla G(x, y) \cdot \nabla \nabla^2 w \right], \tag{3.31}
 \end{aligned}$$

where  $\nabla$  is the gradient operator,  $\nabla^2$  denotes the Laplacian operator, the dot  $\cdot$  gives the scalar (or inner) product of two vectors. One can write (3.31) in a more elaborative form

$$\begin{aligned} & \frac{\partial}{\partial x} \left[ G(x, y) \left( \frac{\partial w}{\partial x} - \ell^2 \nabla^2 \frac{\partial w}{\partial x} \right) \right] + \frac{\partial}{\partial y} \left[ G(x, y) \left( \frac{\partial w}{\partial y} - \ell^2 \nabla^2 \frac{\partial w}{\partial y} \right) \right] \\ & - \ell^2 \left[ \frac{\partial G(x, y)}{\partial x} \frac{\partial^3 w}{\partial x^3} + \frac{\partial G(x, y)}{\partial y} \frac{\partial^3 w}{\partial y^3} + \frac{\partial G(x, y)}{\partial x} \frac{\partial^3 w}{\partial x \partial y^2} + \frac{\partial G(x, y)}{\partial y} \frac{\partial^3 w}{\partial x^2 \partial y} + \right. \\ & \left. \frac{\partial^2 G(x, y)}{\partial x^2} \frac{\partial^2 w}{\partial x^2} + 2 \frac{\partial^2 G(x, y)}{\partial x \partial y} \frac{\partial^2 w}{\partial x \partial y} + \frac{\partial^2 G(x, y)}{\partial y^2} \frac{\partial^2 w}{\partial y^2} \right] = 0. \end{aligned} \quad (3.32)$$

If the shear modulus  $G$  is a function of  $y$  only and takes the exponential form

$$G \equiv G(y) = G_0 e^{\gamma y}, \quad (3.33)$$

then PDE (3.32) becomes

$$-\ell^2 \nabla^4 w - \gamma \ell^2 \frac{\partial}{\partial y} \left( 2 \nabla^2 w + \gamma \frac{\partial w}{\partial y} \right) + \nabla^2 w + \gamma \frac{\partial w}{\partial y} = 0, \quad (3.34)$$

or

$$\left( 1 - \gamma \ell^2 \frac{\partial}{\partial y} - \ell^2 \nabla^2 \right) \left( \nabla^2 + \gamma \frac{\partial}{\partial y} \right) w = 0. \quad (3.35)$$

Paulino (2001) *et al.* [72] has studied the PDE (3.35) in detail. Similarly, in a more general case, if  $G$  is an exponential function of both  $x$  and  $y$

$$G \equiv G(x, y) = G_0 e^{\beta x + \gamma y}, \quad (3.36)$$

then the governing PDE is

$$\left( 1 - \beta \ell^2 \frac{\partial}{\partial x} - \gamma \ell^2 \frac{\partial}{\partial y} - \ell^2 \nabla^2 \right) \left( \nabla^2 + \beta \frac{\partial}{\partial x} + \gamma \frac{\partial}{\partial y} \right) w = 0. \quad (3.37)$$

In Table 1 we list the governing PDEs in antiplane shear problems that correspond to the different combinations of parameter  $\ell$  and various material gradation of the shear modulus  $G$ .

Table 3.1: Governing PDEs in antiplane shear problems.

| Cases  | Governing PDE   | References   |
|--|---|--|
| $\ell = 0, G$ is a constant.                     | Laplace equation:<br>$\nabla^2 w = 0$   | Standard textbooks.<br>[84, 85, 86]  |
| $\ell = 0, G \equiv G(y) = G_0 e^{\gamma y}$     | Perturbed Laplace equation:<br>$(\nabla^2 + \gamma \frac{\partial}{\partial y}) w = 0$  | Erdogan and Ozturk [30].   |
| $\ell = 0, G \equiv G(x) = G_0 e^{\beta x}$      | Perturbed Laplace equation:<br>$(\nabla^2 + \beta \frac{\partial}{\partial x}) w = 0$   | Erdogan [25].<br>Chan <i>et al.</i> [14] and<br>Chapter 2 of<br>the present thesis.            |
| $\ell \neq 0, G$ is a constant.                  | Helmholtz-Laplace equation:<br>$(1 - \ell^2 \nabla^2) \nabla^2 w = 0$   | Fannjiang <i>et al.</i> [36].<br>Vardoulakis <i>et al.</i> [92].<br>Zhang <i>et al.</i> [100]. |
| $\ell \neq 0, G \equiv G(y) = G_0 e^{\gamma y}$  | Equation (3.35):<br>$(1 - \gamma \ell^2 \frac{\partial}{\partial y} - \ell^2 \nabla^2) (\nabla^2 + \gamma \frac{\partial}{\partial y}) w = 0$ | Paulino <i>et al.</i> [72] and<br>Chapter 2 of<br>the present thesis.                          |
| $\ell \neq 0, G \equiv G(x) = G_0 e^{\beta x}$   | $(1 - \beta \ell^2 \frac{\partial}{\partial x} - \ell^2 \nabla^2) (\nabla^2 + \beta \frac{\partial}{\partial x}) w = 0$                       | Chapter 10 of<br>the present thesis.   |
| $\ell \neq 0, \text{ general } G \equiv G(x, y)$ | Eqn. (3.32) or Eqn. (3.31)  | Not available.   |

### 3.3 General State of Stresses

In this section we derive the governing (system of) PDEs of gradient elasticity for a plane problem in functionally graded materials from the strain-energy density function. The process is similar to the one for anti-plane shear case, however, the algebra is more involved.

### 3.3.1 Constitutive Equations

We repeat the strain-energy density function as described in equation (3.5) here:

$$W = \frac{1}{2}\lambda \epsilon_{ii} \epsilon_{jj} + G \epsilon_{ij} \epsilon_{ji} + \frac{1}{2}\lambda \ell^2 (\partial_k \epsilon_{ii})(\partial_k \epsilon_{jj}) + \frac{1}{2}\ell' \nu_k \partial_k (\lambda \epsilon_{ii} \epsilon_{jj}) \\ + G \ell^2 (\partial_k \epsilon_{ij})(\partial_k \epsilon_{ji}) + \ell' \nu_k \partial_k (G \epsilon_{ij} \epsilon_{ji}), \quad \ell, \ell' \geq 0.$$

By the definition of  $\tau_{ij}$ ,  $\mu_{kij}$ , and  $\sigma_{ij}$  in equation (3.8), we have already obtained the (general plane) constitutive equations of gradient elasticity for FGMs in equations (3.9)-(3.11). For homogeneous materials, the constitutive equations are (Exadaktylos [34], Exadaktylos *et. al.* [35]):

$$\tau_{ij} = \lambda \epsilon_{kk} \delta_{ij} + 2G \epsilon_{ij} + \ell' \nu_k \partial_k (\lambda \epsilon_{ii} \delta_{ij} + 2G \epsilon_{ij}) \quad (3.38)$$

$$\mu_{kij} = \lambda \ell^2 \partial_k \epsilon_{ii} \delta_{ij} + 2G \ell' \nu_k \epsilon_{ij} + \lambda \ell' \nu_k \epsilon_{ii} \delta_{ij} + 2G \ell^2 \partial_k \epsilon_{ij} \quad (3.39)$$

$$\sigma_{ij} = \lambda \epsilon_{kk} \delta_{ij} + 2G \epsilon_{ij} - \ell^2 \nabla^2 (\lambda \epsilon_{kk} \delta_{ij} + 2G \epsilon_{ij}). \quad (3.40)$$

Comparing equations (3.9)-(3.11) with (3.38)-(3.40), one notices that the couple stresses  $\mu_{kij}$  in (3.10) and (3.39) take the same form. However, for the total stresses  $\sigma_{ij}$ , there are more terms in (3.11) than in (3.40), and those extra terms will confound the form of the governing (system of) PDEs.

For a 2-dimensional plane problem the components of the strain tensor are given by:

$$\epsilon_{xx} = \frac{\partial u}{\partial x}, \quad \epsilon_{yy} = \frac{\partial v}{\partial y}, \quad \epsilon_{xy} = \frac{1}{2} \left( \frac{\partial u}{\partial y} + \frac{\partial v}{\partial x} \right), \quad \epsilon_{xz} = \epsilon_{yz} = \epsilon_{zx} = 0. \quad (3.41)$$

### 3.3.2 Governing System of PDEs

By imposing the equilibrium equations

$$\frac{\partial \sigma_{xx}}{\partial x} + \frac{\partial \sigma_{xy}}{\partial y} = 0 \quad \text{and} \quad \frac{\partial \sigma_{xy}}{\partial x} + \frac{\partial \sigma_{yy}}{\partial y} = 0, \quad (3.42)$$

and using equations (3.16) and (12.5), one can obtain the following system of PDEs in a compact form:

$$\begin{aligned}
 & G(x, y) \nabla^2 (1 - \ell^2 \nabla^2) \mathbf{u} + [\lambda(x, y) + G(x, y)] \nabla (1 - \ell^2 \nabla^2) \nabla \cdot \mathbf{u} \\
 & + [(1 - \ell^2 \nabla^2) (\nabla \mathbf{u} + \nabla \mathbf{u}^T)] \nabla G(x, y) + [(1 - \ell^2 \nabla^2) \nabla \cdot \mathbf{u}] \nabla \lambda(x, y) \quad (3.43) \\
 & - \ell^2 \left\{ \left( \nabla \frac{\partial}{\partial x} \mathbf{u} \right) \nabla \frac{\partial G(x, y)}{\partial x} + \left( \nabla \frac{\partial}{\partial y} \mathbf{u} \right) \nabla \frac{\partial G(x, y)}{\partial y} - \nabla [\nabla \lambda(x, y) \cdot \nabla \nabla \cdot \mathbf{u}] \right\} \\
 & - \ell^2 \left\{ \frac{\partial}{\partial x} [(\nabla \nabla u) \nabla G(x, y)] + \frac{\partial}{\partial y} [(\nabla \nabla v) \nabla G(x, y)] + (\nabla \nabla^2 \mathbf{u}) \nabla G(x, y) \right\} = 0,
 \end{aligned}$$

where the boldface  $\mathbf{u}$  denotes the displacement vector  $(u, v)$ ,  $\nabla \cdot$  is the divergence operator. If the moduli vary as a function of  $(x, y)$  and assume the exponential form

$$G \equiv G(x, y) = G_0 e^{\beta x + \gamma y}; \quad \lambda \equiv \lambda(x, y) = \frac{3 - \kappa}{\kappa - 1} G(x, y), \quad (3.44)$$

then the system of PDEs is

$$\begin{aligned}
 & \left( 1 - \beta \ell^2 \frac{\partial}{\partial x} - \gamma \ell^2 \frac{\partial}{\partial y} - \ell^2 \nabla^2 \right) \left[ (\kappa + 1) \frac{\partial^2 u}{\partial x^2} + (\kappa - 1) \frac{\partial^2 u}{\partial y^2} + 2 \frac{\partial^2 v}{\partial x \partial y} + \right. \\
 & \left. \beta (\kappa + 1) \frac{\partial u}{\partial x} + \gamma (\kappa - 1) \frac{\partial u}{\partial y} + \gamma (\kappa - 1) \frac{\partial v}{\partial x} + \beta (3 - \kappa) \frac{\partial v}{\partial y} \right] = 0, \quad (3.45)
 \end{aligned}$$

$$\begin{aligned}
 & \left( 1 - \beta \ell^2 \frac{\partial}{\partial x} - \gamma \ell^2 \frac{\partial}{\partial y} - \ell^2 \nabla^2 \right) \left[ (\kappa - 1) \frac{\partial^2 v}{\partial x^2} + (\kappa + 1) \frac{\partial^2 v}{\partial y^2} + 2 \frac{\partial^2 u}{\partial x \partial y} + \right. \\
 & \left. \gamma (3 - \kappa) \frac{\partial u}{\partial x} + \beta (\kappa - 1) \frac{\partial u}{\partial y} + \beta (\kappa - 1) \frac{\partial v}{\partial x} + \gamma (\kappa + 1) \frac{\partial v}{\partial y} \right] = 0, \quad (3.46)
 \end{aligned}$$

where  $\kappa = 3 - 4\nu$  if plane strain is considered;  $\kappa = (3 - \nu)/(1 + \nu)$  if it is a plane stress problem. If  $G$  and  $\lambda$  are constants, then the homogeneous material case is recovered, and the system of PDEs (3.43) is reduced to

$$(1 - \ell^2 \nabla^2) [G \nabla^2 \mathbf{u} + (\lambda + G) \nabla \nabla \cdot \mathbf{u}] = 0, \quad (3.47)$$

which has been studied by Exadaktylos [34].

### 3.3.3 A Point View of Perturbation

In the conventional classical linear elasticity (*i.e.*  $\ell \rightarrow 0$ ), the system of PDEs (3.43) becomes

$$\begin{aligned} G(x, y) \nabla^2 \mathbf{u} + [\lambda(x, y) + G(x, y)] \nabla \nabla \cdot \mathbf{u} + \\ (\nabla \mathbf{u} + \nabla \mathbf{u}^T) \nabla G(x, y) + (\nabla \cdot \mathbf{u}) \nabla \lambda(x, y) = 0. \end{aligned} \quad (3.48)$$

If  $G$  and  $\lambda$  take the form in (3.44), then (3.48) can be expressed as

$$\begin{aligned} (\kappa + 1) \frac{\partial^2 u}{\partial x^2} + (\kappa - 1) \frac{\partial^2 u}{\partial y^2} + 2 \frac{\partial^2 v}{\partial x \partial y} + \\ \beta(\kappa + 1) \frac{\partial u}{\partial x} + \gamma(\kappa - 1) \frac{\partial u}{\partial y} + \gamma(\kappa - 1) \frac{\partial v}{\partial x} + \beta(3 - \kappa) \frac{\partial v}{\partial y} = 0 \end{aligned} \quad (3.49)$$

$$\begin{aligned} (\kappa - 1) \frac{\partial^2 v}{\partial x^2} + (\kappa + 1) \frac{\partial^2 v}{\partial y^2} + 2 \frac{\partial^2 u}{\partial x \partial y} + \\ \gamma(3 - \kappa) \frac{\partial u}{\partial x} + \beta(\kappa - 1) \frac{\partial u}{\partial y} + \beta(\kappa - 1) \frac{\partial v}{\partial x} + \gamma(\kappa + 1) \frac{\partial v}{\partial y} = 0 \end{aligned} \quad (3.50)$$

that has been studied by Konda and Erdogan [51]. For the homogeneous materials, (3.49) and (3.50) can be further simplified to

$$G \nabla^2 \mathbf{u} + (\lambda + G) \nabla \nabla \cdot \mathbf{u} = 0,$$

which is the familiar Navier's equations for the elastic medium.

## 3.4 A Concluding Remark

In the conventional classical linear elasticity, one may derive the governing PDE(s) for FGMs by directly replacing the Lamé constants with the material gradation functions at the level of the constitutive equations. We have shown that this is not true in the case of strain gradient elasticity because of some extra terms may arise in addition to the original constitutive equations that establish the homogeneous materials. These



extra terms come from that the material gradation interplays with the nonlocal effect of the strain gradient. Thus, the constitutive equations for FGMs are different from the ones for homogeneous materials under the consideration of strain gradient elasticity theory (Casal's continuum). The correct and proper way for deriving the governing PDE(s) for FGMs is by using the strain energy density function and the corresponding definitions of the stress fields, which we have presented in this chapter.

## Chapter 4

# Hypersingular Integral Equations for Mode III Fracture in Functionally Graded Materials with Strain-Gradient Effect (Crack Perpendicular to the Material Gradation)

In Chapter 2 we have laid out the method of singular integral equation in classical LEFM, and we have seen that higher singularity may arise by choosing different unknown density function. Another source for hypersingular integral equations to appear is attributing to the underlying continuum theory. For instance, the higher order continuum theory with the strain-gradient effect [35, 37, 92] leads to the formulation of hypersingular integral equations naturally, and it will be exhibited in present

present chapter (see also References [11, 36, 76]) by solving a mode III crack problem in FGMs with strain-gradient effect. Here we choose the geometry that the crack is perpendicular to the material gradation; in Chapter 10 we will deal with the geometry that the crack is parallel to the material gradation.

## 4.1 Constitutive Equations of Gradient Elasticity

In Chapter 3 we have addressed the notations, strain energy density function, constitutive equations, and the governing PDEs. For the sake of clarity, in this section we list the constitutive equations of gradient elasticity for an anti-plane shear crack in FGMs with the shear modulus  $G$  is a function of  $y$ , *i.e.* crack is perpendicular to the material gradation. The constitutive equations of gradient elasticity are:

$$\sigma_{ij} = \lambda(y)\epsilon_{kk}\delta_{ij} + 2G(y)(\epsilon_{ij} - \ell^2\nabla^2\epsilon_{ij}) - 2\ell^2[\partial_k G(y)](\partial_k\epsilon_{ij}) \quad (4.1)$$

$$\tau_{ij} = \lambda(y)\epsilon_{kk}\delta_{ij} + 2G(y)\epsilon_{ij} + 2\ell'\nu_k[\epsilon_{ij}\partial_k G(y) + G(y)\partial_k\epsilon_{ij}] \quad (4.2)$$

$$\mu_{kij} = 2\ell'\nu_k G(y)\epsilon_{ij} + 2\ell^2 G(y)\partial_k\epsilon_{ij}. \quad (4.3)$$

More specifically, each component of the stress fields can be written as following:

$$\begin{aligned} \sigma_{xx} &= \sigma_{yy} = \sigma_{zz} = 0, \quad \sigma_{xy} = 0 \\ \sigma_{xz} &= 2G(y)(\epsilon_{xz} - \ell^2\nabla^2\epsilon_{xz}) - 2\ell^2[\partial_y G(y)](\partial_y\epsilon_{xz}) \neq 0 \\ \sigma_{yz} &= 2G(y)(\epsilon_{yz} - \ell^2\nabla^2\epsilon_{yz}) - 2\ell^2[\partial_y G(y)](\partial_y\epsilon_{yz}) \neq 0 \\ \mu_{xxz} &= 2G(y)\ell^2\partial_x\epsilon_{xz} \\ \mu_{xyz} &= 2G(y)\ell^2\partial_x\epsilon_{yz} \\ \mu_{yxz} &= 2G(y)(\ell^2\partial_y\epsilon_{xz} - \ell'\epsilon_{xz}) \\ \mu_{yyz} &= 2G(y)(\ell^2\partial_y\epsilon_{yz} - \ell'\epsilon_{yz}). \end{aligned} \quad (4.4)$$

Notice that there is an extra term [13] in each of  $\sigma_{xz}$  and  $\sigma_{yz}$  compared with the case of homogeneous materials (see Vardoulakis *et al.* 1996 [95], page 4534).

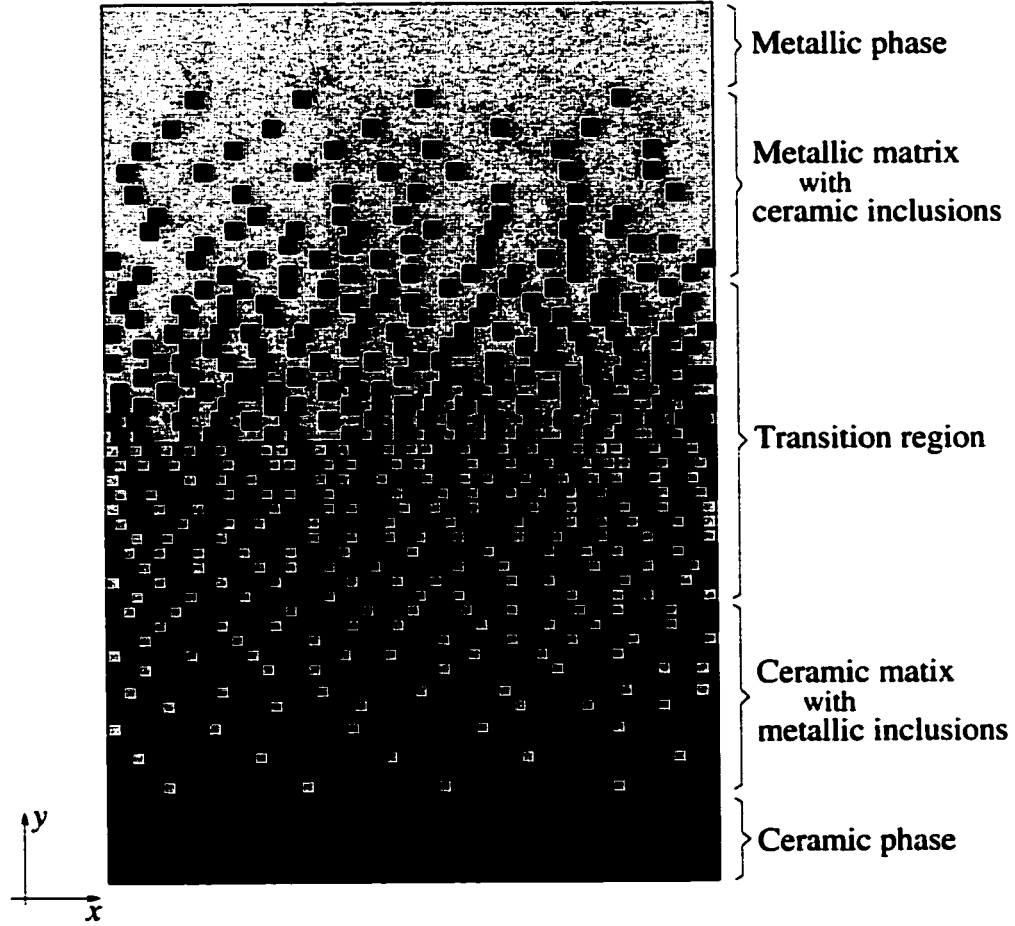


Figure 4.1: FGM with continuously graded microstructure.

## 4.2 Governing Partial Differential Equation

By imposing the only non-trivial equilibrium equation

$$\frac{\partial \sigma_{xz}}{\partial x} + \frac{\partial \sigma_{yz}}{\partial y} = 0, \quad (4.5)$$

and assuming that shear modulus  $G$  is an exponential function of  $y$

$$G \equiv G(y) = G_0 e^{\gamma y}, \quad (4.6)$$

the following PDE is obtained:

$$-\ell^2 \nabla^4 w - 2\gamma \ell^2 \nabla^2 \frac{\partial w}{\partial y} + \nabla^2 w - \gamma^2 \ell^2 \frac{\partial^2 w}{\partial y^2} + \gamma \frac{\partial w}{\partial y} = 0; \quad (4.7)$$

or in a factorized form

$$\left(1 - \gamma \ell^2 \frac{\partial}{\partial y} - \ell^2 \nabla^2\right) \left(\nabla^2 + \gamma \frac{\partial}{\partial y}\right) w = 0. \quad (4.8)$$

In terms of the differential operator notation, (4.8) can be written in the form as

$$\mathbf{H}_\gamma \mathbf{L}_\gamma w = 0; \quad \mathbf{H}_\gamma = 1 - \gamma \ell^2 \frac{\partial}{\partial y} - \ell^2 \nabla^2, \quad \mathbf{L}_\gamma = \nabla^2 + \gamma \frac{\partial}{\partial y}, \quad (4.9)$$

where  $\mathbf{H}_\gamma$  is the perturbed Helmholtz operator,  $\mathbf{L}_\gamma$  is the perturbed Laplacian operator, and the two operators commute, *i.e.*  $\mathbf{H}_\gamma \mathbf{L}_\gamma = \mathbf{L}_\gamma \mathbf{H}_\gamma$ . Thus, PDE (4.8) can be considered as a double perturbation of the composition of the harmonic and Helmholtz's equations

$$(1 - \ell^2 \nabla^2) \nabla^2 w = 0, \quad (4.10)$$

that is, one perturbation is to the Helmholtz operator  $(1 - \ell^2 \nabla^2)$ , the other perturbation happens to the Laplacian operator  $\nabla^2$ . Both the Helmholtz and the Laplacian operators are invariant under the rigid-body motions. FGMs bring in the perturbation and destroy the invariance. By setting  $\gamma \rightarrow 0$  in (4.8), one gets (4.10), the PDE for gradient elasticity.

Another viewpoint of the perturbation is focused on the role of the characteristic length  $\ell$ . By taking  $\ell \rightarrow 0$ , we obtain a lower order of PDE

$$\left(\nabla^2 + \gamma \frac{\partial}{\partial y}\right) w = 0,$$

the perturbed harmonic equation. However, because the corresponding term to the coefficient  $\ell^2$  affects the highest differential in the governing PDE (4.7), a singular perturbation is expected as the limit  $\ell \rightarrow 0$  is considered. By taking both  $\gamma \rightarrow 0$  and  $\ell \rightarrow 0$ , we obtain the harmonic equation for classical elasticity. Various combination of parameters  $\ell$  and  $\gamma$  with the corresponding governing PDE are listed in Table 3.1.

### 4.3 Boundary Conditions

Figure 2.2 shows the geometry of the mode III crack problem in which an FGM, with shear modulus  $G(y) = G_0 e^{\gamma y}$ , bonded to a half space is considered. Thus the problem reduces to the upper half plane, and  $y = 0$  is treated as the boundary. By the principle of virtual work, the following mixed boundary conditions can be derived:

$$\begin{cases} \sigma_{yz}(x, 0) = p(x) , & |x| < a \\ w(x, 0) = 0 , & |x| > a \\ \mu_{yyz}(x, 0) = 0 , & -\infty < x < +\infty , \end{cases} \quad (4.11)$$

which are adopted in this paper. One may observe that the first two boundary conditions (BCs) in (4.11) are from classical elasticity, e.g. linear elastic fracture mechanics (LEFM). The last BC regarding the couple-stress  $\mu_{yyz}$  is needed as the higher order theory is considered.

### 4.4 Fourier Transform

After taking Fourier transform (see (2.6) and (2.7)) to equation (4.7), one obtains

$$\begin{aligned} -\ell^2 \nabla^4 w &= -\ell^2 \left( \frac{\partial^4 w(x, y)}{\partial x^4} + 2 \frac{\partial^4 w(x, y)}{\partial x^2 \partial y^2} + \frac{\partial^4 w(x, y)}{\partial y^4} \right) \\ &= \frac{-\ell^2}{\sqrt{2\pi}} \int_{-\infty}^{\infty} \left( \xi^4 W(\xi, y) - 2\xi^2 \frac{\partial^2 W}{\partial y^2} + \frac{\partial^4 W}{\partial y^4} \right) e^{-ix\xi} d\xi \end{aligned} \quad (4.12)$$

$$\begin{aligned} -\gamma \ell^2 \nabla^2 \frac{\partial w}{\partial y} &= -\gamma \ell^2 \left( \frac{\partial^3 w(x, y)}{\partial x^2 \partial y} + \frac{\partial^3 w(x, y)}{\partial y^3} \right) \\ &= \frac{-\gamma \ell^2}{\sqrt{2\pi}} \int_{-\infty}^{\infty} \left( -\xi^2 \frac{\partial W(\xi, y)}{\partial y} + \frac{\partial^3 W}{\partial y^3} \right) e^{-ix\xi} d\xi \end{aligned} \quad (4.13)$$

$$\begin{aligned} \nabla^2 w &= \frac{\partial^2 w(x, y)}{\partial x^2} + \frac{\partial^2 w(x, y)}{\partial y^2} \\ &= \frac{1}{\sqrt{2\pi}} \int_{-\infty}^{\infty} \left( -\xi^2 W(\xi, y) + \frac{\partial^2 W}{\partial y^2} \right) e^{-ix\xi} d\xi \end{aligned} \quad (4.14)$$

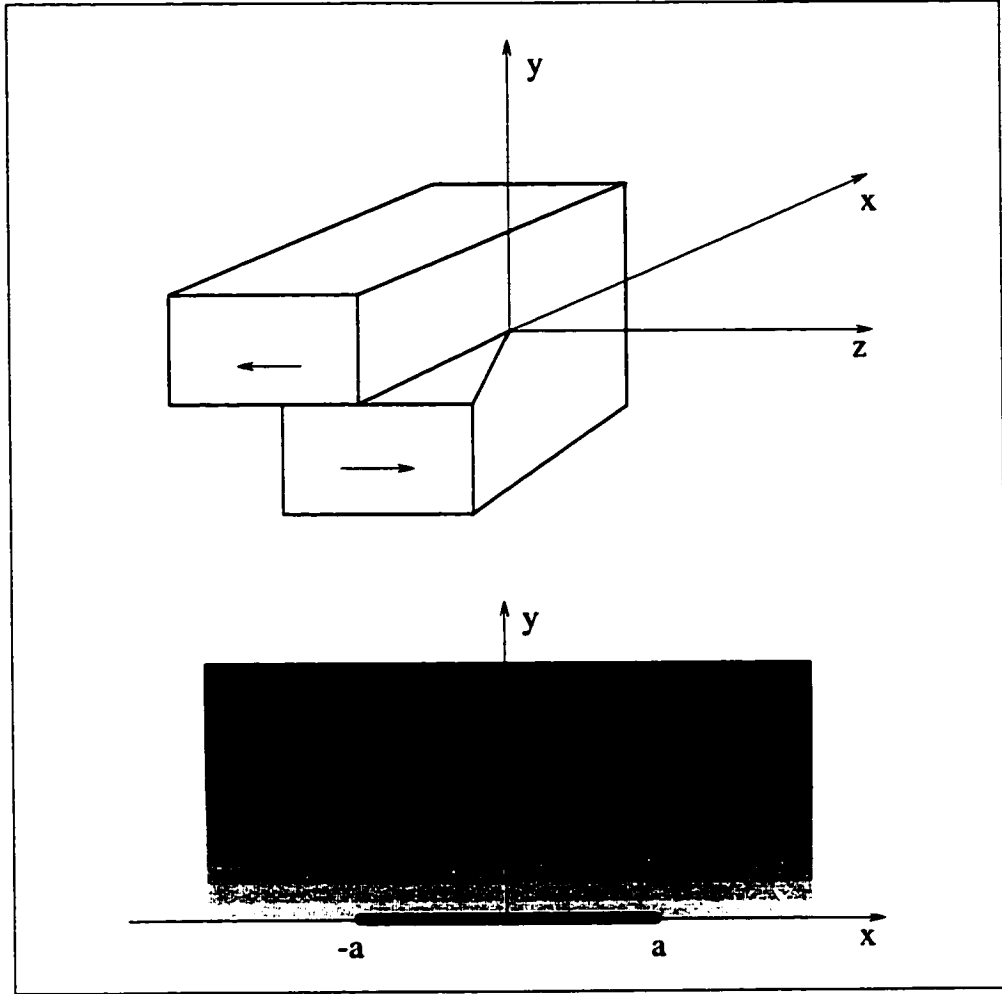


Figure 4.2: Geometry for the mode III crack problem

$$-\gamma^2 \ell^2 \frac{\partial^2 w(x, y)}{\partial y^2} = -\frac{\gamma^2 \ell^2}{\sqrt{2\pi}} \int_{-\infty}^{\infty} \frac{\partial^2 W(\xi, y)}{\partial y^2} e^{-ix\xi} d\xi \quad (4.15)$$

$$\gamma \frac{\partial w(x, y)}{\partial y} = \frac{\gamma}{\sqrt{2\pi}} \int_{-\infty}^{\infty} \frac{\partial W(\xi, y)}{\partial y} e^{-ix\xi} d\xi \quad (4.16)$$

Equations (4.12) to (4.16) are added (according to equation (4.7)), and after simplification, the governing ODE is obtained:

$$\left[ \ell^2 \frac{d^4}{dy^4} + 2\gamma \ell^2 \frac{d^3}{dy^3} - (2\ell^2 \xi^2 + \gamma^2 \ell^2 + 1) \frac{d^2}{dy^2} - \gamma (1 + 2\ell^2 \xi^2) \frac{d}{dy} + (\ell^2 \xi^4 + \xi^2) \right] W = 0. \quad (4.17)$$

The corresponding characteristic equation to the ODE (4.17) is

$$\ell^2 \lambda^4 + 2\gamma \ell^2 \lambda^3 - (2\ell^2 \xi^2 + \gamma^2 \ell^2 + 1) \lambda^2 - \gamma (1 + 2\ell^2 \xi^2) \lambda + (\ell^2 \xi^4 + \xi^2) = 0, \quad (4.18)$$

which can be further factored as

$$[\ell^2 \lambda^2 + \gamma \ell^2 \lambda - (1 + \ell^2 \xi^2)] (\lambda^2 + \gamma \lambda - \xi^2) = 0. \quad (4.19)$$

Clearly the four roots  $\lambda_i$  ( $i = 1, 2, 3, 4$ ) of the polynomial (4.19) above can be obtained as:

$$\lambda_1 = \frac{-\gamma}{2} - \frac{\sqrt{\gamma^2 + 4\xi^2}}{2}, \quad \lambda_2 = \frac{-\gamma}{2} + \frac{\sqrt{\gamma^2 + 4\xi^2}}{2}, \quad (4.20)$$

$$\lambda_3 = \frac{-\gamma}{2} - \sqrt{\xi^2 + \gamma^2/4 + 1/\ell^2}, \quad \lambda_4 = \frac{-\gamma}{2} + \sqrt{\xi^2 + \gamma^2/4 + 1/\ell^2}, \quad (4.21)$$

where we let  $\lambda_1 < 0$  and  $\lambda_3 < 0$ . As  $\gamma \rightarrow 0$ , we recover the roots found by Vardoulakis *et al.* [92] and Fannjiang *et al.* [36]. The roots  $\lambda_1$  and  $\lambda_2$  correspond to the solution of the perturbed harmonic equation, and the roots  $\lambda_3$  and  $\lambda_4$  match with the solution of the Helmholtz's equation. Various choices of parameters  $\ell$  and  $\gamma$  with their corresponding mechanics theories and materials are listed in Table 4.1.

By taking account of the far-field boundary condition

$$w(x, y) \rightarrow 0 \quad \text{as} \quad \sqrt{x^2 + y^2} \rightarrow +\infty, \quad (4.22)$$

and with  $y > 0$  (the upper half plane), one obtains that

$$W(\xi, y) = A(\xi)e^{\lambda_1 y} + B(\xi)e^{\lambda_3 y}. \quad (4.23)$$

Accordingly, the displacement  $w(x, y)$  takes the form

$$w(x, y) = \frac{1}{\sqrt{2\pi}} \int_{-\infty}^{\infty} [A(\xi)e^{\lambda_1 y} + B(\xi)e^{\lambda_3 y}] e^{-ix\xi} d\xi. \quad (4.24)$$

Both  $A(\xi)$  and  $B(\xi)$  are determined by the boundary conditions.



Table 4.1: Roots  $\lambda_i$  together with corresponding mechanics theory and type of material.

| Cases                        | Number of roots | Roots  | Mechanics theory and type of material       | References   |
|------------------------------|-----------------|--|---|--|
| $\ell = 0, \gamma = 0$       | 2               | $\pm \xi $   | Classical LEFM, homogeneous materials       | Standard textbooks.  |
| $\ell = 0, \gamma \neq 0$    | 2               | $-\gamma/2 \pm \sqrt{\gamma^2/4 + \xi^2}$  | Classical LEFM, nonhomogeneous materials    | Erdogan and Ozturk [30].   |
| $\ell \neq 0, \gamma = 0$    | 4               | $\pm \xi , \pm\sqrt{\xi^2 + 1/\ell^2}$   | Gradient theories, homogeneous materials    | Vardoulakis <i>et al.</i> [92].<br>Fannjiang <i>et al.</i> [36]. |
| $\ell \neq 0, \gamma \neq 0$ | 4               | $-\gamma/2 \pm \sqrt{\gamma^2/4 + \xi^2},$<br>$-\gamma/2 \pm \sqrt{\xi^2 + \gamma^2/4 + 1/\ell^2}$ | Gradient theories, nonhomogeneous materials | Studied in this chapter.   |

## 4.5 Hypersingular Integrodifferential Equation

By taking account of the symmetry along the  $x$ -axis, we may consider that  $w(x, y)$  takes the following general solution form (for the upper half plane):

$$\begin{aligned}
 w(x, y) &= \frac{1}{\sqrt{2\pi}} \int_{-\infty}^{\infty} [A(\xi)e^{\lambda_1 y} + B(\xi)e^{\lambda_3 y}] e^{-ix\xi} d\xi, \quad y \geq 0 \\
 &= \frac{1}{\sqrt{2\pi}} \int_{-\infty}^{\infty} \left[ A(\xi)e^{-(\gamma + \sqrt{\gamma^2 + 4\xi^2})y/2} \right. \\
 &\quad \left. + B(\xi)e^{-(\gamma + \sqrt{4\xi^2 + \gamma^2 + 4/\ell^2})y/2} \right] e^{-ix\xi} d\xi, \quad y \geq 0, \quad (4.25)
 \end{aligned}$$

where  $A(\xi)$  and  $B(\xi)$  need to be determined from the boundary conditions (4.11). As equation (4.25) provides the form of the solution for  $w(x, y)$ , it can be substituted in equation (4.4) such that

$$\begin{aligned}
 \sigma_{yz}(x, y) &= 2G(y) (\epsilon_{yz} - \ell^2 \nabla^2 \epsilon_{yz}) - 2\ell^2 [\partial_y G(y)] (\partial_y \epsilon_{yz}) \\
 &= \frac{G(y)}{\sqrt{2\pi}} \int_{-\infty}^{\infty} \lambda_1(\gamma, \xi) A(\xi) e^{-(\gamma + \sqrt{\gamma^2 + 4\xi^2})y/2 - ix\xi} d\xi, \quad y \geq 0. \quad (4.26)
 \end{aligned}$$

Notice that term associated with  $B(\xi)$  has been dropped out from  $\sigma_{yz}(x, y)$ . Moreover,

$$\begin{aligned}
 \mu_{yz}(x, y) &= 2G(y) \left( \ell^2 \frac{\partial \epsilon_{yz}}{\partial y} - \ell' \epsilon_{yz} \right), \quad y \geq 0, \\
 &= \frac{G(y)}{\sqrt{2\pi}} \int_{-\infty}^{\infty} \{ (\ell^2 \lambda_1^2 - \ell' \lambda_1) A(\xi) e^{\lambda_1 y} + (\ell^2 \lambda_3^2 - \ell' \lambda_3) B(\xi) e^{\lambda_3 y} \} e^{-ix\xi} d\xi \\
 &= \frac{G(y)}{\sqrt{2\pi}} \int_{-\infty}^{\infty} \left\{ c_A(\gamma, \xi) A(\xi) e^{-(\gamma + \sqrt{\gamma^2 + 4\xi^2})y/2} \right. \\
 &\quad \left. + c_B(\gamma, \xi) B(\xi) e^{-(\gamma + \sqrt{4\xi^2 + \gamma^2 + 4/\ell^2})y/2} \right\} e^{-ix\xi} d\xi, \quad (4.27)
 \end{aligned}$$

where

$$\begin{aligned}
 c_A(\gamma, \xi) &= \ell^2 \lambda_1^2 - \ell' \lambda_1 \\
 &= \frac{\gamma}{2} (\gamma \ell^2 + \ell') + \frac{1}{2} (\gamma \ell^2 + \ell') \sqrt{\gamma^2 + 4\xi^2} + \ell^2 \xi^2, \quad (4.28)
 \end{aligned}$$

and

$$\begin{aligned}
 c_B(\gamma, \xi) &= \ell^2 \lambda_3^2 - \ell' \lambda_3 \\
 &= \ell^2 \xi^2 + \frac{\gamma}{2} (\gamma \ell^2 + \ell') + 1 + \frac{1}{2} (\gamma \ell^2 + \ell') \sqrt{4\xi^2 + \gamma^2 + 4/\ell^2}. \quad (4.29)
 \end{aligned}$$

In order to derive the Fredholm integral equation, we define the density as the slope function

$$\phi(x) = \partial w(x, 0^+) / \partial x. \quad (4.30)$$

The second boundary condition in (4.11), and equation (4.30), imply that

$$\phi(x) = 0, \quad |x| > a, \quad (4.31)$$

and

$$\int_{-a}^a \phi(x) dx = 0, \quad (4.32)$$

which is the single-valuedness condition. The definition (4.30) together with equation (4.25) lead to

$$\frac{1}{\sqrt{2\pi}} \int_{-\infty}^{\infty} (-i\xi) [A(\xi) + B(\xi)] e^{-ix\xi} d\xi = \phi(x), \quad -\infty < x < \infty. \quad (4.33)$$

By inverting the Fourier transform and using (4.31), one obtains

$$\begin{aligned} (i\xi)[A(\xi) + B(\xi)] &= \frac{-1}{\sqrt{2\pi}} \int_{-\infty}^{\infty} \phi(x) e^{ix\xi} dx, \quad -\infty < x < \infty \\ &= \frac{-1}{\sqrt{2\pi}} \int_{-a}^a \phi(t) e^{i\xi t} dt. \end{aligned} \quad (4.34)$$

The last boundary condition in (4.11), imposed on  $\mu_{yz}(x, y)$ , provides the following pointwise relationship between  $A(\xi)$  and  $B(\xi)$

$$B(\xi) = -\frac{\ell^2 \xi^2 + (\gamma \ell^2 + \ell') \sqrt{\gamma^2/4 + \xi^2} + \gamma(\gamma \ell^2 + \ell')/2}{\ell^2 \xi^2 + 1 + [(\gamma \ell^2 + \ell')/2](\gamma + \sqrt{4\xi^2 + \gamma^2 + 4/\ell^2})} A(\xi) = \rho(\gamma, \xi) A(\xi), \quad (4.35)$$

where the notation  $\rho(\gamma, \xi)$  is introduced here, *i.e.*

$$\rho(\gamma, \xi) = -\frac{\ell^2 \xi^2 + (\gamma \ell^2 + \ell') \sqrt{\gamma^2/4 + \xi^2} + \gamma(\gamma \ell^2 + \ell')/2}{\ell^2 \xi^2 + 1 + [(\gamma \ell^2 + \ell')/2](\gamma + \sqrt{4\xi^2 + \gamma^2 + 4/\ell^2})}. \quad (4.36)$$

Substituting (4.35) into (4.34), one obtains

$$A(\xi) = \frac{-1}{\sqrt{2\pi} i \xi} \left[ \frac{1}{1 + \rho(\gamma, \xi)} \right] \int_{-a}^a \phi(t) e^{i\xi t} dt, \quad (4.37)$$

where

$$\frac{1}{1 + \rho(\gamma, \xi)} = \frac{\ell^2 \xi^2 + 1 + [(\gamma \ell^2 + \ell')/2](\gamma + \sqrt{4\xi^2 + \gamma^2 + 4/\ell^2})}{1 + [(\gamma \ell^2 + \ell')/2](\sqrt{4\xi^2 + \gamma^2 + 4/\ell^2} - \sqrt{4\xi^2 + \gamma^2})}. \quad (4.38)$$

Replacing  $A(\xi)$  in equation (4.26) and using the (first) boundary condition for  $\sigma_{yz}$  (that is,  $\lim_{y \rightarrow 0^+} \sigma_{yz}(x, y) = p(x)$ ,  $|x| < a$ ) in (4.11), one obtains the following integral equation in limit form:

$$\lim_{y \rightarrow 0^+} \frac{G(y)}{2\pi} \int_{-\infty}^{\infty} \left[ \frac{-\lambda_1(\gamma, \xi)}{i\xi(1 + \rho(\gamma, \xi))} \right] \left[ \int_{-a}^a \phi(t) e^{i\xi t} dt \right] e^{-(\gamma + \sqrt{\gamma^2 + 4\xi^2})y/2 - ix\xi} d\xi = p(x), \quad |x| < a. \quad (4.39)$$

By rearranging the order of integration, we obtain

$$\lim_{y \rightarrow 0^+} \frac{G(y)}{2\pi} \int_{-a}^a \phi(t) \int_{-\infty}^{\infty} \frac{-\lambda_1(\gamma, \xi)}{(i\xi)[1 + \rho(\gamma, \xi)]} e^{-(\gamma + \sqrt{\gamma^2 + 4\xi^2})y/2} e^{i\xi(t-x)} d\xi dt = p(x), \quad |x| < a, \quad (4.40)$$

which can be rewritten as

$$\lim_{y \rightarrow 0^+} \frac{G}{2\pi} \int_{-a}^a \phi(t) \int_{-\infty}^{\infty} K(\xi, y) e^{i\xi(t-x)} d\xi dt = p(x), \quad |x| < a, \quad (4.41)$$

with the kernel

$$K(\xi, y) = \frac{-\lambda_1(\gamma, \xi)}{i\xi[1 + \rho(\gamma, \xi)]} e^{-(\gamma + \sqrt{\gamma^2 + 4\xi^2})y/2}. \quad (4.42)$$

Asymptotic analysis allows splitting of the kernel  $K(\xi, y)$  into the singular [ $K_\infty(\xi, y) = \lim_{|\xi| \rightarrow \infty} K(\xi, y)$ ] and nonsingular parts:

$$K(\xi, y) = \underbrace{K_\infty(\xi, y)}_{\text{singular}} + \underbrace{[K(\xi, y) - K_\infty(\xi, y)]}_{\text{nonsingular}}, \quad (4.43)$$

where (as  $y$  is set to zero)

$$K_\infty(\xi, 0) = \frac{|\xi|}{i\xi} \left\{ \left[ \frac{5\ell^2\gamma^2}{8} + \frac{\ell'\gamma}{4} + 1 - \left( \frac{\ell'}{2\ell} \right)^2 \right] + \frac{2\gamma\ell^2 + \ell'}{2} |\xi| + \ell^2\xi^2 \right\}, \quad (4.44)$$

and  $K(\xi, 0) - K_\infty(\xi, 0)$ , denoted by  $N(\xi, 0) = N(\xi)$ , can be expressed as a fraction:

$$N(\xi, 0) = N(\xi) = \frac{P(\xi)}{Q(\xi)}, \quad (4.45)$$

in which

$$Q(\xi) = -i\xi \left( \sqrt{\xi^2 + \gamma^2/4 + 1/\ell^2} + \sqrt{\xi^2 + \gamma^2/4} + \gamma + \ell'/\ell^2 \right). \quad (4.46)$$

and  $P(\xi)$  is given by

$$P(\xi) = P_4(\xi) + P_3(\xi) + P_2(\xi) + P_1(\xi) + P_0(\xi) \quad (4.47)$$

in which

$$P_4(\xi) = \ell^2\xi^2 \times \left( \sqrt{\xi^2 + \gamma^2/4 + 1/\ell^2} \sqrt{\xi^2 + \gamma^2/4} + \xi^2 - |\xi| \sqrt{\xi^2 + \gamma^2/4 + 1/\ell^2} - |\xi| \sqrt{\xi^2 + \gamma^2/4} \right), \quad (4.48)$$

$$P_3(\xi) = \frac{1}{2}(\gamma\ell^2 + \ell')\xi^2 \left( \sqrt{\xi^2 + \gamma^2/4 + 1/\ell^2} + \sqrt{\xi^2 + \gamma^2/4} \right) - (\gamma\ell^2 + \ell')|\xi|^3, \quad (4.49)$$

$$\begin{aligned}
 P_2(\xi) &= [1 + \gamma(\gamma\ell^2 + \ell')] \sqrt{\xi^2 + \gamma^2/4 + 1/\ell^2} \sqrt{\xi^2 + \gamma^2/4} \\
 &+ \left[ 1 + \frac{1}{4}\gamma^2\ell^2 - \frac{1}{2}\left(\frac{\ell'}{\ell}\right)^2 - \frac{1}{2}\gamma\ell' \right] \xi^2 - |\xi| \times \\
 &\left[ 1 + \frac{5}{8}\gamma^2\ell^2 - \left(\frac{\ell'}{2\ell}\right)^2 + \frac{1}{4}\gamma\ell' \right] \left( \sqrt{\xi^2 + \gamma^2/4 + 1/\ell^2} + \sqrt{\xi^2 + \gamma^2/4} \right), \quad (4.50)
 \end{aligned}$$

$$\begin{aligned}
 P_1(\xi) &= \frac{1}{2}\gamma(1 + \gamma^2\ell^2 + \gamma\ell') \sqrt{\xi^2 + \gamma^2/4 + 1/\ell^2} + \left[ \frac{\gamma}{2}(1 + \gamma^2\ell^2 + \gamma\ell') + \frac{\ell'}{\ell^2} \right] \times \\
 &\sqrt{\xi^2 + \gamma^2/4} - \left( \gamma + \frac{\ell'}{\ell^2} \right) \left[ 1 + \frac{5}{8}\gamma^2\ell^2 - \left(\frac{\ell'}{2\ell}\right)^2 + \frac{1}{4}\gamma\ell' \right] |\xi|, \quad (4.51)
 \end{aligned}$$

$$P_0(\xi) = \frac{1}{4}\ell^2\gamma^4 + \frac{3}{4}\gamma^2 + \frac{1}{4}\gamma^3\ell' + \frac{1}{2}\frac{\gamma\ell'}{\ell^2}. \quad (4.52)$$

Substitution of equation (4.44) into (4.41), in the sense of distribution theory [88], leads to

$$\begin{aligned}
 &\lim_{y \rightarrow 0^+} \int_{-\infty}^{\infty} K_{\infty}(\xi, y) e^{i\xi(t-x)} d\xi \\
 &= \frac{-2\ell^2}{(t-x)^3} - \frac{\pi}{2}(2\ell^2\gamma + \ell') \delta'(t-x) + \frac{5\ell^2\gamma^2/8 + \ell'\gamma/4 + 1 - [\ell'/(2\ell)]^2}{t-x},
 \end{aligned}$$

and to the following hypersingular integral equation:

$$\begin{aligned}
 \frac{G_0}{\pi} \int_{-a}^a \left\{ \frac{-2\ell^2}{(t-x)^3} - \frac{\pi}{2}(2\ell^2\gamma + \ell') \delta'(t-x) \right. \\
 \left. + \frac{5\ell^2\gamma^2/8 + \ell'\gamma/4 + 1 - [\ell'/(2\ell)]^2}{t-x} + k(x, t) \right\} \phi(t) dt = p(x), \quad |x| < a, \quad (4.53)
 \end{aligned}$$

where the regular kernel is

$$k(x, t) = \int_0^{\infty} N(\xi) \sin[\xi(t-x)] d\xi \quad (4.54)$$

with  $N(\xi)$  described in equation (4.45). Figure 4.3 permits to graphically evaluate the behavior of the integrand of equation (4.54). Clearly, such kernel is oscillatory, but the magnitude of oscillation decreases and tend to zero as  $\xi$  increases, *i.e.*  $\lim_{\xi \rightarrow \infty} N(\xi) \sin[\xi(t-x)] = 0$ . Another point that we need to be cautious about in equation (4.54) is at  $\xi = 0$ , because of  $N(\xi) = P(\xi)/Q(\xi)$  and  $Q(\xi)$  has the factor  $\xi$ .

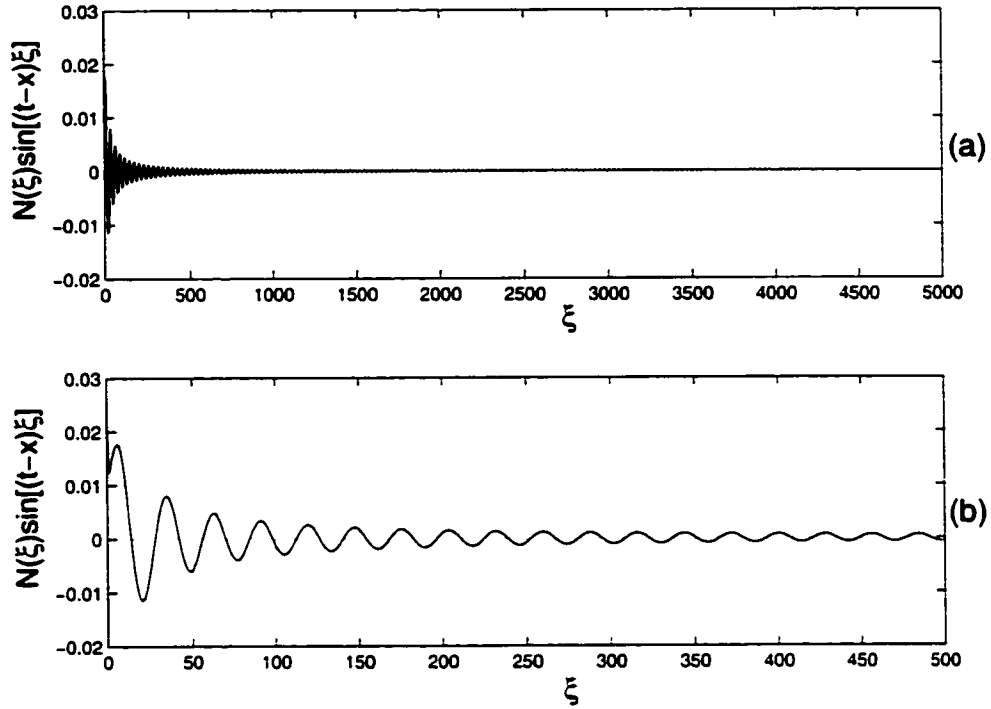


Figure 4.3: Plot of the the integrand in equation (4.54) for  $\ell = 0.05$ ,  $\ell' = 0.005$ ,  $\gamma = 0.1$ ,  $r = \sqrt{3}/7$ , and  $s = \sqrt{2}/3$ . (a)  $\xi \in [0, 5000]$ ; (b) Zoom for the range  $\xi \in [0, 500]$ . Moreover, As  $\xi \rightarrow 0$ , the limit of  $N(\xi) \sin[\xi(s - r)]$  is about  $22.4 \times 10^{-3}$ .

However, this would not affect the integrability of the integrand in equation (4.54) because of the term  $\sin[\xi(t - x)]$ . Thus  $\lim_{\xi \rightarrow 0} N(\xi) \sin[\xi(t - x)]$  exists and is finite, which depends on the values of  $t$ ,  $x$ ,  $\ell$ ,  $\ell'$ , and  $\gamma$ .

As a result of distribution theory [85], the differentiation of a delta function,  $\delta(t)$ , has the following property:

$$\int_{-\infty}^{\infty} \delta'(t - x)\phi(t)dt = -\phi'(x). \quad (4.55)$$

Thus one may rewrite equation (4.53) as

$$\begin{aligned} \frac{G_0}{\pi} \int_{-a}^a \left\{ \frac{-2\ell^2}{(t-x)^3} + \frac{5\ell^2\gamma^2/8 + \ell'\gamma/4 + 1 - (\ell'/\ell)^2/4}{t-x} + k(x, t) \right\} \phi(t) dt \\ + \frac{G_0}{2}(\ell' + 2\ell^2\gamma)\phi'(x) = p(x), \quad |x| < a, \quad (4.56) \end{aligned}$$

which is an integrodifferential equation with both hypersingular and Cauchy singular kernels. In addition to the single-valuedness condition in (4.32), the integrodifferential equation (4.56) is solved under the physical constraint (“smooth closure condition”)

$$\phi(a) = \phi(-a) = 0, \quad (4.57)$$

so that the solution can be found uniquely (see [36] and [60]). Thus it is different from the conventional classical elasticity in which the displacement gradient  $\phi(x)$  has the end-point asymptotics

$$\phi(x) = O\left(\frac{1}{\sqrt{a^2 - x^2}}\right), \quad \text{as } x \rightarrow a^-, (-a)^+. \quad (4.58)$$

Also, an important observation is that once  $\phi(x)$  is solved from equation (4.56) the coefficients  $A(\xi)$  and  $B(\xi)$  can be obtained from (4.35) and (4.37), respectively, and, then, the full field solution  $w(x, y)$  is explicitly given by (4.25).

## 4.6 Numerical Results

Some numerical results are given here. Numerical procedures and the computation of SIFs will be addressed in Chapter 8. The boundary value problem illustrated in Figure 4.1 is considered for all the examples in this paper. To validate the present formulation, consider the case where  $\ell, \ell' \rightarrow 0$  in a certain special limit sense (see Fannjiang *et al.* 2001 [36]), so that the classical elasticity solution is represented. The results for classical SIFs (equations (7.68) and (7.69)) are given in Table 4.2. It is clearly seen from Table 4.2 that the present results are in agreement with those of Erdogan and Ozturk [30]. Note that the SIFs decrease monotonically as  $\gamma$  increases. Moreover, it is interesting to investigate the asymptotic behavior of the SIFs as  $\gamma \rightarrow \pm\infty$ . As  $\gamma \rightarrow \infty$  the stiffness of the medium increases indefinitely and, under finite loading ( $p_0$ ), the crack opening displacement and the SIFs  $K_{III}(a)$  tend to zero. Similarly, as

Table 4.2: Variation of classical (normalized) SIFs with material gradation parameter  $\tilde{\gamma} = \gamma/a$ .

| $\tilde{\gamma}$ | $\frac{K_{III}(-a)}{p_0\sqrt{\pi a}}$ |                         |
|------------------|---------------------------------------|-------------------------|
|                  | Present Study                         | Erdogan and Ozturk [30] |
| -2.0             | 1.476                                 | 1.481                   |
| -1.6             | 1.381                                 | 1.397                   |
| -1.2             | 1.293                                 | 1.308                   |
| -0.8             | 1.204                                 | 1.214                   |
| -0.4             | 1.117                                 | 1.113                   |
| -0.2             | 1.061                                 | 1.059                   |
| 0.0              | 1.000                                 | 1.000                   |
| 0.2              | 0.934                                 | 0.934                   |
| 0.4              | 0.866                                 | 0.869                   |
| 0.6              | 0.807                                 | 0.810                   |
| 0.8              | 0.755                                 | 0.758                   |
| 1.0              | 0.709                                 | 0.712                   |
| 1.2              | 0.669                                 | 0.671                   |
| 1.6              | 0.602                                 | 0.604                   |
| 2.0              | 0.556                                 | 0.550                   |
| 3.0              | 0.458                                 | 0.457                   |
| 5.0              | 0.359                                 | 0.356                   |
| 6.0              | 0.329                                 | 0.324                   |



$\gamma \rightarrow -\infty$  the stiffness of the medium decreases indefinitely, and consequently  $K_{III}(a)$  tend to infinity. These physically expected trends can be observed in Table 4.2.

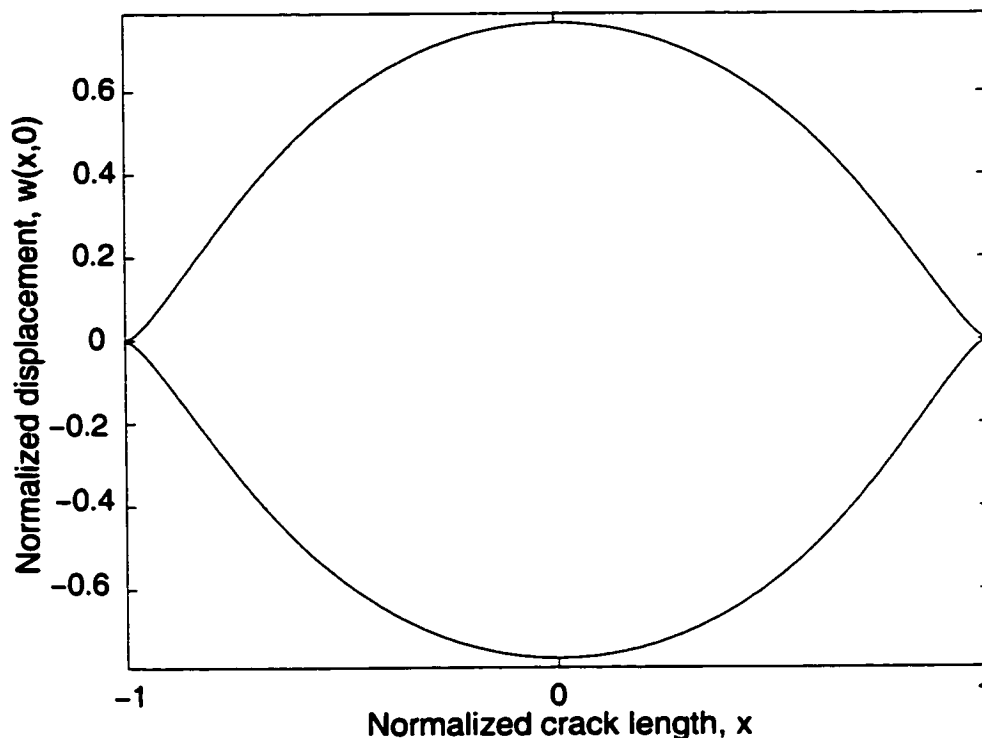


Figure 4.4: Full crack displacement profile in an infinite medium of homogeneous material ( $\tilde{\gamma} = 0$ ) under uniform crack surface shear loading  $\sigma_{yz}(x, 0) = -p_0$  with choice of (normalized)  $\tilde{\ell} = 0.2$  and  $\tilde{\ell}' = 0$ .

Once the slope function is found numerically using the representation (8.3), the crack displacement profile  $w(r, 0)$  can be obtained as

$$w(r, 0) = \int_{-1}^r \Phi(s) ds = \int_{-1}^r \sqrt{1-s^2} \sum_{n=0}^N A_n U_n(s) ds. \quad (4.59)$$

Figure 4 shows the normalized crack displacement profile in an infinite medium of homogeneous material ( $\gamma = 0$ ) under uniform crack surface loading for  $\tilde{\ell} = 0.2$  and  $\tilde{\ell}' = 0$ . Notice that the crack tips form a cusp with zero enclosed angle and zero first derivative of the displacement at the crack tips (see (4.57)). This crack shape is similar to the one obtained by Barenblatt [3] using “cohesive zone theory”, but

without the assumption regarding existence of interatomic forces.

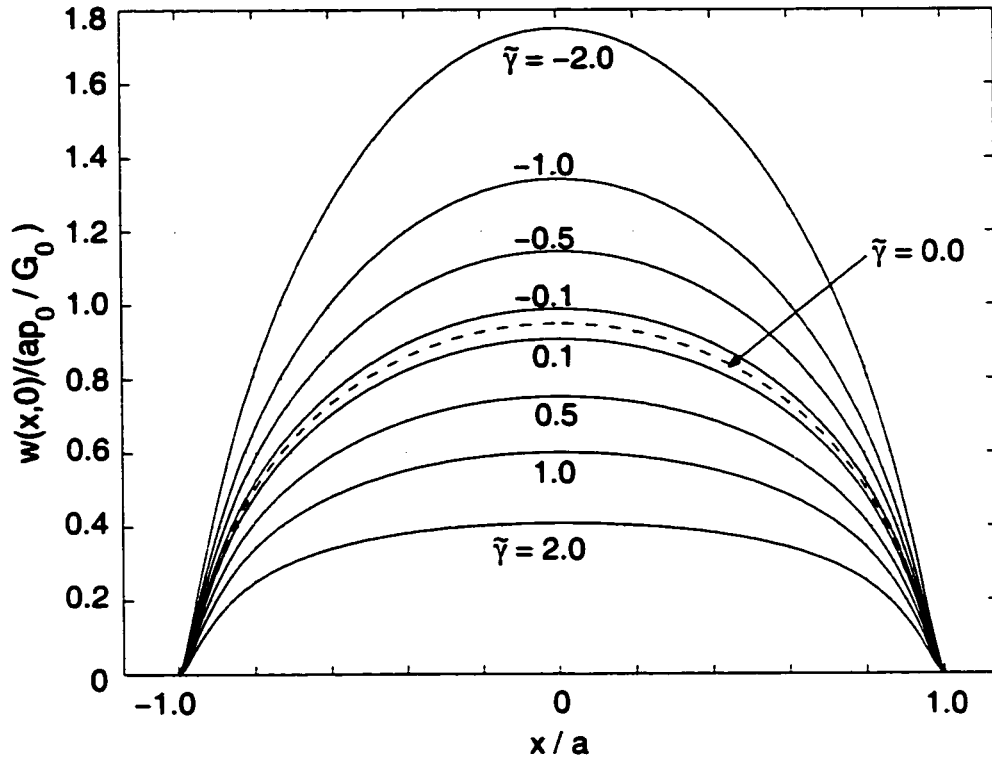


Figure 4.5: Crack surface displacement under uniform crack surface shear loading  $\sigma_{yz}(x, 0) = -p_0$  and shear modulus  $G(y) = G_0 e^{\gamma y}$  with choice of (normalized)  $\bar{\ell} = 0.05$ ,  $\bar{\ell}' = 0$ , and various  $\tilde{\gamma}$ . The dashed line stands for the homogeneous material case ( $\tilde{\gamma} = 0$ ).

The solutions obtained in this study for a nonhomogeneous half-plane having shear modulus  $G \equiv G(y)$ ,  $y > 0$ , is also valid for the corresponding infinite medium in which  $y = 0$  is a plane of symmetry (see Figure 4.2), *i.e.*

$$G(-y) = G(y).$$

Unless otherwise stated, uniform loading is considered on the crack face, *i.e.*  $\sigma_{yz}(x, 0) = -p_0$ , and the normalization  $p_0/G_0$  has been employed.

Further normalized crack displacement profiles for various combinations of the gradient parameters ( $\bar{\ell}$ ,  $\bar{\ell}'$ ) and material gradation parameter ( $\tilde{\gamma}$ ) are presented in Figure 4.5

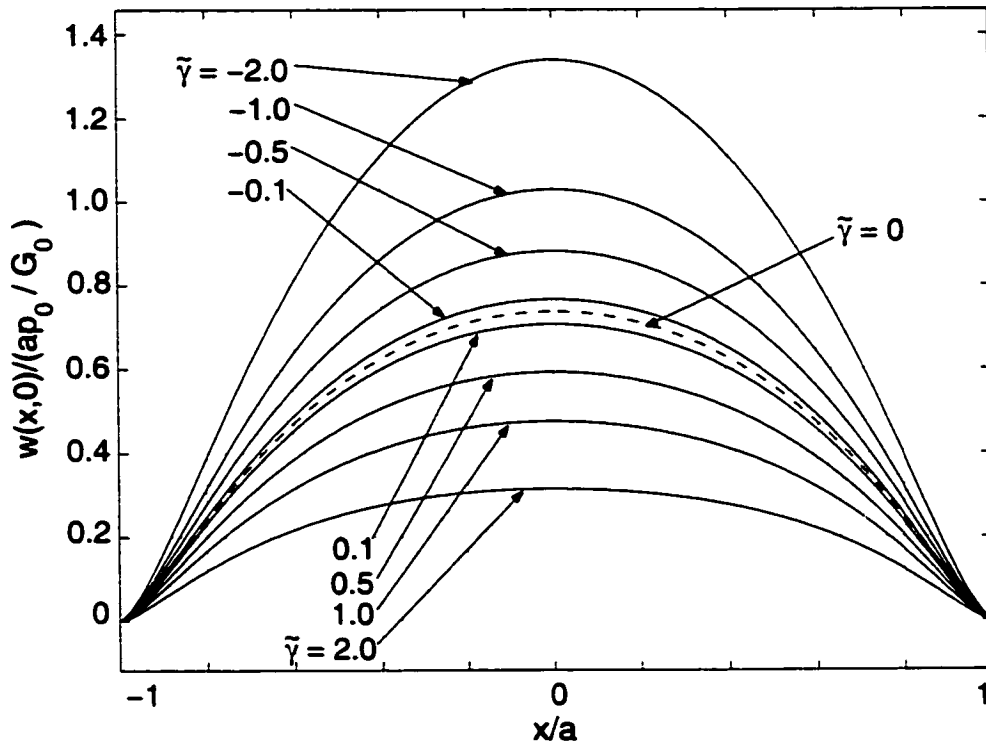


Figure 4.6: Crack surface displacement under uniform crack surface shear loading  $\sigma_{yz}(x, 0) = -p_0$  and shear modulus  $G(y) = G_0 e^{\gamma y}$  with choice of (normalized)  $\bar{\ell} = 0.2$ ,  $\bar{\ell}' = 0.04$ , and various  $\tilde{\gamma}$ . The dashed line stands for the homogeneous material ( $\tilde{\gamma} = 0$ ) in a gradient elastic medium.

to Figure 4.8. Figures 4.5 and 4.6 show crack displacement profiles for selected values of  $\bar{\ell}$ ,  $\bar{\ell}'$ , and various  $\gamma$ . Figure 4.5 considers  $\bar{\ell} = 0.05$ ,  $\bar{\ell}' = 0$  and thus  $\rho = \ell'/\ell = 0$ ; while Figure 4.6 considers  $\bar{\ell} = 0.20$ ,  $\bar{\ell}' = 0.04$  and thus  $\rho = \ell'/\ell = 0.2$ . In both graphs, the broken lines stand for the homogeneous material ( $\gamma = 0$ ) in a gradient elastic medium. A comparison between Figures 4.5 and 4.6 permits to assess the influence of the gradient parameters ( $\ell, \ell'$ ) on the displacement solution. Moreover, as  $\gamma$  increases the displacement magnitude decreases, which is consistent with similar results by Erdogan and Ozturk [30] using classical elasticity to model mode III cracks in FGMs.

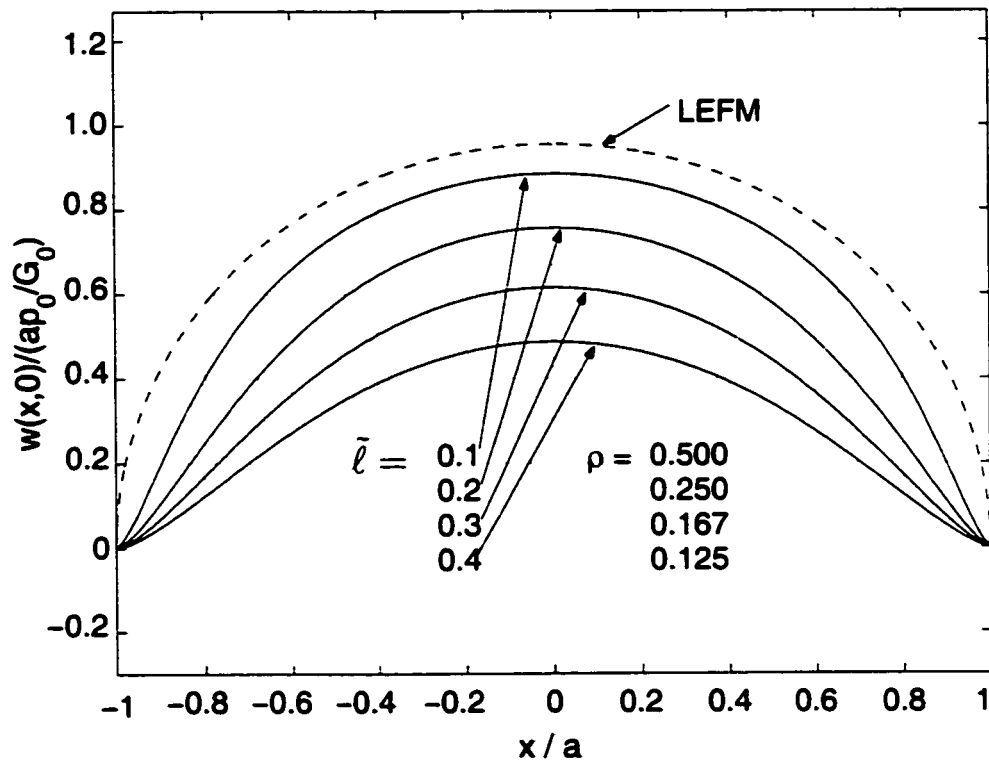


Figure 4.7: Crack surface displacement profiles under uniform crack surface shear loading  $\sigma_{yz}(x, 0) = -p_0$  and shear modulus  $G(y) = G_0 e^{\gamma y}$  with choice of (normalized)  $\bar{\ell}' = 0.05$ ,  $\bar{\gamma} = 0.1$ , and various  $\bar{\ell}$ . The values of  $\bar{\ell}$  are listed in the same order as the solid-line curves.

Figure 4.7 shows crack displacement profiles for  $\bar{\ell}' = 0.05$ ,  $\bar{\gamma} = 0.10$  and various  $\bar{\ell}$ . As  $\bar{\ell}$  increases, the displacement diminishes monotonically, or alternatively the crack

becomes stiffer, in comparison to the classical elasticity theory.

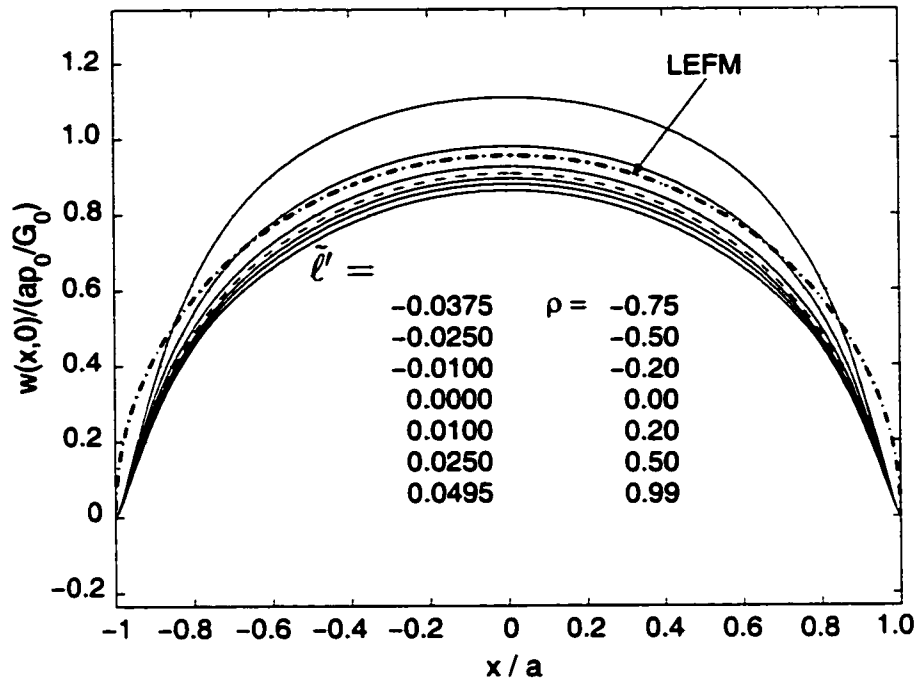


Figure 4.8: Crack surface displacement profiles under uniform crack surface shear loading  $\sigma_{yz}(x, 0) = -p_0$  and shear modulus  $G(y) = G_0 e^{\gamma y}$  with choice of (normalized)  $\tilde{\ell} = 0.05$ ,  $\tilde{\gamma} = 0.1$ , and various  $\tilde{\ell}'$ . The values of  $\tilde{\ell}'$  (and  $\rho$ ) are listed in the same order as the solid-line and dashed-line ( $\rho = 0$ ) curves representing the strain gradient results.

Figure 4.8 shows crack displacement profiles for  $\tilde{\ell} = 0.05$ ,  $\tilde{\gamma} = 0.10$  and various  $\tilde{\ell}'$ . As is apparent from this figure, by maintaining the values of the relative volume energy parameter  $\tilde{\ell}$  constant, the crack stiffening effect becomes more pronounced as the relative surface energy parameter  $\tilde{\ell}'$  increases in the range  $[0, \tilde{\ell}]$ . It is worth mentioning that, from energy considerations, the parameter  $\tilde{\ell}'$  can take negative values [93]. Note from Figure 4.8 that the effect of a negative  $\tilde{\ell}'$  leads to a more compliant crack. In general, this is a desirable property of the mathematical model in regards to describing experimental results and data.

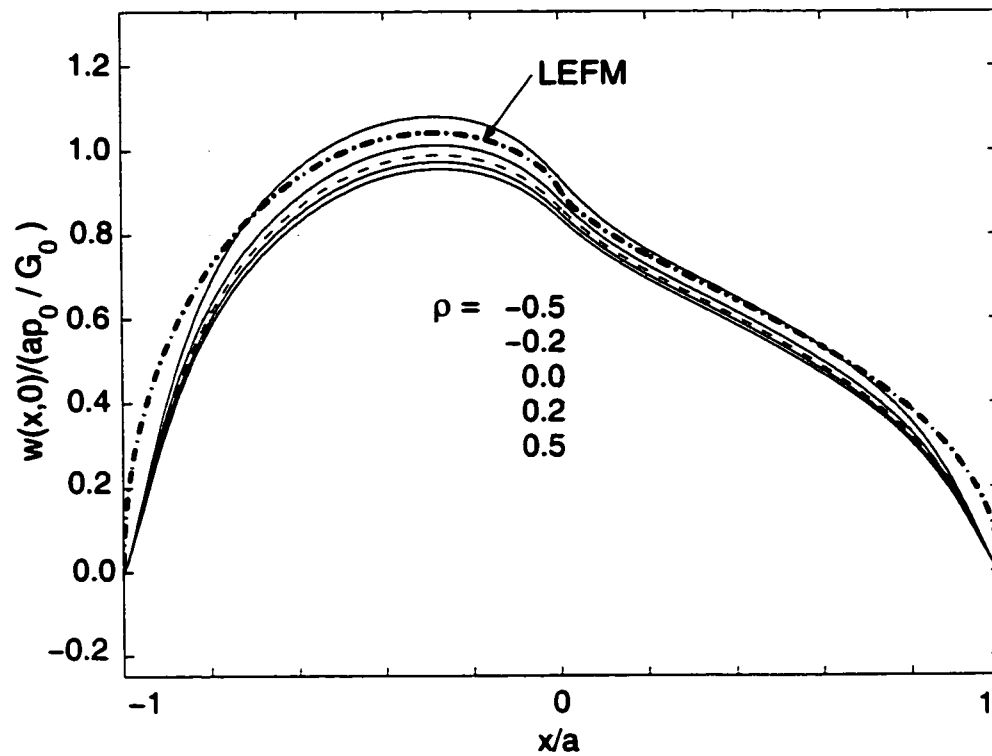


Figure 4.9: Crack surface displacement profiles under discontinuous loading  $p(x/a) = -1 + 0.5\text{sgn}(x/a)$  and shear modulus  $G(y) = G_0 e^{\gamma y}$  with choice of (normalized)  $\bar{\ell} = 0.05$ ,  $\bar{\gamma} = 0.2$ , and various  $\rho$ . The values of  $\rho$  are listed in the same order as the solid-line and dashed-line ( $\rho = 0$ ) curves representing the strain gradient results.

Table 4.3: Convergence of (normalized) generalized SIFs for a mode III crack.

| N  | $\tilde{\gamma} = 0, \tilde{\ell} = 0.05$ |            |   |            | $\tilde{\gamma} = 0.30, \tilde{\ell} = 0.05$ |            |   |            |
|----|---|------------|---|------------|--|------------|---|------------|
|    | $\tilde{\ell}' = 0; \rho = 0$             |            | $\tilde{\ell}' = 0.01; \rho = 0.20$       |            | $\tilde{\ell}' = 0; \rho = 0$                |            | $\tilde{\ell}' = 0.01; \rho = 0.20$       |            |
|    | $\frac{K_{III}(-a)}{\rho_0 \sqrt{\pi a}}$ | Cond. Num. | $\frac{K_{III}(-a)}{\rho_0 \sqrt{\pi a}}$ | Cond. Num. | $\frac{K_{III}(-a)}{\rho_0 \sqrt{\pi a}}$    | Cond. Num. | $\frac{K_{III}(-a)}{\rho_0 \sqrt{\pi a}}$ | Cond. Num. |
| 11 | 0.97292                                   | 9.888      | 0.99640                                   | 17.018     | 0.89258                                      | 15.223     | 0.90773                                   | 15.142     |
| 21 | 0.97467                                   | 83.559     | 0.97375                                   | 1.669e+02  | 0.88381                                      | 1.509e+02  | 0.88337                                   | 1.478e+02  |
| 31 | 0.97467                                   | 3.555e+02  | 0.97355                                   | 7.131e+02  | 0.88376                                      | 6.437e+02  | 0.88287                                   | 6.314e+02  |
| 41 | 0.97467                                   | 1.032e+03  | 0.972256                                  | 2.059e+03  | 0.88336                                      | 1.859e+03  | 0.88133                                   | 1.823e+03  |
| 51 | 0.97467                                   | 2.395e+03  | 0.97109                                   | 4.754e+03  | 0.88301                                      | 4.293e+03  | 0.87999                                   | 4.206e+03  |
| 61 | 0.97467                                   | 4.802e+03  | 0.97113                                   | 9.501e+03  | 0.88301                                      | 8.577e+03  | 0.87996                                   | 8.406e+03  |

Figure 4.9 shows crack displacement profiles considering discontinuous loading

$$p(x) = -1 + 0.5 \operatorname{sgn}(x)$$

and  $\tilde{\ell} = 0.05$ ,  $\tilde{\gamma} = 0.2$ , and various  $\rho = \ell'/\ell$ . Similar comments to those regarding Figure 8 can be made with respect to Figure 4.9. Moreover, qualitatively the results displayed in Figures 4.7 to 4.9 are in agreement with those of Vardoulakis *et al.* [92] for homogeneous materials.

Table 4.3 shows a convergence study for (normalized) generalized SIFs (see equations (8.18), (8.19) and (10.53), (10.54)) involving non-graded ( $\tilde{\gamma} = 0$ ) and graded ( $\tilde{\gamma} \neq 0$ ) gradient elastic materials considering both  $\tilde{\ell}' = 0$  and  $\tilde{\ell}' \neq 0$  ( $\tilde{\ell}' > 0$ ). Note that as the number of collocation points ( $N$ ) increases, the generalized SIF results converge for both materials (*i.e.* non-graded and graded). However, the convergence is worse for the case  $\tilde{\ell}' \neq 0$  than for the case  $\tilde{\ell}' = 0$ . The condition number for all the examples investigated is always satisfactory.

Table 4.4 lists the generalized SIFs (see equations (8.18), (8.19)) for gradient elastic materials considering various values of the material parameter  $\gamma$  and using  $N = 61$  collocation points in the numerical solution. Notice that the SIF monotonically de-

creases as  $\gamma$  increases, which is in full agreement with the early results for classical elasticity considering nonhomogeneous materials (see Table 4.2). Consider, for example, the case  $\bar{\gamma} = 0$ . In this case, the crack stiffening is due to the characteristic material lengths  $\bar{\ell}$  and  $\bar{\ell}'$  ( $\bar{\ell}' > 0$ ) of the structured medium in responsible for lower generalized SIFs ( $< 1.0$ ) and, consequently, lower energy release rates during crack propagation. Notice, from Table 4.4, that similar trends are also observed for  $\bar{\gamma} \neq 0$  (either  $\bar{\gamma} < 0$  or  $\bar{\gamma} > 0$ ). The results indicate that a higher external load, as compared to that of the classical case, must be applied on the crack surfaces (or on the remote boundaries) to propagate it in a material with microstructure.

Table 4.4: Normalized generalized SIFs for a mode III crack at various values of  $\bar{\ell}$ ,  $\bar{\ell}'$ , and  $\bar{\gamma}$ .

|                | $\bar{\ell} = 0.05, \bar{\ell}' = 0$  | $\bar{\ell} = 0.05, \bar{\ell}' = 0.01$ | $\bar{\ell} = 0.2, \bar{\ell}' = 0$   | $\bar{\ell} = 0.2, \bar{\ell}' = 0.04$ |
|----------------|---------------------------------------|---|---------------------------------------|--|
| $\bar{\gamma}$ | $\frac{K_{III}(-a)}{P_0\sqrt{\pi a}}$ | $\frac{K_{III}(-a)}{P_0\sqrt{\pi a}}$   | $\frac{K_{III}(-a)}{P_0\sqrt{\pi a}}$ | $\frac{K_{III}(-a)}{P_0\sqrt{\pi a}}$  |
| -2.00          | 1.42126                               | 1.41617                                 | 1.28917                               | 1.26783                                |
| -1.00          | 1.21749                               | 1.21301                                 | 1.10392                               | 1.08610                                |
| -0.50          | 1.10374                               | 1.09965                                 | 1.00377                               | 0.98768                                |
| -0.10          | 1.00271                               | 0.99903                                 | 0.91696                               | 0.90236                                |
| 0.00           | 0.97467                               | 0.97113                                 | 0.89338                               | 0.87921                                |
| 0.10           | 0.94423                               | 0.94086                                 | 0.86819                               | 0.85450                                |
| 0.50           | 0.82566                               | 0.82282                                 | 0.76878                               | 0.75671                                |
| 1.00           | 0.70597                               | 0.70324                                 | 0.66261                               | 0.65169                                |
| 2.00           | 0.54916                               | 0.54592                                 | 0.50894                               | 0.49937                                |

## 4.7 A Summary

As an end of this chapter we give an outline of the process that leads the boundary value problem to a hypersingular integral equation .

- PDE(s) with mixed-valued boundary conditions (BCs).
- Fourier Transform ( PDE(s)  $\rightarrow$  ODE(s) ).



- Solving ODEs.  $\rightarrow$  Solution is expressed in the Fourier domain.
- Inverting Fourier transform.  $\rightarrow$  Integral equation is formed with unknown coefficients determined by BCs.
- Selection of the density function which can be related to BCs.
- Asymptotic analysis determines the hypersingular kernel(s).
- Splitting out the singularity  $\rightarrow$  Hypersingular integral equation(s) is (are) derived.

Notice that final form of the derived hypersingular integral equation(s) has incorporated the BCs as part of the equation. Thus, solving the integral equation is indeed solving the original PDE(s) with mixed-valued BCs.

## Chapter 5

# Finite Part Integrals and Hypersingular Kernels

In this chapter, we will explain how the hypersingular kernels arise. Essentially, hypersingular kernels are derived by the following three basic ingredients:

- Finite part integrals,
- Identity

$$i^n \frac{d^n}{dy^n} \left[ \frac{1}{y - i(t - x)} \right] = \frac{d^n}{dx^n} \left[ \frac{1}{y - i(t - x)} \right], \quad (5.1)$$

- Plemelj formulas [22, 58, 68].

The key point of identity (5.1) is that it allows one to switch the differentiation from  $d/dx$  to  $d/dy$ , and *vice versa*; it is very straightforward to verify, thus we shall address the other two ingredients.

### 5.1 Finite Part integrals

Unless a proper meaning of integration is given, the first integral in equations (2.32) and (4.56) is meaningless because of the infinity involved. Jacques Hadamard [40] is

the first mathematician who regularized the singular integral by taking “finite part” of the integral. It can be considered as a generalization of the Cauchy principal value integral [32, 60].

### 5.1.1 Cauchy Principal Value Integrals

Equations that involve integrals of the type<sup>1</sup>

$$\int_{-1}^1 \frac{\phi(t)}{t-x} dt, \quad |x| < 1 \quad (5.2)$$

is not integrable in the ordinary (Riemann integral) sense because of the kernel  $1/(t-x)$  is not integrable over any interval that includes the point  $t = x$ . Thus, a special interpretation, called Cauchy principal value integral [50, 67, 79] is given.

**Definition 5.1** (Cauchy principal value integral)

$$\int_{-1}^1 \frac{\phi(t)}{t-x} dt := \lim_{\epsilon \rightarrow 0} \left\{ \int_{-1}^{x-\epsilon} \frac{\phi(t)}{t-x} dt + \int_{x+\epsilon}^1 \frac{\phi(t)}{t-x} dt \right\}, \quad |x| < 1. \quad (5.3)$$

Notice that the  $\epsilon$ -neighborhood about the singular point  $x = t$  must be symmetric, and it is how the principal value integral works out for canceling off the singularity.

Some regularity is required for  $\phi(x)$  in (5.3) so that the Cauchy principal value integral exists.

**Definition 5.2** A function  $\phi : (-1, 1) \rightarrow \mathbb{R}$  is called Hölder continuous on  $(-1, 1)$  (of order  $\alpha$ ) if

$$|\phi(x) - \phi(y)| \leq c|x - y|^\alpha$$

for some constant  $c$ ,  $0 < \alpha \leq 1$ , and all  $x, y \in (-1, 1)$ . We denote  $\phi(x) \in C^{0,\alpha}(-1, 1)$ .

**Proposition 5.1** If  $f(x) \in C^{0,\alpha}(-1, 1)$ , then the principal integral

$$\int_{-1}^1 \frac{\phi(t)}{t-x} dt$$

exists for all values of  $x$  in the interval  $-1 < x < 1$ .

<sup>1</sup>After a step of normalization (change of variables), the integral  $\int_a^b$  can be transformed to  $\int_{-1}^1$ . For the sake of convenience, we use  $\int_{-1}^1$  all through this chapter.

*Proof* By definition, we have

$$\begin{aligned} \int_{-1}^1 \frac{\phi(t)}{t-x} dt &= \lim_{\epsilon \rightarrow 0} \left\{ \int_{|t-x| \geq \epsilon} \frac{\phi(t) - \phi(x)}{t-x} dt + \phi(x) \int_{|t-x| \geq \epsilon} \frac{dt}{t-x} \right\} \\ &= \int_{-1}^1 \frac{\phi(t) - \phi(x)}{t-x} dt + \phi(x) \int_{-1}^1 \frac{dt}{t-x}. \end{aligned} \quad (5.4)$$

Note that for any  $\phi \in C^{0,\alpha}$ ,  $\alpha > 0$ , the first integral on the right side of (5.4) is an ordinary Riemann integral and the second integral is

$$\int_{-1}^1 \frac{dt}{t-x} = \log \frac{1-x}{1+x}, \quad |x| < 1.$$

This completes the proof.

Although Cauchy principal value integral is defined for an interior point in  $(-1, 1)$  above, it can be evaluated separately on both sides of the end points:

$$\int_{-1}^x \frac{\phi(t)}{t-x} dt := \lim_{\epsilon \rightarrow 0} \left\{ \int_{-1}^{x-\epsilon} \frac{\phi(t)}{t-x} dt - \phi(x) \ln \epsilon \right\}, \quad x > -1,$$

and

$$\int_x^1 \frac{\phi(t)}{t-x} dt := \lim_{\epsilon \rightarrow 0} \left\{ \int_{x+\epsilon}^1 \frac{\phi(t)}{t-x} dt + \phi(x) \ln \epsilon \right\}, \quad x < 1.$$

### 5.1.2 The Definition of Finite Part Integrals

Cauchy principal value does not work for a higher singularity. For instance, consider  $\phi(t) = 1$  and  $x = 0$  in

$$\int_a^b \frac{\phi(t)}{(t-x)^2} dt, \quad a < x < b, \quad (5.5)$$

that is,

$$\int_a^b \frac{dt}{t^2}.$$

The integral is not convergent, neither does the principal value exist, since

$$\int_{[a,b] \setminus (-\epsilon, \epsilon)} \frac{dt}{t^2} = \lim_{\epsilon \rightarrow 0} \left( \frac{1}{a} - \frac{1}{b} + \frac{2}{\epsilon} \right)$$

is not finite.

Hadnard finite part integral is defined by disregarding the infinite part,  $2/\epsilon$ , and keeping the finite part, *i.e.*

$$\int_a^b \frac{dt}{t^2} = \frac{1}{a} - \frac{1}{b}. \quad (5.6)$$

**Definition 5.3** ( Finite part integral ) *Let  $\epsilon > 0$ , and denote*

$$F(\epsilon, x) = \int_{[-1, 1] \setminus (x-\epsilon, x+\epsilon)} f(t, x) dt, \quad |x| < 1,$$

*where the singularity appears at the point  $x = t$ . If  $F(\epsilon, x)$  is decomposed into*

$$F(\epsilon, x) = F_0(\epsilon, x) + F_1(\epsilon, x),$$

*and*

$$\lim_{\epsilon \rightarrow 0} F_0(\epsilon, x) < \infty, \quad F_1(\epsilon, x) \xrightarrow{\epsilon \rightarrow 0} \infty,$$

*then the finite part integral is defined by keeping the “finite part”, *i.e.**

$$\int_{-1}^1 f(t, x) dt = \lim_{\epsilon \rightarrow 0} F_0(\epsilon, x).$$

Notice that finite part integral can be considered as a generalization of the principal value in the sense that if the principal value integral exists, then they give the same result [32].

Now, we shall define the finite part integral for integrals with quadratic singularity as in (5.5). Denote by  $C^{m,\alpha}(-1, 1)$  the space of functions whose  $m$ -th derivatives are Hölder continuous on  $(-1, 1)$  with index  $0 < \alpha \leq 1$ .

**Definition 5.4** *If  $\phi(x) \in C^{1,\alpha}(-1, 1)$ , then*

$$\int_{-1}^1 \frac{\phi(t)}{(t-x)^2} dt := \lim_{\epsilon \rightarrow 0} \left[ \int_{-1}^{x-\epsilon} \frac{\phi(t)}{(t-x)^2} dt + \int_{x+\epsilon}^1 \frac{\phi(t)}{(t-x)^2} dt - \frac{2\phi(x)}{\epsilon} \right] \quad (5.7)$$

Like Proposition 5.1, the condition  $\phi(x) \in C^{1,\alpha}(-1, 1)$  is required for the existence of the defined integral [57, 61].

Following observation may help to understand Definition 5.4. By a step of integration by-parts, the first integral under the limit  $\epsilon \rightarrow 0$  in (5.7) can be written as

$$\int_{-1}^{x-\epsilon} \frac{\phi(t)}{(t-x)^2} dt = \frac{\phi(x-\epsilon)}{\epsilon} - \frac{a}{a-x} + \int_{-1}^{x-\epsilon} \frac{\phi'(t)}{t-x} dt.$$

Similarly,

$$\int_{x+\epsilon}^1 \frac{\phi(t)}{(t-x)^2} dt = \frac{\phi(x+\epsilon)}{\epsilon} - \frac{b}{b-x} + \int_{x+\epsilon}^1 \frac{\phi'(t)}{t-x} dt.$$

Thus, the term  $-2\phi(x)/\epsilon$  in (5.7) will kill the singularity  $[\phi(x-\epsilon) + \phi(x+\epsilon)]/\epsilon$ , and under the assumption  $\phi(x) \in C^{1,\alpha}(-1, 1)$  Definition 5.4 indeed takes the finite part of the integral according to Definition 5.3.

Another direction of viewing Definition 5.4 is by taking direct differentiation  $d/dx$  to (5.3) with Leibnitz's rule, *i.e.*

$$\begin{aligned} \frac{d}{dx} \int_{-1}^1 \frac{\phi(t)}{t-x} dt &= \lim_{\epsilon \rightarrow 0} \frac{d}{dx} \left[ \int_{-1}^{x-\epsilon} \frac{\phi(t)}{t-x} dt + \int_{x+\epsilon}^1 \frac{\phi(t)}{t-x} dt \right] \\ &= \lim_{\epsilon \rightarrow 0} \left[ \int_{-1}^{x-\epsilon} \frac{\phi(t)}{(t-x)^2} dt + \int_{x+\epsilon}^1 \frac{\phi(t)}{(t-x)^2} dt - \frac{\phi(x-\epsilon) + \phi(x+\epsilon)}{\epsilon} \right] \end{aligned} \quad (5.8)$$

Comparing (5.8) with (5.7), we can conclude

**Proposition 5.2** *If  $\phi(x) \in C^{1,\alpha}(-1, 1)$ , then*

$$\int_{-1}^1 \frac{\phi(t)}{(t-x)^2} dt = \frac{d}{dx} \int_{-1}^1 \frac{\phi(t)}{t-x} dt \quad (5.9)$$

Alternatively, one can define finite part integrals by equation (5.9) and deduce Definition 5.4 as property. Thus, for general  $n$ , finite part integrals can be defined recursively as follows. We denote  $L^{1+} = \bigcap_{p>1} L^p[-1, 1]$ .

**Definition 5.5** ( Finite part integral ) *For any  $\phi \in C^{n,\alpha}(-1, 1) \cap L^{1+}$  and  $n = 1, 2, 3, \dots$*

$$\int_{-1}^1 \frac{\phi(t)}{(t-x)^{n+1}} dt := \frac{1}{n} \frac{d}{dx} \int_{-1}^1 \frac{\phi(t)}{(t-x)^n} dt, \quad |x| < 1, \quad (5.10)$$

with

$$\int_{-1}^1 \frac{\phi(t)}{t-x} dt := \int_{-1}^1 \frac{\phi(t)}{t-x} dt.$$

By means of (5.4) and the (recursive) definition of finite part integrals, one can deduce [67]

**Proposition 5.3**

$$\begin{aligned} & \int_{-1}^1 \frac{\phi(t)}{(t-x)^n} dt \\ &= \int_{-1}^1 \frac{\phi(t) - \sum_{j=0}^{n-1} \phi^{(j)}(x)(t-x)^j/j!}{(t-x)^n} dt + \sum_{j=0}^{n-1} \phi^{(j)}(x)/j! \int_{-1}^1 \frac{dt}{(t-x)^{n-j}}. \end{aligned} \quad (5.11)$$

For  $\phi \in C^{n,\alpha}(-1, 1) \cap L^{1+}$ , the first integral on the right side of (5.11) is an ordinary Riemann integral. Also, with (5.11) in hand, integration by-parts formula holds for finite part integrals [67].

**Proposition 5.4** For  $\phi \in C^{n,\alpha}(-1, 1) \cap L^{1+}$

$$\int_{-1}^1 \frac{\phi'(t)}{(t-x)^n} dt = n \int_{-1}^1 \frac{\phi(t)}{(t-x)^{n+1}} dt + \frac{\phi(1)}{(1-x)^n} - (-1)^n \frac{\phi(-1)}{(1+x)^n}, \quad n \geq 1$$

and for  $\phi \in C^\alpha(-1, 1) \cap L^{1+}$

$$\int_{-1}^1 \phi'(t) \log|t-x| dt = \int_{-1}^1 \frac{\phi(t)}{t-x} dt + \phi(1) \log|1-x| - \phi(-1) \log|1+x|$$

**5.1.3 A Remark of Finite Part Integrals**

The most commonly used integration in mathematical analysis is Lebesgue integration. Not all the properties for Lebesgue integral can be carried onto finite part integral. For example, properties that involve inequality (*e.g.* monotone convergence theorem, Fatou's lemma, bounded convergence theorem) may not be true for finite part integral anymore. A simple demonstration is (see equation (5.6) and Reference [43])

$$\int_{-1}^1 \frac{dt}{t^2} = -2;$$

clearly,

$$\left| \int_a^b f(x) dx \right| \leq \int_a^b |f(x)| dx$$

is NOT true for finite part integral! However, fortunately, the most relying formula, integration by-parts, is true for finite part integral.

## 5.2 Plemelj Formulas

In general, the Cauchy principal value type of integrals

$$\int_a^b \frac{\phi(t)}{t-x} dt, \quad a < x < b$$

is evaluated indirectly by using complex function theory [64, 76]. Define

$$\Phi(z) = \int_a^b \frac{\phi(t)}{t-z} dt,$$

with  $z$  not on the integration contour. The principal value is then recovered by sending  $z$  to the point  $x$  on the interval  $(a, b)$ , and the result is different as  $z \rightarrow x$  from above and below. Say, define

$$\Phi^+(x) = \lim_{y \rightarrow 0} \Phi(x + i|y|), \quad \Phi^-(x) = \lim_{y \rightarrow 0} \Phi(x - i|y|),$$

then the limits are

$$\Phi^+(x) = \int_a^b \frac{\phi(t)}{t-x} dt + i\pi\phi(x), \tag{5.12}$$

and

$$\Phi^-(x) = \int_a^b \frac{\phi(t)}{t-x} dt - i\pi\phi(x). \tag{5.13}$$

Equations (5.12) and (5.13) are Plemelj formulas [58], sometimes called by the Sokhet-ski formulas. It is (5.12) that we will be using in the derivation of hypersingular kernels.

Notice that  $\phi(x)$  can be recovered from Plemelj formulas, *i.e.*

$$\phi(x) = \frac{\Phi^+(x) - \Phi^-(x)}{2\pi i}.$$



### 5.3 Hypersingular kernels

For the derivation of hypersingular kernels, we use three basic ingredients:

- definition of finite part integrals;
- the identity (5.1)

$$\frac{d^n}{dy^n} \left[ \frac{1}{y - i(t-x)} \right] = i^{-n} \frac{d^n}{dx^n} \left[ \frac{1}{y - i(t-x)} \right];$$

- the Plemelj formula

$$\lim_{\epsilon \rightarrow 0} \int_{-1}^1 \frac{\phi(t)}{(t-x) + i\epsilon} dt = \int_{-1}^1 \frac{\phi(t)}{t-x} dt + \pi i \phi(x), \quad \phi \in L^1.$$

Hypersingular kernels can be derived by observing that

$$\begin{aligned} k_n(t-x, y) &:= \frac{1}{2\pi} \int_{-\infty}^{\infty} i^n |\xi|^n \frac{|\xi|}{i\xi} e^{-|\xi|y + i(t-x)\xi} d\xi \\ &= \sqrt{\frac{2}{\pi}} (-i)^n \operatorname{Im} \left[ \frac{d^n}{dy^n} (y - i(t-x))^{-1} \right] \\ &= (-1)^n \sqrt{\frac{2}{\pi}} \operatorname{Im} \left[ \frac{d^n}{dx^n} (y - i(t-x))^{-1} \right] \\ &= (-1)^n \sqrt{\frac{2}{\pi}} \operatorname{Re} \left[ \frac{d^n}{dx^n} (t-x + iy)^{-1} \right]. \end{aligned}$$

Thus,

$$\begin{aligned} \lim_{y \rightarrow 0^+} \int_{-1}^1 k_n(t-x, y) \phi(t) dt &= \lim_{y \rightarrow 0^+} (-1)^n \sqrt{\frac{2}{\pi}} \int_{-1}^1 \operatorname{Re} \left[ \frac{d^n}{dx^n} (t-x + iy)^{-1} \right] \phi(t) dt \\ &= (-1)^n \sqrt{\frac{2}{\pi}} \operatorname{Re} \left[ \frac{d^n}{dx^n} \lim_{y \rightarrow 0^+} \int_{-1}^1 (t-x + iy)^{-1} \phi(t) dt \right] \\ &= (-1)^n \sqrt{\frac{2}{\pi}} \frac{d^n}{dx^n} \int_{-1}^1 \frac{\phi(t)}{t-x} dt \\ &= n! (-1)^n \sqrt{\frac{2}{\pi}} \int_{-1}^1 \frac{\phi(t)}{(t-x)^{n+1}} dt. \end{aligned}$$

by the Plemelj formula and the definition of finite part integrals.

Note that, when  $n$  is an odd integer,

$$\frac{1}{\sqrt{2\pi}} \int_{-\infty}^{\infty} i^n \xi^n \frac{|\xi|}{i\xi} e^{-|\xi|y+i(t-x)\xi} d\xi = -\sqrt{\frac{2}{\pi}} \operatorname{Im} \left[ \frac{d^n}{dx^n} (t-x+iy)^{-1} \right].$$

Thus we have

$$\begin{aligned} & \int_{-1}^1 dt \phi(t) \lim_{y \rightarrow 0^+} \frac{1}{\sqrt{2\pi}} \int_{-\infty}^{\infty} i^n \xi^n \frac{|\xi|}{i\xi} e^{-|\xi|y+i(t-x)\xi} d\xi \\ &= -\sqrt{\frac{2}{\pi}} \operatorname{Im} \left[ \frac{d^n}{dx^n} \lim_{y \rightarrow 0^+} \int_{-1}^1 \phi(t) (t-x+iy)^{-1} dt \right] \\ &= -\sqrt{2\pi} \frac{d^n}{dx^n} \phi(x), \end{aligned}$$

where the Plemelj formula is used again.

Some examples are:

$$\int_{-\infty}^{\infty} [|\xi|^3 e^{-|\xi|y}] e^{i(t-x)\xi} d\xi \xrightarrow{y \rightarrow 0^+} \frac{12}{(t-x)^4} \quad (5.14)$$

$$\int_{-\infty}^{\infty} [i\xi|\xi| e^{-|\xi|y}] e^{i(t-x)\xi} d\xi \xrightarrow{y \rightarrow 0^+} \frac{4}{(t-x)^3} \quad (5.15)$$

$$\int_{-\infty}^{\infty} [\xi^2 e^{-|\xi|y}] e^{i(t-x)\xi} d\xi \xrightarrow{y \rightarrow 0^+} -2\pi\delta''(t-x) \quad (5.16)$$

$$\int_{-\infty}^{\infty} [|\xi| e^{-|\xi|y}] e^{i(t-x)\xi} d\xi \xrightarrow{y \rightarrow 0^+} \frac{-2}{(t-x)^2} \quad (5.17)$$

$$\int_{-\infty}^{\infty} [i\xi e^{-|\xi|y}] e^{i(t-x)\xi} d\xi \xrightarrow{y \rightarrow 0^+} 2\pi\delta'(t-x) \quad (5.18)$$

$$\int_{-\infty}^{\infty} \left[ i \frac{|\xi|}{\xi} e^{-|\xi|y} \right] e^{i(t-x)\xi} d\xi \xrightarrow{y \rightarrow 0^+} \frac{-2}{t-x} \quad (5.19)$$

$$\int_{-\infty}^{\infty} [1 e^{-|\xi|y}] e^{i(t-x)\xi} d\xi \xrightarrow{y \rightarrow 0^+} 2\pi\delta(t-x) \quad (5.20)$$

We have used  $\delta(x)$  denotes the Dirac delta function.

## Chapter 6

# Asymptotics of Crack-tip Behavior by Mellin Transform

In this chapter we study the crack-tip behavior of the solution to the hypersingular integral equations by using Mellin transform. Martin [63] has proposed using Mellin transform to study the crack-tip (end-point) behaviour of solutions to quadratic hypersingular integral equations. Here we extend the method to investigate cubic and more general hypersingular integral equations.

### 6.1 Mellin Transform

The idea of the Mellin transform and its inversion formula first occurs in a Riemann's memoir [80] on prime numbers in 1876. The explicit formulation was given by Cahen 1894 [5]. The transform bears Mellin's name because Mellin was the first one to give an accurate and elaborate discussion on it [66]. Mellin transform arises in solving the boundary value problems associated with the geometry as an infinite wedge [20, 88], and it also plays an important role in the asymptotic expansions of integrals [4]. Properties and applications of Mellin transform can be found in [20, 74, 88]. Extensive

tables of Mellin transform are provided in [23, 71]. Its definition is given by

**Definition 6.1**

$$M[f; z] = \tilde{f}(z) := \int_0^{\infty} x^{z-1} f(x) dx. \quad (6.1)$$

$M[f; z]$ , or  $\tilde{f}(z)$ , the “ $(z - 1)$ th” moment of function  $f(x)$  is called the Mellin transform of  $f$ . From now on, we use the notation

$$z = \sigma + i\tau \quad (6.2)$$

to denote the real and imaginary parts of complex variable  $z$ . Using complex Fourier transform, one can derive the inverse Mellin transform as

$$f(x) = \frac{1}{2\pi i} \int_{c-i\infty}^{c+i\infty} \tilde{f}(z) x^{-z} dz, \quad \text{for some } c \in \mathbb{R}. \quad (6.3)$$

The following three examples motivate how the Mellin transform contributes in the asymptotic analysis.

**Example 6.1**

$$\phi_1(x) = \begin{cases} x^\nu, & 0 < x < a \\ 0, & x > a \end{cases} \Rightarrow \tilde{\phi}_1(z) = \frac{1}{z + \nu} a^{z+\nu}, \quad \Re(z) > -\Re(\nu)$$

The integral  $\int_0^{\infty} \phi_1(x) x^{z-1} dx$  exists and is equal to  $\tilde{\phi}_1(z) = a^{z+\nu}/(z + \nu)$ , as  $\Re(z) > -\Re(\nu)$ . However,  $\tilde{\phi}_1(z)$  can be analytically continued to the whole complex plane, still being  $a^{z+\nu}/(z + \nu)$ , with a simple pole at  $z = -\nu$ .

**Example 6.2**

$$\phi_2(x) = \begin{cases} 0, & 0 < x < a \\ x^\nu, & x > a \end{cases} \Rightarrow \tilde{\phi}_2(z) = \frac{-1}{z + \nu} a^{z+\nu}, \quad \Re(z) < -\Re(\nu)$$

The integral  $\int_0^{\infty} \phi_2(x) x^{z-1} dx$  exists and is equal to  $\tilde{\phi}_2(z) = -a^{z+\nu}/(z + \nu)$  as  $\Re(z) < -\Re(\nu)$ . However,  $\tilde{\phi}_2(z)$  can be analytically continued to the whole complex plane, still being  $-a^{z+\nu}/(z + \nu)$ , with a simple pole at  $z = -\nu$ .

**Example 6.3**

$$\phi_3(x) = \begin{cases} x^\nu, & 0 < a < x < b \\ 0, & x \in \mathbb{R} \setminus [a, b] \end{cases} \Rightarrow \tilde{\phi}_3(z) = \frac{1}{z + \nu} (b^{z+\nu} - a^{z+\nu}), \quad z \neq -\nu$$

$\tilde{\phi}_3(z)$  is analytic except a simple pole at  $z = -\nu$ .

From the three examples above we can observe that by studying the pole(s) of the Mellin transform one can gain the knowledge of the asymptotics of the original function. For instance, function  $\phi_1(x)$  has asymptotics  $x^\nu$  at  $x \rightarrow 0^+$ , then its Mellin transform  $\tilde{\phi}_1(z)$  is analytic on a right half-plane and has a simple pole at  $z = -\nu$  after analytic continuation. Function  $\phi_2(x)$  has asymptotics  $x^\nu$  as  $x \rightarrow \infty$ , then its Mellin transform  $\tilde{\phi}_2(z)$  is analytic on a left half-plane and has a simple pole at  $z = -\nu$  after analytic continuation.

**6.2 Three Prototypes of Asymptotics**

The three examples in the last section only serve to the motivation of the role of Mellin transform has played in the asymptotic analysis. Of course, there are a lot of functions with various asymptotics. For the sake of completeness, we list the three prototypes of asymptotics and their Mellin transforms that can be found in Bleistein and Handelsman [4], page 109–110.

**Example 6.4**

$$M[e^{-x}; z] = \Gamma(z).$$

The function  $f_1(x) = e^{-x}$  decays exponentially as  $x \rightarrow \infty$ , and its Mellin transform  $\tilde{f}_1(z) = \Gamma(z)$  is analytic in the right half-plane  $\Re(z) > 0$ .

**Example 6.5**

$$M[e^{ix}; z] = e^{\pi iz/2} \Gamma(z).$$

The function  $f_2(x) = e^{ix}$  oscillates as  $x \rightarrow \infty$ , then its Mellin transform  $\tilde{f}_2(z)$  is analytic in the strip  $0 < \Re(z) < 1$  and can be analytically continued into a holomorphic function in  $\Re(z) \geq 1$ .

**Example 6.6**

$$M \left[ \frac{1}{1+x}; z \right] = \frac{\pi}{\sin \pi z}.$$

The function  $f_3(x) = 1/(1+x)$  decays algebraically and monotonically as  $x \rightarrow \infty$ , then its Mellin transform  $\tilde{f}_3(z)$  is analytic in the strip  $0 < \Re(z) < 1$  and can be analytically continued to a meromorphic function in  $\Re(z) \geq 1$ .  $\tilde{f}_3(z)$  has simple poles at the positive integers in the region  $\Re(z) \geq 1$ .

The three examples illustrate the following:

1. If  $f(x)$  decays exponentially as  $x \rightarrow \infty$ , then  $\tilde{f}(z)$  is holomorphic in a right half-plane  $\Re(z) > c$ , for some  $c \in \mathbb{R}$ .
2. If  $f(x)$  oscillates as  $x \rightarrow \infty$ , then  $\tilde{f}(z)$  can be analytically continued into a right half-plane holomorphic function.
3. If  $f(x)$  decays algebraically and monotonically as  $x \rightarrow \infty$ , then  $\tilde{f}(z)$  can be analytically continued into a right half-plane meromorphic function.

Thus, by studying the Mellin transform  $\tilde{f}(z)$  and determining where  $\tilde{f}(z)$  is analytic, where the isolated singularities (poles) of  $\tilde{f}(z)$  are, one can gain the knowledge of the asymptotics of function  $f(x)$  as  $x \rightarrow \infty$ . For the purpose of our applications, we are interested in determining the asymptotics of function  $f(x)$  as  $x \rightarrow x_0$ , for some finite point  $x_0 \in \mathbb{R}$ . Without loss of generality, we assume the interval  $(0, a)$  to be the crack surface, and  $f(x)$  is only defined for  $0 < x < a$ . We extend  $f(x)$  by zero for  $x > a$ , so that  $\tilde{f}(z)$  exists and it is analytic in some right half-plane  $\sigma > c$  with

$$|\tilde{f}(\sigma + i\tau)| \rightarrow 0, \quad \text{as } |\tau| \rightarrow \infty. \quad (6.4)$$

### 6.3 Two Main Theorems

Martin [60] first proposed using Mellin transform to find the end-point behaviour of solutions to the quadratic hypersingular integral equations. The two main useful theorems are

**Theorem 6.1** (*Bleistein and Handelsman [4], Lemma 4.3.6*)

Given that  $f(x) = 0$  for  $x > a$  and

$$f(x) \sim \sum_{m=0}^{\infty} \sum_{n=0}^{N(m)} A_{mn} x^{a_m} (\ln x)^n \quad \text{as } x \rightarrow 0^+, \quad (6.5)$$

where  $\Re(a_0) \leq \Re(a_1) \leq \dots \leq \Re(a_m)$ , and  $0 \leq N(m)$ , a finite integer. Then  $\tilde{f}(z)$  is analytic in the right half-plane  $\Re(z) > -\Re(a_0)$  and can be analytically continued into  $\Re(z) \leq -\Re(a_0)$ , with poles at  $z = -a_m$ . The principal part of the Laurent expansion of  $\tilde{f}(z)$  about  $z = -a_m$  is

$$\sum_{n=0}^{N(m)} A_{mn} \frac{(-1)^n n!}{(z + a_m)^{n+1}}. \quad (6.6)$$

Also, (6.4) holds for all values of  $\sigma$ .

That is, the asymptotic expansion of  $f(x)$  for  $x \rightarrow 0^+$  completely determines the poles of  $\tilde{f}(z)$ . In (6.5), the exponents  $a_m$  to the variable  $x$  determines where the poles of  $\tilde{f}(z)$  are, and the powers  $n$  to function  $\ln x$  give the order of the poles. For our purpose, we need the other way of determination, *i.e.* given the knowledge of the pole(s) of  $\tilde{f}(z)$ , one can determine the corresponding asymptotic expansion of  $f(x)$  as  $x \rightarrow 0^+$ , and it is provided in the following theorem.

**Theorem 6.2** (*Oberhettinger [71], page 7*)

Suppose that  $\tilde{f}(z)$  is analytic in a left hand half-plane,  $\sigma \leq c$ , apart from poles at  $z = -a_m$ ,  $m = 0, 1, 2, \dots$ ; let the principal part of the Laurent expansion of  $\tilde{f}(z)$  about  $z = -a_m$  be given by (6.6). Assume that (6.4) holds for  $c' \leq \sigma \leq c$ . Then, if  $c'$

can be chosen so that

$$-\Re(a_{M+1}) < c' < -\Re(a_M) \quad \text{for some } M,$$

we have

$$f(x) = \sum_{m=0}^{\infty} \sum_{n=0}^{N(m)} A_{mn} x^{a_m} (\ln x)^n + R_M(x), \quad (6.7)$$

where

$$R_M(x) = \frac{1}{2\pi i} \int_{c'-i\infty}^{c'+i\infty} \tilde{f}(z) x^{-z} dz = \frac{x^{-c'}}{2\pi} \int_{-\infty}^{\infty} \tilde{f}(c' + i\tau) x^{-i\tau} d\tau. \quad (6.8)$$

The remainder  $R_M(x)$  is of order  $o(x^{\Re(a_M)})$  if, for instance,

$$\int_{-\infty}^{\infty} |\tilde{f}(c' + i\tau)| d\tau < \infty, \quad (6.9)$$

hence (6.7) is an asymptotic approximation.

Thus, we will focus on how to determine the pole(s) of  $\tilde{f}(z)$ , the Mellin transform of the unknown density function  $f(x)$ .

## 6.4 Crack-tip Asymptotics by the Mellin Transform

We demonstrate how the Mellin transform helps to determine the asymptotics of crack-tip behavior by giving some examples. Throughout the demonstration the following two equations turn out to be very useful.

$$\int_0^{\infty} \frac{x^z}{t-x} dx = \pi t^z \cot(\pi z) \quad \text{for } -1 < \sigma < 0. \quad (6.10)$$

$$\int_0^{\infty} \frac{x^z}{(t-x)^2} dx = -\pi z t^{z-1} \cot(\pi z) \quad \text{for } -1 < \sigma < 1. \quad (6.11)$$

$$\int_0^{\infty} \frac{x^{z+1}}{(t-x)^3} dx = \frac{\pi}{2} z(z+1) t^{z-1} \cot(\pi z) \quad \text{for } -2 < \sigma < 1. \quad (6.12)$$

Equation (6.10) can be found in many textbooks, for example, see Ref. [32]. Equations (6.11) and (6.12) is a combined result of (6.10) and (5.10).



### 6.4.1 Cauchy Singular Integral Equations

Recall that the crack problem for nonhomogeneous materials in classical LEFM if one chooses using slope  $(\partial/\partial x)w(x, 0) = \phi(x)$  as the density function, then equation (2.40) is obtained:

$$\frac{G(x)}{\pi} \int_c^d \left[ \frac{1}{t-x} + \frac{\beta}{2} \log|t-x| + \tilde{N}(x, t) \right] \phi(t) dt = p(x), \quad c < x < d.$$

In case of a homogeneous material is considered, equation above is reduced to a Cauchy singular integral equation

$$\frac{G}{\pi} \int_c^d \frac{\phi(t)}{t-x} dt = p(x), \quad c < x < d, \quad \text{with} \quad \int_c^d \phi(x) dx = 0. \quad (6.13)$$

Without loss of generality we have replaced the crack surface  $(c, d)$  to  $(0, a)$  in (6.13), and it has the exact solution

$$\phi(x) = \frac{1}{\pi G \sqrt{x(a-x)}} \int_0^a \frac{p(t) \sqrt{x(a-x)}}{x-t} dt.$$

Clearly, one may see that  $1/\sqrt{x(a-x)}$  is an admissible behavior of  $\phi(x)$  around the crack tips. Here we use Mellin transform to see the same conclusion is drawn.

**Proposition 6.1** *If  $\phi \in C^{0,\alpha}(0, a)$ ,  $0 < \alpha \leq 1$ , and  $\phi(x) = 0$ , for  $x > a$ . Also  $\phi(x)$  satisfies*

$$\frac{G}{\pi} \int_0^a \frac{\phi(t)}{t-x} dt = p(x), \quad 0 < x < a, \quad \int_0^a \phi(x) dx = 0, \quad (6.14)$$

where  $p(x)$  is integrable and

$$\lim_{x \rightarrow 0^+} p(x) < \infty, \quad \lim_{x \rightarrow a^-} p(x) < \infty.$$

Then,  $\phi(x)$  has the following admissible asymptotics:

$$\phi(x) \sim \frac{1}{\sqrt{x}}, \quad \text{as } x \rightarrow 0^+.$$

*Proof* Taking Mellin transform on both side of the Cauchy singular integral equation (6.14), one has

$$\frac{G}{\pi} \int_0^\infty \int_0^a \frac{\phi(t)}{t-x} dt x^{z-1} dx = \tilde{p}(z),$$

$$\begin{aligned}
 &\Rightarrow \frac{G}{\pi} \int_0^a \phi(t) \int_0^\infty \frac{x^{z-1}}{t-x} dx dt = \bar{p}(z), \\
 &\Rightarrow \frac{G}{\pi} \int_0^a \phi(t) \pi t^{z-1} \cot(\pi z) dt = \bar{p}(z), \\
 &\Rightarrow G \cot(\pi z) \int_0^a \phi(t) t^{z-1} dt = \bar{p}(z), \\
 &\Rightarrow G \tilde{\phi}(z) = \bar{p}(z) / \cot(\pi z), \\
 &\Rightarrow \phi(x) \sim \frac{1}{\sqrt{x}}, \text{ as } x \rightarrow 0^+, \text{ is admissible.}
 \end{aligned}$$

This completes the proof.

**Proposition 6.2** *If  $\phi(x)$  satisfies the conditions as in Proposition 6.1 except the Cauchy singular integral equation (6.14) is replaced by*

$$\frac{G}{\pi} \int_0^a \frac{\phi(t)}{t-x} dt + \int_0^a k(x,t)\phi(t) dt = p(x), \quad 0 < x < a, \quad \int_0^a \phi(x) dx = 0, \quad (6.15)$$

*Then,  $\phi(x)$  has the following admissible asymptotics:*

$$\phi(x) \sim \frac{1}{\sqrt{x}}, \text{ as } x \rightarrow 0^+.$$

*Proof* Denote

$$(K\phi)(x) = \int_0^a k(x,t)\phi(t) dt.$$

The regularity of the nonsingular  $k(x,t)$  makes

$$(K\phi)(x) \sim \begin{cases} c_\infty x^{-\alpha}, & \text{as } x \rightarrow \infty, \quad \alpha > 1 \\ c_0 x^\beta, & \text{as } x \rightarrow 0, \quad \beta > -1/2 \end{cases}$$

Similar to the proof for Proposition 6.1, by taking Mellin transform on both side of (6.15), one obtains

$$G \cot(\pi z) \tilde{\phi}(z) + K \tilde{\phi}(z) = \tilde{p}(z),$$

which leads to

$$\begin{aligned} G \tilde{\phi}(z) &= [\tilde{p}(z) - K \tilde{\phi}(z)] / \cot(\pi z), \\ \Rightarrow \phi(x) &\sim \frac{1}{\sqrt{x}}, \quad \text{as } x \rightarrow 0^+, \quad \text{is admissible.} \end{aligned}$$

This completes the proof.

### 6.4.2 Quadratic Hypersingular Integral Equations

The study of crack-tip asymptotics of quadratic hypersingular integral equations by using Mellin transform has been addressed by Martin [60], thus we shall be brief in this subsection. Recall that equation (2.34)

$$\frac{G_0}{\pi} \int_c^d \frac{w(t, 0^+)}{(t-x)^2} dt = p(x), \quad c < x < d.$$

in Chapter 2 is a quadratic hypersingular integral equation.

**Proposition 6.3** *If  $\phi \in C^{1,\alpha}(0, a)$ ,  $0 < \alpha \leq 1$ , and  $\phi(0) = \phi(a) = 0$ . Also  $\phi(x)$  satisfies*

$$\frac{1}{\pi} \int_0^a \frac{\phi(t)}{(t-x)^2} dt = p(x), \quad 0 < x < a, \quad (6.16)$$

where  $p(x)$  is integrable and

$$\lim_{x \rightarrow 0^+} p(x) < \infty, \quad \lim_{x \rightarrow a^-} p(x) < \infty.$$

Then,  $\phi(x)$  has the following admissible asymptotics:

$$\phi(x) \sim \sqrt{x}, \quad \text{as } x \rightarrow 0^+.$$

*Proof* When  $x > a$ ,  $p(x)$  is defined by the left-hand-side of (6.16), thus  $p(x) \sim 1/x^2$  as  $x \rightarrow \infty$ , and the Mellin transform  $\tilde{\phi}(z)$  of  $p(x)$  is analytic for  $0 < \text{Re}(z) < 2$ . Taking the “zth moment” Mellin transform on both side of the quadratic hypersingular

integral equation (6.16), one obtains

$$\begin{aligned}
 & \frac{1}{\pi} \int_0^\infty \int_0^a \frac{\phi(t)}{(t-x)^2} dt x^z dx = \bar{p}(z+1), \\
 \Rightarrow & \frac{1}{\pi} \int_0^a \phi(t) \int_0^\infty \frac{x^z}{(t-x)^2} dx dt = \bar{p}(z+1), \\
 \Rightarrow & \frac{1}{\pi} \int_0^a \phi(t) (-\pi) z t^{z-1} \cot(\pi z) dt = \bar{p}(z+1), \\
 \Rightarrow & -z \cot(\pi z) \int_0^a \phi(t) t^{z-1} dt = \bar{p}(z+1), \\
 \Rightarrow & -z \cot(\pi z) \tilde{\phi}(z) = \bar{p}(z+1),
 \end{aligned}$$

If  $\lim_{z \rightarrow -1/2} \bar{p}(z+1) = \lim_{z \rightarrow 1/2} \bar{p}(z) \neq 0$ , then  $\phi(x) \sim \sqrt{x}$ , as  $x \rightarrow 0^+$ .

This completes the proof.

### 6.4.3 Cubic Hypersingular Integral Equations

In this subsection we study the crack-tip asymptotics of cubic hypersingular integral equations by using Mellin transform.

**Proposition 6.4** *If  $\phi \in C^{2,\alpha}(0, a)$ ,  $0 < \alpha \leq 1$ , and  $\phi(0) = \phi(a) = 0$ . Also  $\phi(x)$  satisfies*

$$\frac{1}{\pi} \int_0^a \frac{\phi(t)}{(t-x)^3} dt = p(x), \quad 0 < x < a, \quad (6.17)$$

where  $p(x)$  is integrable and

$$\lim_{x \rightarrow 0^+} p(x) < \infty, \quad \lim_{x \rightarrow a^-} p(x) < \infty.$$

Then,  $\phi(x)$  has the following admissible asymptotics:

$$\phi(x) \sim \sqrt{x}, \quad \text{as } x \rightarrow 0^+.$$

*Proof* When  $x > a$ ,  $p(x)$  is defined by the left-hand-side of (6.17), thus  $p(x) \sim 1/x^3$  as  $x \rightarrow \infty$ , and the Mellin transform  $\tilde{\phi}(z)$  of  $p(x)$  is analytic for  $0 < \operatorname{Re}(z) < 3$ . Taking the “ $(z + 1)$ th moment” Mellin transform on both side of the cubic hypersingular integral equation (6.17), one obtains

$$\begin{aligned} & \frac{1}{\pi} \int_0^\infty \int_0^a \frac{\phi(t)}{(t-x)^3} dt x^{z+1} dx = \bar{p}(z+2), \\ \Rightarrow & \frac{1}{\pi} \int_0^a \phi(t) \int_0^\infty \frac{x^{z+1}}{(t-x)^3} dx dt = \bar{p}(z+2), \\ \Rightarrow & \frac{1}{\pi} \int_0^a \phi(t) \frac{\pi}{2} z(z+1) t^{z-1} \cot(\pi z) dt = \bar{p}(z+2), \\ \Rightarrow & \frac{1}{2} z(z+1) \cot(\pi z) \int_0^a \phi(t) t^{z-1} dt = \bar{p}(z+2), \\ \Rightarrow & \frac{1}{2} z(z+1) \cot(\pi z) \tilde{\phi}(z) = \bar{p}(z+2), \end{aligned}$$

*Case I* If

$$\lim_{z \rightarrow -1/2} \bar{p}(z+2) = \lim_{z \rightarrow 3/2} \bar{p}(z) \neq 0,$$

then  $\tilde{\phi}(z)$  has a simple pole at  $z = -1/2$ . Thus

$$\phi(x) \sim \sqrt{x}, \quad \text{as } x \rightarrow 0^+.$$

*Case II* If

$$\lim_{z \rightarrow -1/2} \bar{p}(z+2) = \lim_{z \rightarrow 3/2} \bar{p}(z) = 0,$$

and

$$\lim_{z \rightarrow -3/2} \bar{p}(z+2) = \lim_{z \rightarrow 1/2} \bar{p}(z) \neq 0,$$

then  $\tilde{\phi}(z)$  has a simple pole at  $z = -3/2$ . Thus

$$\phi(x) \sim x^{3/2}, \quad \text{as } x \rightarrow 0^+.$$

This completes the proof.

## Chapter 7

# Evaluation of Hypersingular Integrals

The focus of this chapter is to exactly evaluate hypersingular integrals of the type

$$I_\alpha(T_n, m, r) = \int_{-1}^1 \frac{T_n(s)(1-s^2)^{m-\frac{1}{2}}}{(s-r)^\alpha} ds, \quad |r| < 1 \quad (7.1)$$

and

$$I_\alpha(U_n, m, r) = \int_{-1}^1 \frac{U_n(s)(1-s^2)^{m-\frac{1}{2}}}{(s-r)^\alpha} ds, \quad |r| < 1 \quad (7.2)$$

for general integers  $\alpha$  (positive) and  $m$  (non-negative), where  $T_n(s)$  and  $U_n(s)$  are the Chebyshev polynomials of the 1st and 2nd kinds, respectively. Exact formulas are derived for the cases  $\alpha = 1, 2, 3, 4$  and  $m = 0, 1, 2, 3$ .

### 7.1 Theoretical Aspects

From Chapter 2 and Chapter 4 we learn that the final form of hypersingular integral equation can be written as

$$\int_c^d \frac{c_\alpha D(t)}{(t-x)^\alpha} dt + \int_c^d k(x, t)D(t) dt + f(x) = p(x), \quad c < x < d, \quad (7.3)$$

where  $\int$  denotes an improper integral;  $c_\alpha$  is a constant associated to the singular kernel  $1/(t-x)^\alpha$ ;  $k(x, t)$  is the nonsingular (regular) kernel;  $f(x)$  is a function standing for some extra term;  $p(x)$  is generally for the force function. The parameter  $\alpha$  is a positive integer which determines the degree of the singularity. If  $\alpha = 1$ , the integral equation (7.3) is called a Cauchy singular integral equation, and the singular term is evaluated as a Cauchy principal value (CPV) integral. If  $\alpha \geq 2$ , it is called a hypersingular integral equation and the singular term is evaluated as a Hadamard finite part (HFP) integral [50, 54, 61, 67, 70, 80, 81]. Here the notation  $\int$  and  $\int$  refer to CPV and HFP integrals, respectively.

### 7.1.1 Integration and Approximation

As far as the integration and numerical procedures are concerned, the integral equation (7.3) may be normalized through the following change of variables

$$s = \frac{2}{d-c} \left( t - \frac{c+d}{2} \right) \quad \text{and} \quad r = \frac{2}{d-c} \left( x - \frac{c+d}{2} \right), \quad (7.4)$$

which leads to the normalized version of the integral equation (7.3) written as<sup>1</sup>

$$\int_{-1}^1 \frac{D(s)}{(s-r)^\alpha} ds + \int_{-1}^1 \mathcal{K}(r, s) D(s) ds + F(r) = P(r), \quad -1 < r < 1. \quad (7.5)$$

The density function  $D(s)$  is further assumed to have the representation

$$D(s) = R(s)W(s). \quad (7.6)$$

The weight function  $W(s)$  determines the singular behavior of the solution  $D(s)$  and has the form

$$W(s) = (1-s)^{m_1}(1+s)^{m_2}. \quad (7.7)$$

---

<sup>1</sup>The notations in this thesis have been chosen as following:  $x$  and  $t$  refer to the physical quantities and have dimension of "Length";  $r$  and  $s$  are normalized (dimensionless) variables, corresponding to  $x$  and  $t$ , respectively. This choice of convention has been consistently used in the rest of the thesis.

In general,  $m_1 \neq m_2$ , and the corresponding integrals, which involve Jacobi polynomials  $P_n^{(m_1, m_2)}(s)$ , are of the type

$$\int_{-1}^1 \frac{(1-s)^{m_1}(1+s)^{m_2} P_n^{(m_1, m_2)}(s)}{s-r} ds, \quad (7.8)$$

and can be expressed in terms of gamma and hypergeometric functions [42, 53]. In this paper, only the case  $m_1 = m_2$  is considered and  $m_1, m_2$  are set to be

$$m_1 = m_2 = m - \frac{1}{2}. \quad (7.9)$$

Thus  $W(s)$  can be expressed as

$$W(s) = (1-s^2)^{m-\frac{1}{2}} \quad m = 0, 1, 2, \dots \quad (7.10)$$

The value of  $m$  is determined by the order of singularity  $\alpha$ . As  $\alpha = 1$ , one may apply Muskhelishvili's procedure [68, 69] to the corresponding (Cauchy) singular integral equation and find  $m = 0$ . Thus the solution  $D(s)$  to the Cauchy singular integral equation (7.5) takes the form

$$D(s) = \frac{R(s)}{\sqrt{1-s^2}}. \quad (7.11)$$

In this case, which consists of the majority of the work involving applications of integral equations to fracture mechanics (Wang and Karihaloo [95]; Erdogan [24]; Meguid and Wang [62]),  $R(s)$  is chosen to be

$$R(s) = \sum_n^{\infty} a_n T_n(s); \quad (7.12)$$

and because of that, the CPV integral  $I_1(T_n, 0, r)$  can be evaluated exactly [50, 42, 30]:

$$I_1(T_n, 0, r) = \int_{-1}^1 \frac{T_n(s)}{(s-r)\sqrt{1-s^2}} ds = \begin{cases} 0, & n = 0 \\ \pi U_{n-1}(r), & n \geq 1. \end{cases} \quad (7.13)$$

Another reason for choosing the expansion (7.12) is that with respect to the weight function  $W(s) = 1/\sqrt{1-s^2}$ , the class of the Chebyshev polynomials of first kind



$T_n(s)$  is an orthogonal family (Hochstrasser [42]):

$$\int_{-1}^1 \frac{T_m(s)T_n(s)}{\sqrt{1-s^2}} ds = \begin{cases} \pi & m = n = 0 \\ \pi/2 & m = n; \quad m, n = 1, 2, 3, \dots \\ 0 & m \neq n; \quad m, n = 0, 1, 2, \dots \end{cases} \quad (7.14)$$

With this orthogonal property a Galerkin-type method (Krenk [52]) may be applied to find the coefficients  $a_n$  in equation (7.12).

If  $\alpha = 2$ , then  $m = 1$ , and the solution  $D(s)$  to the hypersingular integral equation (7.5) is characterized by

$$D(s) = R(s)\sqrt{1-s^2}. \quad (7.15)$$

Correspondingly,  $R(s)$  is chosen to be

$$R(s) = \sum_n^{\infty} b_n U_n(s), \quad (7.16)$$

because of the same reasons for the case  $\alpha = 1$ , namely, analytical evaluation and orthogonal property. With respect to the first reason, the HFP integral  $I_2(U_n, 1, r)$  can be evaluated analytically (Kaya and Erdogan [50]):

$$I_2(U_n, 1, r) = \oint_{-1}^1 \frac{U_n(s)\sqrt{1-s^2}}{(s-r)^2} ds = -(n+1)\pi U_n(r), \quad n \geq 0. \quad (7.17)$$

According to the second reason, by orthogonality,

$$\int_{-1}^1 U_m(s)U_n(s)\sqrt{1-s^2} ds = \begin{cases} \pi/2 & m = n; \quad m, n = 0, 1, 2, \dots \\ 0 & m \neq n; \quad m, n = 0, 1, 2, \dots \end{cases}, \quad (7.18)$$

and one may apply Galerkin-type methods (Krenk [52]) to find the coefficients  $b_n$  in equation (7.16).

When  $\alpha = 3$ , then  $m \geq 1$ . For instance, with  $m = 2$ , the weight function  $W(s) = (1-s^2)^{3/2}$ , neither  $T_n(s)$  nor  $U_n(s)$  is an orthogonal family. *However, if collocation*

method is applied, one does not need the orthogonal property, as long as the expansion function  $R(s)$  is chosen such that

$$\int_{-1}^1 \frac{R(s)(1-s^2)^{\frac{3}{2}}}{(s-r)^3} ds$$

can be evaluated analytically. For example, if  $R(s)$  is expanded as a Chebyshev polynomial of the 1st kind  $T_n(s)$  or the 2nd kind  $U_n(s)$ , i.e.

$$R(s) = \sum_n a_n T_n(s) \quad \text{or} \quad R(s) = \sum_n b_n U_n(s), \quad (7.19)$$

then the evaluation of

$$I_\alpha(T_n, m, r) = \int_{-1}^1 \frac{T_n(s)(1-s^2)^{m-\frac{1}{2}}}{(s-r)^\alpha} ds$$

or

$$I_\alpha(U_n, m, r) = \int_{-1}^1 \frac{U_n(s)(1-s^2)^{m-\frac{1}{2}}}{(s-r)^\alpha} ds$$

for general  $m = 0, 1, 2, \dots$  and  $\alpha = 1, 2, 3, \dots$  is a necessary step for the numerical approach to the integral equation (7.5). This is the one of main tasks in this paper and is addressed in Sections 7.4 and 7.5 .

### 7.1.2 Selection of the Density Function

Usually the unknown function  $D(t)$  in equation (7.3) can be chosen as the displacement profile (e.g.  $u(t)$  – a displacement function), the (first) derivative of the displacement function ( $du(t)/dt$ , denoted by  $\phi(t)$  – the slope function), or a higher derivative of  $u(t)$ . The choice of the unknown function  $D(t)$  will affect the degree of singularity in the formulation. For example, consider the standard mode III crack problem in a free space (Gdoutos [39]) and a linear elastic fracture mechanics (LEFM) setting. If  $D(t)$  is chosen to be the slope function  $\phi(t)$ , then the governing integral equation is the Cauchy singular integral equation

$$D(t) \equiv \phi(t) \quad , \quad \int_c^d \frac{\phi(t)}{t-x} dt = p(x) \quad , \quad c < x < d . \quad (7.20)$$

However, if  $D(t)$  is chosen to be the displacement function  $w(t)$ , then the hypersingular integral equation with  $\alpha = 2$  is obtained,

$$D(t) \equiv w(t) \ , \ \oint_c^d \frac{w(t)}{(t-x)^2} dt = p(x) \ , \ c < x < d . \quad (7.21)$$

The differences between the above two formulations are discussed next.

Note that the higher singularity in (7.21) does *not* constitute more difficulty in solving the equation since hypersingular integrals in both (7.20) and (7.21) can be evaluated exactly with the suitable basis functions. So the choice of the density functions should be dictated by considerations other than the order of singularity in the resulting equations. There are situations, however, in which the displacements appear to be more natural than the slopes, e.g., in periodic (Schulze and Erdogan [78]) or three dimensional crack problems. Sometimes, a formulation with higher singular kernels results in simpler nonsingular kernels in the decomposition (2.24) (see Section 7 for discussion of examples).

### 7.1.3 Properties of Chebyshev Polynomials

The evaluation of Cauchy singular and hypersingular integrals which involve the Chebyshev polynomials  $T_n(s)$  and  $U_n(s)$  highly depends on the special properties of these polynomials. They are listed here for the sake of completeness and because they will be of much use later in the development of this work. Most of them (but not all) can be found in Hochstrasser [42] and Kaya and Erdogan [50].

- Definition of Chebyshev polynomials of the first kind:

$$T_n(s) = \cos[n \cos^{-1}(s)] \ , \quad n = 0, 1, 2, \dots \quad (7.22)$$

- Definition of Chebyshev polynomials of the second kind:

$$U_n(s) = \frac{\sin[(n+1) \cos^{-1}(s)]}{\sin[\cos^{-1}(s)]} \ , \quad n = 0, 1, 2, \dots \quad (7.23)$$

• Iterative (recursive) properties:

$$sT_n(s) = \frac{1}{2}[T_{n+1}(s) + T_{n-1}(s)] , \quad n \geq 1 \quad (7.24)$$

$$sU_n(s) = \frac{1}{2}[U_{n+1}(s) + U_{n-1}(s)] , \quad n \geq 1 \quad (7.25)$$

$$T_n(s) = \frac{1}{2}[U_n(s) - U_{n-2}(s)] , \quad n \geq 2 \quad (7.26)$$

$$U_n(s)(1 - s^2) = sT_{n+1}(s) - T_{n+2}(s) , \quad n \geq 0 \quad (7.27)$$

By means of equation (7.24), one may rewrite equation (7.27) above as

$$U_n(s) = \frac{1}{2(1 - s^2)}[T_n(s) - T_{n+2}(s)] , \quad n \geq 0 \quad (7.28)$$

Thus an additional equality, which is useful in handling cubic hypersingular integrals can be derived<sup>2</sup>:

$$\begin{aligned} U_n(s)(1 - s^2)^{\frac{3}{2}} &\stackrel{(7.28)}{=} \frac{1}{2}[T_n(s) - T_{n+2}(s)]\sqrt{1 - s^2} \\ &\stackrel{(7.26)}{=} -\frac{1}{2}\left[\frac{1}{2}U_{n+2}(s) - U_n(s) + \frac{1}{2}U_{n-2}(s)\right]\sqrt{1 - s^2} , \quad n \geq 2 \\ &= -\frac{1}{4}[U_{n+2}(s) - 2U_n(s) + U_{n-2}(s)]\sqrt{1 - s^2} , \quad n \geq 2 \end{aligned} \quad (7.29)$$

• Derivatives:

$$\frac{dT_n(s)}{ds} = nU_{n-1}(s) , \quad n \geq 1 \quad (7.30)$$

$$\frac{dU_n(s)}{ds} = \frac{1}{1 - s^2}\left[\frac{n+2}{2}U_{n-1}(s) - \frac{n}{2}U_{n+1}(s)\right] , \quad n \geq 1 \quad (7.31)$$

---

<sup>2</sup>The equation number is stacked above the equal sign to show how the equations are being derived and connected.

## 7.2 Cauchy Singular Integral Formulas ( $\alpha = 1$ )

This section mainly evaluates  $I_1(T_n, m, r)$  and  $I_1(U_n, m, r)$ , which are defined in equations (7.1) and (7.2). The new result here is that the singular integral formulas are found for general  $m$ . In order to obtain this new result, two well known Cauchy singular integral formulas are introduced (Hochstrasser [42]): one is already stated in equation (7.13), and the other one is

$$I_1(U_n, 1, r) = \int_{-1}^1 \frac{U_n(s)\sqrt{1-s^2}}{s-r} ds = -\pi T_{n+1}(r), \quad n \geq 0, \quad (7.32)$$

which can be obtained as follows

$$\begin{aligned} I_1(U_n, 1, r) &= \int_{-1}^1 \frac{U_n(s)\sqrt{1-s^2}}{s-r} ds \\ &\stackrel{(7.28)}{=} \frac{1}{2} \int_{-1}^1 \frac{T_n(s) - T_{n+2}(s)}{\sqrt{1-s^2}(s-r)} ds \\ &\stackrel{(7.13)}{=} \frac{\pi}{2} [U_{n-1}(r) - U_{n+1}(r)] \\ &\stackrel{(7.26)}{=} -\pi T_{n+1}(r). \end{aligned}$$

The integral formulas for  $m = 0, 1, 2, 3, \dots$  are derived below. The general formulas have the restriction of minimum  $n$ . For instance, equations (7.26) and (7.29) are only true for  $n \geq 2$ , and equations (7.30) and (7.31) are valid for  $n \geq 1$ . The lower  $n$  terms can not be derived by general formulas, and are given in Appendix A.

### 7.2.1 $I_1(T_n, m, r)$ , $m = 0, 1, 2, 3$

- $I_1(T_n, 0, r)$ : This is equation (7.13).

- $I_1(T_n, 1, r)$ :

$$\begin{aligned} \int_{-1}^1 \frac{T_n(s)\sqrt{1-s^2}}{s-r} ds &\stackrel{(7.26)}{=} \frac{1}{2} \int_{-1}^1 \frac{[U_n(s) - U_{n-2}(s)]\sqrt{1-s^2}}{s-r} ds \\ &\stackrel{(7.32)}{=} \frac{\pi}{2} [T_{n-1}(r) - T_{n+1}(r)], \quad n \geq 2. \end{aligned} \quad (7.33)$$

- $I_1(T_n, 2, r)$ :

$$\begin{aligned}
 & \int_{-1}^1 \frac{T_n(s)(1-s^2)^{\frac{3}{2}}}{s-r} ds \stackrel{(7.26)}{=} \int_{-1}^1 \frac{\frac{1}{2}[U_n(s) - U_{n-2}(s)](1-s^2)^{\frac{3}{2}}}{s-r} ds \\
 & \stackrel{(7.36)}{=} \frac{\pi}{8} \{ [T_{n-1}(r) - 2T_{n+1}(r) + T_{n+3}(r)] - [T_{n-3}(r) - 2T_{n-1}(r) + T_{n+1}(r)] \} \\
 & = -\frac{\pi}{8} [T_{n-3}(r) - 3T_{n-1}(r) + 3T_{n+1}(r) - T_{n+3}(r)] , \quad n \geq 4 \quad (7.34)
 \end{aligned}$$

- $I_1(T_n, 3, r)$ :

$$\begin{aligned}
 & \int_{-1}^1 \frac{T_n(s)(1-s^2)^{\frac{5}{2}}}{s-r} ds \stackrel{(7.26)}{=} \int_{-1}^1 \frac{\frac{1}{2}[U_n(s) - U_{n-2}(s)](1-s^2)^{\frac{5}{2}}}{s-r} ds \\
 & \stackrel{(7.37)}{=} \frac{\pi}{32} \{ [T_{n-5}(r) - 4T_{n-3}(r) + 6T_{n-1}(r) - 4T_{n+1}(r) + T_{n+3}(r)] - \\
 & \quad [T_{n-3}(r) - 4T_{n-1}(r) + 6T_{n+1}(r) - 4T_{n+3}(r) + T_{n+5}(r)] \} , \quad n \geq 6 \\
 & = \frac{\pi}{32} [T_{n-5}(r) - 5T_{n-3}(r) + 10T_{n-1}(r) \\
 & \quad - 10T_{n+1}(r) + 5T_{n+3}(r) - T_{n+5}(r)] , \quad n \geq 6 \quad (7.35)
 \end{aligned}$$

### 7.2.2 $I_1(U_n, m, r)$ , $m = 1, 2, 3$

- $I_1(U_n, 1, r)$ : This is equation (7.32).

- $I_1(U_n, 2, r)$ :

$$\begin{aligned}
 & \int_{-1}^1 \frac{U_n(s)(1-s^2)^{\frac{3}{2}}}{s-r} ds \stackrel{(7.28)}{=} \frac{1}{2} \int_{-1}^1 \frac{[T_n(s) - T_{n+2}(s)]\sqrt{1-s^2}}{s-r} ds \\
 & \stackrel{(7.33)}{=} \frac{\pi}{4} \{ [T_{n-1}(r) - T_{n+1}(r)] - [T_{n+1}(r) - T_{n+3}(r)] \} , \quad n \geq 2 \\
 & = \frac{\pi}{4} [T_{n-1}(r) - 2T_{n+1}(r) + T_{n+3}(r)] , \quad n \geq 2 \quad (7.36)
 \end{aligned}$$

- $I_1(U_n, 3, r)$ :

$$\begin{aligned}
 & \int_{-1}^1 \frac{U_n(s)(1-s^2)^{\frac{5}{2}}}{s-r} ds \stackrel{(7.28)}{=} \frac{1}{2} \int_{-1}^1 \frac{[T_n(s) - T_{n+2}(s)](1-s^2)^{\frac{3}{2}}}{s-r} ds \\
 & \stackrel{(7.34)}{=} \frac{\pi}{16} \{ [T_{n-1}(r) - 3T_{n+1}(r) + 3T_{n+3}(r) - T_{n+5}(r)] - \\
 & \quad [T_{n-3}(r) - 3T_{n-1}(r) + 3T_{n+1}(r) - 3T_{n+3}(r)] \} , \quad n \geq 4 \\
 & = -\frac{\pi}{16} [T_{n-3}(r) - 4T_{n-1}(r) + 6T_{n+1}(r) - 4T_{n+3}(r) + T_{n+5}(r)] . \quad (7.37)
 \end{aligned}$$

**7.2.3  $I_1(T_n, m, r)$  and  $I_1(U_n, m, r)$**

At this point one may easily see the procedural steps above, which take advantage of recursive properties (7.26) and (7.28) between the Chebyshev polynomials  $T_n(s)$  and  $U_n(s)$ . For instance, evaluation of  $I_1(T_n, 4, r) = \int_{-1}^1 T_n(s)(1 - s^2)^{7/2}/(s - r)ds$  can be reduced to evaluation of  $I_1(U_n, 4, r) = \int_{-1}^1 U_n(s)(1 - s^2)^{7/2}/(s - r)ds$ , which, in turn, can be reduced to evaluation of  $I_1(T_n, 3, r) = \int_{-1}^1 T_n(s)(1 - s^2)^{5/2}/(s - r)ds$ . After a suitable number of steps, this reduction leads to either (7.13) or (7.32). This procedure can be summarized as the following flow chart:

$$\begin{aligned}
 & \int_{-1}^1 \frac{T_n(s)(1 - s^2)^{m+\frac{1}{2}}}{s - r} ds \\
 & \quad \Downarrow (7.26) \\
 & \int_{-1}^1 \frac{U_n(s)(1 - s^2)^{m+\frac{1}{2}}}{s - r} ds \\
 & \quad \Downarrow (7.28) \\
 & \int_{-1}^1 \frac{T_n(s)(1 - s^2)^{m-\frac{1}{2}}}{s - r} ds \\
 & \quad \Downarrow (7.26) \\
 & \int_{-1}^1 \frac{U_n(s)(1 - s^2)^{m-\frac{1}{2}}}{s - r} ds \\
 & \quad \Downarrow (7.28) \\
 & \quad \vdots \\
 & \quad \Downarrow \\
 & \text{Equation (7.13) or (7.32)}
 \end{aligned}$$

This procedure reduces integrals with higher  $m$  to those with lower  $m$ . Another way of evaluating  $I_1(T_n, m, r)$  and  $I_1(U_n, m, r)$  is by using the recursive property through  $T_n(s)$  only, which is discussed in Section 7.2.4.

- $I_1(T_n, m, r)$ , where  $m \geq 1$ , and  $n \geq 2m$

$$\int_{-1}^1 \frac{T_n(s)(1-s^2)^{m-\frac{1}{2}}}{s-r} ds = \pi(-1)^{m+1} 2^{1-2m} \sum_{j=0}^{2m-1} (-1)^j \binom{2m-1}{j} T_{n+1-2m+2j}(r) \quad (7.38)$$

- $I_1(U_n, m, r)$ , where  $m \geq 2$ , and  $n \geq 2m - 2$

$$\int_{-1}^1 \frac{U_n(s)(1-s^2)^{m-\frac{1}{2}}}{s-r} ds = \pi(-1)^m \left(\frac{1}{2}\right)^{2m-2} \sum_{j=0}^{2m-2} (-1)^j \binom{2m-2}{j} T_{n+3-2m+2j}(r) \quad (7.39)$$

The usual notation

$$\binom{m}{j} = \frac{(m)!}{j!(m-j)!}$$

denotes the binomial coefficients.

#### 7.2.4 Alternative Approach

Instead of using the recursive property between the Chebyshev polynomials  $T_n(s)$  and  $U_n(s)$ , *i.e.* equations (7.26) and (7.28), another way of evaluating  $I_1(T_n, m, r)$  and  $I_1(U_n, m, r)$  is by using the recursive property through  $T_n(s)$  only. By equations (7.26) and (7.28) one may obtain

$$T_n(s)(1-s^2) = -\frac{1}{4}T_{n-2}(s) + \frac{1}{2}T_n(s) - \frac{1}{4}T_{n+2}(s), \quad n \geq 2. \quad (7.40)$$

Thus both the integrals  $I_1(T_n, m+1, r)$  and  $I_1(U_n, m+1, r)$  can be deduced from knowing  $I_1(T_n, m, r)$ . For example, an alternative way of deriving equation (7.33) is

$$\begin{aligned} & \int_{-1}^1 \frac{T_n(s)\sqrt{1-s^2}}{s-r} ds \stackrel{(7.40)}{=} \\ & -\frac{1}{4} \int_{-1}^1 \frac{T_{n-2}(s)}{(s-r)\sqrt{1-s^2}} + \frac{1}{2} \int_{-1}^1 \frac{T_n(s)}{(s-r)\sqrt{1-s^2}} - \frac{1}{4} \int_{-1}^1 \frac{T_{n+2}(s)}{(s-r)\sqrt{1-s^2}} \end{aligned}$$



$$\begin{aligned}
 &= \begin{cases} \frac{\pi}{2}[T_1(r) - T_3(r)] , & n = 2 \\ \frac{\pi}{4}[U_{n-3}(r) + 2U_{n-1}(r) - U_{n+1}(r)] , & n \geq 3 \end{cases} \\
 &= \frac{\pi}{2}[T_{n-1}(r) - T_{n+1}(r)] , \quad n \geq 2 .
 \end{aligned}$$

This alternative derivation applies to all the other formulas derived in this paper, such as equations (7.38), (7.39), (7.45), (7.49), (7.55), (7.59), (7.64), and (7.67).

### 7.3 Hypersingular Integral Formulas ( $\alpha \geq 2$ )

Once a Cauchy singular integral formula has been reached, all other hypersingular integral formulas may be obtained successively by taking differentiation with respect to  $r$  through the recursive definition of the finite part integral (5.10).

#### 7.3.1 $I_2(T_n, m, r)$

By means of

$$\int_{-1}^1 \frac{T_n(s)(1-s^2)^{m-\frac{1}{2}}}{(s-r)^2} ds = \frac{d}{dr} \int_{-1}^1 \frac{T_n(s)(1-s^2)^{m-\frac{1}{2}}}{s-r} ds ,$$

one readily obtains

- $I_2(T_n, 0, r)$  (see also Kaya and Erdogan [50]):

$$\begin{aligned}
 &\int_{-1}^1 \frac{T_n(s)}{\sqrt{1-s^2}(s-r)^2} ds = \pi \frac{d}{dr} U_{n-1}(r) \\
 &\stackrel{(7.31)}{=} \frac{\pi}{1-r^2} \left[ \frac{n+1}{2} U_{n-2}(r) - \frac{n-1}{2} U_n(r) \right] , \quad n \geq 2 \quad (7.41)
 \end{aligned}$$

- $I_2(T_n, 1, r)$ :

$$\begin{aligned}
 &\int_{-1}^1 \frac{T_n(s)\sqrt{1-s^2}}{(s-r)^2} ds = \frac{\pi}{2} \frac{d}{dr} [T_{n-1}(r) - T_{n+1}(r)] \\
 &\stackrel{(7.30)}{=} \frac{\pi}{2} [(n-1)U_{n-2}(r) - (n+1)U_n(r)] , \quad n \geq 2 \quad (7.42)
 \end{aligned}$$

- $I_2(T_n, 2, r)$ :

$$\begin{aligned} \int_{-1}^1 \frac{T_n(s)(1-s^2)^{\frac{3}{2}}}{(s-r)^2} ds &= -\frac{\pi}{8} \frac{d}{dr} [T_{n-3}(r) - 3T_{n-1}(r) + 3T_{n+1}(r) - T_{n+3}(r)] \\ &\stackrel{(7.30)}{=} -\frac{\pi}{8} [(n-3)U_{n-4}(r) - 3(n-1)U_{n-2}(r) + 3(n+1)U_n(r) - \\ &\quad (n+3)U_{n+2}(r)], \quad n \geq 4 \end{aligned} \quad (7.43)$$

- $I_2(T_n, 3, r)$ :

$$\begin{aligned} \int_{-1}^1 \frac{T_n(s)(1-s^2)^{\frac{5}{2}}}{(s-r)^2} ds &= \frac{\pi}{32} \frac{d}{dr} [T_{n-5}(r) - 5T_{n-3}(r) + 10T_{n-1}(r) - 10T_{n+1}(r) + 5T_{n+3}(r) - T_{n+5}(r)] \\ &\stackrel{(7.30)}{=} \frac{\pi}{32} [(n-5)U_{n-6}(r) - 5(n-3)U_{n-4}(r) + 10(n-1)U_{n-2}(r) \\ &\quad - 10(n+1)U_n(r) + 5(n+3)U_{n+2}(r) - (n+5)U_{n+4}(r)], \quad n \geq 6 \end{aligned} \quad (7.44)$$

- $I_2(T_n, m, r)$ , where  $m \geq 1$ , and  $n \geq 2m + 1$ :

$$\begin{aligned} \frac{1}{\pi} \int_{-1}^1 \frac{T_n(s)(1-s^2)^{m-1/2}}{(s-r)^2} ds &= \\ &(-1)^{m+1} 2^{1-2m} \sum_{j=0}^{2m-1} (-1)^j \binom{2m-1}{j} (n+1-2m+2j) U_{n-2m+2j}(r) \end{aligned} \quad (7.45)$$

### 7.3.2 $I_2(U_n, m, r)$

The following equality

$$\int_{-1}^1 \frac{U_n(s)(1-s^2)^{m-\frac{1}{2}}}{(s-r)^2} ds = \frac{d}{dr} \int_{-1}^1 \frac{U_n(s)(1-s^2)^{m-\frac{1}{2}}}{s-r} ds$$

leads to:

- $I_2(U_n, 1, r)$  (see also Kaya and Erdogan [50]):

$$\int_{-1}^1 \frac{U_n(s)\sqrt{1-s^2}}{(s-r)^2} ds = -\pi \frac{d}{dr} T_{n+1}(r) \stackrel{(7.30)}{=} -\pi(n+1)U_n(r), \quad n \geq 0, \quad (7.46)$$

which is the same as (7.17).

- $I_2(U_n, 2, r)$ : For  $n \geq 2$ ,

$$\begin{aligned} \int_{-1}^1 \frac{U_n(s)(1-s^2)^{\frac{3}{2}}}{(s-r)^2} ds &= \frac{\pi}{4} \frac{d}{dr} [T_{n-1}(r) - 2T_{n+1}(r) + T_{n+3}(r)] \\ &\stackrel{(7.30)}{=} \frac{\pi}{4} [(n-1)U_{n-2}(r) - 2(n+1)U_n(r) + (n+3)U_{n+2}(r)] \end{aligned} \quad (7.47)$$

- $I_2(U_n, 3, r)$ :

$$\begin{aligned} \int_{-1}^1 \frac{U_n(s)(1-s^2)^{\frac{5}{2}}}{(s-r)^2} ds &= -\frac{\pi}{16} \frac{d}{dr} [T_{n-3}(r) - 4T_{n-1}(r) + 6T_{n+1}(r) - 4T_{n+3}(r) + T_{n+5}(r)] \\ &\stackrel{(7.30)}{=} -\frac{\pi}{16} [(n-3)U_{n-4}(r) - 4(n-1)U_{n-2}(r) + 6(n+1)U_n(r) \\ &\quad - 4(n+3)U_{n+2}(r) + (n+5)U_{n+4}(r)], \quad n \geq 4 \end{aligned} \quad (7.48)$$

- $I_2(U_n, m, r)$ , where  $m \geq 2$ , and  $n \geq 2m - 1$ :

$$\begin{aligned} \frac{1}{\pi} \int_{-1}^1 \frac{U_n(s)(1-s^2)^{m-\frac{1}{2}}}{(s-r)^2} ds &= \\ &(-1)^m 2^{2-2m} \sum_{j=0}^{2m-2} (-1)^j \binom{2m-2}{j} (n+3-2m+2j) U_{n+2-2m+2j}(r) \end{aligned} \quad (7.49)$$

### 7.3.3 $I_3(T_n, m, r)$

By means of

$$\int_{-1}^1 \frac{T_n(s)(1-s^2)^{m-\frac{1}{2}}}{(s-r)^3} ds = \frac{1}{2} \frac{d}{dr} \int_{-1}^1 \frac{T_n(s)(1-s^2)^{m-\frac{1}{2}}}{(s-r)^2} ds,$$

one obtains:

- $I_3(T_n, 0, r)$ :

$$\begin{aligned} \int_{-1}^1 \frac{T_n(s)}{\sqrt{1-s^2}(s-r)^3} ds &= \frac{\pi}{8(1-r^2)^2} [(n+1)(n+2)U_{n-3}(r) \\ &\quad - 2(n^2-3)U_{n-1}(r) + (n-1)^2 U_{n+1}(r)], \quad n \geq 3 \end{aligned} \quad (7.50)$$

- $I_3(T_n, 1, r)$ :

$$\begin{aligned} \int_{-1}^1 \frac{T_n(s)\sqrt{1-s^2}}{(s-r)^3} ds &= \frac{\pi}{8(1-r^2)} [(n^2 - n)U_{n-3}(r) \\ &\quad - 2(n^2 + 2)U_{n-1}(r) + (n^2 + n)U_{n+1}(r)], \quad n \geq 3 \end{aligned} \quad (7.51)$$

- $I_3(T_n, 2, r)$ :  $n \geq 5$

$$\begin{aligned} \int_{-1}^1 \frac{T_n(s)(1-s^2)^{\frac{3}{2}}}{(s-r)^3} ds &= \frac{\pi}{32(1-r^2)} \{ -(n+3)(n+2)U_{n+3}(r) \\ &\quad + [(n+3)(n+4) + 3n(n+1)]U_{n+1}(r) - [3(n+1)(n+2) + 3(n-1)(n-2)] \\ &\quad \times U_{n-1}(r) + [3n(n-1) + (n-3)(n-4)]U_{n-3}(r) - (n-3)(n-2)U_{n-5}(r) \} \end{aligned} \quad (7.52)$$

- $I_3(T_n, 3, r)$ :

$$\begin{aligned} \int_{-1}^1 \frac{T_n(s)(1-s^2)^{\frac{5}{2}}}{(s-r)^3} ds &= \frac{\pi}{128(1-r^2)} [(n^2 + 9n + 20)U_{n+5}(r) \\ &\quad - 6(n^2 + 6n + 10)U_{n+3}(r) + 15(n^2 + 3n + 4)U_{n+1}(r) \\ &\quad - 20(n^2 + 2)U_{n-1}(r) + 15(n^2 - 3n + 4)U_{n-3}(r) - 6(n^2 - 6n + 10)U_{n-5}(r) \\ &\quad + (n^2 - 9n + 2)U_{n-7}(r)], \quad n \geq 7 \end{aligned} \quad (7.53)$$

- $I_3(T_n, m, r)$ , where  $m \geq 1$ , and  $n \geq 2m + 2$ :

$$\begin{aligned} \frac{1-r^2}{\pi} \int_{-1}^1 \frac{T_n(s)(1-s^2)^{m-\frac{1}{2}}}{(s-r)^3} ds &= \\ &= (-1)^{m+1} 2^{-2m-1} \sum_{j=0}^{2m-1} (-1)^j \binom{2m-1}{j} (n+1-2m+2j) \times \\ &= [(n+2-2m+2j)U_{n-1-2m+2j}(r) - (n-2m+2j)U_{n+1-2m+2j}(r)] \end{aligned} \quad (7.54)$$

### 7.3.4 $I_3(U_n, m, r)$

By means of

$$\int_{-1}^1 \frac{U_n(s)(1-s^2)^{m-\frac{1}{2}}}{(s-r)^3} ds = \frac{1}{2} \frac{d}{dr} \int_{-1}^1 \frac{U_n(s)(1-s^2)^{m-\frac{1}{2}}}{(s-r)^2} ds,$$

one gets:

- $I_3(U_n, 1, r)$ : For  $n \geq 1$ ,

$$\begin{aligned} & \int_{-1}^1 \frac{U_n(s)\sqrt{1-s^2}}{(s-r)^3} ds \\ &= \frac{\pi}{4(1-r^2)} \{-(n^2+3n+2)U_{n-1}(r) + (n^2+n)U_{n+1}(r)\} \end{aligned} \quad (7.55)$$

- $I_3(U_n, 2, r)$ :

$$\begin{aligned} & \int_{-1}^1 \frac{U_n(s)(1-s^2)^{\frac{1}{2}}}{(s-r)^3} ds = \frac{\pi}{16(1-r^2)} [-(n^2+5n+6)U_{n+3}(r) \\ &+ (3n^2+9n+12)U_{n+1}(r) - (3n^2+3n+6)U_{n-1}(r) \\ &+ (n^2-n)U_{n-3}(r)], \quad n \geq 3 \end{aligned} \quad (7.56)$$

- $I_3(U_n, 3, r)$ : For  $n \geq 5$ ,

$$\begin{aligned} & \int_{-1}^1 \frac{U_n(s)(1-s^2)^{\frac{3}{2}}}{(s-r)^3} ds = \frac{\pi}{64(1-r^2)} [(n^2+9n+20)U_{n+5}(r) \\ &- (5n^2+31n+54)U_{n+3}(r) + (10n^2+34n+48)U_{n+1}(r) - (10n^2+6n+20) \\ &\times U_{n-1}(r) + (5n^2-11n+12)U_{n-3}(r) - (n^2-5n+6)U_{n-5}(r)] \end{aligned} \quad (7.57)$$

- $I_3(U_n, m, r)$ , where  $m \geq 2$ , and  $n \geq 2m$ :

$$\begin{aligned} & \frac{1-r^2}{\pi} \int_{-1}^1 \frac{U_n(s)(1-s^2)^{m-\frac{1}{2}}}{(s-r)^3} ds = \\ & (-1)^m 2^{-2m} \sum_{j=0}^{2m-2} (-1)^j \binom{2m-2}{j} (n+3-2m+2j) \times \\ & [(n+4-2m+2j)U_{n+1-2m+2j}(r) - (n+2-2m+2j)U_{n+3-2m+2j}(r)] \end{aligned} \quad (7.58)$$

### 7.3.5 $I_4(T_n, m, r)$

By means of

$$\int_{-1}^1 \frac{T_n(s)(1-s^2)^{m-\frac{1}{2}}}{(s-r)^4} ds = \frac{1}{3} \frac{d}{dr} \int_{-1}^1 \frac{T_n(s)(1-s^2)^{m-\frac{1}{2}}}{(s-r)^3} ds,$$

one reaches the following results:

- $I_4(T_n, 0, r)$ :

$$\begin{aligned} \int_{-1}^1 \frac{T_n(s)}{(s-r)^4 \sqrt{1-s^2}} ds &= \frac{\pi}{48(1-r^2)^3} [(n^3 + 6n^2 + 11n + 6)U_{n-4}(r) \\ &\quad - (3n^3 + 6n^2 - 25n - 44)U_{n-2}(r) + (3n^3 - 5n^2 - 19n + 37)U_n(r) \\ &\quad - (n^3 - 5n^2 + 7n - 3)U_{n+2}(r)], \quad n \geq 4 \end{aligned} \quad (7.59)$$

- $I_4(T_n, 1, r)$ :

$$\begin{aligned} \int_{-1}^1 \frac{T_n(s) \sqrt{1-s^2}}{(s-r)^4} ds &= \frac{\pi}{48(1-r^2)^2} [ \\ &\quad (n^3 - n)U_{n-4}(r) - (3n^3 + 9n + 12)U_{n-2}(r) + (3n^3 + 9n - 12)U_n(r) \\ &\quad - (n^3 - n)U_{n+2}(r)], \quad n \geq 4 \end{aligned} \quad (7.60)$$

- $I_4(T_n, 2, r)$ :

$$\begin{aligned} \int_{-1}^1 \frac{T_n(s)(1-s^2)^{\frac{3}{2}}}{(s-r)^4} ds &= \frac{\pi}{192(1-r^2)^2} [(n^3 + 6n^2 + 11n + 6)U_{n+4}(r) \\ &\quad - (5n^3 + 18n^2 + 43n + 30)U_{n+2}(r) + (10n^3 + 12n^2 + 134n - 36)U_n(r) \\ &\quad - (10n^3 - 12n^2 + 134n + 36)U_{n-2}(r) + (5n^3 - 18n^2 + 43n - 30)U_{n-4}(r) \\ &\quad - (n^3 - 6n^2 + 11n - 6)U_{n-6}(r)], \quad n \geq 6 \end{aligned} \quad (7.61)$$

- $I_4(T_n, 3, r)$ :

$$\begin{aligned} \int_{-1}^1 \frac{T_n(s)(1-s^2)^{\frac{5}{2}}}{(s-r)^4} ds &= \frac{\pi}{384(1-r^2)^2} [ -(\frac{1}{2}n^3 + 6n^2 + \frac{47}{2}n + 30)U_{n+6}(r) \\ &\quad + (\frac{7}{2}n^3 + 30n^2 + \frac{197}{2}n + 120)U_{n+4}(r) - (\frac{21}{2}n^3 + 54n^2 + \frac{327}{2}n + 180)U_{n+2}(r) \\ &\quad + (\frac{35}{2}n^3 + 30n^2 + \frac{325}{2}n + 90)U_n(r) - (\frac{35}{2}n^3 - 30n^2 + \frac{325}{2}n - 90)U_{n-2}(r) \\ &\quad + (\frac{21}{2}n^3 - 54n^2 + \frac{327}{2}n - 180)U_{n-4}(r) - (\frac{7}{2}n^3 - 30n^2 + \frac{197}{2}n - 120)U_{n-6}(r) \\ &\quad + (\frac{1}{2}n^3 - 6n^2 + \frac{47}{2}n - 30)U_{n-8}(r)], \quad n \geq 8 \end{aligned} \quad (7.62)$$

- $I_4(T_n, m, r)$ , where  $m \geq 1$ , and  $n \geq 2m + 3$ :

$$\begin{aligned}
 & \frac{3(1-r^2)^2}{\pi} \int_{-1}^1 \frac{T_n(s)(1-s^2)^{m-\frac{1}{2}}}{(s-r)^4} ds = \\
 & (-1)^{m+1} 2^{-2m-2} \sum_{j=0}^{2m-1} (-1)^j \binom{2m-1}{j} (n+1-2m+2j) \times \\
 & \{ [(n+2-2m+2j)(n+3-2m+2j)] U_{n-2-2m+2j}(r) \\
 & - [2(n-2m+2j)^2 + 4(n-2m+2j) - 6] U_{n-2m+2j}(r) \\
 & + [(n-2m+2j)(n-1-2m+2j)] U_{n+2-2m+2j}(r) \} \quad (7.63)
 \end{aligned}$$

### 7.3.6 $I_4(U_n, m, r)$ :

By means of

$$\int_{-1}^1 \frac{U_n(s)(1-s^2)^{m-\frac{1}{2}}}{(s-r)^4} ds = \frac{1}{3} \frac{d}{dr} \int_{-1}^1 \frac{U_n(s)(1-s^2)^{m-\frac{1}{2}}}{(s-r)^3} ds,$$

one obtains

- $I_4(U_n, 1, r)$ :

$$\begin{aligned}
 & \int_{-1}^1 \frac{U_n(s)(1-s^2)^{\frac{1}{2}}}{(s-r)^4} ds = \frac{\pi}{24(1-r^2)^2} [ \\
 & -(2n^3 + 9n^2 + 11n + 6)U_{n-2}(r) + (3n^3 + 3n^2 - 2n - 6)U_n(r) \\
 & -(n^3 - n)U_{n+2}(r) ], \quad n \geq 2 \quad (7.64)
 \end{aligned}$$

- $I_4(U_n, 2, r)$ :

$$\begin{aligned}
 & \int_{-1}^1 \frac{U_n(s)(1-s^2)^{\frac{3}{2}}}{(s-r)^4} ds = \frac{\pi}{96(1-r^2)^2} [(n^3 + 6n^2 + 11n + 6)U_{n+4}(r) \\
 & -(4n^3 + 18n^2 + 44n + 30)U_{n+2}(r) + (6n^3 + 18n^2 + 54n + 42)U_n(r) \\
 & -(4n^3 + 6n^2 + 20n + 18)U_{n-2}(r) + (n^3 - n)U_{n-4}(r) ], \quad n \geq 4 \quad (7.65)
 \end{aligned}$$

- $I_4(U_n, 3, r)$ :

$$\begin{aligned}
 \int_{-1}^1 \frac{U_n(s)(1-s^2)^{\frac{5}{2}}}{(s-r)^4} ds &= \frac{\pi}{192(1-r^2)^2} \left[ -\left(\frac{1}{2}n^3 + 6n^2 + \frac{47}{2}n + 320\right)U_{n+6}(r) \right. \\
 &+ (3n^3 + 27n^2 + 93n + 117)U_{n+4}(r) - \left(\frac{15}{2}n^3 + 45n^2 + \frac{285}{2}n + 165\right)U_{n+2}(r) \\
 &+ (10n^3 + 30n^2 + 110n + 90)U_n(r) - \left(\frac{15}{2}n^3 + \frac{105}{2}n\right)U_{n-2}(r) \\
 &+ (3n^3 - 9n^2 + 21n - 15)U_{n-4}(r) \\
 &\left. - \left(\frac{1}{2}n^3 + 3n^2 + \frac{11}{2}n - 3\right)U_{n-6}(r) \right], \quad n \geq 6
 \end{aligned} \tag{7.66}$$

- $I_4(U_n, m, r)$ , where  $m \geq 2$ , and  $n \geq 2m + 1$ :

$$\begin{aligned}
 \frac{3(1-r^2)^2}{\pi} \int_{-1}^1 \frac{U_n(s)(1-s^2)^{m-\frac{1}{2}}}{(s-r)^4} ds &= \\
 (-1)^{m2-2m-1} \sum_{j=0}^{2m-2} (-1)^j \binom{2m-2}{j} (n+3-2m+2j) \times \\
 \{ &[(n+4-2m+2j)(n+5-2m+2j)]U_{n-2m+2j}(r) \\
 &- [2(n-2m+2j)^2 + 10(n-2m+2j) + 10]U_{n+2-2m+2j}(r) \\
 &+ [(n+2-2m+2j)(n-1-2m+2j)]U_{n+4-2m+2j}(r) \}
 \end{aligned} \tag{7.67}$$

## 7.4 Evaluation of Stress Intensity Factors (SIFs)

An important task is to evaluate the stress intensity factors (SIFs) at both crack tips, since the propagation of a crack starts around its tips. In mode III crack problems, standard SIFs can be calculated from

$$K_{III}(d) = \lim_{x \rightarrow d^+} \sqrt{2\pi(x-d)} \sigma_{yz}(x, 0), \quad (x > d) \tag{7.68}$$

and

$$K_{III}(c) = \lim_{x \rightarrow c^-} \sqrt{2\pi(c-x)} \sigma_{yz}(x, 0), \quad (x < c). \tag{7.69}$$

Note that the limit is taken from outside of the crack surfaces and towards both tips. Usually the left hand side of integral equation (7.3) is the expression for  $\sigma_{yz}(x, 0)$



which is valid for  $x$  is inside the crack surfaces  $(c, d)$  as well as outside of  $(c, d)$ . Thus to calculate SIFs, the key is to evaluate the following integrals (after proper normalization and a change of variables described in equation (7.4)):

$$S_\alpha(T_n, m, r) = \int_{-1}^1 \frac{T_n(s)(1-s^2)^{m-(1/2)}}{(s-r)^\alpha} ds, \quad r \notin (-1, 1) \quad (7.70)$$

and

$$S_\alpha(U_n, m, r) = \int_{-1}^1 \frac{U_n(s)(1-s^2)^{m-(1/2)}}{(s-r)^\alpha} ds, \quad r \notin (-1, 1). \quad (7.71)$$

Note that the above integrals are not singular as  $x \neq t$  for  $t \in (c, d)$  and  $x \notin (c, d)$ .

The strategy to evaluate  $S_\alpha(T_n, m, r)$  and  $S_\alpha(U_n, m, r)$  for general integers  $\alpha$  (positive) and  $m$  (non-negative) is similar to the process for evaluating  $I_\alpha(T_n, m, r)$  and  $I_\alpha(U_n, m, r)$ . It consists of evaluating the integrals  $S_1(T_n, m, r)$  and  $S_1(U_n, m, r)$  by means of the reduction procedure described in Subsection 7.2.3, and taking differentiation (with respect to  $r$ ) to obtain  $S_\alpha(T_n, m, r)$  and  $S_\alpha(U_n, m, r)$  for  $\alpha \geq 2$ . The relevant derivations are provided below. The range of  $r$  is restricted to  $|r| > 1$  for each formula provided in the rest of present Section.

#### 7.4.1 $S_1(T_n, m, r)$ and $S_1(U_n, m, r)$

- $S_1(T_n, 0, r)$ :

This is a well known integral (Erdogan and Ozturk [30]):

$$S_1(T_n, 0, r) = \int_{-1}^1 \frac{T_n(s)}{(s-r)\sqrt{1-s^2}} ds \quad (7.72)$$

$$= -\pi \frac{(r - \sqrt{r^2 - 1}|r|/r)^n}{\sqrt{r^2 - 1}|r|/r}, \quad n \geq 0. \quad (7.73)$$

- $S_1(U_n, 1, r)$ :

$$\begin{aligned}
 & \int_{-1}^1 \frac{U_n(s)\sqrt{1-s^2}}{s-r} ds \\
 & \stackrel{(7.28)}{=} \frac{1}{2} \int_{-1}^1 \frac{T_n(s)}{(s-r)\sqrt{1-s^2}} ds - \frac{1}{2} \int_{-1}^1 \frac{T_{n+2}(s)}{(s-r)\sqrt{1-s^2}} ds \\
 & \stackrel{(7.73)}{=} -\pi \left( r - \frac{|r|}{r} \sqrt{r^2-1} \right)^{n+1}, \quad n \geq 0. \tag{7.74}
 \end{aligned}$$

- $S_1(T_n, 1, r)$ :

$$\begin{aligned}
 & \int_{-1}^1 \frac{T_n(s)\sqrt{1-s^2}}{s-r} ds \\
 & \stackrel{(7.26)}{=} \frac{1}{2} \int_{-1}^1 \frac{U_n(s)\sqrt{1-s^2}}{s-r} ds - \frac{1}{2} \int_{-1}^1 \frac{U_{n-2}(s)\sqrt{1-s^2}}{s-r} ds \\
 & \stackrel{(7.74)}{=} \pi \frac{|r|}{r} \sqrt{r^2-1} \left( r - \frac{|r|}{r} \sqrt{r^2-1} \right)^n, \quad n \geq 2. \tag{7.75}
 \end{aligned}$$

- $S_1(U_n, 2, r)$ :

$$\begin{aligned}
 & \int_{-1}^1 \frac{U_n(s)(1-s^2)^{\frac{3}{2}}}{s-r} ds \\
 & \stackrel{(7.28)}{=} \frac{1}{2} \int_{-1}^1 \frac{T_n(s)\sqrt{1-s^2}}{s-r} ds - \frac{1}{2} \int_{-1}^1 \frac{T_{n+2}(s)\sqrt{1-s^2}}{s-r} ds \\
 & \stackrel{(7.75)}{=} \pi(r^2-1) \left( r - \frac{|r|}{r} \sqrt{r^2-1} \right)^{n+1}, \quad n \geq 2. \tag{7.76}
 \end{aligned}$$

- $S_1(T_0, 2, r)$ :

$$\int_{-1}^1 \frac{T_0(s)(1-s^2)^{\frac{3}{2}}}{s-r} ds = \pi(r^2-1) \left( r - \frac{|r|}{r} \sqrt{r^2-1} \right). \tag{7.77}$$

- $S_1(T_1, 2, r)$ :

$$\int_{-1}^1 \frac{T_1(s)(1-s^2)^{\frac{3}{2}}}{s-r} ds = \frac{\pi}{2}(r^2-1) \left( r - \frac{|r|}{r} \sqrt{r^2-1} \right)^2. \tag{7.78}$$

- $S_1(T_n, 2, r)$ :

$$\int_{-1}^1 \frac{T_n(s)(1-s^2)^{\frac{3}{2}}}{s-r} ds \stackrel{(7.26),(7.76)}{=} -\frac{\pi|r|}{r}(r^2-1)^{\frac{3}{2}} \left( r - \frac{|r|}{r} \sqrt{r^2-1} \right)^n, \quad n \geq 2. \tag{7.79}$$

Thus we obtain the following formulas for  $S_1(T_n, m, r)$  and  $S_1(U_n, m, r)$ :

$$\begin{aligned} S_1(T_n, m, r) &= \int_{-1}^1 \frac{T_n(s)(1-s^2)^{m-\frac{1}{2}}}{s-r} ds \\ &= \pi(-1)^{m+1} \frac{|r|}{r} (r^2-1)^{m-\frac{1}{2}} \left( r - \frac{|r|}{r} \sqrt{r^2-1} \right)^n, \quad m \geq 0 \text{ and } n \geq 2m. \end{aligned} \quad (7.80)$$

$$\begin{aligned} S_1(U_n, m, r) &= \int_{-1}^1 \frac{U_n(s)(1-s^2)^{m-\frac{1}{2}}}{s-r} ds \\ &= \pi(-1)^m (r^2-1)^{m-1} \left( r - \frac{|r|}{r} \sqrt{r^2-1} \right)^n, \quad m \geq 1 \text{ and } n \geq 2m-2. \end{aligned} \quad (7.81)$$

#### 7.4.2 $S_2(T_n, m, r)$ and $S_2(U_n, m, r)$

Differentiating (with respect to  $r$ ) the formulas for  $S_1(T_n, m, r)$  and  $S_1(U_n, m, r)$ , we obtain the formulas for  $S_2(T_n, m, r)$  and  $S_2(U_n, m, r)$ .

$$\begin{aligned} \int_{-1}^1 \frac{U_n(s)(1-s^2)^{\frac{3}{2}}}{(s-r)^2} ds &= -\pi(n+1) \frac{|r|}{r} \sqrt{r^2-1} \left( r - \frac{|r|}{r} \sqrt{r^2-1} \right)^{n+1} \\ &\quad + 2\pi r \left( r - \frac{|r|}{r} \sqrt{r^2-1} \right)^{n+1}, \quad n \geq 0 \end{aligned} \quad (7.82)$$

and

$$\int_{-1}^1 \frac{T_n(s)(1-s^2)^{\frac{3}{2}}}{(s-r)^2} ds = -\frac{\pi|r|}{r} (r^2-1)^{\frac{3}{2}} \left( r - \frac{|r|}{r} \sqrt{r^2-1} \right)^n, \quad n \geq 2. \quad (7.83)$$

Formulas (7.82) and (7.83) are used in calculating SIFs in Chapters 10 and 12.

#### 7.4.3 $S_3(T_n, m, r)$ and $S_3(U_n, m, r)$

The following formulas are obtained by differentiating twice (with respect to  $r$ ) the corresponding formulas obtained in Subsection 7.4.1.

$$\begin{aligned} \int_{-1}^1 \frac{U_n(s)(1-s^2)^{\frac{3}{2}}}{(s-r)^3} ds &= \frac{\pi}{2} \left[ (n^2+2n+3) - 3(n+1) \frac{|r|}{\sqrt{r^2-1}} \right] \\ &\quad \times \left( r - \frac{|r|}{r} \sqrt{r^2-1} \right)^{n+1}, \quad n \geq 0. \end{aligned} \quad (7.84)$$

$$\int_{-1}^1 \frac{T_1(s)(1-s^2)^{\frac{3}{2}}}{(s-r)^3} ds = \frac{3\pi}{2} \left( r - \frac{|r|}{r} \sqrt{r^2-1} \right)^2 \left( 1 - \frac{|r|}{\sqrt{r^2-1}} \right). \quad (7.85)$$

$$\int_{-1}^1 \frac{T_0(s)(1-s^2)^{\frac{3}{2}}}{(s-r)^3} ds = \frac{3\pi}{2} \left( r - \frac{|r|}{r} \sqrt{r^2-1} \right) \left( 1 - \frac{|r|}{\sqrt{r^2-1}} \right). \quad (7.86)$$

$$\begin{aligned} & \int_{-1}^1 \frac{T_n(s)(1-s^2)^{\frac{3}{2}}}{(s-r)^3} ds \\ &= \frac{\pi}{4} \left\{ \left( r - \frac{|r|}{r} \sqrt{r^2-1} \right)^{n+1} \left[ (n^2+2n+3) - 3(n+1) \frac{|r|}{\sqrt{r^2-1}} \right] \right. \\ & \quad \left. - \left( r - \frac{|r|}{r} \sqrt{r^2-1} \right)^{n-1} \left[ (n^2-2n+3) - 3(n-1) \frac{|r|}{\sqrt{r^2-1}} \right] \right\}, \quad n \geq 2. \quad (7.87) \end{aligned}$$

The above formulas are used in calculating the SIFs all through the thesis, like in Chapters 4, 10, 11, and 12.

## 7.5 Integrals associated with lower order $n$

The general formula given in the text, *e.g.* equations (7.38), (7.39), (7.45), (7.49), (7.55), (7.59), (7.64), and (7.67) are only valid above certain values of  $n$ . Thus the goal of this section is to provide the expressions for integrals associated with lower order  $n$ .

### 7.5.1 $I_1(T_n, 1, r)$ , $n = 0, 1$

$$\frac{1}{\pi} \int_{-1}^1 \frac{T_0(s)\sqrt{1-s^2}}{s-r} ds = -r, \quad |r| < 1 \quad (7.88)$$

$$\frac{1}{\pi} \int_{-1}^1 \frac{T_1(s)\sqrt{1-s^2}}{s-r} ds = -r^2 + \frac{1}{2}, \quad |r| < 1 \quad (7.89)$$

7.5.2  $I_1(T_n, 2, r)$ ,  $n = 0 \cdots 5$ ,  $|r| < 1$

$$\frac{1}{\pi} \int_{-1}^1 \frac{T_0(s)(1-s^2)^{\frac{3}{2}}}{s-r} ds = r^3 - \frac{3}{2}r \quad (7.90)$$

$$\frac{1}{\pi} \int_{-1}^1 \frac{T_1(s)(1-s^2)^{\frac{3}{2}}}{s-r} ds = r^4 - \frac{3}{2}r^2 + \frac{3}{8} \quad (7.91)$$

$$\frac{1}{\pi} \int_{-1}^1 \frac{T_2(s)(1-s^2)^{\frac{3}{2}}}{s-r} ds = 2r^5 - 4r^3 + \frac{9}{4}r \quad (7.92)$$

$$\frac{1}{\pi} \int_{-1}^1 \frac{T_3(s)(1-s^2)^{\frac{3}{2}}}{s-r} ds = 4r^6 - 9r^4 + 6r^2 - \frac{7}{8} \quad (7.93)$$

$$\frac{1}{\pi} \int_{-1}^1 \frac{T_4(s)(1-s^2)^{\frac{3}{2}}}{s-r} ds = 8r^7 - 20r^5 + 16r^3 - 4r \quad (7.94)$$

$$\frac{1}{\pi} \int_{-1}^1 \frac{T_5(s)(1-s^2)^{\frac{3}{2}}}{s-r} ds = 16r^8 - 44r^6 + 41r^4 - 14r^2 + 1 \quad (7.95)$$

7.5.3  $I_1(T_n, 3, r)$ ,  $n = 0 \cdots 5$ ,  $|r| < 1$

$$\frac{1}{\pi} \int_{-1}^1 \frac{T_0(s)(1-s^2)^{\frac{5}{2}}}{s-r} ds = -\frac{15}{8}r + \frac{5}{2}r^3 - r^5 \quad (7.96)$$

$$\frac{1}{\pi} \int_{-1}^1 \frac{T_1(s)(1-s^2)^{\frac{5}{2}}}{s-r} ds = \frac{5}{16} - \frac{15}{8}r^2 + \frac{5}{2}r^4 - r^6 \quad (7.97)$$

$$\frac{1}{\pi} \int_{-1}^1 \frac{T_2(s)(1-s^2)^{\frac{5}{2}}}{s-r} ds = \frac{5}{12}r - \frac{25}{4}r^3 + 6r^5 - 2r^7 \quad (7.98)$$

$$\frac{1}{\pi} \int_{-1}^1 \frac{T_3(s)(1-s^2)^{\frac{5}{2}}}{s-r} ds = -\frac{25}{32} + \frac{55}{8}r^2 - 15r^4 + 13r^6 - 4r^8 \quad (7.99)$$

$$\frac{1}{\pi} \int_{-1}^1 \frac{T_4(s)(1-s^2)^{\frac{5}{2}}}{s-r} ds = -\frac{65}{16}r + 20r^3 - 36r^5 + 28r^7 - 8r^9 \quad (7.100)$$

$$\frac{1}{\pi} \int_{-1}^1 \frac{T_5(s)(1-s^2)^{\frac{5}{2}}}{s-r} ds = \frac{31}{32} - 15r^2 + 55r^4 - 85r^6 + 60r^8 - 16r^{10} \quad (7.101)$$

**7.5.4**  $I_1(U_n, 3, r)$ ,  $n = 0 \dots 5$ ,  $|r| < 1$

$$\frac{1}{\pi} \int_{-1}^1 \frac{U_0(s)(1-s^2)^{\frac{5}{2}}}{s-r} ds = -\frac{15}{8}r + \frac{5}{2}r^3 - r^5 \quad (7.102)$$

$$\frac{1}{\pi} \int_{-1}^1 \frac{U_1(s)(1-s^2)^{\frac{5}{2}}}{s-r} ds = \frac{5}{8} - \frac{15}{4}r^2 + 5r^4 - 2r^6 \quad (7.103)$$

$$\frac{1}{\pi} \int_{-1}^1 \frac{U_2(s)(1-s^2)^{\frac{5}{2}}}{s-r} ds = \frac{25}{8}r - 10r^3 + 11r^5 - 4r^7 \quad (7.104)$$

$$\frac{1}{\pi} \int_{-1}^1 \frac{U_3(s)(1-s^2)^{\frac{5}{2}}}{s-r} ds = -\frac{15}{16} + 10r^2 - 25r^4 + 24r^6 - 8r^8 \quad (7.105)$$

$$\frac{1}{\pi} \int_{-1}^1 \frac{U_4(s)(1-s^2)^{\frac{5}{2}}}{s-r} ds = -5r + 30r^3 - 61r^5 + 52r^7 - 16r^9 \quad (7.106)$$

$$\frac{1}{\pi} \int_{-1}^1 \frac{U_5(s)(1-s^2)^{\frac{5}{2}}}{s-r} ds = 1 - 20r^2 + 85r^4 - 146r^6 + 112r^8 - 32r^{10} \quad (7.107)$$

**7.5.5**  $I_2(T_n, 3, r)$ ,  $n = 0 \dots 6$ ,  $|r| < 1$

$$\frac{1}{\pi} \int_{-1}^1 \frac{T_0(s)(1-s^2)^{\frac{5}{2}}}{(s-r)^2} ds = -5r^4 + \frac{15}{2}r^2 - \frac{15}{8} \quad (7.108)$$

$$\frac{1}{\pi} \int_{-1}^1 \frac{T_1(s)(1-s^2)^{\frac{5}{2}}}{(s-r)^2} ds = -6r^5 + 10r^3 - \frac{15}{4}r \quad (7.109)$$

$$\frac{1}{\pi} \int_{-1}^1 \frac{T_2(s)(1-s^2)^{\frac{5}{2}}}{(s-r)^2} ds = -14r^6 + 30r^4 - \frac{75}{4}r^2 + \frac{5}{2} \quad (7.110)$$

$$\frac{1}{\pi} \int_{-1}^1 \frac{T_3(s)(1-s^2)^{\frac{5}{2}}}{(s-r)^2} ds = -32r^7 + 78r^5 - 60r^3 + \frac{55}{4}r \quad (7.111)$$

$$\frac{1}{\pi} \int_{-1}^1 \frac{T_4(s)(1-s^2)^{\frac{5}{2}}}{(s-r)^2} ds = -72r^8 + 196r^6 - 180r^4 + 60r^2 - \frac{65}{16} \quad (7.112)$$

$$\frac{1}{\pi} \int_{-1}^1 \frac{T_5(s)(1-s^2)^{\frac{5}{2}}}{(s-r)^2} ds = -160r^9 + 480r^7 - 510r^5 + 220r^3 - 30r \quad (7.113)$$

$$\frac{1}{\pi} \int_{-1}^1 \frac{T_6(s)(1-s^2)^{\frac{5}{2}}}{(s-r)^2} ds = -352r^{10} + 1152r^8 - 1386r^6 + 730r^4 - 150r^2 + 6 \quad (7.114)$$

**7.5.6**  $I_2(U_n, 3, r)$ ,  $n = 0 \cdots 6$ ,  $|r| < 1$

$$\frac{1}{\pi} \int_{-1}^1 \frac{U_0(s)(1-s^2)^{\frac{5}{2}}}{(s-r)^2} ds = -5r^4 + \frac{15}{2}r^2 - \frac{15}{8} \quad (7.115)$$

$$\frac{1}{\pi} \int_{-1}^1 \frac{U_1(s)(1-s^2)^{\frac{5}{2}}}{(s-r)^2} ds = -12r^5 + 20r^3 - \frac{15}{2}r \quad (7.116)$$

$$\frac{1}{\pi} \int_{-1}^1 \frac{U_2(s)(1-s^2)^{\frac{5}{2}}}{(s-r)^2} ds = -28r^6 + 55r^4 - 30r^2 + \frac{25}{8} \quad (7.117)$$

$$\frac{1}{\pi} \int_{-1}^1 \frac{U_3(s)(1-s^2)^{\frac{5}{2}}}{(s-r)^2} ds = -64r^7 + 144r^5 - 100r^3 + 20r \quad (7.118)$$

$$\frac{1}{\pi} \int_{-1}^1 \frac{U_4(s)(1-s^2)^{\frac{5}{2}}}{(s-r)^2} ds = -144r^8 + 364r^6 - 305r^4 + 90r^2 - 5 \quad (7.119)$$

$$\frac{1}{\pi} \int_{-1}^1 \frac{U_5(s)(1-s^2)^{\frac{5}{2}}}{(s-r)^2} ds = -320r^9 + 896r^7 - 876r^5 + 340r^3 - 40r \quad (7.120)$$

$$\frac{1}{\pi} \int_{-1}^1 \frac{U_6(s)(1-s^2)^{\frac{5}{2}}}{(s-r)^2} ds = -704r^{10} + 2160r^8 - 2408r^6 + 1155r^4 - 210r^2 + 7 \quad (7.121)$$

7.5.7  $I_3(T_n, 2, r)$ ,  $n = 0 \cdots 4$ ,  $|r| < 1$

$$\frac{1}{\pi} \int_{-1}^1 \frac{T_0(s)(1-s^2)^{\frac{3}{2}}}{(s-r)^3} ds = 3r \quad (7.122)$$

$$\frac{1}{\pi} \int_{-1}^1 \frac{T_1(s)(1-s^2)^{\frac{3}{2}}}{(s-r)^3} ds = 6r^2 - \frac{3}{2} \quad (7.123)$$

$$\frac{1}{\pi} \int_{-1}^1 \frac{T_2(s)(1-s^2)^{\frac{3}{2}}}{(s-r)^3} ds = 20r^3 - 12r \quad (7.124)$$

$$\frac{1}{\pi} \int_{-1}^1 \frac{T_3(s)(1-s^2)^{\frac{3}{2}}}{(s-r)^3} ds = 60r^4 - 54r^2 + 6 \quad (7.125)$$

$$\frac{1}{\pi} \int_{-1}^1 \frac{T_4(s)(1-s^2)^{\frac{3}{2}}}{(s-r)^3} ds = 168r^5 - 200r^3 + 48r \quad (7.126)$$

7.5.8  $I_3(T_n, 3, r)$ ,  $n = 0 \cdots 7$ ,  $|r| < 1$

$$\frac{1}{\pi} \int_{-1}^1 \frac{T_0(s)(1-s^2)^{\frac{5}{2}}}{(s-r)^3} ds = -10r^3 + \frac{15}{2}r \quad (7.127)$$

$$\frac{1}{\pi} \int_{-1}^1 \frac{T_1(s)(1-s^2)^{\frac{5}{2}}}{(s-r)^3} ds = -15r^4 + 15r^2 - \frac{15}{8} \quad (7.128)$$

$$\frac{1}{\pi} \int_{-1}^1 \frac{T_2(s)(1-s^2)^{\frac{5}{2}}}{(s-r)^3} ds = -42r^5 + 60r^3 - \frac{75}{4}r \quad (7.129)$$

$$\frac{1}{\pi} \int_{-1}^1 \frac{T_3(s)(1-s^2)^{\frac{5}{2}}}{(s-r)^3} ds = -112r^6 + 195r^4 - 90r^2 + \frac{55}{8} \quad (7.130)$$

$$\frac{1}{\pi} \int_{-1}^1 \frac{T_4(s)(1-s^2)^{\frac{5}{2}}}{(s-r)^3} ds = -288r^7 + 588r^5 - 360r^3 + 60r \quad (7.131)$$

$$\frac{1}{\pi} \int_{-1}^1 \frac{T_5(s)(1-s^2)^{\frac{5}{2}}}{(s-r)^3} ds = -720r^8 + 1680r^6 - 1275r^4 + 330r^2 - 15 \quad (7.132)$$



$$\frac{1}{\pi} \int_{-1}^1 \frac{T_6(s)(1-s^2)^{\frac{5}{2}}}{(s-r)^3} ds = -1760r^9 + 4608r^7 - 4158r^5 + 1460r^3 - 150r \quad (7.133)$$

$$\begin{aligned} \frac{1}{\pi} \int_{-1}^1 \frac{T_7(s)(1-s^2)^{\frac{5}{2}}}{(s-r)^3} ds = \\ -4224r^{10} + 12240r^8 - 12768r^6 + 5655r^4 - 930r^2 + 27 \end{aligned} \quad (7.134)$$

**7.5.9**  $I_3(U_n, 3, r)$ ,  $n = 0 \dots 6$ ,  $|r| < 1$

$$\frac{1}{\pi} \int_{-1}^1 \frac{U_0(s)(1-s^2)^{\frac{5}{2}}}{(s-r)^3} ds = -10r^3 + \frac{15}{2}r \quad (7.135)$$

$$\frac{1}{\pi} \int_{-1}^1 \frac{U_1(s)(1-s^2)^{\frac{5}{2}}}{(s-r)^3} ds = -30r^4 + 30r^2 - \frac{15}{4} \quad (7.136)$$

$$\frac{1}{\pi} \int_{-1}^1 \frac{U_2(s)(1-s^2)^{\frac{5}{2}}}{(s-r)^3} ds = -84r^5 + 110r^3 - 30r \quad (7.137)$$

$$\frac{1}{\pi} \int_{-1}^1 \frac{U_3(s)(1-s^2)^{\frac{5}{2}}}{(s-r)^3} ds = -224r^6 + 360r^4 - 150r^2 + 10 \quad (7.138)$$

$$\frac{1}{\pi} \int_{-1}^1 \frac{U_4(s)(1-s^2)^{\frac{5}{2}}}{(s-r)^3} ds = -576r^7 + 1092r^5 - 610r^3 + 90r \quad (7.139)$$

$$\frac{1}{\pi} \int_{-1}^1 \frac{U_5(s)(1-s^2)^{\frac{5}{2}}}{(s-r)^3} ds = -1440r^8 + 3136r^6 - 2190r^4 + 510r^2 - 20 \quad (7.140)$$

$$\frac{1}{\pi} \int_{-1}^1 \frac{U_6(s)(1-s^2)^{\frac{5}{2}}}{(s-r)^3} ds = -3520r^9 + 8640r^7 - 7224r^5 + 2310r^3 - 210r \quad (7.141)$$

**7.5.10**  $I_4(T_n, 3, r)$ ,  $n = 0 \dots 8$ ,  $|r| < 1$

$$\frac{1}{\pi} \int_{-1}^1 \frac{T_0(s)(1-s^2)^{\frac{5}{2}}}{(s-r)^4} ds = -10r^2 + \frac{5}{2} \quad (7.142)$$

$$\frac{1}{\pi} \int_{-1}^1 \frac{T_1(s)(1-s^2)^{\frac{5}{2}}}{(s-r)^4} ds = -20r^3 + 10r \quad (7.143)$$

$$\frac{1}{\pi} \int_{-1}^1 \frac{T_2(s)(1-s^2)^{\frac{5}{2}}}{(s-r)^4} ds = -70r^4 + 60r^2 - \frac{25}{4} \quad (7.144)$$

$$\frac{1}{\pi} \int_{-1}^1 \frac{T_3(s)(1-s^2)^{\frac{5}{2}}}{(s-r)^4} ds = -224r^5 + 260r^3 - 60r \quad (7.145)$$

$$\frac{1}{\pi} \int_{-1}^1 \frac{T_4(s)(1-s^2)^{\frac{5}{2}}}{(s-r)^4} ds = -672r^6 + 980r^4 - 360r^2 + 20 \quad (7.146)$$

$$\frac{1}{\pi} \int_{-1}^1 \frac{T_5(s)(1-s^2)^{\frac{5}{2}}}{(s-r)^4} ds = -1920r^7 + 3360r^5 - 1700r^3 + 220r \quad (7.147)$$

$$\frac{1}{\pi} \int_{-1}^1 \frac{T_6(s)(1-s^2)^{\frac{5}{2}}}{(s-r)^4} ds = -5280r^8 + 10752r^6 - 6930r^4 + 1460r^2 - 50 \quad (7.148)$$

$$\frac{1}{\pi} \int_{-1}^1 \frac{T_7(s)(1-s^2)^{\frac{5}{2}}}{(s-r)^4} ds = -14080r^9 + 32640r^7 - 25536r^5 + 7540r^3 - 620r \quad (7.149)$$

$$\frac{1}{\pi} \int_{-1}^1 \frac{T_8(s)(1-s^2)^{\frac{5}{2}}}{(s-r)^4} ds = -36608r^{10} + 95040r^8 - 87360r^6 + 33320r^4 - 4560r^2 + 104 \quad (7.150)$$

**7.5.11**  $I_4(U_n, 3, r)$ ,  $n = 0 \dots 6$ ,  $|r| < 1$

$$\frac{1}{\pi} \int_{-1}^1 \frac{U_0(s)(1-s^2)^{\frac{5}{2}}}{(s-r)^4} ds = -10r^2 + \frac{5}{2} \quad (7.151)$$

$$\frac{1}{\pi} \int_{-1}^1 \frac{U_1(s)(1-s^2)^{\frac{5}{2}}}{(s-r)^4} ds = -40r^3 + 20r \quad (7.152)$$

$$\frac{1}{\pi} \int_{-1}^1 \frac{U_2(s)(1-s^2)^{\frac{5}{2}}}{(s-r)^4} ds = -140r^4 + 110r^2 - 10 \quad (7.153)$$

$$\frac{1}{\pi} \int_{-1}^1 \frac{U_3(s)(1-s^2)^{\frac{5}{2}}}{(s-r)^4} ds = -448r^5 + 480r^3 - 100r \quad (7.154)$$

$$\frac{1}{\pi} \int_{-1}^1 \frac{U_4(s)(1-s^2)^{\frac{5}{2}}}{(s-r)^4} ds = -1344r^6 + 1820r^4 - 610r^2 + 30 \quad (7.155)$$

$$\frac{1}{\pi} \int_{-1}^1 \frac{U_5(s)(1-s^2)^{\frac{5}{2}}}{(s-r)^4} ds = -3840r^7 + 6272r^5 - 2920r^3 + 340r \quad (7.156)$$

$$\frac{1}{\pi} \int_{-1}^1 \frac{U_6(s)(1-s^2)^{\frac{5}{2}}}{(s-r)^4} ds = -10560r^8 + 20160r^6 - 12040r^4 + 2310r^2 - 70 \quad (7.157)$$

### 7.5.12 Others

$$\int_{-1}^1 (1-t^2)^{\frac{3}{2}} T_0(t) dt = \int_{-1}^1 (1-t^2)^{\frac{3}{2}} dt = \frac{3}{8}\pi \quad (7.158)$$

$$\int_{-1}^1 (1-t^2)^{\frac{3}{2}} T_2(t) dt = -\frac{\pi}{4} \quad (7.159)$$

$$\int_{-1}^1 (1-t^2)^{\frac{3}{2}} T_4(t) dt = \frac{\pi}{16} \quad (7.160)$$

$$\int_{-1}^1 (1-t^2)^{\frac{3}{2}} T_n(t) dt = 0 \quad , \quad \text{for all } n, \quad \text{and } n \neq 0, 2, 4. \quad (7.161)$$

## Chapter 8

# Numerical Approximation

## Procedures

One of the main merits for the formulation of hypersingular integral equations is that once a hypersingular integral equation is formulated, then its numerical solution is readily to find. In this chapter we give a detail accounts of the numerical approximation procedures which, in general, is called the collocation method [28, 29]. It can be divided into the following steps:

- Normalization.
- Representation of the Density Function.
- Chebyshev Polynomial Expansion.
- Evaluation of the Derivative of the Density Function.
- Formation of the Linear System of Equations.
- Evaluation of Singular and Hypersingular Integrals.
- Evaluation of Non-singular Integral.

Relevant details for each of the above items are given below by using equation (4.56)

$$\frac{G_0}{\pi} \int_{-a}^a \left\{ \frac{-2\ell^2}{(t-x)^3} + \frac{5\ell^2\gamma^2/8 + \ell'\gamma/4 + 1 - (\ell'/\ell)^2/4}{t-x} + k(x,t) \right\} \phi(t) dt + \frac{G}{2}(\ell' + 2\ell^2\gamma)\phi'(x) = p(x), \quad |x| < a$$

as an example. After the numerical approximation we show how to compute the stress intensity factors (SIFs), then at the end of the chapter we demonstrate that we can use either Chebyshev polynomials  $T_n$  or  $U_n$  to be in the expansion by giving another numerical example.

## 8.1 Normalization

By the following change of variables

$$s = [2/(d-c)][t - (c+d)/2]$$

one may convert the integral  $\int_c^d g(t)dt$  into the form of  $\int_{-1}^1 f(s)ds$ . Because the crack surface is located in the range  $(-a, a)$ , a convenient change of variables becomes

$$t/a = s \quad \text{and} \quad x/a = r,$$

which is the normalization of the variables  $t$  and  $x$ , respectively. Thus equation (4.56) can be written in the normalized fashion as:

$$\frac{1}{\pi} \int_{-1}^1 \left\{ \frac{-2(\ell/a)^2}{(s-r)^3} + \frac{5(\ell/a)^2(a\gamma)^2/8 + (\ell'/a)(a\gamma)/4 + 1 - [(\ell'/a)/(\ell/a)]^2/4}{s-r} + \mathcal{K}(r,s) \right\} \Phi(s) ds + [\ell'/a + 2(\ell/a)^2(a\gamma)] \Phi'(r)/2 = \mathcal{P}(r)/G_0, \quad |r| < 1, \quad (8.1)$$

where

$$\Phi(r) = \phi(ar), \quad \mathcal{P}(r) = p(ar), \quad \mathcal{K}(r,s) = ak(ar, as).$$

As clearly seen in equation (8.1), the quantities  $\ell/a$ ,  $\ell'/a$ , and  $a\gamma$  are dimensionless parameters. Thus the following dimensionless parameters are defined

$$\bar{\ell} = \ell/a, \quad \bar{\ell}' = \ell'/a, \quad \bar{\gamma} = a\gamma, \quad (8.2)$$

which will be used in the numerical implementation and results.

## 8.2 Representation of the Density Function

The next step of the numerical approach to the (normalized) hypersingular integral equation (8.1) is to establish the correct behavior of the unknown density function  $\Phi(s)$  around the two crack tips  $s = \pm 1$ . For example, the governing integral equation in classical LEFM has Cauchy singularity if the slope function, say  $\Phi(s)_{\text{LEFM}}$ , is chosen to be the unknown density function. A well-known representation is [28, 29]:

$$\Phi(s)_{\text{LEFM}} = f(s)/\sqrt{1-s^2}, \quad |s| < 1,$$

where  $f(\pm 1) \neq 0$ . For the cubic hypersingular integral, equation (8.1), the representation of  $\Phi(s)$  is found to be [36]:

$$\Phi(s)_{\text{GE}} \equiv \Phi(s) = g(s)\sqrt{1-s^2}, \quad (8.3)$$

where  $g(\pm 1)$  is finite,  $g(\pm 1) \neq 0$ , and the subscript GE stands for gradient elasticity. Thus by approximating  $g(s)$ , one can find the numerical solution to  $\Phi(s)$ .

## 8.3 Chebyshev Polynomial Expansion

The approximation of  $g(s)$  in equation (8.3) is accomplished by means of Chebyshev polynomials expansion. Either Chebyshev polynomials of the first kind  $T_n(s)$ , or of the second kind  $U_n(s)$ , may be employed in the approximation, *i.e.*

$$g(s) = \sum_{n=0}^{\infty} a_n T_n(s) \quad \text{or} \quad g(s) = \sum_{n=0}^{\infty} A_n U_n(s). \quad (8.4)$$

The coefficients  $a_n$ 's or  $A_n$ 's are determined numerically by the collocation method. As shown by Chan *et al.* [14], the two expansions should lead to the same numerical

results. In this paper, the expansion using  $U_n(s)$  is adopted, *i.e.*

$$\Phi(s) = \sqrt{1-s^2} \sum_{n=0}^{\infty} A_n U_n(s) , \quad (8.5)$$

where  $U_n(s)$  is defined, as usual, by

$$U_n(s) = \frac{\sin[(n+1)\cos^{-1}(s)]}{\sin[\cos^{-1}(s)]} , \quad n = 0, 1, 2, \dots \quad (8.6)$$

Satisfaction of the single-valuedness condition (4.32), or equivalently,  $\int_{-1}^1 \Phi(s) ds = 0$ , requires that the following relation holds

$$A_0 = 0 . \quad (8.7)$$

## 8.4 Evaluation of the Derivative of the Density Function

The term  $\Phi'(r)$  in equation (8.1) is evaluated using the expansion (8.5) and the fact that

$$\frac{d}{dr} \left[ U_n(r) \sqrt{1-r^2} \right] = -\frac{n+1}{\sqrt{1-r^2}} T_{n+1}(r) , \quad n \geq 0 . \quad (8.8)$$

Thus

$$\Phi'(r) = \frac{d}{dr} \left[ \sqrt{1-r^2} \sum_{n=0}^{\infty} A_n U_n(r) \right] = \frac{-1}{\sqrt{1-r^2}} \sum_{n=0}^{\infty} (n+1) A_n T_n(r) . \quad (8.9)$$

## 8.5 Formation of the Linear System of Equations

The strategy to determine the coefficients  $A_n$ 's consists of forming a set of linear algebraic equations. Replacing  $\Phi(s)$  in (8.1) by the representation (8.5), and using

(8.9) one obtains the governing integral equation in discretized form:

$$\begin{aligned}
 & -2\tilde{\ell}^2 \sum_{n=1}^{\infty} \frac{A_n}{\pi} \int_{-1}^1 \frac{U_n(s)\sqrt{1-s^2}}{(s-r)^3} ds + \left[ 1 + \frac{5\tilde{\ell}^2\tilde{\gamma}^2}{8} + \frac{\tilde{\ell}'\tilde{\gamma}}{4} - \left( \frac{\tilde{\ell}'}{2\tilde{\ell}} \right)^2 \right] \times \\
 & \sum_{n=1}^{\infty} \frac{A_n}{\pi} \int_{-1}^1 \frac{U_n(s)\sqrt{1-s^2}}{s-r} ds + \sum_{n=1}^{\infty} \frac{A_n}{\pi} \int_{-1}^1 \sqrt{1-s^2} U_n(s) \mathcal{K}(r,s) ds \\
 & - \frac{\tilde{\ell}' + 2\tilde{\ell}^2\tilde{\gamma}}{2\sqrt{1-r^2}} \sum_{n=1}^{\infty} A_n(n+1)T_{n+1}(r) = \frac{\mathcal{P}(r)}{G_0}, |r| < 1. \tag{8.10}
 \end{aligned}$$

Notice that the running index  $n$  starts from 1 instead of 0 (see (8.7)).

## 8.6 Evaluation of Singular and Hypersingular Integrals

The governing integrodifferential equation (4.56), and its discretized version, equation (8.10), contains both Cauchy singular and hypersingular integrals (cubic singularity), which need to be evaluated. Erdogan *et al.* [28, 29] have presented formulas for evaluating Cauchy singular integrals, and Chan *et al.* [11] have presented formulas for evaluating a broad class of hypersingular integrals, which generalizes previous derivations [28, 29, 50] in the literature. For easy reference, the ones being used in the present numerical example are listed here: For  $|r| < 1$ ,

$$\frac{1}{\pi} \int_{-1}^1 \frac{U_n(s)\sqrt{1-s^2}}{s-r} ds = -T_{n+1}(r), \quad n \geq 0, \tag{8.11}$$

$$\frac{1}{\pi} \int_{-1}^1 \frac{U_n(s)\sqrt{1-s^2}}{(s-r)^2} ds = -(n+1)U_n(r), \quad n \geq 0 \tag{8.12}$$

$$\frac{1}{\pi} \int_{-1}^1 \frac{U_n(s)\sqrt{1-s^2}}{(s-r)^3} ds = \begin{cases} -1, & n = 0, \\ [(n^2+n)U_{n+1}(r) - (n^2+3n+2)U_{n-1}(r)] / [4(1-r^2)], & n \geq 1. \end{cases} \tag{8.13}$$



## 8.7 Evaluation of Non-singular Integral

Combining all the results obtained so far in the numerical approximation, one may rewrite equation (8.10) in the following form

$$\begin{aligned}
 & \frac{-\tilde{\ell}^2}{2(1-r^2)} \sum_{n=1}^{\infty} A_n [(n^2+n)U_{n+1}(r) - (n^2+3n+2)U_{n-1}(r)] \\
 & - \left[ 1 + \frac{5\tilde{\ell}^2\tilde{\gamma}^2}{8} + \frac{\tilde{\ell}'\tilde{\gamma}}{4} - \left( \frac{\tilde{\ell}'}{2\tilde{\ell}} \right)^2 \right] \sum_{n=1}^{\infty} A_n T_{n+1}(r) + \sum_{n=1}^{\infty} \frac{A_n}{\pi} \int_{-1}^1 \sqrt{1-s^2} U_n(s) \mathcal{K}(r,s) ds \\
 & - \frac{\tilde{\ell}' + 2\tilde{\ell}^2\tilde{\gamma}}{2\sqrt{1-r^2}} \sum_{n=1}^{\infty} A_n (n+1) T_{n+1}(r) = \frac{\mathcal{P}(r)}{G}, \quad |r| < 1. \tag{8.14}
 \end{aligned}$$

Thus the last step to apply the collocation method is to know the evaluation of the (regular) integral in (8.14), which is actually a double integral, *i.e.*

$$\begin{aligned}
 \int_{-1}^1 \sqrt{1-s^2} U_n(s) \mathcal{K}(r,s) ds &= \int_{-1}^1 \sqrt{1-s^2} U_n(s) ak(ar, as) ds \\
 &= \int_{-1}^1 \sqrt{1-s^2} U_n(s) \int_0^{\infty} aN(\xi) \sin[a\xi(s-r)] d\xi ds.
 \end{aligned}$$

with  $N(\xi)$  described in equation (4.45). **Figure 4.3** permits to graphically evaluate the behavior of the integrand of equation (4.54). Clearly, such kernel is oscillatory, but the magnitude of oscillation decreases and tend to zero as  $\xi$  increases, *i.e.*  $\lim_{\xi \rightarrow \infty} N(\xi) \sin[\xi(t-x)] = 0$ . Another point that we need to be cautious about in equation (4.54) is at  $\xi = 0$ , because of  $N(\xi) = P(\xi)/Q(\xi)$  and  $Q(\xi)$  has the factor  $\xi$ . However, this would not affect the integrability of the integrand in equation (4.54) because of the term  $\sin[\xi(t-x)]$ . Thus  $\lim_{\xi \rightarrow 0} N(\xi) \sin[\xi(t-x)]$  exists and is finite, which depends on the values of  $t$ ,  $x$ ,  $\ell$ ,  $\ell'$ , and  $\gamma$ . The integral along  $[0, \infty)$  is a Fourier sine transform, and can be efficiently evaluated by applying fast Fourier transform (FFT) [19, 38, 89]. The integral along  $[-1, 1]$  can be readily obtained by the Gaussian quadrature method [87].

## 8.8 Stress Intensity Factors

Since the propagation of a crack starts around its tips, it is very important to study and determine the stress intensity factors (SIFs) at both crack tips. In classical LEFM the stress  $\sigma_{yz}(x, 0)$  has  $1/\sqrt{x-a}$  singularity as  $x \rightarrow a^+$  (or  $1/\sqrt{x+a}$ , as  $x \rightarrow -a^-$ ), and thus SIFs are defined and can be calculated by

$$K_{III}(a) = \lim_{x \rightarrow a^+} \sqrt{2\pi(x-a)} \sigma_{yz}(x, 0), \quad (x > a), \quad (8.15)$$

and

$$K_{III}(-a) = \lim_{x \rightarrow -a^-} \sqrt{2\pi(-a-x)} \sigma_{yz}(x, 0), \quad (x < -a). \quad (8.16)$$

However, the same definition may not hold for strain-gradient elasticity because  $\sigma_{yz}(x, 0)$  may have a stronger singularity [100]. Thus SIFs will be redefined in the development below.

First, note that the limit in equations (8.15) and (8.16) is taken from outside of the crack surfaces toward both tips, and the integral equation (4.56) is the expression for  $\sigma_{yz}(x, 0)$  which is valid for  $|x| > a$  as well as  $|x| < a$ , *i.e.*

$$\begin{aligned} \sigma_{yz}(x, 0) = & \frac{G}{\pi} \int_{-a}^a \left\{ \frac{-2\ell^2}{(t-x)^3} + \frac{5\ell^2\gamma^2/8 + \ell'\gamma/4 + 1 - (\ell'/\ell)^2/4}{t-x} + k(x, t) \right\} \phi(t) dt \\ & + \frac{G}{2} (\ell' + 2\ell^2\gamma) \phi'(x), \quad |x| > a. \end{aligned} \quad (8.17)$$

Second, after normalization and with the density function  $\Phi(t)$  expanded by Chebyshev polynomials of the second kind  $U_n$ , some integral formulas, which are useful for deriving SIFs, need to be developed for  $|r| > 1$  (Chan *et al.* [11]), and are listed in Appendix B (see equations (8.23) to (8.25)). Notice that the highest singularity in the equations (8.23) to (8.25) appears in the last term in equation (8.25), and it has singularity  $(r^2 - 1)^{-3/2}$  as  $r \rightarrow 1^+$  or  $r \rightarrow -1^-$ . Motivated by such asymptotic behavior, we generalize the SIFs for strain gradient elasticity from those of classical

LEFM. Thus

$$\ell K_{III}(a) = \lim_{x \rightarrow a^+} 2\sqrt{2\pi(x-a)}(x-a) \sigma_{yz}(x, 0), \quad (8.18)$$

$$\ell K_{III}(-a) = \lim_{x \rightarrow -a^-} 2\sqrt{2\pi(x+a)}(x+a) \sigma_{yz}(x, 0). \quad (8.19)$$

Therefore, the following formulas for the normalized mode III SIFs in the strain-gradient elasticity theory may be derived:

$$\begin{aligned} \ell K_{III}(a) &= \lim_{x \rightarrow a^+} 2\sqrt{2\pi(x-a)}(x-a) \sigma_{yz}(x, 0), \quad (x > a) \\ &= \lim_{r \rightarrow 1^+} 2\sqrt{2\pi(ar-a)}(ar-a) \sigma_{yz}(ar, 0), \quad (r > 1) \\ &= 2a\sqrt{\pi a} G_0 \lim_{r \rightarrow 1^+} \sqrt{2(r-1)}(r-1) \frac{-2\ell^2}{\pi a^2} \int_{-1}^1 \frac{\Phi(s)}{(s-r)^3} ds, \quad (r > 1). \end{aligned} \quad (8.20)$$

After cancellation of the common terms, equation (8.20) can be continued by introducing formula (8.25), and using the representation (8.5), *i.e.*

$$\begin{aligned} K_{III}(a) &= 2\sqrt{2\pi a} \left( \frac{-2\ell}{a} \right) G_0 \lim_{r \rightarrow 1^+} (r-1)^{3/2} \times \\ &\quad \sum_{n=0}^N \frac{-(n+1)}{2} \left( r - \frac{|r|}{r} \sqrt{r^2-1} \right)^{n-1} \left[ n \left( 1 - \frac{|r|}{\sqrt{r^2-1}} \right)^2 + \frac{r - \frac{|r|}{r} \sqrt{r^2-1}}{\sqrt{r^2-1}^3} \right] A_n \\ &= \sqrt{\pi a} G_0 (\ell/a) \sum_{n=0}^{\infty} (n+1) A_n. \end{aligned} \quad (8.21)$$

Similarly,

$$K_{III}(-a) = \sqrt{\pi a} G_0 (\ell/a) \sum_{n=0}^{\infty} (-1)^n (n+1) A_n. \quad (8.22)$$

Formulas (8.21) and (8.22) are used to obtain numerical results for SIFs (see Tables 4.3 & 4.3).

The calculation of stress intensity factors (8.21) and (8.22) requires knowledge about integrals like

$$\frac{1}{\pi} \int_{-1}^1 \frac{U_n(s) \sqrt{1-s^2}}{(s-r)^\alpha} ds, \quad |r| > 1 \quad n \geq 0.$$

The derivation has been addressed in Chapter 7. For easy reference, we list the following formulas here: For  $|r| > 1$ ,

$$\frac{1}{\pi} \int_{-1}^1 \frac{U_n(s) \sqrt{1-s^2}}{s-r} ds = - \left( r - \frac{|r|}{r} \sqrt{r^2-1} \right)^{n+1}, \quad n \geq 0 \quad (8.23)$$

$$\frac{1}{\pi} \int_{-1}^1 \frac{U_n(s) \sqrt{1-s^2}}{(s-r)^2} ds = -(n+1) \left( 1 - \frac{|r|}{\sqrt{r^2-1}} \right) \left( r - \frac{|r|}{r} \sqrt{r^2-1} \right)^n, \quad n \geq 0 \quad (8.24)$$

$$\begin{aligned} \frac{1}{\pi} \int_{-1}^1 \frac{U_n(s) \sqrt{1-s^2}}{(s-r)^3} ds &= \frac{-1}{2} (n+1) \left( r - \frac{|r|}{r} \sqrt{r^2-1} \right)^{n-1} \\ &\times \left[ n \left( 1 - \frac{|r|}{\sqrt{r^2-1}} \right)^2 + \frac{r - \frac{|r|}{r} \sqrt{r^2-1}}{\sqrt{r^2-1}^3} \right], \quad n \geq 0 \end{aligned} \quad (8.25)$$

### 8.9 $T_n$ vs. $U_n$

By giving a numerical example, we demonstrate that we can use either Chebyshev polynomials  $T_n$  or  $U_n$  to be in the expansion of the unknown density function. Consider a crack in an infinite strip of homogeneous material, as illustrated in Figure 8.1.

The governing PDE and boundary conditions are:

$$\begin{aligned} \nabla^2 u(x, y) + \frac{2}{\kappa-1} \left( \frac{\partial^2 u(x, y)}{\partial x^2} + \frac{\partial^2 u(x, y)}{\partial x \partial y} \right) &= 0, & -\infty < x, y < \infty, \\ \nabla^2 v(x, y) + \frac{2}{\kappa-1} \left( \frac{\partial^2 v(x, y)}{\partial y^2} + \frac{\partial^2 v(x, y)}{\partial x \partial y} \right) &= 0, & -\infty < x, y < \infty, \\ \sigma_{xx}(0, y) = \sigma_{xy}(0, y) = \sigma_{xx}(h, y) = \sigma_{xy}(h, y) &= 0, & -\infty < y < \infty, \\ \sigma_{xy}(x, 0) = 0, & & 0 < x < h, \\ \sigma_{yy}(x, 0) = -p(x), & & x \in (c, d), \\ v(x, 0) = 0, & & x \notin [c, d], \end{aligned} \quad (8.26)$$

where  $u$  and  $v$  are the  $x$  and  $y$  components of the displacement vector;  $\sigma_{ij}$  is the stress tensor;  $\kappa$  is an elastic constant ( $\kappa = 3 - 4\nu$  for plane strain,  $\kappa = (3 - \nu)/(1 + \nu)$  for plane stress, and  $\nu$  is the Poisson's ratio.) This problem has been studied by Kaya

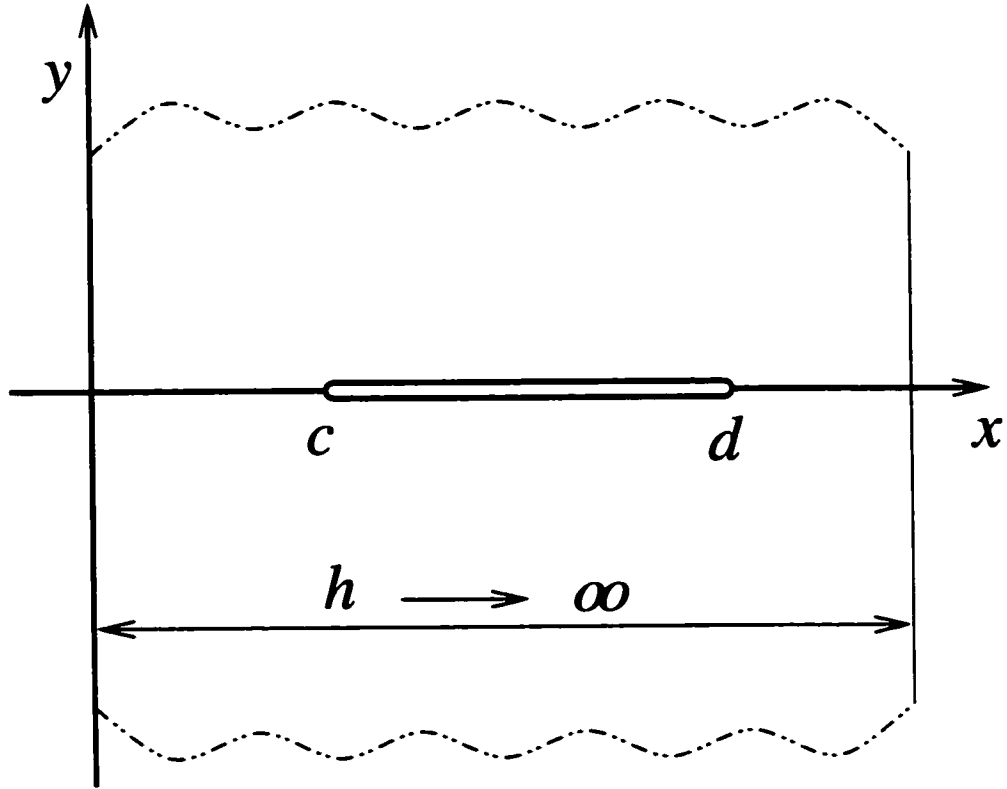


Figure 8.1: A mode I crack in an infinite strip.

and Erdogan [50] by means of a  $U_n$  representation, and it has also been used as a benchmark problem by Kabir *et al.* [47]. Here both  $U_n$  and  $T_n$  are employed and compared.

The governing integral equation can be written in the form given by equation (7.3) as in Kaya and Erdogan [50]

$$\int_c^d \frac{\Delta v(t)}{(t-x)^2} dt + \int_c^d k(x,t) \Delta v(t) dt = -\pi \left( \frac{1+\kappa}{2G} \right) p(x), \quad c < x < d, \quad (8.27)$$

where  $G \equiv \mu$  is the shear modulus, the primary variable is the crack opening displacement  $\Delta v$  given by

$$\Delta v(x) = v(x, 0^+) - v(x, 0^-), \quad c < x < d,$$

and the kernel  $k(x, t)$  is given in Kaya and Erdogan [50], equations (51) – (54c), page 112. It is worth noting that as  $h \rightarrow \infty$  (see Figure 8.1), the integral equation for the half plane is recovered and the kernel  $k(x, t)$  is reduced to a much simpler form<sup>1</sup>

$$k(x, t) = \frac{-1}{(t+x)^2} + \frac{12x}{(t+x)^3} - \frac{12x^2}{(t+x)^4}.$$

After normalization, the corresponding integral equation can be written in a fashion similar to equation (7.5), *i.e.*<sup>2</sup>

$$\oint_{-1}^1 \frac{D(s)}{(s-r)^2} ds + \int_{-1}^1 \mathcal{K}(r, s) D(s) ds = P(r), \quad -1 < r < 1, \quad (8.28)$$

where  $D(s)$  is the unknown displacement function, the regular kernel is

$$\mathcal{K}(r, s) = \frac{-1}{\left[(r+s) + 2\left(\frac{d+c}{d-c}\right)\right]^2} + \frac{12\left[s + \left(\frac{d+c}{d-c}\right)\right]}{\left[(r+s) + 2\left(\frac{d+c}{d-c}\right)\right]^3} - \frac{12\left[s + \left(\frac{d+c}{d-c}\right)\right]^2}{\left[(r+s) + 2\left(\frac{d+c}{d-c}\right)\right]^4},$$

and the loading function is

$$P(s) = -\pi \left(\frac{1+\kappa}{2G}\right) p \left(\left(\frac{d-c}{2}\right)s + \frac{d+c}{2}\right).$$

The case  $c > 0$  represents an internal crack, which is the case of interest in this work. Based on the dominant behavior of the singular kernels of the integral equation (8.28), the solution takes the form

$$D(s) = R(s)\sqrt{1-s^2}.$$

Here the representation function  $R(s)$  is approximated in terms of Chebyshev polynomials of 1st and 2nd kinds, *i.e.*

$$R(s) = \sum_{n=0}^N a_n U_n(s) \quad \text{and} \quad R(s) = \sum_{n=0}^N b_n T_n(s).$$

The unknown coefficients  $a_n$  and  $b_n$  are determined by selecting an appropriate set of collocation points

$$r_j = \cos\left(\frac{(2n-1)\pi}{2(N+1)}\right), \quad j = 1, 2, \dots, N+1; \quad \text{for } U_n \text{ representation}.$$

<sup>1</sup>To be consistent with the notation adopted in this section, we have used symbols different from those used by Kaya and Erdogan [50]. For instance, upper case  $K(t, x)$  is used by Kaya and Erdogan [50], instead of  $k(t, x)$ .

<sup>2</sup>Again, the notation is different from the one adopted by Kaya and Erdogan [50].

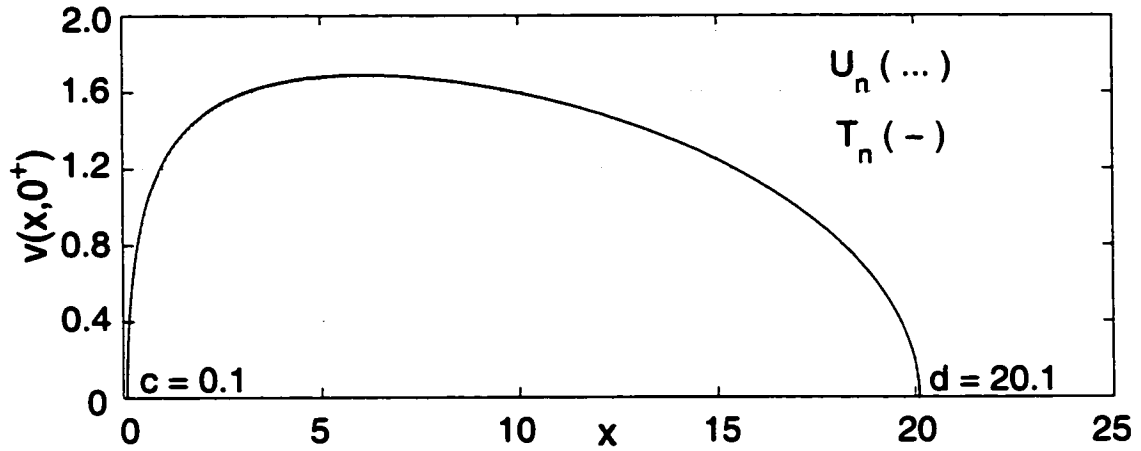


Figure 8.2: Displacement profiles for a mode I crack in an infinite strip obtained by means of  $U_n$  and  $T_n$  representations ( $N + 1 = 15$ ). Here  $c = 0.1$ ,  $d = 20.1$ ,  $2a = 20$ , and  $(c + d)/(d - c) = 1.01$ . The crack is tilted to the left because of the “edge effect”.

$$r_j = \cos\left(\frac{n\pi}{N+2}\right), \quad j = 1, 2, \dots, N+1; \quad \text{for } T_n \text{ representation.}$$

Once the solution is obtained, the SIFs can be calculated from <sup>3</sup>

$$\begin{aligned} K_I(c) &= \lim_{x \rightarrow c^-} \sqrt{2\pi(c-x)} \sigma_{yy}(x, 0), \quad (x < c) \\ &= \left(\frac{2G}{1+\kappa}\right) \lim_{x \rightarrow c^+} \frac{D(x)}{\sqrt{2\pi(x-c)}}, \quad (x > c) \\ &= \left(\frac{2G}{1+\kappa}\right) \sqrt{\frac{d-c}{2\pi}} R(-1) \end{aligned} \quad (8.29)$$

and

$$\begin{aligned} K_I(d) &= \lim_{x \rightarrow d^+} \sqrt{2\pi(x-d)} \sigma_{yy}(x, 0), \quad (x > d) \\ &= \left(\frac{2G}{1+\kappa}\right) \lim_{x \rightarrow d^-} \frac{D(x)}{\sqrt{2\pi(d-x)}}, \quad (x < d) \\ &= \left(\frac{2G}{1+\kappa}\right) \sqrt{\frac{d-c}{2\pi}} R(+1) \end{aligned} \quad (8.30)$$

<sup>3</sup>Kaya and Erdogan [50] do not consider the factor  $\sqrt{\pi}$  in the definition of SIFs, equations (8.29) and (8.30). Note that this does not affect the normalized SIFs (e.g. see Table 8.1).

which are obtained from equation (8.27) by observing that its left-hand-side gives the stress component  $\sigma_{yy}(x, 0)$  outside the crack interval  $(c, d)$ .

Table 8.1: Normalized stress intensity factors (SIFs) for an internal crack in a half-plane.  $N + 1$  terms are used in approximating the primary variable.

| $\frac{d+c}{d-c}$ | $N + 1$ | $U_n$ Representation                   |  | $T_n$ Representation                   |  | Kaya and Erdogan [50]                  |  |
|-------------------|---------|--|--|--|--|--|--|
|                   |         | $\frac{K_I(c)/p_0}{\sqrt{\pi(d-c)/2}}$ | $\frac{K_I(d)/p_0}{\sqrt{\pi(d-c)/2}}$ | $\frac{K_I(c)/p_0}{\sqrt{\pi(d-c)/2}}$ | $\frac{K_I(d)/p_0}{\sqrt{\pi(d-c)/2}}$ | $\frac{K_I(c)/p_0}{\sqrt{\pi(d-c)/2}}$ | $\frac{K_I(d)/p_0}{\sqrt{\pi(d-c)/2}}$ |
| 1.01              | 15      | 3.6437                                 | 1.3292                                 | 3.8037                                 | 1.3313                                 | 3.6387                                 | 1.3298                                 |
| 1.05              | 10      | 2.1541                                 | 1.2535                                 | 2.1920                                 | 1.2543                                 | 2.1547                                 | 1.2536                                 |
| 1.1               | 10      | 1.7583                                 | 1.2108                                 | 1.7655                                 | 1.2111                                 | 1.7587                                 | 1.2108                                 |
| 1.2               | 6       | 1.4637                                 | 1.1625                                 | 1.4728                                 | 1.1632                                 | 1.4637                                 | 1.1626                                 |
| 1.3               | 6       | 1.3316                                 | 1.1331                                 | 1.3346                                 | 1.1335                                 | 1.3316                                 | 1.1331                                 |
| 1.4               | 6       | 1.2544                                 | 1.1123                                 | 1.2556                                 | 1.1125                                 | 1.2544                                 | 1.1123                                 |
| 1.5               | 4       | 1.2036                                 | 1.0966                                 | 1.2066                                 | 1.0969                                 | 1.2035                                 | 1.0967                                 |
| 2.0               | 4       | 1.0913                                 | 1.0539                                 | 1.0916                                 | 1.0540                                 | 1.0913                                 | 1.0539                                 |
| 3.0               | 4       | 1.0345                                 | 1.0246                                 | 1.0346                                 | 1.0246                                 | 1.0345                                 | 1.0246                                 |
| 4.0               | 4       | 1.0182                                 | 1.0141                                 | 1.0182                                 | 1.0141                                 | 1.0182                                 | 1.0141                                 |
| 5.0               | 4       | 1.0112                                 | 1.0092                                 | 1.0112                                 | 1.0092                                 | 1.0112                                 | 1.0092                                 |
| 10.0              | 4       | 1.0026                                 | 1.0024                                 | 1.0026                                 | 1.0024                                 | 1.0026                                 | 1.0024                                 |
| 20.0              | 4       | 1.0006                                 | 1.0006                                 | 1.0006                                 | 1.0006                                 | 1.0006                                 | 1.0006                                 |

Table 8.1 presents the SIFs at both tips of an internal crack in a half-plane ( $h \rightarrow \infty$ ) under uniform load ( $p(x) = p_0$ ) obtained with both  $U_n$  and  $T_n$  representations. First, it is worth noting that the present SIF results for the  $U_n$  representation compare well with those reported in Table 1 (page 114) of the paper by Kaya and Erdogan [50] for the entire range of values describing the relative position of the crack, *i.e.*  $1.01 < (d + c)/(d - c) < 20$ . Next, comparing the SIFs obtained with the  $U_n$  and  $T_n$  representations in Table 8.1, we note that the results compare quite well, except when  $(d + c)/(d - c) \approx 1.0$ , and the discrepancy is bigger at the left-hand-side (LHS) than at the right-hand-side (RHS) crack tip. This occurs because of the “edge



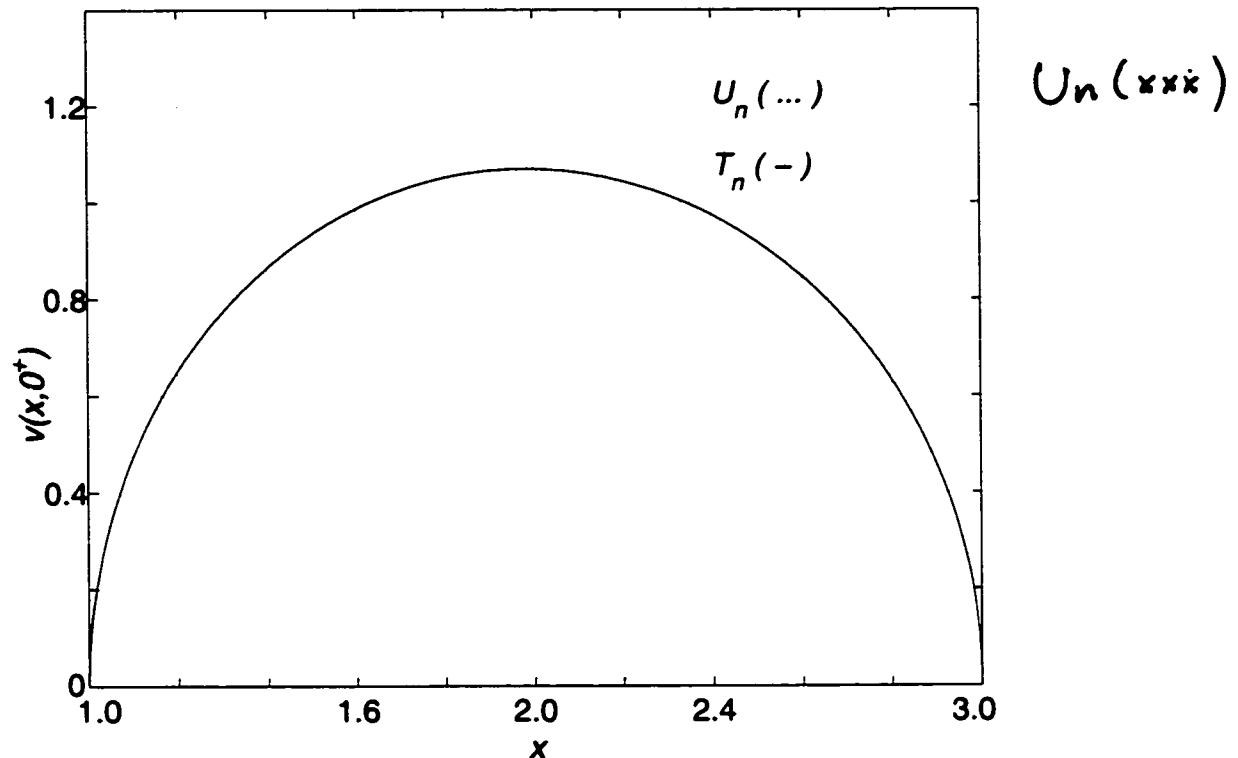


Figure 8.3: Displacement profiles for a mode I crack in an infinite strip obtained by means of  $U_n$  and  $T_n$  representations ( $N + 1 = 8$ ). Here  $c = 1$ ,  $d = 3$ ,  $2a = 2$ , and  $(c + d)/(d - c) = 2$ .

effect” (Paulino *et al.* [74]). If 42 terms (*i.e.*  $N + 1 = 42$ ) and  $T_n$  representation are considered for the case  $(d + c)/(d - c) = 1.01$ , then the normalized SIFs at the LHS and RHS crack tips are 3.6437 and 1.3302, respectively. Thus, when there is an “edge effect”, the results are sensitive to the discretization adopted. Moreover, for the same number of collocation points, the level of accuracy attained with the  $U_n$  representation is slightly different from that with the  $T_n$  representation.

Figure 8.2 and Figure 8.3 compare the crack profiles for  $U_n$  and  $T_n$  representations. One may observe that the displacement profiles obtained from both representations practically agree within plotting accuracy, especially in Figure 8.3. Note that the displacement profile in Figure 8.2 is tilted to the left because of the “edge effect”. Such effect is negligible in Figure 8.3.

## Chapter 9

# Mode III Crack Problems with Strain-Gradient Effect — A Case with Closed Form Solution

In Chapter 4 we have derived:

$$\frac{G_0}{\pi} \int_{-a}^a \left\{ \frac{-2\ell^2}{(t-x)^3} + \frac{5\ell^2\gamma^2/8 + \ell'\gamma/4 + 1 - (\ell'/\ell)^2/4}{t-x} + k(x,t) \right\} \phi(t) dt + \frac{G}{2}(\ell' + 2\ell^2\gamma) \phi'(x) = p(x), \quad |x| < a. \quad (4.56)$$

If  $\gamma = 0$ , *i.e.* for the case of homogeneous materials, equation (4.56) becomes

$$\frac{G_0}{\pi} \int_{-a}^a \left\{ \frac{-2\ell^2}{(t-x)^3} + \frac{1 - (\ell'/\ell)^2/4}{t-x} + K_0(x,t) \right\} \phi(t) dt + \frac{G_0\ell'}{2} \phi'(x) = p(x), \quad |x| < a, \quad (9.1)$$

where the regular kernel  $K_0(x,t)$  will be addressed later in this chapter. Two main goals are set in this chapter:

1. We show that there is a closed form solution to (9.1) if  $\ell' = 0$ .

2. The crack-tips asymptotics for the unknown density function  $\phi(x)$  in (9.1) is

$$\phi(x) \sim \sqrt{a^2 - x^2} \quad \text{as } x \rightarrow \pm a, \quad (9.2)$$

instead of

$$\phi(x) \sim (a^2 - x^2)^{3/2} \quad \text{as } x \rightarrow \pm a.$$

Of course, once goal one is achieved, goal two should follow right away. However, historically, we faced the problem without knowing the closed form solution first. Also, at the end of the chapter we will discuss briefly the strain-gradient effect on Mode III cracks for the more general strain energy density.

## 9.1 Hypersingular integrodifferential equations

The derivation of (9.1) has been done in Chapter 4, thus we will not repeat here. However, because the regular kernel is different, we shall start off

$$\lim_{y \rightarrow 0^+} \frac{G}{2\pi} \int_{-a}^a \phi(t) \int_{-\infty}^{\infty} \hat{K}(\xi, y) e^{i\xi(x-t)} d\xi dt = -p(x), \quad |x| < a \quad (9.3)$$

with the kernel

$$\hat{K}(\xi, y) = \frac{|\xi| (\ell'/\ell) \sqrt{\ell^2 \xi^2 + 1} + \ell^2 \xi^2 + 1}{i\xi (\ell'/\ell) \sqrt{\ell^2 \xi^2 + 1} - \ell' |\xi| + 1} e^{-|\xi|y}.$$

The limit  $y \rightarrow 0^+$  in (9.3) is singular since  $\hat{K}(\xi, 0)$  does not decay in  $\xi$ . So we write

$$\hat{K}(\xi, 0) = \hat{K}_{\infty}(\xi) + \hat{K}_0(\xi)$$

with the nondecaying part  $\hat{K}_{\infty}(\xi, 0)$  given by

$$\hat{K}_{\infty}(\xi, 0) = \frac{|\xi|}{i\xi} \left[ 1 - \frac{1}{4} \left( \frac{\ell'}{\ell} \right)^2 + \frac{\ell'}{2} |\xi| + \ell^2 \xi^2 \right] \quad (9.4)$$

and the decaying part  $\hat{K}_0(\xi)$  given by

$$\begin{aligned}
 \hat{K}_0(\xi) &= \frac{|\xi| [\ell'|\xi|/2 + (\ell'/2\ell)^2] \left( \sqrt{\ell^2\xi^2 + 1} - \ell|\xi| \right) + (\ell'/\ell)^3/4}{i\xi \left( \ell'/\ell + \sqrt{\ell^2\xi^2 + 1} + \ell|\xi| \right)} \\
 &= \rho \frac{|\xi| (\ell|\xi|/2 + \rho/4) \left( \sqrt{\ell^2\xi^2 + 1} - \ell|\xi| \right) + \rho^2/4}{i\xi \left( \rho + \sqrt{\ell^2\xi^2 + 1} + \ell|\xi| \right)}, \quad \rho = \ell'/\ell. \quad (9.5)
 \end{aligned}$$

By (9.4) and the results of Chapter 5

$$\int_{-\infty}^{\infty} \hat{K}_\infty(\xi, y) e^{i\xi(x-t)} d\xi$$

converges, as  $y \rightarrow 0^+$ , in the sense of distribution, to the hypersingular kernels of the following equation (9.6) whereas  $\hat{K}_0(\xi)$  gives rise to the regular kernel  $K_0$ . Thus, as  $y \rightarrow 0^+$ , equation (9.3) becomes

$$\begin{aligned}
 -\frac{2\ell^2}{\pi} \int_{-a}^a \frac{\phi(t)}{(t-x)^3} dt + \frac{1-\rho^2/4}{\pi} \int_{-a}^a \frac{\phi(t)}{t-x} dt + \frac{1}{\pi} \int_{-a}^a K_0(t-x)\phi(t) dt \\
 - \frac{\ell'}{2} \phi'(x) = \frac{p(x)}{G}, \quad |x| < a, \quad (9.6)
 \end{aligned}$$

where the regular kernel  $K_0$  can be written as

$$K_0(t-x) = 2 \int_0^\infty \hat{K}_0(\xi) \sin[\xi(t-x)] d\xi \quad (9.7)$$

in view of the anti-symmetry of  $\hat{K}_0(\xi)$ . Recall that since the dominant kernel in (9.6) is cubically singular, we need to furnish, in addition to (4.32), the crack-tip condition (4.57).

## 9.2 Solutions of the integral equations

It is convenient to nondimensionalize equation (9.6) by the half crack length  $a$ . In view of the fact that both  $\phi(x)$  and  $p(x)/G$  are dimensionless, this amounts to normalizing the variables by  $a$  in the equation and replacing  $\ell, \ell'$  by  $\bar{\ell} = \ell/a, \bar{\ell}' = \ell'/a$ , respectively.

### 9.2.1 Case $\ell' = 0$ : closed form solution

Note that the regular kernel  $K_0(t-x)$  in equation (9.6) has a factor  $\ell'$ , so it drops out from the equation when  $\ell' = 0$ . After normalizing by the half crack length  $a$ , equation (9.6) becomes:

$$-\frac{2\ell^2}{\pi} \int_{-1}^1 \frac{\phi(t)}{(t-x)^3} dt + \frac{1}{\pi} \int_{-1}^1 \frac{1}{t-x} \phi(t) dt = p(x)/G, \quad |x| < 1. \quad (9.8)$$

Let  $\mathbf{H}$  denote the finite Hilbert transform

$$\mathbf{H}[\phi](x) = \frac{1}{\pi} \int_{-1}^1 \frac{\phi(t)}{t-x} dt.$$

Then, by the definition of Hadamard's finite part integrals (see Chapter 5), equation (9.8) is a second order differential equation for  $\mathbf{H}[\phi](x)$ :

$$-\ell^2 \mathbf{H}[\phi]''(x) + \mathbf{H}[\phi](x) = p(x)/G,$$

which has the general solution

$$\mathbf{H}[\phi](x) = -\frac{1}{\ell^2} e^{x/\ell} \int_{-1}^x \left[ e^{-2s/\ell} \int_{-1}^s e^{t/\ell} \frac{p(t)}{G} dt \right] ds + C_1 e^{x/\ell} + C_2 e^{-x/\ell}. \quad (9.9)$$

Set

$$f(x) = -\frac{1}{\ell^2} e^{x/\ell} \int_{-1}^x \left[ e^{-2s/\ell} \int_{-1}^s e^{t/\ell} \frac{p(t)}{G} dt \right] ds,$$

then we have

$$\frac{1}{\pi} \int_{-1}^1 \frac{1}{t-x} \phi(t) dt = f(x) + C_1 e^{x/\ell} + C_2 e^{-x/\ell} \equiv g(x). \quad (9.10)$$

It is well known (Tricomi 1957 [91]) that the solution  $\phi(x)$  of equation (9.10) is unique in  $L^p[-1, 1]$  for any  $p > 1$ , where  $L^p[-1, 1]$  is defined by

$$L^p[-1, 1] = \left\{ f : [-1, 1] \rightarrow \mathcal{R} \mid \|f\|_p = \left[ \int_{-1}^1 |f(x)|^p dx \right]^{1/p} < \infty \right\},$$

and  $\phi(x)$  can be written as

$$\begin{aligned} \phi(x) = & \frac{\sqrt{1-x^2}}{\pi} \int_{-1}^1 \frac{g(t)}{\sqrt{1-t^2}(x-t)} dt + \frac{x}{\pi\sqrt{1-x^2}} \int_{-1}^1 \frac{g(t)}{\sqrt{1-t^2}} dt \\ & + \frac{1}{\pi\sqrt{1-x^2}} \int_{-1}^1 \frac{tg(t)}{\sqrt{1-t^2}} dt + \frac{1}{\pi\sqrt{1-x^2}} \int_{-1}^1 \phi(t) dt \end{aligned} \quad (9.11)$$

provided that equation (9.11) is well-defined. For this, it suffices, for example, that  $g(x) \in L^p[-1, 1]$  for some  $p > 2$ , so  $g(t)/\sqrt{1-t^2} \in L^{1+}[-1, 1]$ .

Under condition (4.32) and a stronger integrability condition,  $\phi \in L^p[-1, 1]$  for some  $p > 2$  (instead of condition (4.57)), we then have the conditions determining  $g(x)$

$$\int_{-1}^1 \frac{g(t)}{\sqrt{1-t^2}} dt = 0, \quad \int_{-1}^1 \frac{tg(t)}{\sqrt{1-t^2}} dt = 0$$

or equivalently

$$\int_{-1}^1 \frac{f(t)}{\sqrt{1-t^2}} dt + C_1 \int_{-1}^1 \frac{e^{t/\ell}}{\sqrt{1-t^2}} dt + C_2 \int_{-1}^1 \frac{e^{-t/\ell}}{\sqrt{1-t^2}} dt = 0 \quad (9.12)$$

$$\int_{-1}^1 \frac{tf(t)}{\sqrt{1-t^2}} dt + C_1 \int_{-1}^1 \frac{te^{t/\ell}}{\sqrt{1-t^2}} dt + C_2 \int_{-1}^1 \frac{te^{-t/\ell}}{\sqrt{1-t^2}} dt = 0 \quad (9.13)$$

which determine uniquely the constants  $C_1, C_2$ :

$$C_1 = - \left( 2 \int_{-1}^1 \frac{e^{t/\ell}}{\sqrt{1-t^2}} dt \right)^{-1} \int_{-1}^1 \frac{f(t)}{\sqrt{1-t^2}} dt - \left( 2 \int_{-1}^1 \frac{te^{t/\ell}}{\sqrt{1-t^2}} dt \right)^{-1} \int_{-1}^1 \frac{tf(t)}{\sqrt{1-t^2}} dt$$

$$C_2 = - \left( 2 \int_{-1}^1 \frac{e^{t/\ell}}{\sqrt{1-t^2}} dt \right)^{-1} \int_{-1}^1 \frac{f(t)}{\sqrt{1-t^2}} dt + \left( 2 \int_{-1}^1 \frac{te^{t/\ell}}{\sqrt{1-t^2}} dt \right)^{-1} \int_{-1}^1 \frac{tf(t)}{\sqrt{1-t^2}} dt.$$

With the above proviso, equation (9.11) becomes

$$\phi(x) = \frac{\sqrt{1-x^2}}{\pi} \int_{-1}^1 \frac{g(t)}{\sqrt{1-t^2}(x-t)} dt. \quad (9.14)$$

While the form (9.14) makes explicit the crack-tip asymptotics  $O(\sqrt{1-x^2})$  for the slope  $\phi(x)$ , the following alternative form [75] is also useful for analyzing the limiting behavior as  $\ell \rightarrow 0$ :

$$\phi(x) = \frac{1}{\pi\sqrt{1-x^2}} \times$$

$$\left[ \int_{-1}^1 \frac{\sqrt{1-t^2} f(t)}{x-t} dt + C_1 \int_{-1}^1 \frac{\sqrt{1-t^2} e^{t/\ell}}{x-t} dt + C_2 \int_{-1}^1 \frac{\sqrt{1-t^2} e^{-t/\ell}}{x-t} dt \right] \quad (9.15)$$

since the limit has the singularity like  $(\sqrt{1-x^2})^{-1}$  near the crack-tips. To be consistent with the expression (9.14), the apparent singularity in (9.15) must be canceled.

The unique solution satisfying (4.57) corresponds to the following choice of  $C_1, C_2$ .

First we note that, for  $f(x) \in L^p[-1, 1], p > 2$ ,

$$\mathbf{H}[\sqrt{1-t^2}f](-1) = \frac{1}{\pi} \int_{-1}^1 \sqrt{\frac{1-t}{1+t}} f(t) dt < \infty$$

$$\mathbf{H}[\sqrt{1-t^2}f](1) = -\frac{1}{\pi} \int_{-1}^1 \sqrt{\frac{1+t}{1-t}} f(t) dt < \infty$$

$$\begin{aligned} \mathbf{H}[\sqrt{1-t^2}e^{-t/\ell}](-1) &= \frac{1}{\pi} \int_{-1}^1 \sqrt{\frac{1-t}{1+t}} e^{-t/\ell} dt = \frac{1}{\pi} \int_{-1}^1 \sqrt{\frac{1+t}{1-t}} e^{t/\ell} dt \\ &= -\mathbf{H}[\sqrt{1-t^2}e^{t/\ell}](1) < \infty \end{aligned}$$

$$\begin{aligned} -\mathbf{H}[\sqrt{1-t^2}e^{-t/\ell}](1) &= \frac{1}{\pi} \int_{-1}^1 \sqrt{\frac{1+t}{1-t}} e^{-t/\ell} dt = \frac{1}{\pi} \int_{-1}^1 \sqrt{\frac{1-t}{1+t}} e^{t/\ell} dt \\ &= \mathbf{H}[\sqrt{1-t^2}e^{t/\ell}](-1) < \infty \end{aligned}$$

Thus, in the presence of the factor  $1/\sqrt{1-x^2}$  in equation (9.15), the constants  $C_1$  and  $C_2$  must satisfy

$$\mathbf{H}[\sqrt{1-t^2}f](-1) + C_1 \mathbf{H}[\sqrt{1-t^2}e^{t/\ell}](-1) + C_2 \mathbf{H}[\sqrt{1-t^2}e^{-t/\ell}](-1) = 0 \quad (9.16)$$

$$\mathbf{H}[\sqrt{1-t^2}f](1) + C_1 \mathbf{H}[\sqrt{1-t^2}e^{t/\ell}](1) + C_2 \mathbf{H}[\sqrt{1-t^2}e^{-t/\ell}](1) = 0. \quad (9.17)$$

The determinant of the above system is

$$\begin{aligned} &\mathbf{H}[\sqrt{1-t^2}e^{t/\ell}](-1)\mathbf{H}[\sqrt{1-t^2}e^{-t/\ell}](1) - \mathbf{H}[\sqrt{1-t^2}e^{-t/\ell}](-1)\mathbf{H}[\sqrt{1-t^2}e^{t/\ell}](1) \\ &= \left\{ \mathbf{H}[\sqrt{1-t^2}e^{t/\ell}](-1) \right\}^2 - \left\{ \mathbf{H}[\sqrt{1-t^2}e^{t/\ell}](1) \right\}^2 \\ &\neq 0 \end{aligned}$$

so  $C_1$  and  $C_2$  are uniquely determined by (9.16)-(9.17). It can be shown directly that with this choice of  $C_1, C_2$ , equation (9.15) has the crack-tip asymptotics  $O(\sqrt{1-x^2})$ .

The idea is that the expression

$$\int_{-1}^1 \frac{\sqrt{1-t^2} f(t)}{t-x} dt + C_1 \int_{-1}^1 \frac{\sqrt{1-t^2} e^{t/\ell}}{t-x} dt + C_2 \int_{-1}^1 \frac{\sqrt{1-t^2} e^{-t/\ell}}{t-x} dt$$

generally has the asymptotics  $O(1-x^2)$  near the crack tips  $x = \pm 1$ . We will address the asymptotics in Section 9.3.

### 9.2.2 Case $\ell' \neq 0$ : A Regular Perturbation

Integrating eq. (9.6) once in  $x$ , we obtain

$$\begin{aligned} & -\frac{\ell^2}{\pi} \int_{-1}^1 \frac{\phi(t)}{(t-x)^2} dt + \frac{1-\rho^2/4}{\pi} \int_{-1}^1 \log|t-x|\phi(t) dt \\ & + \frac{1}{\pi} \int_{-1}^1 \tilde{K}_0(t-x)\phi(t) dt - \frac{\ell'}{2}\phi(x) = \int_0^x p(t)/G dt + C_0, \quad |x| < 1, \end{aligned} \quad (9.18)$$

where  $\tilde{K}_0(t)$  is a primitive function of the regular kernel  $K_0$ :  $\tilde{K}_0'(t) = K_0(t)$ . The constant  $C_0$  is to be determined by the condition (4.32). With condition (4.57), equation (9.18) is a type of quadratically singular integral equation, studied in Martin 1991 [60] in which the end-point asymptotics of  $\phi(x)$  was proved to be  $O(\sqrt{1-x^2})$  by using the Mellin transform.

The crack-tip asymptotics can also be derived in another way. Integrating equation (9.6) twice in  $x$ , we obtain

$$\begin{aligned} & -\ell^2 \mathbf{H}[\phi](x) + \frac{1-\rho^2/4}{\pi} \int_{-1}^1 \int_{-1}^x \log|t-s| ds \phi(t) dt - \frac{\ell'}{2} \int_{-1}^x \phi(t) dt \\ & + \frac{1}{\pi} \int_{-1}^1 \int_{-1}^x ds \int_{-1}^s d\sigma K_0(t-\sigma)\phi(t) dt = \frac{1}{G} \int_{-1}^x ds \int_{-1}^s d\sigma p(\sigma) + C_1 x + C_0, \end{aligned}$$

which is a generalized Cauchy singular integral equation

$$-\ell^2 \mathbf{H}[\phi](x) + \int_{-1}^1 K(x,t)\phi(t) dt = \int_{-1}^x ds \int_{-1}^s d\sigma p(\sigma)/G + C_1 x + C_0 \quad (9.19)$$

with a regular kernel

$$K(x,t) = \frac{1-(\ell'/2\ell)^2}{\pi} \int_{-1}^x \log|t-s| ds + \frac{1}{\pi} \int_{-1}^x ds \int_{-1}^s d\sigma K_0(t-\sigma) - \frac{\ell'}{2} \mathbf{I}_{[-1, x]}(t),$$

where  $\mathbf{I}_{[-1, x]}$  is the characteristic function of the interval  $[-1, x]$ ,  $\forall |x| < 1$ , i.e.

$$\mathbf{I}_{[-1, x]}(t) = \begin{cases} 1, & \text{if } t \in [-1, x], \\ 0, & \text{if } t \notin [-1, x]. \end{cases}$$

Since

$$\int_{-1}^1 \int_{-1}^1 K^2(x,t) dt dx < \infty,$$



the integral operator

$$\mathbf{K}[\phi](x) \equiv \int_{-1}^1 K(x, t)\phi(t)dt$$

is a Hilbert-Schmidt operator on  $L^2[-1, 1]$ . Therefore the solution  $\phi$  has the same end-point asymptotics as that of the solutions  $\tilde{\phi}$  of the dominant equation

$$-\ell^2 \mathbf{H}[\phi](x) = f(x) + C_1 x + C_0 \quad (9.20)$$

subject to the same set of end-point conditions (Muskhelishvili 1953 [68]). The end-point asymptotics of the solution of equation (9.20) can be analyzed as before.

### 9.3 Crack-Tips Asymptotics for the Unknown Density Function $\phi(x)$

Here we show the end-point asymptotics of the closed form solution (9.15) is  $O(\sqrt{1-x^2})$ , instead of  $O((1-x^2)^{3/2})$ .

For the first question, with the developed numerical tool in hand, it is very easy to show that the end-point asymptotics of the closed form solution (9.15) is  $O(\sqrt{1-x^2})$ , and it is demonstrated in Figure 9.1 which shows the numerical solution vs. closed form solution (9.15).

The answer to the second part: If the closed form solution (9.15) has end-point asymptotics  $O((1-x^2)^{3/2})$ , then  $\phi(x)$  needs to satisfy the solution for the following boundary value problem:

$$-\ell^2 \phi''(x) + \phi(x) = f(x), \quad \text{with } \phi(\pm 1) = 0 \quad \text{and} \quad \phi'(\pm 1) = 0, \quad (9.21)$$

where  $f(x) = x/(\pi \sqrt{1-x^2})$  if the loading is uniform, *i.e.*  $p(x)/G = 1$ . One problem arises immediately: there are four BCs imposed to a 2nd order ODE (9.21)! Existence of solution is jeopardized. A simple calculation gives the general solution to (9.21):

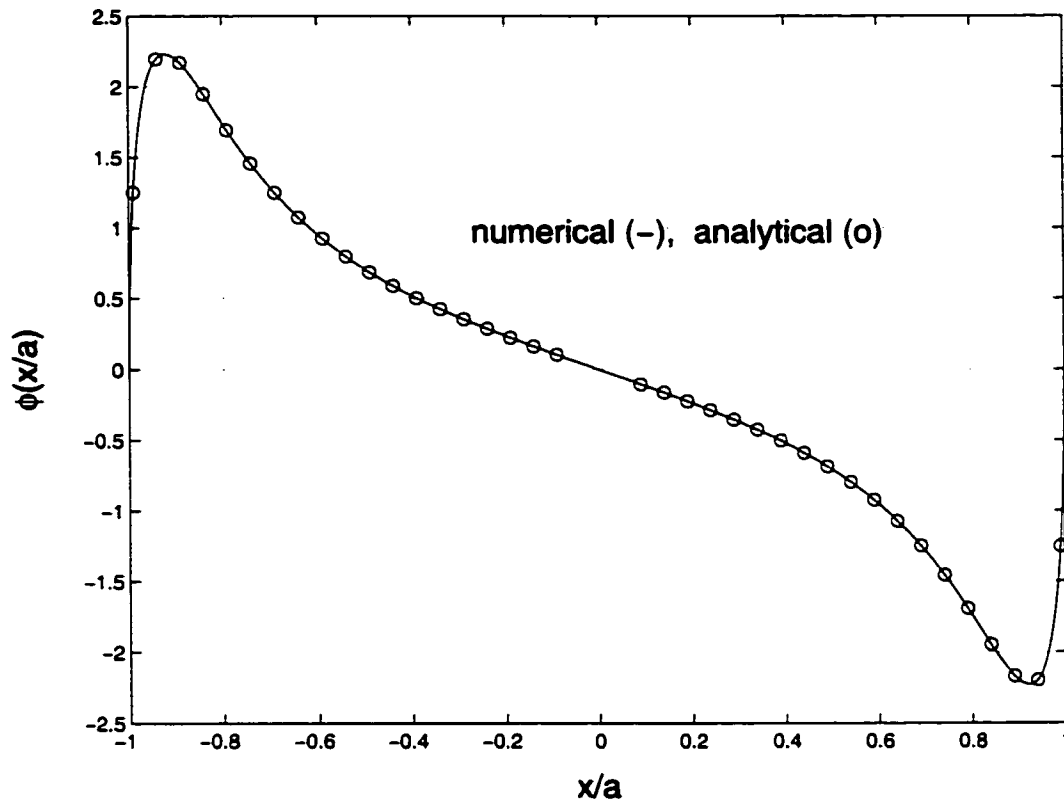


Figure 9.1: Numerical solution vs. closed form solution (9.15)

$$\begin{aligned} \phi(x) = & \frac{-1}{2\ell} e^{x/\ell} \int_{-1}^x e^{-s/\ell} f(s) ds + \frac{1}{2\ell} e^{-x/\ell} \int_{-1}^x e^{s/\ell} f(s) ds \\ & + C_1 e^{x/\ell} + C_2 e^{-x/\ell}, \end{aligned}$$

where  $C_1$  and  $C_2$  are some constants determined by the four BCs. It can be easily shown that the problem does not have a solution. Otherwise, a contradiction,  $e^{2/\ell} = 1$ , will be reached. Thus, we conclude that

$$\phi(x) \text{ does not have end-point asymptotics } O((1-x^2)^{3/2}).$$

## 9.4 More General Form of Strain Energy Density Function

The strain-energy density function for Mode III fracture is

$$\mathcal{W} = \frac{1}{2} \lambda \epsilon_{ii} \epsilon_{jj} + G \epsilon_{ij} \epsilon_{ji} + \ell^2 G (\partial_k \epsilon_{ij})(\partial_k \epsilon_{ji}) + \ell' \nu_k \partial_k (G \epsilon_{ij} \epsilon_{ji}),$$

which appeared as equation (3.17) in Chapter 3. As anti-plane shear problems are considered, in terms of the nonzero strains  $\epsilon_{xz}$  and  $\epsilon_{yz}$ , density function (3.17) can be written as

$$\mathcal{W} = 2 [G(\epsilon_{xz}^2 + \epsilon_{yz}^2) + G\ell^2(|\nabla\epsilon_{xz}|^2 + |\nabla\epsilon_{yz}|^2) + G\ell'\nu_k\partial_k(\epsilon_{xz}^2 + \epsilon_{yz}^2)], \quad (9.22)$$

which leads to

$$-\ell^2 \nabla^4 w + \nabla^2 w = 0 \quad \text{or} \quad (1 - \ell^2 \nabla^2) \nabla^2 w = 0. \quad (9.23)$$

The hypersingular integral equation (9.6) is derived from PDE (9.23).

A more general form of strain energy density function is by adding an extra Laplacian term,  $\frac{1}{2}G\hat{\ell}^2(\Delta w)^2$ , to (9.6), that is,

$$\mathcal{W} \Rightarrow \mathcal{W} + 2G\hat{\ell}^2(\epsilon_{xz,x} + \epsilon_{yz,y})^2 = \mathcal{W} + \frac{1}{2}G\hat{\ell}^2(\Delta w)^2,$$

then the kernel  $\hat{K}(\xi, y)$  (corresponding to (9.5)) becomes

$$\hat{K}(\xi, y) = \frac{|\xi|}{i\xi} \frac{\left(\ell'/\sqrt{\ell^2 + \hat{\ell}^2}\right) \sqrt{(\ell^2 + \hat{\ell}^2)\xi^2 + 1 + \ell^2\xi^2 + 1}}{\left(\ell'/\sqrt{\ell^2 + \hat{\ell}^2}\right) \sqrt{(\ell^2 + \hat{\ell}^2)\xi^2 + 1 - \ell'|\xi| + 1}} e^{-|\xi|y}.$$

Asymptotics (as  $|\xi| \rightarrow \infty$ ) is given by

$$\hat{K}_\infty(\xi, 0) = \frac{|\xi|}{i\xi} \left[ \frac{1}{4} \frac{4\ell^4 - (\ell\ell')^2 + 8(\ell\hat{\ell})^2 + 4\hat{\ell}^4 - 2(\hat{\ell}\ell')^2}{(\ell^2 + \hat{\ell}^2)^2} + \frac{1}{2} \frac{\ell'(\ell^2 + 2\hat{\ell}^2)}{\ell^2 + \hat{\ell}^2} |\xi| + \ell^2\xi^2 \right]$$

The decaying part  $\hat{K}_0(\xi)$  is

$$\hat{K}_0(\xi) = \frac{|\xi|}{i\xi} \frac{p(\xi)}{\ell'/\sqrt{\ell^2 + \hat{\ell}^2} + \sqrt{(\ell^2 + \hat{\ell}^2)\xi^2 + 1} + \sqrt{\ell^2 + \hat{\ell}^2}|\xi|},$$

where

$$p(\xi) = \left[ \frac{\ell' \ell^2 |\xi|}{2(\ell^2 + \hat{\ell}^2)} + \frac{\ell'^2}{4(\ell^2 + \hat{\ell}^2)} \left( 1 + \frac{\hat{\ell}^2}{\ell^2 + \hat{\ell}^2} \right) \right] \left[ \sqrt{(\ell^2 + \hat{\ell}^2)\xi^2 + 1} - \sqrt{\ell^2 + \hat{\ell}^2} |\xi| \right] + \frac{1}{4} \left( \frac{\ell'}{\sqrt{\ell^2 + \hat{\ell}^2}} \right)^3 \left( 1 + \frac{\hat{\ell}^2}{\ell^2 + \hat{\ell}^2} \right)$$

$\hat{K}_0(\xi)$  can be written as

$$\rho \frac{|\xi|}{i\xi} \frac{\left[ \frac{\ell^2 |\xi|}{2\sqrt{\ell^2 + \hat{\ell}^2}} + \frac{\ell}{4}(1 + \hat{\rho}^2) \right] \left[ \sqrt{(\ell^2 + \hat{\ell}^2)\xi^2 + 1} - \sqrt{\ell^2 + \hat{\ell}^2} |\xi| \right] + \frac{\ell^2}{4}(1 + \hat{\rho}^2)}{\rho + \sqrt{(\ell^2 + \hat{\ell}^2)\xi^2 + 1} + \sqrt{\ell^2 + \hat{\ell}^2} |\xi|},$$

where

$$\rho = \frac{\ell'}{\sqrt{\ell^2 + \hat{\ell}^2}}, \quad \hat{\rho} = \frac{\hat{\ell}}{\sqrt{\ell^2 + \hat{\ell}^2}}$$

Thus,  $\hat{K}_0(\xi)$  still has  $\ell'$  as a factor!

## Chapter 10

# Hypersingular Integral Equations for Mode III Fracture in Functionally Graded Materials with Strain-Gradient Effect (Crack Parallel to the Material Gradation)

This chapter can be considered as a second part of Chapter 4. In Chapter 4, we considered a plane elasticity problem in which the medium contains a finite crack on the  $y = 0$  plane and the material gradation is perpendicular to the crack. In this chapter, the material gradation is parallel to the crack (see Figure 10.1). In Chapter 4, the shear modulus  $G$  (that rules the material gradation) is a function of  $y$  only,  $G \equiv G(y) = G_0 e^{\gamma y}$ ; while in this chapter it is a function of  $x$ , *i.e.*  $G \equiv G(x) = G_0 e^{\beta x}$ . An immediate consequence of the difference in geometry, which is indicated in Figure 10.1, is that the location of the crack in Chapter 4 is rather irrelevant to the problem

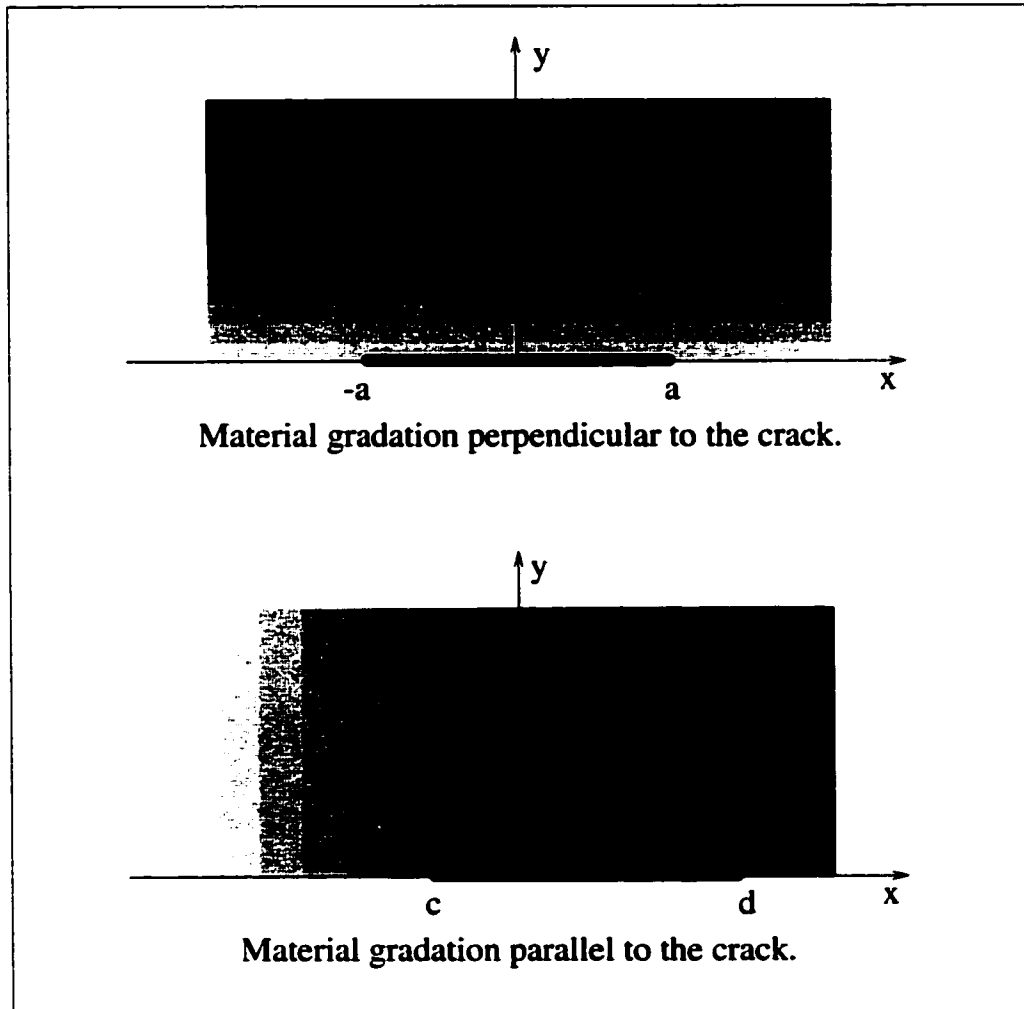


Figure 10.1: A geometric comparison of the material gradation with respect to the crack location.

and thus can be shifted so that the center is at the origin point  $(0, 0)$ . On the other hand, if the material gradation is parallel to the crack, then the location of the crack is pertinent to the solution of the problem.

The method of solution is essentially the same in both Chapters 4 and 10, *i.e.* the integral equation method. However, because of differences in the geometrical configurations, some changes are expected. For instance, in Chapters 4 the crack opening displacement profile is symmetric with respect to the  $y$  axis, while in this chapter the

symmetry of the crack profiles no longer exists. Thus some interesting questions arise:

- How are the crack opening displacement profiles affected by the gradient elasticity and the gradation of the material?
- How are the stresses influenced under the gradient elasticity?
- How are the stress intensity factors (SIFs) calculated?
- How do the results compare with the classical linear elastic fracture mechanics (LEFM)?

We will address all the above questions.

## 10.1 Constitutive Equations of Gradient Elasticity

For the sake of completeness, the constitutive equations of gradient elasticity for an anti-plane shear crack in FGMs are briefly given in this section and particularized to the case of an exponentially graded material along the  $x$ -direction, and they are (Chan *et al.* [13], Paulino *et al.* [72]):

$$\begin{aligned} \sigma_{ij} = & \lambda(x)\epsilon_{kk}\delta_{ij} + 2G(x)(\epsilon_{ij} - \ell^2\nabla^2\epsilon_{ij}) \\ & - \ell^2[\partial_k\lambda(x)](\partial_k\epsilon_{ll})\delta_{ij} - 2\ell^2[\partial_k G(x)](\partial_k\epsilon_{ij}) \end{aligned} \quad (10.1)$$

$$\tau_{ij} = \lambda(x)\epsilon_{kk}\delta_{ij} + 2G(x)\epsilon_{ij} + 2\ell'\nu_k[\epsilon_{ij}\partial_k G(x) + G(x)\partial_k\epsilon_{ij}] \quad (10.2)$$

$$\mu_{kij} = 2\ell'\nu_k G(x)\epsilon_{ij} + 2\ell^2 G(x)\partial_k\epsilon_{ij}, \quad (10.3)$$

For a mode-III problem, each component of the stress fields can be written specifically as following:

$$\begin{aligned}
 \sigma_{xx} &= \sigma_{yy} = \sigma_{zz} = 0, \quad \sigma_{xy} = 0 \\
 \sigma_{xz} &= 2G(x)(\epsilon_{xz} - \ell^2 \nabla^2 \epsilon_{xz}) - 2\ell^2 [\partial_x G(x)] (\partial_x \epsilon_{xz}) \neq 0 \\
 \sigma_{yz} &= 2G(x)(\epsilon_{yz} - \ell^2 \nabla^2 \epsilon_{yz}) - 2\ell^2 [\partial_x G(x)] (\partial_x \epsilon_{yz}) \neq 0 \\
 \mu_{xxz} &= 2G(x) \ell^2 \partial \epsilon_{xz} / \partial x \\
 \mu_{xyz} &= 2G(x) \ell^2 \partial \epsilon_{yz} / \partial x \\
 \mu_{yxz} &= 2G(x) (\ell^2 \partial \epsilon_{xz} / \partial y - \ell' \epsilon_{xz}) \\
 \mu_{yyz} &= 2G(x) (\ell^2 \partial \epsilon_{yz} / \partial y - \ell' \epsilon_{yz}).
 \end{aligned} \tag{10.4}$$

It is worth to point out that each of the total stresses  $\sigma_{xz}$  and  $\sigma_{yz}$  in (10.4) has an extra term than the ones in homogeneous materials (see Vardoulakis *et al.* 1996 [92], page 4534) due to the material gradation interplays with the strain gradient effect (Chan *et al.* [13]).

## 10.2 Governing Partial Differential Equation and Boundary Conditions

The following PDE is obtained by applying the balance of force:

$$\begin{aligned}
 & \frac{\partial}{\partial x} \left[ G(x) \left( \frac{\partial w}{\partial x} - \ell^2 \nabla^2 \frac{\partial w}{\partial x} \right) \right] + \frac{\partial}{\partial y} \left[ G(x) \left( \frac{\partial w}{\partial y} - \ell^2 \nabla^2 \frac{\partial w}{\partial y} \right) \right] \\
 & - \ell^2 \left[ \frac{\partial^2 G(x)}{\partial x^2} \frac{\partial^2 w}{\partial x^2} + \frac{\partial G(x)}{\partial x} \frac{\partial^3 w}{\partial x^3} + \frac{\partial G(x)}{\partial x} \frac{\partial^3 w}{\partial x \partial y^2} \right] = 0.
 \end{aligned} \tag{10.5}$$

If the shear modulus  $G$  is assumed as an exponential function of  $x$  (see Figure 10.2):

$$G = G(x) = G_0 e^{\beta x}, \tag{10.6}$$

then PDE (10.5) can be simplified as

$$-\ell^2 \nabla^4 w - 2\beta \ell^2 \nabla^2 \frac{\partial w}{\partial x} + \nabla^2 w - \beta^2 \ell^2 \frac{\partial^2 w}{\partial x^2} + \beta \frac{\partial w}{\partial x} = 0, \tag{10.7}$$



or

$$\left(1 - \beta \ell^2 \frac{\partial}{\partial x} - \ell^2 \nabla^2\right) \left(\nabla^2 + \beta \frac{\partial}{\partial x}\right) w = 0, \quad (10.8)$$

which is the governing PDE solved in the present chapter.

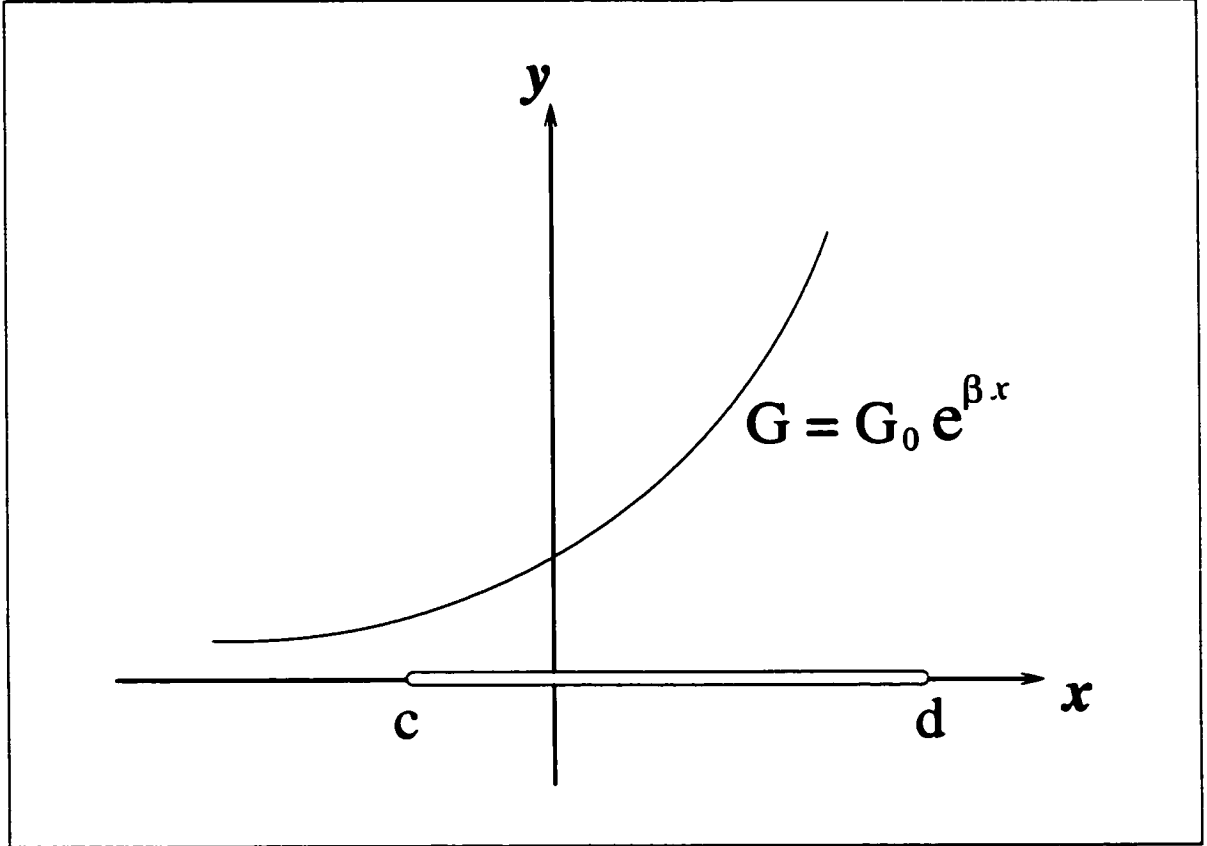


Figure 10.2: Geometry of the crack problem.

It may be seen, from a viewpoint of perturbation, that PDE (10.8) can be expressed in an operator form, *i.e.*

$$\mathbf{H}_\beta \mathbf{L}_\beta w = 0; \quad \mathbf{H}_\beta = 1 - \beta \ell^2 \frac{\partial}{\partial x} - \ell^2 \nabla^2, \quad \mathbf{L}_\beta = \nabla^2 + \beta \frac{\partial}{\partial x}, \quad (10.9)$$

where  $\mathbf{H}_\beta$  is the perturbed Helmholtz operator,  $\mathbf{L}_\beta$  is the perturbed Laplacian operator, and the two operators commute ( $\mathbf{H}_\beta \mathbf{L}_\beta = \mathbf{L}_\beta \mathbf{H}_\beta$ ). By sending  $\beta \rightarrow 0$ , we get the PDE [36, 92]

$$(1 - \ell^2 \nabla^2) \nabla^2 w = 0, \quad \text{or} \quad \mathbf{H}\mathbf{L}w = 0, \quad (10.10)$$

where the Helmholtz operator  $H = 1 - \ell^2 \nabla^2$  and the Laplacian operator  $L = \nabla^2$  are invariant under any change of variables by rotations and translations. FGM creates the perturbation and ruins the invariance. However, the perturbing term “ $-\beta \ell^2 \frac{\partial}{\partial x}$ ” in  $L_\beta$ , which is not purely caused by the gradation of the material, involves both the gradation parameter  $\beta$  and the characteristic length  $\ell$  (the product of  $\beta$  and  $\ell^2$ ). It can be interpreted as a consequence of the interaction of the material gradation and the strain gradient effect [13].

If we let  $\ell \rightarrow 0$  alone, then the perturbed Helmholtz differential operator  $L_\beta$  will be dropped, and one reduces PDE (10.8) to

$$\left( \nabla^2 + \beta \frac{\partial}{\partial x} \right) w = 0, \quad (10.11)$$

the perturbed Laplace equation, which is the PDE that governs the mode III crack problem for nonhomogeneous materials with shear modulus  $G(x) = G_0 e^{\beta x}$  [14, 25]. The limit of sending  $\ell \rightarrow 0$  will lower the fourth order PDE (10.7) to a second order one, (10.11). Thus, based upon the general theory for linear elliptic PDEs – the solution is mainly influenced by the highest order of the differential operator, one expects a singular perturbation to occur. By taking both limits  $\beta \rightarrow 0$  and  $\ell \rightarrow 0$ , one obtains the harmonic equation for classical elasticity. Various combination of parameters  $\ell$  and  $\gamma$  with the corresponding governing PDE are listed in Table 3.1.

One may notice that in the governing PDE (10.8) there is no surface term parameter  $\ell'$  involved. However,  $\ell'$  does come into the picture of the solution when the boundary conditions are considered. By the principle of virtual work the following boundary conditions can be derived:

$$\begin{cases} \sigma_{yz}(x, 0) = p(x) , & |x| < a \\ w(x, 0) = 0 , & |x| > a \\ \mu_{yyz}(x, 0) = 0 , & -\infty < x < +\infty . \end{cases} \quad (10.12)$$

One may observe that the first two boundary conditions in (10.12) are from the classical LEFM, and the last one, regarding the couple-stress  $\mu_{yyz}$ , is needed as the higher order theory is considered.

### 10.3 Solutions of the ODE

As we have demonstrated in Chapter 4, the following ODE is obtained by a Fourier transform technique:

$$\begin{aligned} \ell^2 \frac{d^4}{dy^4} W - (2\ell^2 \xi^2 + 2i\beta\ell^2 \xi + 1) \frac{d^2}{dy^2} W \\ + (\ell^2 \xi^4 + 2i\beta\ell^2 \xi^3 - \beta^2 \ell^2 \xi^2 + \xi^2 + i\beta\xi) W = 0 . \end{aligned} \quad (10.13)$$

The corresponding characteristic equation to the ODE (10.13) is

$$\ell^2 \lambda^4 - (2\ell^2 \xi^2 + 2i\beta\ell^2 \xi + 1) \lambda^2 + (\ell^2 \xi^4 + 2i\beta\ell^2 \xi^3 - \beta^2 \ell^2 \xi^2 + \xi^2 + i\beta\xi) = 0 , \quad (10.14)$$

which can be further factored as

$$[\ell^2 \lambda^2 - (1 + i\beta\ell^2 \xi + \ell^2 \xi^2)] (\lambda^2 - \xi^2 - i\beta\xi) = 0 . \quad (10.15)$$

Clearly the four roots  $\lambda_i$  ( $i = 1, 2, 3, 4$ ) of the polynomial (10.15) above can be obtained as:

$$\lambda_1 = \frac{-1}{\sqrt{2}} \sqrt{\sqrt{\xi^4 + \beta^2 \xi^2} + \xi^2} - \frac{i}{\sqrt{2}} \frac{\beta \xi}{\sqrt{\sqrt{\xi^4 + \beta^2 \xi^2} + \xi^2}} , \quad (10.16)$$

$$\lambda_2 = \frac{1}{\sqrt{2}} \sqrt{\sqrt{\xi^4 + \beta^2 \xi^2} + \xi^2} + \frac{i}{\sqrt{2}} \frac{\beta \xi}{\sqrt{\sqrt{\xi^4 + \beta^2 \xi^2} + \xi^2}} , \quad (10.17)$$

$$\lambda_3 = \frac{-1}{\sqrt{2}} \sqrt{\sqrt{(\xi^2 + 1/\ell^2)^2 + \beta^2 \xi^2} + \xi^2 + 1/\ell^2} - \frac{i}{\sqrt{2}} \frac{\beta \xi}{\sqrt{\sqrt{(\xi^2 + 1/\ell^2)^2 + \beta^2 \xi^2} + \xi^2 + 1/\ell^2}}, \quad (10.18)$$

$$\lambda_4 = \frac{1}{\sqrt{2}} \sqrt{\sqrt{(\xi^2 + 1/\ell^2)^2 + \beta^2 \xi^2} + \xi^2 + 1/\ell^2} + \frac{i}{\sqrt{2}} \frac{\beta \xi}{\sqrt{\sqrt{(\xi^2 + 1/\ell^2)^2 + \beta^2 \xi^2} + \xi^2 + 1/\ell^2}}, \quad (10.19)$$

where we have let  $\Re(\lambda_1)$  and  $\Re(\lambda_3)$ , the real part of  $\lambda_1$  and  $\lambda_3$ , be non-positive. If  $\beta \rightarrow 0$ , then the imaginary part of each root  $\lambda_i$  ( $i = 1, \dots, 4$ ) disappears. Thus we have exactly the same roots found by Vardoulakis *et. al.* [92] and Fannjiang *et al.* [36]. The root  $\lambda_1$  corresponds to the solution of the perturbed harmonic equation,  $\nabla^2 w + \beta \partial w / \partial x = 0$ ; the root  $\lambda_3$  agrees with the solution of the perturbed Helmholtz equation,  $(1 - \beta \ell^2 \partial / \partial x - \ell^2 \nabla^2) w = 0$ . Various choices of parameters  $\ell$  and  $\gamma$  with their corresponding mechanics theories and materials are listed in Table 10.1.

One remark is made here: In comparison with the four roots (all reals) found in Chapter 4, the four roots in here are all complex and admit a more complicated expression. It turns out that in the process of solving the problem, asymptotic analysis of those roots is needed. The simpler the roots are, the easier the asymptotic analysis is. Thus, in this sense, one may say that problems with material gradation perpendicular to the crack are easier to solve than the ones with material gradation parallel to the crack.

By taking account of the far-field boundary condition, one obtains

$$w(x, y) \rightarrow 0 \quad \text{as} \quad \sqrt{x^2 + y^2} \rightarrow +\infty, \quad (10.20)$$

Table 10.1: Roots  $\lambda_i$  together with corresponding mechanics theory and type of material.

| Cases                       | Number of roots | Roots   | Mechanics theory and type of material       | References   |
|-----------------------------|-----------------|---|---|--|
| $\ell = 0, \beta = 0$       | 2               | $\pm \xi $  | Classical LEFM, homogeneous materials.      | Standard textbooks.  |
| $\ell = 0, \beta \neq 0$    | 2               | $\lambda_1$ and $\lambda_2$ in equations (10.16) and (10.17), respectively. | Classical LEFM, nonhomogeneous materials    | Erdogan [25].  |
| $\ell \neq 0, \beta = 0$    | 4               | $\pm \xi , \pm\sqrt{\xi^2 + 1/\ell^2}$                                      | Gradient theories, homogeneous materials.   | Vardoulakis <i>et al.</i> [92].<br>Fannjiang <i>et al.</i> [36]. |
| $\ell \neq 0, \beta \neq 0$ | 4               | The four roots $\lambda_1 - \lambda_4$ in equations (10.16) - (10.19).      | Gradient theories, nonhomogeneous materials | Studied in this chapter.   |

and with  $y > 0$  (the upper half plane), the following expression results:

$$W(\xi, y) = A(\xi)e^{\lambda_1 y} + B(\xi)e^{\lambda_3 y}. \quad (10.21)$$

Accordingly, the displacement  $w(x, y)$  takes the form

$$w(x, y) = \frac{1}{\sqrt{2\pi}} \int_{-\infty}^{\infty} [A(\xi)e^{\lambda_1 y} + B(\xi)e^{\lambda_3 y}] e^{-ix\xi} d\xi. \quad (10.22)$$

Both  $A(\xi)$  and  $B(\xi)$  are determined by the boundary conditions.

## 10.4 Hypersingular Integrodifferential Equation

By taking account of the symmetry along the  $x$ -axis, we may consider that  $w(x, y)$  takes the following form (for the upper half plane):

$$w(x, y) = \frac{1}{\sqrt{2\pi}} \int_{-\infty}^{\infty} \left\{ A(\xi)e^{[-a(\xi)/\sqrt{2} - i\beta\xi/[\sqrt{2}a(\xi)]]y} + B(\xi)e^{[-b(\xi)/\sqrt{2} - i\beta\xi/[\sqrt{2}b(\xi)]]y} \right\} e^{-ix\xi} d\xi, \quad (10.23)$$

where

$$a(\xi) = \sqrt{\sqrt{\xi^4 + \beta^2 \xi^2} + \xi^2}, \quad b(\xi) = \sqrt{\sqrt{(\xi^2 + 1/\ell^2)^2 + \beta^2 \xi^2} + \xi^2 + 1/\ell^2}.$$

As equation (10.23) provides the form of the solution for  $w(x, y)$ , it can be substituted into  $\sigma_{yz}$  and  $\mu_{yyz}$  of equations (10.4) so that the boundary conditions (10.12) can be imposed. Thus,  $\sigma_{yz}$  can be expressed as

$$\begin{aligned} \sigma_{yz}(x, y) &= 2G(x) (\epsilon_{yz} - \ell^2 \nabla^2 \epsilon_{yz}) - 2\ell^2 [\partial_x G(x)] \partial_x \epsilon_{yz} \\ &= \frac{G(x)}{\sqrt{2\pi}} \int_{-\infty}^{\infty} [\lambda_1 A(\xi) e^{\lambda_1 y}] e^{-iz\xi} d\xi, \quad y \geq 0, \end{aligned} \quad (10.24)$$

and  $\mu_{yyz}$  can be written as

$$\begin{aligned} \mu_{yyz}(x, y) &= 2G(x) \left( \ell^2 \frac{\partial \epsilon_{yz}}{\partial y} - \ell' \epsilon_{yz} \right) \\ &= \frac{G(x)}{\sqrt{2\pi}} \int_{-\infty}^{\infty} \{ (\ell^2 \lambda_1^2 - \ell' \lambda_1) A(\xi) e^{\lambda_1 y} + (\ell^2 \lambda_3^2 - \ell' \lambda_3) B(\xi) e^{\lambda_3 y} \} e^{-iz\xi} d\xi \end{aligned} \quad (10.25)$$

By the boundary condition imposed on the couple-stress  $\mu_{yyz}$  (*i.e.*  $\mu_{yyz}(x, 0) = 0$  for  $-\infty < x < \infty$ ) and the expression obtained in equation (10.25), one may get the following relationship between  $A(\xi)$  and  $B(\xi)$

$$B(\xi) = \frac{\ell' \lambda_1 - \ell^2 \lambda_1^2}{\ell^2 \lambda_3^2 - \ell' \lambda_3} A(\xi) = \rho(\beta, \xi) A(\xi), \quad (10.26)$$

where the notation  $\rho(\beta, \xi)$  is introduced such that

$$\rho(\beta, \xi) = \frac{\ell' \lambda_1 - \ell^2 \lambda_1^2}{\ell^2 \lambda_3^2 - \ell' \lambda_3} = -\frac{\ell^2 \xi^2 + i\beta \ell^2 \xi + \ell' \sqrt{\xi^2 + i\beta \xi}}{\ell' \sqrt{\xi^2 + i\beta \xi + 1/\ell^2} + (\ell^2 \xi^2 + i\beta \ell^2 \xi + 1)}. \quad (10.27)$$

Let's denote

$$\begin{aligned} \phi(x) &= \frac{\partial}{\partial x} w(x, 0^+) = \frac{1}{\sqrt{2\pi}} \int_{-\infty}^{\infty} (-i\xi) [A(\xi) + B(\xi)] e^{-iz\xi} d\xi \\ &= \text{the inverse Fourier transform of } \{(-i\xi)[A(\xi) + B(\xi)]\}. \end{aligned} \quad (10.28)$$

The second boundary condition in (10.12), and equation (10.28), imply that

$$\phi(x) = 0, \quad x \notin [c, d], \quad (10.29)$$

and

$$\int_c^d \phi(x) dx = 0, \quad (10.30)$$

which is the single-valuedness condition. By inverting the Fourier transform and using the boundary condition that is imposed on the displacement function  $w(x, y)$ , i.e.  $w(x, 0) = 0$  for  $x \notin [c, d]$ , one obtains

$$\begin{aligned} (-i\xi)[A(\xi) + B(\xi)] &= \frac{1}{\sqrt{2\pi}} \int_{-\infty}^{\infty} \phi(x) e^{ix\xi} dx \\ &= \frac{1}{\sqrt{2\pi}} \int_c^d \phi(t) e^{i\xi t} dt. \end{aligned} \quad (10.31)$$

Substituting (10.26) into (10.31) above, one gets

$$A(\xi) = \frac{1}{\sqrt{2\pi}} \left[ \frac{1}{(-i\xi)[1 + \rho(\beta, \xi)]} \right] \int_c^d \phi(t) e^{i\xi t} dt, \quad (10.32)$$

where

$$\frac{1}{1 + \rho(\beta, \xi)} = \frac{(\ell^2 \xi^2 + i\beta \ell^2 \xi + 1) + \ell' \sqrt{\xi^2 + i\beta \xi + 1/\ell^2}}{1 + \ell' \sqrt{\xi^2 + i\beta \xi + 1/\ell^2} - \ell' \sqrt{\xi^2 + i\beta \xi}}. \quad (10.33)$$

Replacing the  $A(\xi)$  in equation (10.24) by (10.32) and using the (first) boundary condition for  $\sigma_{yz}$  (that is,  $\lim_{y \rightarrow 0^+} \sigma_{yz}(x, y) = p(x)$ ,  $|x| < a$ ) in (10.12), one obtains the following integral equation in limit form:

$$\begin{aligned} \lim_{y \rightarrow 0^+} \sigma_{yz}(x, y) &= \lim_{y \rightarrow 0^+} \frac{G(x)}{2\pi} \int_{-\infty}^{\infty} \left[ \frac{\lambda_1(\beta, \xi)}{(-i\xi)[1 + \rho(\beta, \xi)]} \int_c^d \phi(t) e^{i\xi t} dt \right] e^{\lambda_1 y} e^{-ix\xi} d\xi \\ &= \lim_{y \rightarrow 0^+} \frac{G(x)}{2\pi} \int_c^d \phi(t) \int_{-\infty}^{\infty} \left[ \frac{\lambda_1(\beta, \xi)}{(-i\xi)[1 + \rho(\beta, \xi)]} e^{\lambda_1 y} \right] e^{i(t-x)\xi} d\xi dt \\ &= p(x), \quad c < x < d. \end{aligned} \quad (10.34)$$

By denoting

$$K(\xi, y) = \frac{\lambda_1(\beta, \xi)}{(-i\xi)[1 + \rho(\beta, \xi)]} e^{\lambda_1 y}, \quad (10.35)$$

one can rewrite (10.34) as

$$\lim_{y \rightarrow 0^+} \frac{G}{2\pi} \int_c^d \phi(t) \int_{-\infty}^{\infty} K(\xi, y) e^{i\xi(t-x)} d\xi dt = p(x), \quad c < x < d. \quad (10.36)$$

Asymptotic analysis allows us to split  $K(\xi, y)$  into the singular

$$K_\infty(\xi, y) = \lim_{|\xi| \rightarrow \infty} K(\xi, y), \quad (10.37)$$

and nonsingular part

$$N(\xi, y) = K(\xi, y) - K_\infty(\xi, y). \quad (10.38)$$

As  $y$  is set to be 0, the kernel of equation (10.37) is given by

$$K_\infty(\xi, 0) = -i\ell^2|\xi|\xi - \frac{\ell'}{2}i\xi + \frac{3\beta\ell^2}{2}|\xi| + \frac{\ell'\beta}{2} + \left[ \left( \frac{\ell'}{2\ell} \right)^2 + \frac{3\ell^2\beta^2}{8} - 1 \right] \frac{i\xi}{|\xi|}. \quad (10.39)$$

Note that the real and the imaginary parts of  $K_\infty(\xi, 0)$ , described in equation (10.39), are even and odd functions of  $\xi$ , respectively. The following limit

$$\lim_{y \rightarrow 0^+} K_\infty(\xi, y) e^{i\xi(t-x)} d\xi$$

converges in the distribution sense, as  $y \rightarrow 0^+$ , to the hypersingular kernels. The derivation of hypersingular kernels has been addressed in Chapter 5 (see (5.14)–(5.20)). Here we repeat and list some we are using below:

$$\int_{-\infty}^{\infty} [i\xi|\xi|e^{-|\xi|y}] e^{i(t-x)\xi} d\xi \xrightarrow{y \rightarrow 0^+} \frac{4}{(t-x)^3} \quad (10.40)$$

$$\int_{-\infty}^{\infty} [|\xi|e^{-|\xi|y}] e^{i(t-x)\xi} d\xi \xrightarrow{y \rightarrow 0^+} \frac{-2}{(t-x)^2} \quad (10.41)$$

$$\int_{-\infty}^{\infty} [i\xi e^{-|\xi|y}] e^{i(t-x)\xi} d\xi \xrightarrow{y \rightarrow 0^+} 2\pi\delta'(t-x) \quad (10.42)$$

$$\int_{-\infty}^{\infty} \left[ i \frac{|\xi|}{\xi} e^{-|\xi|y} \right] e^{i(t-x)\xi} d\xi \xrightarrow{y \rightarrow 0^+} \frac{-2}{t-x} \quad (10.43)$$

$$\int_{-\infty}^{\infty} [1e^{-|\xi|y}] e^{i(t-x)\xi} d\xi \xrightarrow{y \rightarrow 0^+} 2\pi\delta(t-x) \quad (10.44)$$

We have used  $\delta(x)$  to denote the Dirac delta function.

By means of the limits that are evaluated from equations (10.40)–(10.44), one may reach the following governing hypersingular integrodifferential equation:

$$\begin{aligned} \frac{1}{\pi} \int_c^d \left\{ \frac{-2\ell^2}{(t-x)^3} - \frac{3\beta\ell^2}{2(t-x)^2} + \frac{1-3\beta^2\ell^2/8 - [\ell'/(2\ell)]^2}{t-x} + k(x, t) \right\} \phi(t) dt \\ + \frac{\ell'}{2} \phi'(x) + \frac{\beta\ell'}{2} \phi(x) = p(x)/G, \quad c < x < d, \quad (10.45) \end{aligned}$$



where we have applied the property about the differentiation of the delta function  $\delta(t)$  in the distribution theory sense, *i.e.*

$$\int_{-\infty}^{\infty} \delta^{(n)}(t-x)D(t)dt = (-1)^n \frac{d^n}{dx^n} D(x).$$

The regular kernel is given by

$$k(x, t) = \int_0^{\infty} N(\xi)e^{i(t-x)\xi}d\xi \quad (10.46)$$

with the function  $N(\xi)$  defined in equation (10.38) by setting  $y = 0$  (*i.e.*  $N(\xi) = N(\xi, 0)$ ). Thus a second kind Fredholm integral equation has been formulated with the cubic-hypersingular and Cauchy-singular kernels, a derivative term, and a free term.

## 10.5 Numerical Solution and Results

Numerical procedures and the computation of SIFs have been addressed in Chapter 8. Some numerical results including crack surface displacements, strains, stresses, and SIFs are given in this section.

### 10.5.1 Numerical Solution

Numerical solution is obtained by discretizing (10.45) to be

$$\begin{aligned} & -2\bar{\ell}^2 \sum_{n=1}^{\infty} \frac{A_n}{\pi} \int_{-1}^1 \frac{U_n(s)\sqrt{1-s^2}}{(s-r)^3} ds - \frac{3\bar{\ell}^2\bar{\beta}}{2} \sum_{n=1}^{\infty} \frac{A_n}{\pi} \int_{-1}^1 \frac{U_n(s)\sqrt{1-s^2}}{(s-r)^2} ds \\ & + \left[ 1 - \frac{3\bar{\ell}^2\bar{\beta}^2}{8} \left( \frac{\bar{\ell}'}{2\bar{\ell}} \right)^2 \right] \sum_{n=1}^{\infty} \frac{A_n}{\pi} \int_{-1}^1 \frac{U_n(s)\sqrt{1-s^2}}{s-r} ds + \sum_{n=1}^{\infty} \frac{A_n}{\pi} \int_{-1}^1 \sqrt{1-s^2} U_n(s) \mathcal{K}(r, s) ds \\ & - \frac{\bar{\ell}'}{2\sqrt{1-r^2}} \sum_{n=1}^{\infty} (n+1) A_n T_{n+1}(r) + \frac{\bar{\ell}'\bar{\beta}}{2} \sqrt{1-r^2} \sum_{n=1}^{\infty} A_n U_n(r) = \frac{\mathcal{P}(r)}{G(r)}, |r| < 1, \end{aligned} \quad (10.47)$$

Where we have normalized  $\phi(x)$  to be  $\Phi(s)$  and used the representation

$$\Phi(s) = \sqrt{1-s^2} \sum_{n=1}^{\infty} A_n U_n(s). \quad (10.48)$$

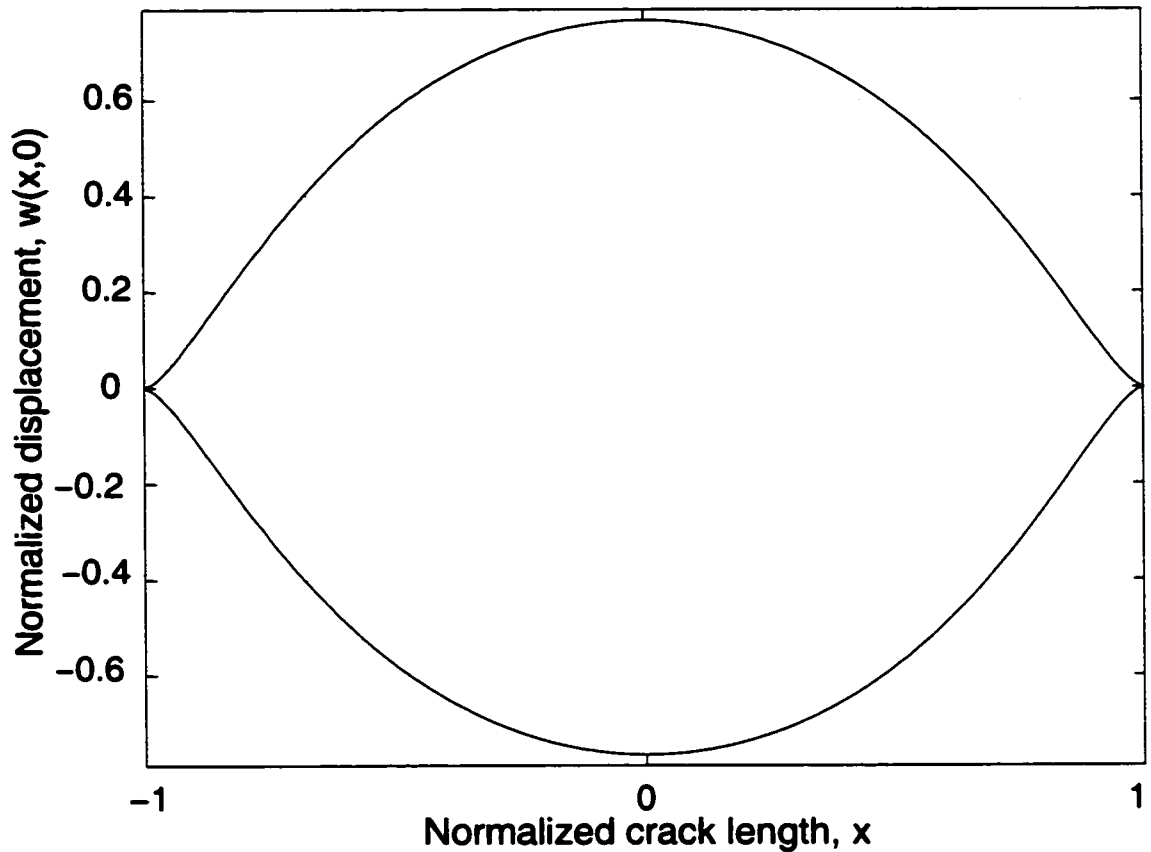


Figure 10.3: Full crack displacement profile for homogeneous material ( $\bar{\beta} = 0$ ) under uniform crack surface shear loading  $\sigma_{yz}(x, 0) = -p_0$  with choice of (normalized)  $\bar{\ell} = 0.2$  and  $\bar{\ell}' = 0$ .

Notice that the running index  $n$  starts from 1 instead of 0 because of the condition (10.30).

### 10.5.2 Crack Surface Displacements

The crack surface displacements are reported in Figures 10.3–10.7. The most prominent feature is the cusping phenomena around the crack tips as shown in Figures 10.3, 10.6 and 10.7. Figure 10.3 shows a full normalized crack sliding displacement profile for a homogeneous medium ( $\bar{\beta} = 0$ ) under the strain-gradient effect.

The crack profile in Figure 10.3 is symmetric because the material is homogeneous.

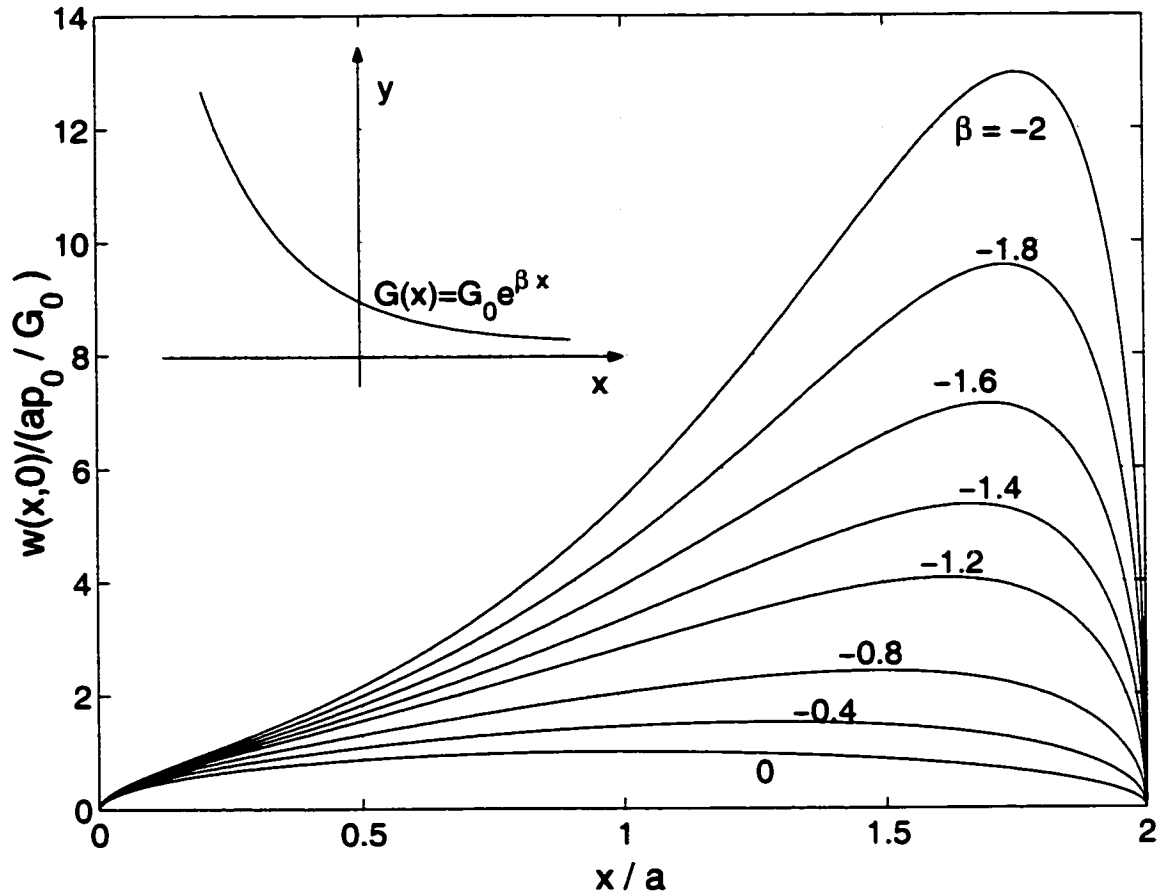


Figure 10.4: Classical LEFM, *i.e.*  $\bar{\ell} = \bar{\ell}' \rightarrow 0$ . Crack surface displacement in an infinite nonhomogeneous plane under uniform crack surface shear loading  $\sigma_{yz}(x,0) = -p_0$  and shear modulus  $G(x) = G_0 e^{\beta x}$ . Here  $a = (d - c)/2$  denotes the half crack length.

Figures 10.4 and 10.5 display the crack sliding profiles in classical LEFM. As  $\beta < 0$ , the material has larger shear modulus at the left side of the crack than at the right side, and thus the material is stiffer on the left and more compliant on the right as shown in Figure 10.4 (and 10.6). Similarly, Figure 10.5 (and 10.7) illustrates the case of  $\beta > 0$ , and confirm that the material is stiffer on the right and more compliant on the left. Figures 10.6 and 10.7 demonstrate the crack surface displacement profiles in FGMs under the strain-gradient effect. The variation of the shear modulus destroys the symmetry of the displacement profiles. In Figure 10.6,  $\beta < 0$ , and the displacement

profiles tilt to the right; while in Figure 10.7,  $\beta > 0$ , and the displacement profiles tilt to the left.

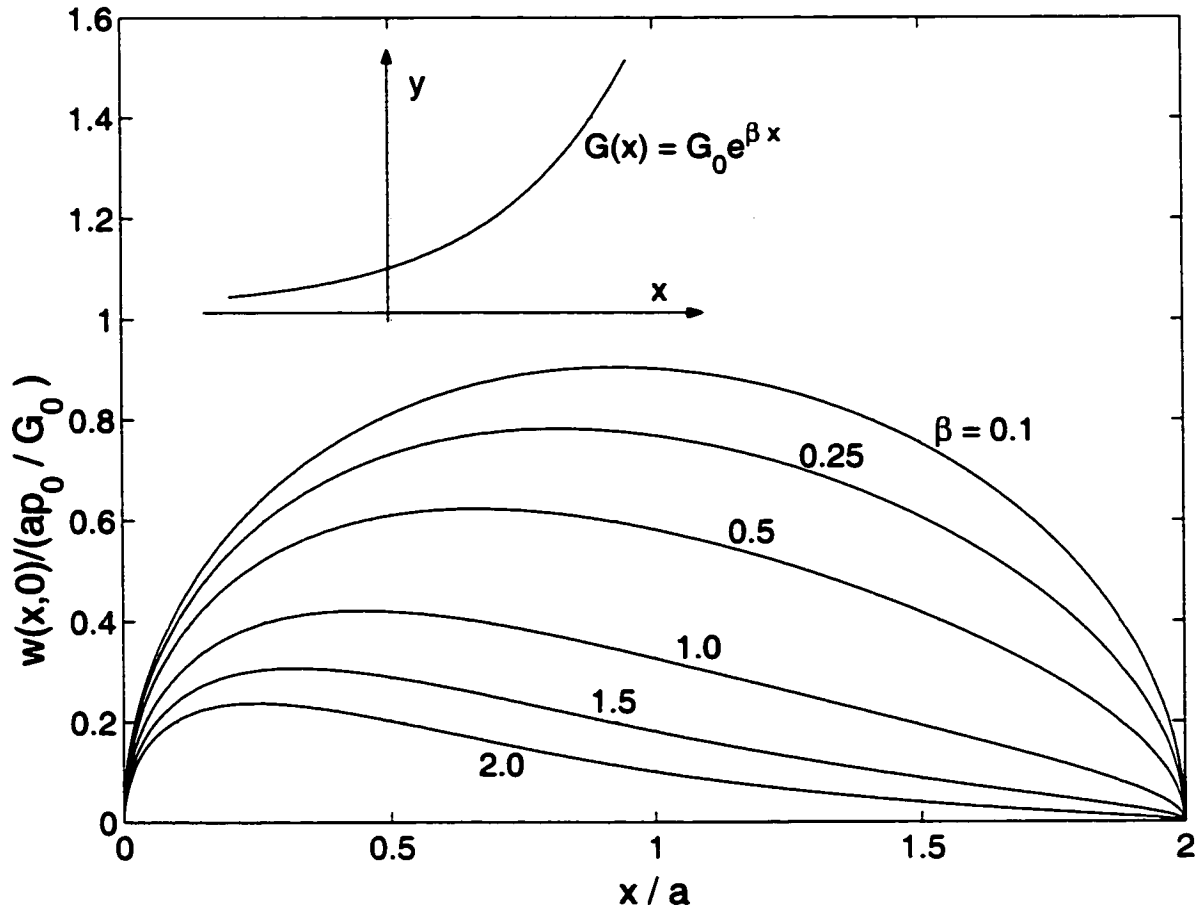


Figure 10.5: Classical LEFM, *i.e.*  $\bar{\ell} = \bar{\ell}' \rightarrow 0$ . Crack surface displacement in an infinite nonhomogeneous plane under uniform crack surface shear loading  $\sigma_{yz}(x, 0) = -p_0$  and shear modulus  $G(x) = G_0 e^{\beta x}$ . Here  $a = (d - c)/2$  denotes the half crack length.

The difference between Figures 10.4 and 10.5 and Figures 10.6 and 10.7 is the cusp at the crack tips. In Figures 10.4 and 10.5, one may observe that the profiles have a tangent line with infinite slope at the crack tips, which is a common crack behavior exhibited in the classical LEFM, although less physical. However, such is not the case in gradient theory as evidenced by the numerical results shown.

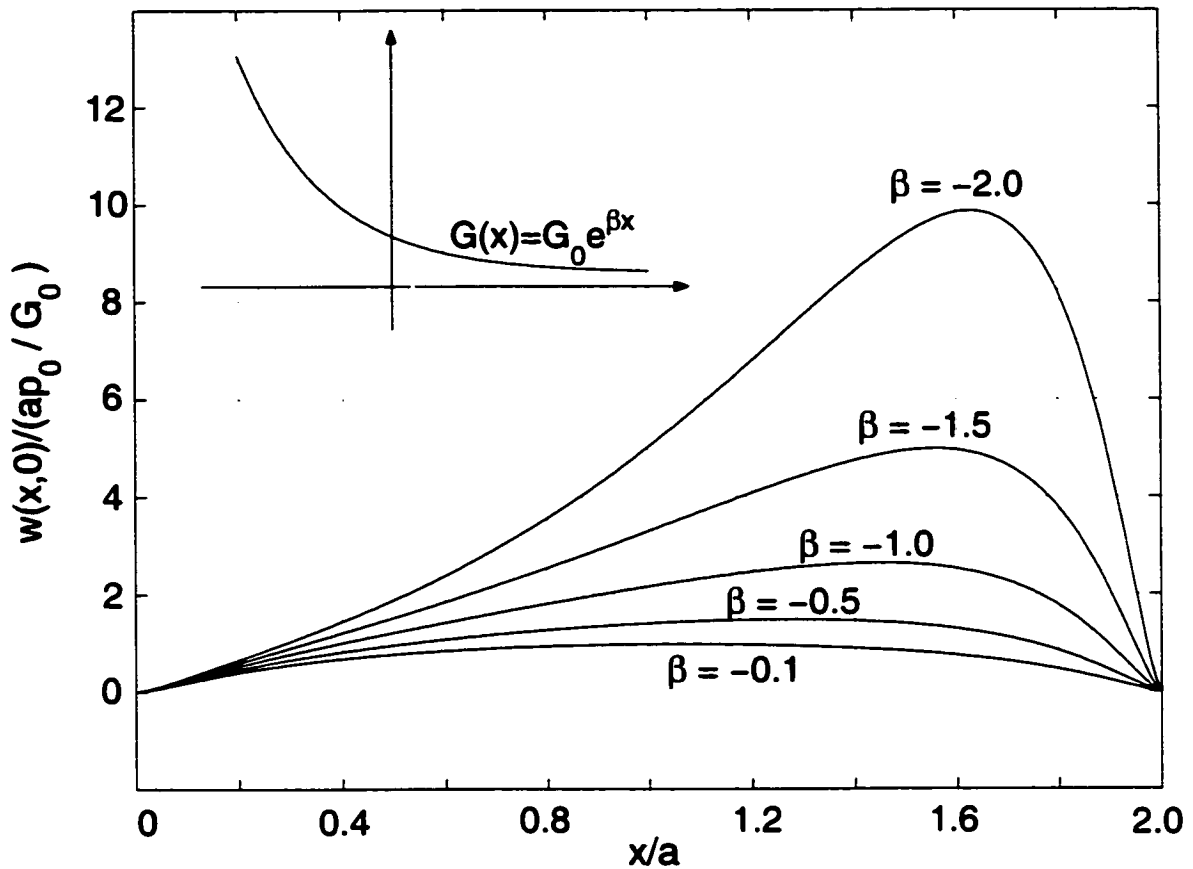


Figure 10.6: Crack surface displacement in an infinite nonhomogeneous plane under uniform crack surface shear loading  $\sigma_{yz}(x, 0) = -p_0$  and shear modulus  $G(x) = G_0 e^{\beta x}$  with choice of (normalized)  $\bar{\ell} = 0.10$  and  $\bar{\ell}' = 0.01$ . Here  $a = (d - c)/2$  denotes the half crack length.

### 10.5.3 Strains

We have used the strain-like field,  $\phi(x)$  (the slope function), as the unknown density function in our integral equation formulation. The plot of  $\phi(x)$  under various choices of different values of  $\bar{\ell}$  is displayed in Figure 10.8. A completely different aspect from the classical LEFM is observed here where  $\phi(x)$  is finite at the crack tips. The finiteness of the strain is equivalent to the crack surface displacement profiles having cusps at the crack tips because it can be obtained by integrating the slope function  $\phi(x)$ . Thus, if the normalized  $\phi(x)$ ,  $\Phi(s)$ , is found numerically by using the Chebyshev

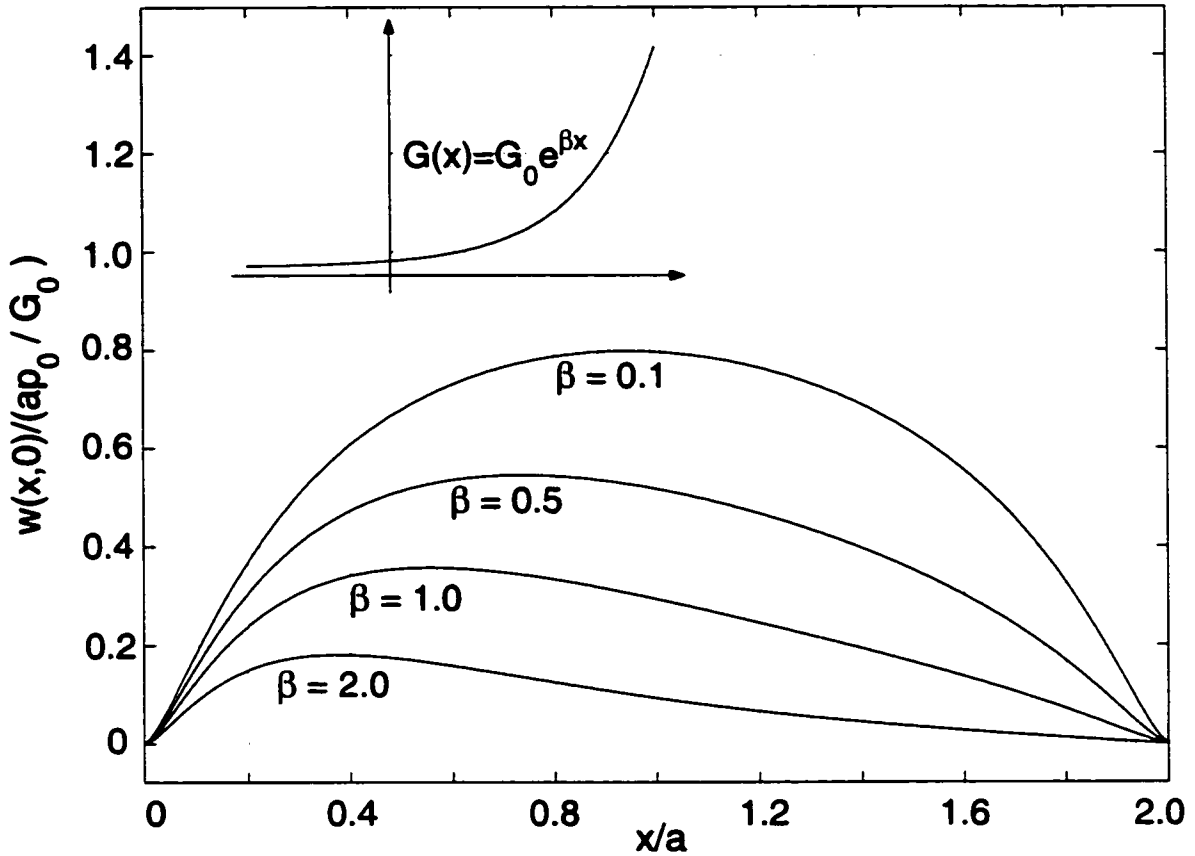


Figure 10.7: Crack surface displacement in an infinite nonhomogeneous plane under uniform crack surface shear loading  $\sigma_{yz}(x, 0) = -p_0$  and shear modulus  $G(x) = G_0 e^{\beta x}$  with choice of (normalized)  $\tilde{\ell} = 0.10$  and  $\tilde{\ell}' = 0.01$ . Here  $a = (d - c)/2$  denotes the half crack length.

expansion (10.48), then the crack displacement profile  $w(r, 0)$  can be obtained by

$$w(r, 0) = \int_{-1}^r \phi(s) ds = \int_{-1}^r \sqrt{1 - s^2} \sum_{n=0}^N A_n U_n(s) ds. \quad (10.49)$$

Notice in Figure 10.8 that the plot of the slope function  $\phi(x)$  is not symmetric due to the gradation of the material. As  $\ell$  decreases, the interior part (*i.e.* the region apart from the two crack tips) of  $\phi(x)$  seems to converge to the slope function of the classical LEFM case. However, the limit of  $\ell \rightarrow 0$  leads to a singular perturbation problem, and a boundary layer may arise.

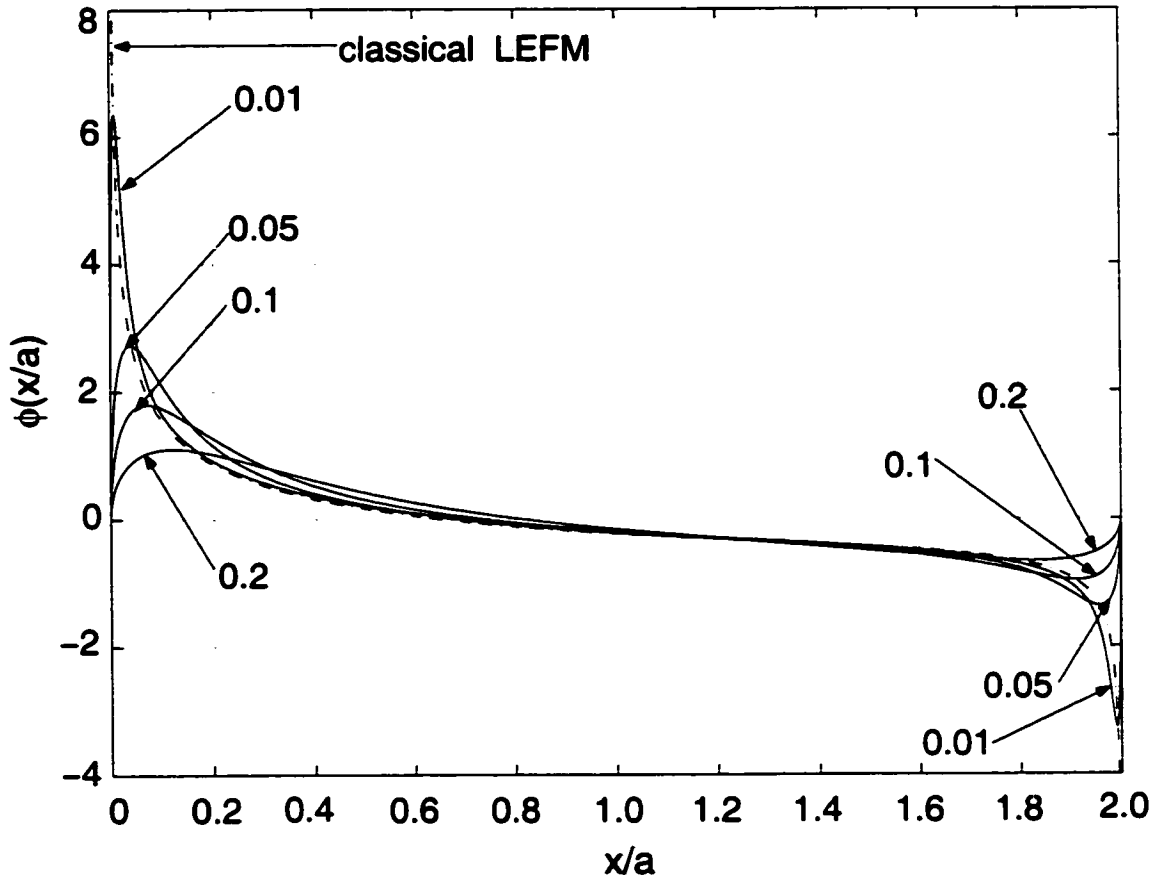


Figure 10.8: Strain  $\phi(x/a)$  along the crack surface  $(c, d) = (0, 2)$  for  $\tilde{\beta} = 0.5$ ,  $\tilde{\ell}' = 0$ , and various  $\tilde{\ell}$  in an infinite nonhomogeneous plane under uniform crack surface shear loading  $\sigma_{yz}(x, 0) = -p_0$  and shear modulus  $G(x) = G_0 e^{\beta x}$ . Here  $a = (d - c)/2$  denotes the half crack length.

#### 10.5.4 Stresses

A very interesting and extraordinary phenomena appears as the stress field is investigated. Similar to classical LEFM, the stress  $\sigma_{yz}(x, 0)$  is still not finite as  $x$  approaches the crack tips from the ligament. However, the sign of the stress is changed. This invalidity of physical meaning has also been reported by Zhang *et al.* [100] for mode III crack problems and by Shi *et al.* [82] for both mode I and mode II crack problems. Similar to the case of the strain, as  $\ell$  decreases, the interior part (*i.e.* the region apart from the two crack tips) of  $\sigma_{yz}(x, 0)$  seems to converge to the solution of classical

LEFM. Further exploration is needed along the line of singular perturbation and the existence of boundary layer.

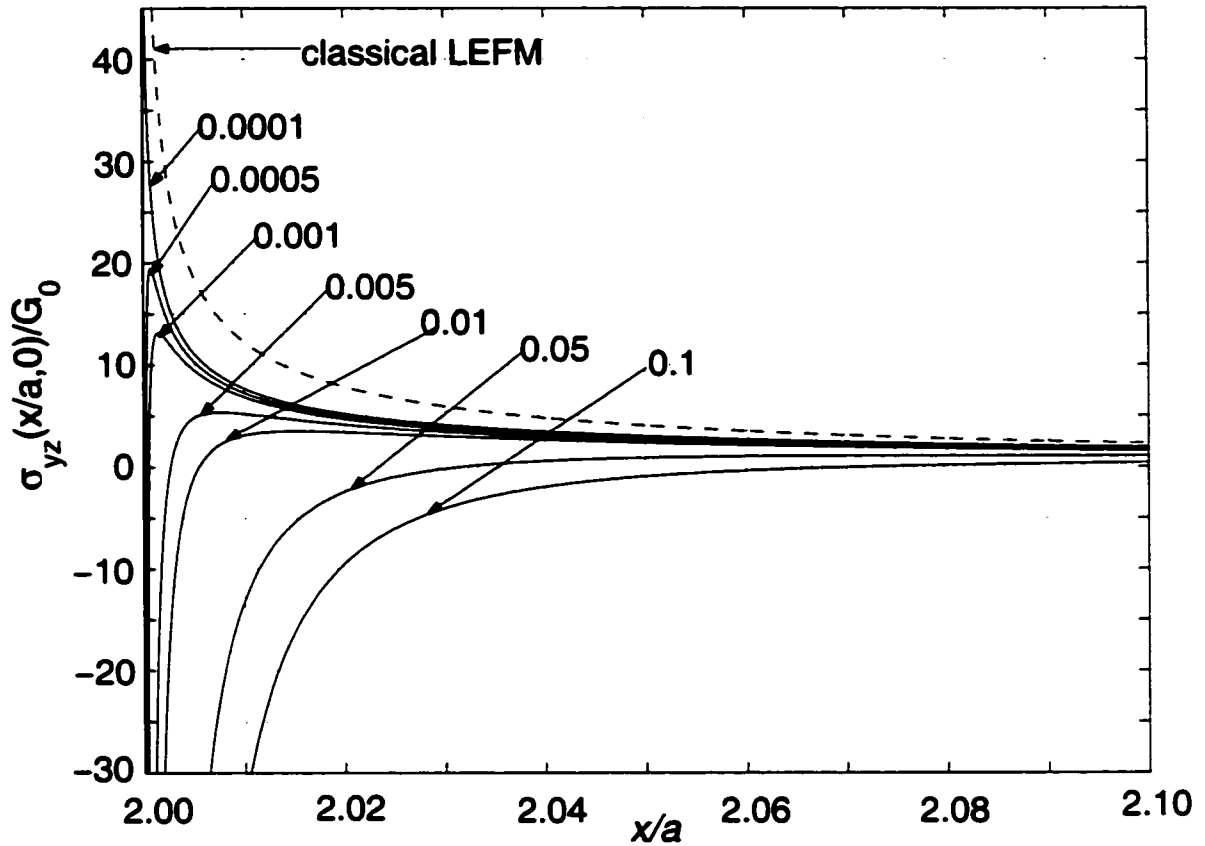


Figure 10.9: Stress  $\sigma_{yz}(x/a, 0)/G_0$  along the ligament for  $\bar{\beta} = 0.5$ ,  $\bar{\ell}' = 0$ , and various  $\bar{\ell}$ . Crack surface  $(c, d) = (0, 2)$  located in an infinite nonhomogeneous plane is assumed to be under uniform crack surface shear loading  $\sigma_{yz}(x, 0) = -p_0$  and shear modulus  $G(x) = G_0 e^{\beta x}$ . Here  $a = (d - c)/2$  denotes the half crack length.

### 10.5.5 Stress Intensity Factors (SIFs)

In Chapter 8 we have showed how to generalize the conventional definition of SIFs and derive the numerical formulas for them. Here, we briefly list them.

$$\ell K_{III}(d) = \lim_{x \rightarrow d^+} 2\sqrt{2\pi(x-d)}(x-d)\sigma_{yz}(x, 0), \quad (x > d) \quad (10.50)$$



$$\ell K_{III}(c) = \lim_{x \rightarrow c^-} 2\sqrt{2\pi(c-x)}(c-x)\sigma_{yz}(x, 0), \quad (x < c). \quad (10.51)$$

It leads to (for  $x > d$ , or  $r > 1$ )

$$\begin{aligned} \ell K_{III}(d) &= \lim_{x \rightarrow d^+} 2\sqrt{2\pi(x-d)}(x-d)\sigma_{yz}(x, 0), \\ &= \lim_{r \rightarrow 1^+} 2\sqrt{2\pi \left[ \left( \frac{d-c}{2} \right) r + \frac{c+d}{2} - d \right]} (ar-a)\sigma_{yz} \left( \frac{d-c}{2}r + \frac{c+d}{2}, 0 \right) \\ &= 2a\sqrt{2\pi a} \lim_{r \rightarrow 1^+} \sqrt{(r-1)}(r-1) \sigma_{yz}((d-c)r/2 + (c+d)/2, 0) \\ &= 2a\sqrt{2\pi a} \lim_{r \rightarrow 1^+} \sqrt{(r-1)}(r-1) G_0 e^{a\beta r} e^{\beta(d+c)/2} \left( \frac{-2\ell^2}{\pi a^2} \right) \times \\ &\quad \int_{-1}^1 \frac{\Phi(s)}{(s-r)^3} ds. \end{aligned} \quad (10.52)$$

Thus

$$\begin{aligned} K_{III}(d) &= 2\sqrt{2\pi a} \left( \frac{2\ell}{a} \right) G_0 e^{\beta d} \lim_{r \rightarrow 1^+} (r-1)^{3/2} \sum_{n=0}^N \frac{n+1}{2} \left( r - \frac{|r|}{r} \sqrt{r^2-1} \right)^{n-1} \\ &\quad \times \left[ n \left( 1 - \frac{|r|}{\sqrt{r^2-1}} \right)^2 + \frac{r - \frac{|r|}{r} \sqrt{r^2-1}}{\sqrt{r^2-1}^3} \right] A_n \\ &= \sqrt{\pi a} G_0 e^{\beta d} (\ell/a) \sum_{n=0}^{\infty} (n+1) A_n. \end{aligned} \quad (10.53)$$

Similarly,

$$K_{III}(c) = \sqrt{\pi a} G_0 e^{\beta c} (\ell/a) \sum_{n=0}^{\infty} (-1)^n (n+1) A_n. \quad (10.54)$$

Recall that  $a = (d-c)/2$  is half of the crack length and  $\ell/a = \tilde{\ell}$  is the normalized  $\ell$  which is dimensionless.

Table 10.2 contains the (normalized) SIFs for the special case of classical LEFM (*i.e.*  $\ell = \ell' \rightarrow 0$ ) by using both  $T_n$  and  $U_n$  Chebyshev polynomials expansions [see Eqns. (8.3) and (8.4)]. By choosing displacement as the unknown density function, one may found the following formulas (see Chan *et al.* [14]):

Table 10.2: Normalized SIFs for mode III crack problem in an FGM. ( $\ell = \ell' \rightarrow 0$ )

| $\beta(\frac{d-c}{2})$ | $U_n$ Representation                      |   | $T_n$ Representation                      |   |
|------------------------|---|---|---|---|
|                        | $\frac{K_{III}(c)}{p_0\sqrt{\pi(d-c)/2}}$ | $\frac{K_{III}(d)}{p_0\sqrt{\pi(d-c)/2}}$ | $\frac{K_{III}(c)}{p_0\sqrt{\pi(d-c)/2}}$ | $\frac{K_{III}(d)}{p_0\sqrt{\pi(d-c)/2}}$ |
| -2.00                  | 1.21779                                   | 0.55672                                   | 1.21779                                   | 0.55672                                   |
| -1.50                  | 1.17801                                   | 0.63007                                   | 1.17801                                   | 0.63007                                   |
| -1.00                  | 1.14307                                   | 0.72845                                   | 1.14307                                   | 0.72845                                   |
| -0.50                  | 1.09036                                   | 0.85676                                   | 1.09036                                   | 0.85676                                   |
| -0.10                  | 1.02289                                   | 0.97312                                   | 1.02289                                   | 0.97312                                   |
| 0.00                   | 1.00000                                   | 1.00000                                   | 1.00000                                   | 1.00000                                   |
| 0.10                   | 0.97312                                   | 1.02289                                   | 0.97312                                   | 1.02289                                   |
| 0.50                   | 0.85676                                   | 1.09036                                   | 0.85676                                   | 1.09036                                   |
| 1.00                   | 0.72845                                   | 1.14307                                   | 0.72845                                   | 1.14307                                   |
| 1.50                   | 0.63007                                   | 1.17801                                   | 0.63007                                   | 1.17801                                   |
| 2.00                   | 0.55672                                   | 1.21779                                   | 0.55672                                   | 1.21779                                   |

- With  $T_n$  expansion:

$$\frac{K_{III}(c)}{G_0\sqrt{\pi(d-c)/2}} = e^{\beta c} \sum_0^N (-1)^n a_n, \quad \frac{K_{III}(d)}{G_0\sqrt{\pi(d-c)/2}} = e^{\beta d} \sum_0^N a_n. \quad (10.55)$$

- With  $U_n$  expansion:

$$\frac{K_{III}(c)}{G_0\sqrt{\pi(d-c)/2}} = e^{\beta c} \sum_0^N (-1)^n (n+1) A_n, \quad \frac{K_{III}(d)}{G_0\sqrt{\pi(d-c)/2}} = e^{\beta d} \sum_0^N (n+1) A_n. \quad (10.56)$$

The SIFs in Table 3 have been obtained by using equations (10.55) and (10.56), and they are consistent with the trend of the SIF results reported by Erdogan [25].

Table 10.3 contains the (normalized) generalized SIFs for the case of strain gradient elasticity at  $\bar{\ell} = 0.1$  and  $\bar{\ell}' = 0.01$ . One can observe that the trend of decreasing  $K_{III}(c)$  and increasing  $K_{III}(d)$  as  $\bar{\beta}$  increases is similar to the trend reported in Table 3. However, the support of experimental data is needed here to provide the physical justification.

Table 10.3: Normalized generalized SIFs for a mode III crack at  $\bar{\ell} = 0.1$ ,  $\bar{\ell}' = 0.01$ , and various values of  $\bar{\beta}$

| $\bar{\beta}$ | $\frac{K_{III}(c)}{p_0 \sqrt{\pi(d-c)/2}}$ | $\frac{K_{III}(d)}{p_0 \sqrt{\pi(d-c)/2}}$ |
|---------------|--|--|
| -2.00         | 1.23969                                    | 0.49938                                    |
| -1.00         | 1.12585                                    | 0.67600                                    |
| -0.50         | 1.04849                                    | 0.80248                                    |
| -0.10         | 0.96814                                    | 0.91658                                    |
| 0.00          | 0.94385                                    | 0.94385                                    |
| 0.10          | 0.91677                                    | 0.96828                                    |
| 0.50          | 0.80277                                    | 1.04854                                    |
| 1.00          | 0.67637                                    | 1.12584                                    |
| 2.00          | 0.49938                                    | 1.23969                                    |

## Chapter 11

# Gradient Elasticity Theory for Mode I Fracture in Homogeneous Materials

Previous chapters dealt with anti-plane shear mode, a scalar-valued problem. In terms of PDE, the problem is governed by one single partial differential equation. In the present and next chapters we investigate the solutions to the mode I fracture problems for homogeneous materials and FGMs, respectively. Thus, a vector-valued problem is involved, and the governing PDE is a system of partial differential equations, which gives rise to a system of hypersingular integral equations. Exadaktylos [34] has investigated the mode I problem by applying gradient elasticity with surface energy in homogeneous materials. The homogeneous case is revisited by using the hypersingular integral equation method, which is different from the approach by Exadaktylos [34].

## 11.1 Formulation of the Crack Problem

For the sake of continuation and completeness, we list all ingredients that are related to the formulation of the problem.

### 11.1.1 Constitutive Equations

For homogeneous materials, the constitutive equations of gradient elasticity are (Exadaktylos [34], Exadaktylos *et. al.* [35])

$$\tau_{ij} = \lambda \epsilon_{kk} \delta_{ij} + 2G \epsilon_{ij} + \ell' \nu_k \partial_k (\lambda \epsilon_{ll} \delta_{ij} + 2G \epsilon_{ij}), \quad (11.1)$$

$$\mu_{kij} = \lambda \ell^2 \partial_k \epsilon_{ll} \delta_{ij} + 2G \ell' \nu_k \epsilon_{ij} + \lambda \ell' \nu_k \epsilon_{ll} \delta_{ij} + 2G \ell^2 \partial_k \epsilon_{ij}, \quad (11.2)$$

$$\sigma_{ij} = \lambda \epsilon_{kk} \delta_{ij} + 2G \epsilon_{ij} - \ell^2 \nabla^2 (\lambda \epsilon_{kk} \delta_{ij} + 2G \epsilon_{ij}), \quad (11.3)$$

which have been stated in (3.38), (3.39), and (3.40). Each component of the stress fields for the homogeneous materials are [34]:

$$\left\{ \begin{array}{l} \sigma_{xz} = \sigma_{yz} = 0 \\ \sigma_{xx} = (\lambda + 2G) \epsilon_{xx} + \lambda \epsilon_{yy} - (\lambda + 2G) \ell^2 \nabla^2 \epsilon_{xx} - \lambda \ell^2 \nabla^2 \epsilon_{yy} \\ \sigma_{yy} = (\lambda + 2G) \epsilon_{yy} + \lambda \epsilon_{xx} - (\lambda + 2G) \ell^2 \nabla^2 \epsilon_{yy} - \lambda \ell^2 \nabla^2 \epsilon_{xx} \\ \sigma_{xy} = \sigma_{yx} = 2G \epsilon_{xy} - 2G \ell^2 \nabla^2 \epsilon_{xy} \\ \sigma_{zz} = \lambda (\epsilon_{xx} + \epsilon_{yy}) - \lambda \ell^2 \nabla^2 (\epsilon_{xx} + \epsilon_{yy}), \end{array} \right. \quad (11.4)$$

$$\left\{ \begin{array}{l} \mu_{xxx} = (\lambda + 2G) \ell^2 \partial_x \epsilon_{xx} + \lambda \ell^2 \partial_x \epsilon_{yy} \\ \mu_{yxx} = -(\lambda + 2G) \ell' \epsilon_{xx} - \lambda \ell' \epsilon_{yy} + (\lambda + 2G) \ell^2 \partial_y \epsilon_{xx} + \lambda \ell^2 \partial_y \epsilon_{yy} \\ \mu_{xyy} = (\lambda + 2G) \ell^2 \partial_x \epsilon_{yy} + \lambda \ell^2 \partial_x \epsilon_{xx} \\ \mu_{yyy} = -(\lambda + 2G) \ell' \epsilon_{yy} - \lambda \ell' \epsilon_{xx} + (\lambda + 2G) \ell^2 \partial_y \epsilon_{yy} + \lambda \ell^2 \partial_y \epsilon_{xx} \\ \mu_{txy} = \mu_{txx} = 2G \ell^2 \partial_x \epsilon_{xy} \\ \mu_{yyx} = \mu_{yxy} = -2G \ell' \epsilon_{xy} + 2G \ell^2 \partial_y \epsilon_{xy}. \end{array} \right. \quad (11.5)$$

### 11.1.2 Governing System of PDEs and Boundary Conditions

By imposing the equilibrium equations

$$\frac{\partial \sigma_{xx}}{\partial x} + \frac{\partial \sigma_{xy}}{\partial y} = 0 \quad \text{and} \quad \frac{\partial \sigma_{xy}}{\partial x} + \frac{\partial \sigma_{yy}}{\partial y} = 0, \quad (11.6)$$

and using equations (3.16) and (11.4), one can obtain the following system of PDEs:

$$(1 - \ell^2 \nabla^2) \left[ (\kappa + 1) \frac{\partial^2 u}{\partial x^2} + (\kappa - 1) \frac{\partial^2 u}{\partial y^2} + 2 \frac{\partial^2 v}{\partial x \partial y} \right] = 0, \quad (11.7)$$

$$(1 - \ell^2 \nabla^2) \left[ (\kappa - 1) \frac{\partial^2 v}{\partial x^2} + (\kappa + 1) \frac{\partial^2 v}{\partial y^2} + 2 \frac{\partial^2 u}{\partial x \partial y} \right] = 0. \quad (11.8)$$

Boundary conditions are derived from the principle of virtual work:

$$\begin{cases} \sigma_{xy}(x, 0^+) = 0, & -\infty < x < \infty \\ \sigma_{yy}(x, 0^+) = p(x), & |x| < a \\ v(x, 0^+) = 0, & |x| > a \end{cases} \quad (11.9)$$

$$\begin{cases} \mu_{yyx}(x, 0^+) = 0, & -\infty < x < \infty \\ \mu_{yyy}(x, 0^+) = 0, & |x| < a \\ \frac{\partial}{\partial y} v(x, 0^+) = 0, & |x| > a, \end{cases} \quad (11.10)$$

where  $p(x)$  is the crack surface tractions. Also,  $u(x, y)$  and  $v(x, y)$  are assumed to satisfy the far-field condition:

$$u(x, y), v(x, y) \rightarrow 0 \quad \text{as} \quad \sqrt{x^2 + y^2} \rightarrow \infty. \quad (11.11)$$

## 11.2 Derivation for the System of Integral Equations

By defining

$$u(x, y) = \frac{1}{\sqrt{2\pi}} \int_{-\infty}^{\infty} \hat{u}(\xi, y) e^{-ix\xi} d\xi \quad (11.12)$$

and

$$v(x, y) = \frac{1}{\sqrt{2\pi}} \int_{-\infty}^{\infty} \hat{v}(\xi, y) e^{-ix\xi} d\xi \quad (11.13)$$

through Fourier transform, the system PDEs (11.7) and (11.8) becomes a system of ODEs:

$$\begin{aligned}
 -\ell^2(\kappa - 1) \frac{d^4 \hat{u}}{dy^4} + [(\kappa - 1) + 2\ell^2 \kappa \xi^2] \frac{d^2 \hat{u}}{dy^2} + [(\kappa + 1)\xi^2 + \ell^2(\kappa + 1)\xi^4] \hat{u} \\
 + (2i\ell^2 \xi) \frac{d^3 \hat{v}}{dy^3} - (2i\xi + 2i\ell^2 \xi^3) \frac{d\hat{v}}{dy} = 0, \quad (11.14)
 \end{aligned}$$

$$\begin{aligned}
 -\ell^2(\kappa + 1) \frac{d^4 \hat{v}}{dy^4} - [(\kappa + 1) + 2\ell^2 \kappa \xi^2] \frac{d^2 \hat{v}}{dy^2} - (\kappa - 1)(i\beta \xi + \xi^2 + \ell^2 \xi^4) \hat{v} \\
 (2i\ell^2 \xi) \frac{d^3 \hat{u}}{dy^3} - (2i\xi + 2i\ell^2 \xi^3) \frac{d\hat{u}}{dy} = 0. \quad (11.15)
 \end{aligned}$$

The corresponding characteristic polynomial<sup>1</sup> to the system of ODEs (11.14) and (11.15)

$$[\lambda^2 - (\xi^2 + 1/\ell^2)]^2 (\lambda^2 - \xi^2)^2 = 0 \quad (11.16)$$

has six eigenvalues contributing to the solution:

$$\begin{aligned}
 \lambda_1(\xi) = \lambda_2(\xi) = -|\xi|, \quad \lambda_3(\xi) = -\sqrt{\frac{\ell^2 \xi^2 + 1}{\ell^2}}, \quad (11.17) \\
 -\lambda_1(\xi), \quad -\lambda_2(\xi), \quad \text{and} \quad -\lambda_3(\xi).
 \end{aligned}$$

By the far-field condition (11.11), only negative roots  $\lambda_1$ ,  $\lambda_2$ , and  $\lambda_3$  are considered.

Notice that  $\lambda_1$  and  $\lambda_2$  are repeated root. We can express  $\hat{v}(\xi, y)$  and  $\hat{u}(\xi, y)$  as

$$\begin{aligned}
 \hat{v}(\xi, y) = a_1(\xi)e^{-|\xi|y} + a_2(\xi)ye^{-|\xi|y} + a_3(\xi)e^{\lambda_3(\xi)y} \\
 \hat{u}(\xi, y) = b_1(\xi)e^{-|\xi|y} + b_2(\xi)ye^{-|\xi|y} + b_3(\xi)e^{\lambda_3(\xi)y}
 \end{aligned} \quad (11.18)$$

Substitution of the general solutions  $\hat{v}(\xi, y)$  and  $\hat{u}(\xi, y)$  into ODEs (11.14) and (11.15) leads to the following relations:

$$b_1(\xi) = i \frac{\xi}{|\xi|} a_1(\xi) - \frac{i\kappa}{\xi} a_2(\xi) \quad \text{and} \quad b_2(\xi) = i \frac{\xi}{|\xi|} a_2(\xi). \quad (11.19)$$

At this point, we are left to solve the four unknown coefficients  $a_1(\xi)$ ,  $a_2(\xi)$ ,  $a_3(\xi)$ , and  $b_3(\xi)$ , which are determined by employing the boundary conditions.

<sup>1</sup>Case of the homogeneous material can be considered as a special case of FGM. Thus, the detail of forming the corresponding characteristic equation and solving their eigenvalues will be included and addressed in Chapter 12.

### 11.2.1 System of Fredholm Integral Equations

By the symmetry of this mode I problem, one may consider only the upper half plane ( $y \geq 0$ ) and express  $v(x, y)$  and  $u(x, y)$  as:

$$v(x, y) = \frac{1}{\sqrt{2\pi}} \int_{-\infty}^{\infty} [a_1(\xi)e^{-|\xi|y} + a_2(\xi)ye^{-|\xi|y} + a_3(\xi)e^{\lambda_3(\xi)y}] e^{-ix\xi} d\xi, \quad y \geq 0, \quad (11.20)$$

$$u(x, y) = \frac{1}{\sqrt{2\pi}} \int_{-\infty}^{\infty} [b_1(\xi)e^{-|\xi|y} + b_2(\xi)ye^{-|\xi|y} + b_3(\xi)e^{\lambda_3(\xi)y}] e^{-ix\xi} d\xi, \quad y \geq 0. \quad (11.21)$$

Recall that the four unknown coefficients are  $a_1(\xi)$ ,  $a_2(\xi)$ ,  $a_3(\xi)$ , and  $b_3(\xi)$ .

By the first boundary condition in (11.9) one can establish

$$a_1(\xi) = \left[ \frac{\kappa + 1}{2|\xi|} - 2\ell^2|\xi| \right] a_2(\xi). \quad (11.22)$$

Also, by the first boundary condition in (11.10),  $b_3(\xi)$  can be expressed as

$$b_3(\xi) = \frac{-1}{\lambda_3(\xi) [\ell' + \ell^2\lambda_3(\xi)]} \{ (\ell'|\xi| + \ell^2\xi^2)b_1(\xi) - (\ell' + 2\ell^2|\xi|)b_2(\xi) + i\xi(\ell' + 2\ell^2|\xi|)a_1(\xi) - i\ell^2\xi a_2(\xi) + i\xi [\ell' + \ell^2\lambda_3(\xi)] a_3(\xi) \}. \quad (11.23)$$

Thus there are only two unknowns,  $a_2(\xi)$  and  $a_3(\xi)$ , left to be determined now.

Define

$$\phi_0(x) = \frac{\partial}{\partial x} v(x, 0) \quad \text{and} \quad \psi_0(x) = \frac{\partial}{\partial x} \left[ \frac{\partial}{\partial y} v(x, 0) \right], \quad (11.24)$$

then by the third conditions of (11.9) and (11.10), after a step of inverting the Fourier transform, one may get

$$\begin{cases} \left[ -i\frac{\kappa+1}{2} \frac{\xi}{|\xi|} + 2i\ell^2|\xi|\xi \right] a_2(\xi) - i\xi a_3(\xi) & = \frac{1}{\sqrt{2\pi}} \int_{-a}^a \phi_0(t) e^{it\xi} dt \\ (-i\xi) \left[ \frac{1-\kappa}{2} + 2\ell^2\xi^2 \right] a_2(\xi) - i\xi\lambda_3(\xi)a_3(\xi) & = \frac{1}{\sqrt{2\pi}} \int_{-a}^a \psi_0(t) e^{it\xi} dt. \end{cases} \quad (11.25)$$

Solving (11.25) for  $a_2(\xi)$  and  $a_3(\xi)$ , then by the second conditions of (11.9) and



(11.10), one obtains the following system of integral equations in the limit form:

$$\begin{cases} \lim_{y \rightarrow 0} \frac{1}{2\pi} \int_{-a}^a \int_{-\infty}^{\infty} [K_{11}(\xi, y)\phi_0(t) + K_{12}(\xi, y)\psi_0(t)] e^{i(t-x)\xi} d\xi dt = \frac{p(x)}{G_0}, & |x| < a \\ \lim_{y \rightarrow 0} \frac{1}{2\pi} \int_{-a}^a \int_{-\infty}^{\infty} [K_{21}(\xi, y)\phi_0(t) + K_{22}(\xi, y)\psi_0(t)] e^{i(t-x)\xi} d\xi dt = 0, & |x| < a, \end{cases} \quad (11.26)$$

where the four kernels  $K_{ij}$  ( $i, j = 1, 2$ ) can be described by:

$$K_{ij}(\xi) = \lim_{y \rightarrow 0} K_{ij}(\xi, y) = \frac{N_{ij}(\xi)}{D(\xi)}, \quad i, j = 1, 2 \quad (11.27)$$

where

$$D(\xi) = \left[ -i \left( \frac{\kappa + 1}{2} \right) \frac{\xi}{|\xi|} + 2i\ell^2 |\xi| \xi \right] \lambda_3(\xi) + (i\xi) \left( \frac{1 - \kappa}{2} + 2\ell^2 \xi^2 \right) \quad (11.28)$$

$$N_{11}(\xi) = -2\lambda_3(\xi), \quad N_{12}(\xi) = -2; \quad (11.29)$$

$$\begin{aligned} N_{21}(\xi) &= (i\xi) \left( \frac{3 - \kappa}{\kappa - 1} \right) \left[ \ell' + \ell^2 |\xi| + \frac{\ell' |\xi| + \ell^2 \xi^2}{\lambda_3} \right] \left[ \frac{i(1 - \kappa)}{2\xi} - 2i\ell^2 \xi \right] \lambda_3 \\ &+ (i\xi) \left( \frac{3 - \kappa}{\kappa - 1} \right) \left[ -\ell^2 - \frac{\ell' + \ell^2 |\xi|}{\lambda_3} \right] \frac{i\xi \lambda_3}{|\xi|} \\ &+ \left[ (i\xi) \left( \frac{3 - \kappa}{\kappa - 1} \right) \frac{(i\xi)(\ell' + \ell^2 |\xi|)}{\lambda_3} + \left( \frac{\kappa + 1}{\kappa - 1} \right) (\ell' |\xi| + \ell^2 \xi^2) \right] \times \\ &\quad \left[ \frac{(\kappa + 1)}{2|\xi|} - 2\ell^2 |\xi| \right] \lambda_3 \\ &+ \left[ -(i\xi) \left( \frac{3 - \kappa}{\kappa - 1} \right) \frac{i\ell^2 \xi}{\lambda_3} - \left( \frac{\kappa + 1}{\kappa - 1} \right) (\ell' + 2\ell^2 |\xi|) \right] \lambda_3 \\ &- \left[ (i\xi) \left( \frac{3 - \kappa}{\kappa - 1} \right) \frac{(i\xi)(\ell' - \ell^2 \lambda_3)}{\lambda_3} - \left( \frac{\kappa + 1}{\kappa - 1} \right) \lambda_3 (\ell' - \ell^2 \lambda_3) \right] \times \\ &\quad \left[ \frac{1 - \kappa}{2} + 2\ell^2 \xi^2 \right] \end{aligned} \quad (11.30)$$

$$\begin{aligned}
 N_{22}(\xi) = & -(i\xi) \left( \frac{3-\kappa}{\kappa-1} \right) \left[ \ell' + \ell^2|\xi| + \frac{\ell'|\xi| + \ell^2\xi^2}{\lambda_3} \right] \left[ \frac{i(1-\kappa)}{2\xi} - 2i\ell^2\xi \right] \\
 & - (i\xi) \left( \frac{3-\kappa}{\kappa-1} \right) \left[ -\ell^2 - \frac{\ell' + \ell^2|\xi|}{\lambda_3} \right] \frac{i\xi}{|\xi|} \\
 & - \left[ (i\xi) \left( \frac{3-\kappa}{\kappa-1} \right) \frac{(i\xi)(\ell' + \ell^2|\xi|)}{\lambda_3} + \left( \frac{\kappa+1}{\kappa-1} \right) (\ell'|\xi| + \ell^2\xi^2) \right] \left[ \frac{(\kappa+1)}{2|\xi|} - 2\ell^2|\xi| \right] \\
 & - \left[ -(i\xi) \left( \frac{3-\kappa}{\kappa-1} \right) \frac{i\ell^2\xi}{\lambda_3} - \left( \frac{\kappa+1}{\kappa-1} \right) (\ell' + 2\ell^2|\xi|) \right] \\
 & + \left[ (i\xi) \left( \frac{3-\kappa}{\kappa-1} \right) \frac{(i\xi)(\ell' - \ell^2\lambda_3)}{\lambda_3} - \left( \frac{\kappa+1}{\kappa-1} \right) \lambda_3(\ell' - \ell^2\lambda_3) \right] \times \\
 & \left[ \frac{\kappa+1}{2|\xi|} - 2\ell^2|\xi| \right] \tag{11.31}
 \end{aligned}$$

Splitting the singularity from the four kernels  $K_{ij}$  ( $i, j = 1, 2$ ) by performing the asymptotic analysis, one can reach the following system of hypersingular integral equations:

$$\begin{aligned}
 \frac{1}{\pi} \int_{-a}^a \left[ \frac{-16\ell^2}{\kappa+2} \frac{1}{(t-x)^3} + \frac{2(3\kappa+7)}{(\kappa+2)^2} \frac{1}{t-x} + k_{11}(x, t) \right] \phi_0(t) dt \\
 + \frac{8\ell^2}{\kappa+2} \psi_0'(x) + \frac{1}{\pi} \int_{-a}^a k_{12}(x, t) \psi_0(t) dt = p(x)/G_0, \quad |x| < a \tag{11.32}
 \end{aligned}$$

$$\begin{aligned}
 \frac{1}{\pi} \int_{-a}^a \left[ \frac{2\ell'\kappa(\kappa-3)}{(\kappa+2)(\kappa-1)} \frac{1}{t-x} + k_{21}(x, t) \right] \phi_0(t) dt + \frac{2\ell^2\kappa}{\kappa+2} \phi_0'(x) \\
 + \frac{1}{\pi} \int_{-a}^a \left[ \frac{2\ell^2(\kappa^2 + \kappa + 4)}{(\kappa+2)(\kappa-1)} \frac{1}{t-x} + k_{22}(x, t) \right] \psi_0(t) dt = 0, \quad |x| < a, \tag{11.33}
 \end{aligned}$$

which is the final and main hypersingular integral equations that are solved together with the single-valuedness condition

$$\int_{-a}^a \phi_0(x) dx = 0, \quad \int_{-a}^a \psi_0(x) dx = 0. \tag{11.34}$$

### 11.3 Numerical Results

By choosing the dimensionless variables

$$r = x/a, \quad s = t/a, \quad \bar{\ell} = \ell/a, \quad \text{and} \quad \bar{\ell}' = \ell'/a,$$

where  $a$  is the half crack length, the hypersingular integrodifferential equations (11.32) and (11.33) can be treated only on the normalized interval  $(-1, 1)$ . Denote the normalized  $\phi_0(x)$  and  $\psi_0(x)$  by  $\Phi_0(r)$  and  $\Psi_0(r)$ , respectively. Based on the order of singularity of the derived hypersingular integral equations,  $\Phi_0$  and  $\Psi_0$  can be expanded by the Chebyshev polynomials of the second kind  $U_n(s)$ :

$$\Phi_0(s) = \sqrt{1-s^2} \sum_{n=0}^{\infty} a_n U_n(s), \quad \Psi_0(s) = \sqrt{1-s^2} \sum_{n=0}^{\infty} b_n U_n(s). \quad (11.35)$$

Here  $a_n$  and  $b_n$  are the expansion coefficients, and condition (11.34) implies that

$$a_0 = 0 \quad \text{and} \quad b_0 = 0.$$

It is worth to point out that although  $\psi_0(x)$  is defined to be

$$\psi_0(x) = \frac{\partial}{\partial x} \left[ \frac{\partial}{\partial y} v(x, 0) \right],$$

a second derivative of displacement  $v(x, y)$ , the crack-tip asymptotics is still the same as  $\phi_0(x)$ . It can be seen from following simple analysis. Assume  $v(x, y)$  takes form

$$v(x, y) = h(x, y) [1 - (x^2 + y^2)]^{3/2},$$

where  $h(x, y)$  is some well-behavior function. Then

$$\frac{\partial v(x, y)}{\partial y} = \frac{\partial h(x, y)}{\partial y} [1 - (x^2 + y^2)]^{3/2} - 3yh(x, y) \sqrt{x^2 + y^2}.$$

Clearly, after plugging  $y = 0$ ,  $\partial v(x, 0)/\partial y$  does not lose the “three-half” power of  $[1 - (x^2 + y^2)]$ . Thus, undertaken another differentiation with respect to  $x$ ,  $\psi_0(x)$  has crack-tip behavior  $\sqrt{x^2 + y^2}$ .

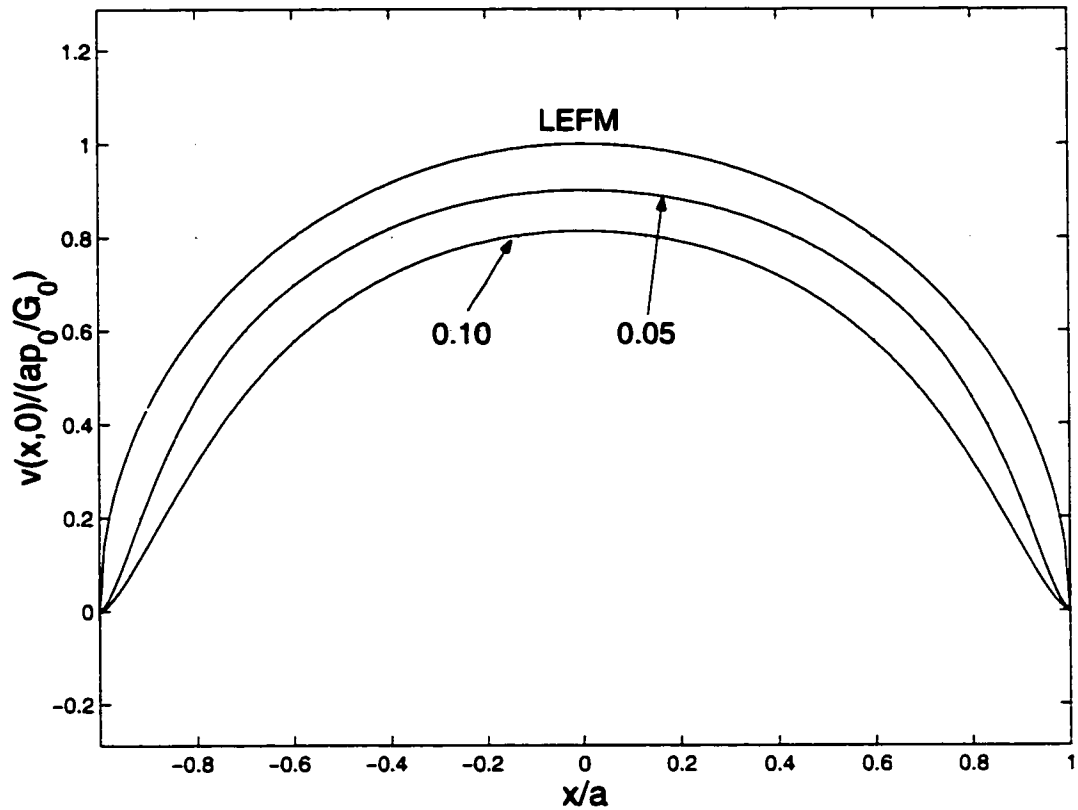


Figure 11.1: Mode I normalized crack profiles for homogeneous materials at  $\bar{\ell} = 0.05, 0.1$ ,  $\bar{\ell}' = 0.0$ , and  $\nu = 0.25$ .

Homogeneous materials can be treated as a particular case of the graded materials by letting the gradation parameters get closer to zero. A more detail of the numerical results will be given in next chapter, here we provide a Mode I crack opening displacement (COD) profiles shown in Figure 11.1. The contrast between the classical LEFM and the strain-gradient effect is clearly seen at the two ends of the crack!

## Chapter 12

# Gradient Elasticity Theory for Mode I Fracture in Functionally Graded Materials

Chapter 11 dealt with homogeneous materials. In this chapter, we focus on FGMs with strain-gradient effect for mode I crack problems. It is a vector-valued problem involved with much more complicated algebra than the previous chapter. However, a system of hypersingular integral equations is also derived; the difference is that there are additional terms, corresponding to the material gradation, appear in the governing integral equations. Konda and Erdogan [51] have solved the mixed mode problem (including Mode I) for classical elasticity in FGMs. Exadaktylos [34] has investigated the mode I problem in homogeneous materials by applying gradient elasticity with surface energy. This chapter can be considered as a combination of both.

## 12.1 Formulation of the Crack Problem

For the sake of continuation and clarity, again, we list all related ingredients for the formulation of the mode I crack problem for FGMs.

### 12.1.1 Constitutive Equations

Constitutive equations for nonhomogeneous materials are

$$\begin{aligned} \tau_{ij} = & \lambda(\mathbf{x})\epsilon_{kk}\delta_{ij} + 2G(\mathbf{x})\epsilon_{ij} + \ell'\nu_k[\epsilon_{ll}\partial_k\lambda(\mathbf{x}) + \lambda(\mathbf{x})\partial_k\epsilon_{ll}]\delta_{ij} \\ & + 2\ell'\nu_k[\epsilon_{ij}\partial_k G(\mathbf{x}) + G(\mathbf{x})\partial_k\epsilon_{ij}], \end{aligned} \quad (12.1)$$

$$\mu_{kij} = \ell'\nu_k\lambda(\mathbf{x})\epsilon_{ll}\delta_{ij} + \ell^2\lambda(\mathbf{x})\partial_k\epsilon_{ll}\delta_{ij} + 2\ell'\nu_k G(\mathbf{x})\epsilon_{ij} + 2\ell^2 G(\mathbf{x})\partial_k\epsilon_{ij}, \quad (12.2)$$

$$\begin{aligned} \sigma_{ij} = & \lambda(\mathbf{x})(\epsilon_{kk} - \ell^2\nabla^2\epsilon_{kk})\delta_{ij} + 2G(\mathbf{x})(\epsilon_{ij} - \ell^2\nabla^2\epsilon_{ij}) \\ & - \ell^2[\partial_k\lambda(\mathbf{x})](\partial_k\epsilon_{ll})\delta_{ij} - 2\ell^2[\partial_k G(\mathbf{x})](\partial_k\epsilon_{ij}), \end{aligned} \quad (12.3)$$

which have been stated in (3.9), (3.10), and (3.11).

For nonhomogeneous materials, the couple stresses  $\mu_{kij}$  have the same form as in (11.5), except that the Lamé constants  $\lambda$  and  $G$  are not constants anymore, and they are functions of  $(x, y)$  according to the gradation of the materials:

$$\left\{ \begin{aligned} \mu_{xxx} &= [\lambda(x, y) + 2G(x, y)]\ell^2\partial_x\epsilon_{xx} + \lambda(x, y)\ell^2\partial_x\epsilon_{yy} \\ \mu_{yxx} &= -[\lambda(x, y) + 2G(x, y)]\ell'\epsilon_{xx} - \lambda(x, y)\ell'\epsilon_{yy} \\ &\quad + [\lambda(x, y) + 2G(x, y)]\ell^2\partial_y\epsilon_{xx} + \lambda(x, y)\ell^2\partial_y\epsilon_{yy} \\ \mu_{xyy} &= [\lambda(x, y) + 2G(x, y)]\ell^2\partial_x\epsilon_{yy} + \lambda(x, y)\ell^2\partial_x\epsilon_{xx} \\ \mu_{yyy} &= -[\lambda(x, y) + 2G(x, y)]\ell'\epsilon_{yy} - \lambda(x, y)\ell'\epsilon_{xx} \\ &\quad + [\lambda(x, y) + 2G(x, y)]\ell^2\partial_y\epsilon_{yy} + \lambda(x, y)\ell^2\partial_y\epsilon_{xx} \\ \mu_{xxy} &= \mu_{xyx} = 2G\ell^2\partial_x\epsilon_{xy} \\ \mu_{yyx} &= \mu_{yxy} = -2G\ell'\epsilon_{xy} + 2G\ell^2\partial_y\epsilon_{xy}. \end{aligned} \right. \quad (12.4)$$

The total stresses  $\sigma_{ij}$  have more terms than in (11.4), and they are:

$$\left\{ \begin{array}{l}
 \sigma_{xz} = \sigma_{yz} = 0 \\
 \sigma_{xx} = [\lambda(x, y) + 2G(x, y)](1 - \ell^2 \nabla^2) \epsilon_{xx} + \lambda(x, y)(1 - \ell^2 \nabla^2) \epsilon_{yy} \\
 \quad - \ell^2 \{ [\partial_x \lambda(x, y)] \partial_x (\epsilon_{xx} + \epsilon_{yy}) + [\partial_y \lambda(x, y)] \partial_y (\epsilon_{xx} + \epsilon_{yy}) \} \\
 \quad - 2\ell^2 \{ [\partial_x G(x, y)] \partial_x \epsilon_{xx} + [\partial_y G(x, y)] \partial_y \epsilon_{xx} \} \\
 \sigma_{yy} = [\lambda(x, y) + 2G(x, y)](1 - \ell^2 \nabla^2) \epsilon_{yy} + \lambda(x, y)(1 - \ell^2 \nabla^2) \epsilon_{xx} \\
 \quad - \ell^2 \{ [\partial_x \lambda(x, y)] \partial_x (\epsilon_{xx} + \epsilon_{yy}) + [\partial_y \lambda(x, y)] \partial_y (\epsilon_{xx} + \epsilon_{yy}) \} \\
 \quad - 2\ell^2 \{ [\partial_x G(x, y)] \partial_x \epsilon_{yy} + [\partial_y G(x, y)] \partial_y \epsilon_{yy} \} \\
 \sigma_{xy} = \sigma_{yx} = 2G(x, y)(\epsilon_{xy} - \ell^2 \nabla^2 \epsilon_{xy}) - \\
 \quad 2\ell^2 \{ [\partial_x G(x, y)] \partial_x \epsilon_{xy} + [\partial_y G(x, y)] \partial_y \epsilon_{xy} \} \\
 \sigma_{zz} = \lambda(x, y)[(\epsilon_{xx} + \epsilon_{yy}) - \ell^2 \nabla^2 (\epsilon_{xx} + \epsilon_{yy})] \\
 \quad - \ell^2 \{ [\partial_x \lambda(x, y)] \partial_x (\epsilon_{xx} + \epsilon_{yy}) + [\partial_y \lambda(x, y)] \partial_y (\epsilon_{xx} + \epsilon_{yy}) \} .
 \end{array} \right. \quad (12.5)$$

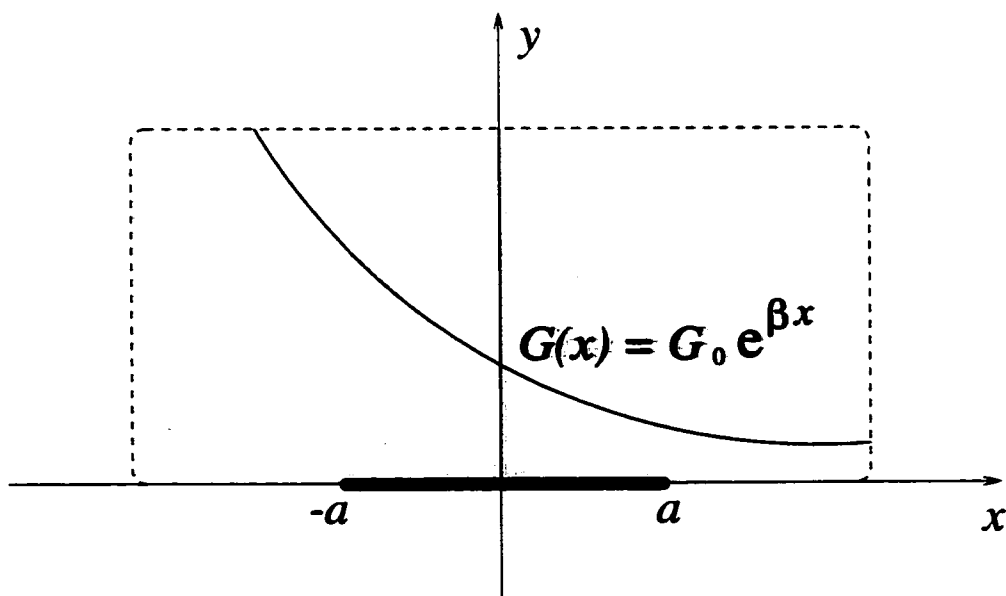


Figure 12.1: Geometry of the problem.

### 12.1.2 Governing System of PDEs and Boundary Conditions

We assume that the shear modulus varies in the  $x$ -direction and it takes the exponential form (see Figure 12.1):

$$G \equiv G(x) = G_0 e^{\beta x}, \quad (12.6)$$

where  $G_0$  and  $\beta$  are material constants. Also,

$$\lambda \equiv \lambda(x) = \frac{3 - \kappa}{\kappa - 1} G(x) \quad (12.7)$$

is a function of  $x$ , where  $\kappa = 3 - 4\nu$  as plane strain is considered in this paper. By imposing the equilibrium equations (11.6)

$$\frac{\partial \sigma_{xx}}{\partial x} + \frac{\partial \sigma_{xy}}{\partial y} = 0 \quad \text{and} \quad \frac{\partial \sigma_{xy}}{\partial x} + \frac{\partial \sigma_{yy}}{\partial y} = 0,$$

and using equations (3.16) and (12.5), one can obtain the following system of PDEs:

$$\left(1 - \beta \ell^2 \frac{\partial}{\partial x} - \ell^2 \nabla^2\right) \left[ (\kappa + 1) \frac{\partial^2 u}{\partial x^2} + (\kappa - 1) \frac{\partial^2 u}{\partial y^2} + 2 \frac{\partial^2 v}{\partial x \partial y} + \beta(\kappa + 1) \frac{\partial u}{\partial x} + \beta(3 - \kappa) \frac{\partial v}{\partial y} \right] = 0, \quad (12.8)$$

$$\left(1 - \beta \ell^2 \frac{\partial}{\partial x} - \ell^2 \nabla^2\right) \left[ (\kappa - 1) \frac{\partial^2 v}{\partial x^2} + (\kappa + 1) \frac{\partial^2 v}{\partial y^2} + 2 \frac{\partial^2 u}{\partial x \partial y} + \beta(\kappa - 1) \frac{\partial u}{\partial y} + \beta(\kappa - 1) \frac{\partial v}{\partial x} \right] = 0. \quad (12.9)$$

Boundary conditions are same as (11.9) and (11.10); the far-field condition is (11.11).

## 12.2 Derivation for the System of Integral Equations

After a Fourier transform

$$u(x, y) = \frac{1}{\sqrt{2\pi}} \int_{-\infty}^{\infty} \hat{u}(\xi, y) e^{-ix\xi} d\xi, \quad v(x, y) = \frac{1}{\sqrt{2\pi}} \int_{-\infty}^{\infty} \hat{v}(\xi, y) e^{-ix\xi} d\xi,$$



the system PDEs (12.8) and (12.9) becomes a system of ODEs:

$$\begin{aligned}
 & -\ell^2(\kappa - 1) \frac{d^4 \hat{u}}{dy^4} + (\kappa - 1 + 2\ell^2 \kappa \xi^2 + 2i\beta \ell^2 \kappa \xi) \frac{d^2 \hat{u}}{dy^2} - \\
 & (\kappa + 1) (\xi^2 + i\beta \xi + \ell^2 \xi^4 + 2i\beta \ell^2 \xi^3 - \beta^2 \ell^2 \xi^2) \hat{u} + [2i\ell^2 \xi - \beta \ell^2 (3 - \kappa)] \frac{d^3 \hat{v}}{dy^3} \\
 & - [2i\xi + 2i\ell^2 \xi^3 - \beta(3 - \kappa) - \beta \ell^2 (5 - \kappa) \xi^2 - i\beta^2 \ell^2 (3 - \kappa) \xi] \frac{d\hat{v}}{dy} = 0, \quad (12.10)
 \end{aligned}$$

$$\begin{aligned}
 & -\ell^2(\kappa + 1) \frac{d^4 \hat{v}}{dy^4} + (\kappa + 1 + 2\ell^2 \kappa \xi^2 + 2i\beta \ell^2 \kappa \xi) \frac{d^2 \hat{v}}{dy^2} - \\
 & (\kappa - 1) (i\beta \xi + \xi^2 + 2i\beta \ell^2 \xi^3 + \ell^2 \xi^4 - \beta^2 \ell^2 \xi^2) \hat{v} + [2i\ell^2 \xi - \beta \ell^2 (\kappa - 1)] \frac{d^3 \hat{u}}{dy^3} \\
 & - [2i\xi - \beta(\kappa - 1) + 2i\ell^2 \xi^3 - \beta \ell^2 (\kappa + 1) \xi^2 - i\beta^2 \ell^2 (\kappa - 1) \xi] \frac{d\hat{u}}{dy} = 0. \quad (12.11)
 \end{aligned}$$

### 12.2.1 Finding Roots of System of ODEs

Define the new variables  $U$  and  $V$  by

$$U = \frac{d}{dy} \hat{u} = \hat{u}', \quad \text{and} \quad V = \frac{d}{dy} \hat{v} = \hat{v}', \quad (12.12)$$

then the system of ODEs (12.10) and (12.11) can be put into the following matrix form  $\mathbf{x}' = \mathbf{A}\mathbf{x}$  for an  $8 \times 8$  linear system of first-order equations, that is,

$$\begin{bmatrix} U \\ U' \\ U'' \\ U''' \\ V \\ V' \\ V'' \\ V''' \end{bmatrix} = \begin{bmatrix} 0 & 1 & 0 & 0 & 0 & 0 & 0 & 0 \\ 0 & 0 & 1 & 0 & 0 & 0 & 0 & 0 \\ 0 & 0 & 0 & 1 & 0 & 0 & 0 & 0 \\ a_{41} & 0 & a_{43} & 0 & 0 & a_{46} & 0 & a_{48} \\ 0 & 0 & 0 & 0 & 0 & 1 & 0 & 0 \\ 0 & 0 & 0 & 0 & 0 & 0 & 1 & 0 \\ 0 & 0 & 0 & 0 & 0 & 0 & 0 & 1 \\ 0 & a_{82} & 0 & a_{84} & a_{85} & 0 & a_{87} & 0 \end{bmatrix} \begin{bmatrix} \hat{u} \\ \hat{u}' \\ \hat{u}'' \\ \hat{u}''' \\ \hat{v} \\ \hat{v}' \\ \hat{v}'' \\ \hat{v}''' \end{bmatrix} \quad (12.13)$$

where

$$a_{41} = -\frac{(\kappa + 1) (i\beta \xi + \xi^2 + 2i\beta \ell^2 \xi^3 + \ell^2 \xi^4 - \beta^2 \ell^2 \xi^2)}{\ell^2 (\kappa - 1)}$$

$$a_{43} = \frac{\kappa - 1 + 2\ell^2\kappa\xi^2 + 2i\ell^2\beta\kappa\xi}{\ell^2(\kappa - 1)}$$

$$a_{46} = -\frac{2i\xi - \beta(3 - \kappa) + 2i\ell^2\xi^3 - \beta\ell^2(5 - \kappa)\xi^2 - \beta\ell^2(5 - \kappa)\xi^2 - i\beta^2\ell^2(3 - \kappa)\xi}{\ell^2(\kappa - 1)}$$

$$a_{48} = \frac{2i\ell^2\xi - \beta\ell^2(3 - \kappa)}{\ell^2(\kappa - 1)}$$

$$a_{82} = -\frac{2i\xi - \beta(\kappa - 1) + 2i\ell^2\xi^3 - \beta\ell^2(\kappa + 1)\xi^2 - i\beta^2\ell^2(\kappa - 1)\xi}{\ell^2(\kappa + 1)}$$

$$a_{84} = \frac{2i\ell^2\xi - \ell^2\beta(\kappa - 1)}{\ell^2(\kappa + 1)}$$

$$a_{85} = -\frac{(\kappa - 1)(i\beta\xi + \xi^2 + 2i\beta\ell^2\xi^3 + \ell^2\xi^4 - \beta^2\ell^2\xi^2)}{\ell^2(\kappa + 1)}$$

$$a_{87} = \frac{\kappa + 1 + 2\ell^2\kappa\xi^2 + 2i\beta\ell^2\kappa\xi}{\ell^2(\kappa + 1)}$$

The corresponding characteristic polynomial to the  $8 \times 8$  matrix in (12.13) can be found to be:

$$[\lambda^2 - (\xi^2 + i\beta\xi + 1/\ell^2)]^2 \{ \lambda^4 - [2\xi(\xi + i\beta) - \beta^2(3 - \kappa)/(\kappa + 1)]\lambda^2 + \xi^2(\xi^2 + 2i\beta\xi - \beta^2) \} = 0. \quad (12.14)$$

*Note:*

If the shear modulus  $G$  takes form  $G = G(x, y) = G_0 e^{\beta x + \gamma y}$ , then it is a mixed mode problem to be solved, and the corresponding characteristic polynomial (to an  $8 \times 8$  matrix) is

$$[\lambda^2 + \gamma\lambda - (\xi^2 + i\beta\xi + 1/\ell^2)]^2 \{ \lambda^4 + 2\gamma\lambda^3 - [2\xi(\xi + i\beta) - \gamma^2 - \beta^2(3 - \kappa)/(\kappa + 1)]\lambda^2 + \xi^2[\xi^2 + 2i\beta\xi - \beta^2 + \gamma^2(3 - \kappa)/(\kappa + 1)] \} = 0. \quad (12.15)$$

By using MAPLE [96, 97], a computer algebra system, to solve characteristic polynomial (12.14), one may find that there are six eigenvalues,  $\lambda_1(\xi) - \lambda_6(\xi)$ , to be considered:

$$\lambda_1(\xi) = -\frac{\beta\sqrt{(3-\kappa)/(\kappa+1)}}{2} - \frac{\sqrt{\beta^2(3-\kappa)/(\kappa+1) + 4(\xi^2 + i\beta\xi)}}{2} \quad (12.16)$$

$$\lambda_2(\xi) = \frac{\beta\sqrt{(3-\kappa)/(\kappa+1)}}{2} - \frac{\sqrt{\beta^2(3-\kappa)/(\kappa+1) + 4(\xi^2 + i\beta\xi)}}{2} \quad (12.17)$$

$$\begin{aligned} \lambda_3 = & \frac{-1}{\sqrt{2}} \sqrt{\sqrt{(\xi^2 + 1/\ell^2)^2 + \beta^2\xi^2} + \xi^2 + 1/\ell^2} \\ & - \frac{i}{\sqrt{2}} \frac{\beta\xi}{\sqrt{\sqrt{(\xi^2 + 1/\ell^2)^2 + \beta^2\xi^2} + \xi^2 + 1/\ell^2}} \end{aligned} \quad (12.18)$$

$$\lambda_4(\xi) = -\frac{\beta\sqrt{(3-\kappa)/(\kappa+1)}}{2} + \frac{\sqrt{\beta^2(3-\kappa)/(\kappa+1) + 4\xi^2 + i\beta\xi}}{2} \quad (12.19)$$

$$\lambda_5(\xi) = \frac{\beta\sqrt{(3-\kappa)/(\kappa+1)}}{2} + \frac{\sqrt{\beta^2(3-\kappa)/(\kappa+1) + 4\xi^2 + i\beta\xi}}{2} \quad (12.20)$$

$$\begin{aligned} \lambda_6 = & \frac{1}{\sqrt{2}} \sqrt{\sqrt{(\xi^2 + 1/\ell^2)^2 + \beta^2\xi^2} + \xi^2 + 1/\ell^2} \\ & - \frac{i}{\sqrt{2}} \frac{\beta\xi}{\sqrt{\sqrt{(\xi^2 + 1/\ell^2)^2 + \beta^2\xi^2} + \xi^2 + 1/\ell^2}}. \end{aligned} \quad (12.21)$$

### 12.2.2 Representation of the Solution

The mode I problem is simplified by considering the upper-half plane ( $y \geq 0$ ). Thus by taking into account the far-field conditions

$$u(x, y), v(x, y) \rightarrow 0 \text{ as } \sqrt{x^2 + y^2} \rightarrow \infty,$$

the roots ( $\lambda_4, \lambda_5$ , and  $\lambda_6$ ) with positive real parts are disregarded and only the roots  $\lambda_1, \lambda_2$ , and  $\lambda_3$  are considered herein. So the general solutions of  $\hat{v}(\xi, y)$  and  $\hat{u}(\xi, y)$

can be expressed as

$$\hat{v}(\xi, y) = c_1(\xi)e^{\lambda_1(\xi)y} + c_2(\xi)e^{\lambda_2(\xi)y} + c_3(\xi)e^{\lambda_3(\xi)y} \quad (12.22)$$

$$\hat{u}(\xi, y) = d_1(\xi)e^{\lambda_1(\xi)y} + d_2(\xi)e^{\lambda_2(\xi)y} + d_3(\xi)e^{\lambda_3(\xi)y} .$$

The system of ODEs (12.10) and (12.11) imposes the following restriction:

$$\hat{u}(\xi, y) = \eta_1(\xi)c_1(\xi)e^{\lambda_1(\xi)y} + \eta_2(\xi)c_2(\xi)e^{\lambda_2(\xi)y} + d_3(\xi)e^{\lambda_3(\xi)y} , \quad (12.23)$$

in which

$$\eta_1(\xi) = \frac{\lambda_1(\xi) + \lambda_2(\xi) - \beta\kappa\sqrt{\frac{3-\kappa}{\kappa+1}}}{2i\xi - \beta(\kappa - 1)} \quad (12.24)$$

$$\eta_2(\xi) = \frac{\lambda_1(\xi) + \lambda_2(\xi) + \beta\kappa\sqrt{\frac{3-\kappa}{\kappa+1}}}{2i\xi - \beta(\kappa - 1)} . \quad (12.25)$$

Thus,  $v(x, y)$  and  $u(x, y)$  can be expressed as

$$v(x, y) = \frac{1}{\sqrt{2\pi}} \int_{-\infty}^{\infty} [c_1(\xi)e^{\lambda_1(\xi)y} + c_2(\xi)e^{\lambda_2(\xi)y} + c_3(\xi)e^{\lambda_3(\xi)y}] e^{-ix\xi} d\xi , \quad y \geq 0 , \quad (12.26)$$

$$u(x, y) = \frac{1}{\sqrt{2\pi}} \int_{-\infty}^{\infty} [\eta_1(\xi)c_1(\xi)e^{\lambda_1(\xi)y} + \eta_2(\xi)c_2(\xi)e^{\lambda_2(\xi)y} + d_3(\xi)e^{\lambda_3(\xi)y}] e^{-ix\xi} d\xi , \quad y \geq 0 . \quad (12.27)$$

Again, like the homogeneous case, there are four unknown coefficients  $c_1(\xi)$ ,  $c_2(\xi)$ ,  $c_3(\xi)$ , and  $d_3(\xi)$  to be determined by means of the boundary conditions.

### 12.2.3 System of Fredholm Integral Equations

Imposing the first boundary condition in (11.9), one obtains

$$c_2(\xi) = \frac{g_1(\xi)}{g_2(\xi)} c_1(\xi) , \quad (12.28)$$

where

$$\begin{aligned} g_1(\xi) &= \eta_1\lambda_1 - i\xi + \ell^2\xi^2\eta_1\lambda_1 - \ell^2\eta_1\lambda_1^3 - i\ell^2\xi^3 + i\ell^2\xi\lambda_1^2 + i\beta\ell^2\xi(\eta_1\lambda_1 - i\xi) \\ &= (\eta_1\lambda_1 - i\xi)(1 + i\beta\ell^2\xi + \ell^2\xi^2 - \ell^2\lambda_1^2) , \end{aligned} \quad (12.29)$$

$$\begin{aligned}
 g_2(\xi) &= i\xi - \eta_2\lambda_2 - \ell^2\xi^2\eta_2\lambda_2 + \ell^2\eta_2\lambda_2^3 + i\ell^2\xi^3 - i\ell^2\xi\lambda_2^2 + i\beta\ell^2\xi(i\xi - \eta_2\lambda_2) \\
 &= (i\xi - \eta_2\lambda_2)(1 + i\beta\ell^2\xi + \ell^2\xi^2 - \ell^2\lambda_2^2).
 \end{aligned} \tag{12.30}$$

Also, by the first boundary condition in (11.10),  $d_3(\xi)$  may be expressed as

$$d_3(\xi) = q_1(\xi)c_1(\xi) + q_2(\xi)c_2(\xi) + q_3(\xi)c_3(\xi), \tag{12.31}$$

where

$$q_1(\xi) = \frac{\ell'(i\xi - \eta_1\lambda_1) + \ell^2(\eta_1\lambda_1^2 - i\xi\lambda_1)}{\ell'\lambda_3 - \ell^2\lambda_3^2} = \frac{(i\xi - \eta_1\lambda_1)(\ell' - \ell^2\lambda_1)}{\lambda_3(\ell' - \ell^2\lambda_3)}, \tag{12.32}$$

$$q_2(\xi) = \frac{\ell'(i\xi - \eta_2\lambda_2) + \ell^2(\eta_2\lambda_2^2 - i\xi\lambda_2)}{\ell'\lambda_3 - \ell^2\lambda_3^2} = \frac{(i\xi - \eta_2\lambda_2)(\ell' - \ell^2\lambda_2)}{\lambda_3(\ell' - \ell^2\lambda_3)}, \tag{12.33}$$

$$q_3(\xi) = \frac{i\xi}{\lambda_3}. \tag{12.34}$$

Follow the same route as the homogeneous case, and define

$$\phi(x) = \frac{\partial}{\partial x}v(x, 0) \quad \text{and} \quad \psi(x) = \frac{\partial}{\partial x} \left[ \frac{\partial}{\partial y}v(x, 0) \right], \tag{12.35}$$

one may translate the two mixed-valued boundary conditions into the following system of integral equations in the limit form:

$$\lim_{y \rightarrow 0} \frac{1}{2\pi} \int_{-a}^a \int_{-\infty}^{\infty} [\mathcal{K}_{11}(\xi, y)\phi(t) + \mathcal{K}_{12}(\xi, y)\psi(t)] e^{i(t-x)\xi} d\xi dt = \frac{p(x)}{G(x)}, \quad |x| < a \tag{12.36}$$

$$\lim_{y \rightarrow 0} \frac{1}{2\pi} \int_{-a}^a \int_{-\infty}^{\infty} [\mathcal{K}_{21}(\xi, y)\phi(t) + \mathcal{K}_{22}(\xi, y)\psi(t)] e^{i(t-x)\xi} d\xi dt = 0, \quad |x| < a, \tag{12.37}$$

where the four kernels  $\mathcal{K}_{ij}$  ( $i, j = 1, 2$ ) are described as follows:

$$\mathcal{K}_{ij}(\xi) = \lim_{y \rightarrow 0} \mathcal{K}_{ij}(\xi, y) = \frac{\mathcal{N}_{ij}(\xi)}{\mathcal{D}(\xi)}, \quad i, j = 1, 2 \tag{12.38}$$

where

$$\mathcal{D}(\xi) = (-i\xi)[(g_1 + g_2)\lambda_3 - (\lambda_1g_2 + \lambda_2g_1)], \tag{12.39}$$

$$\mathcal{N}_{11}(\xi) = \lambda_3(m_1g_2 + m_2g_1), \quad \mathcal{N}_{12}(\xi) = -(m_1g_2 + m_2g_1), \tag{12.40}$$

$$\begin{aligned} \mathcal{N}_{21}(\xi) &= \lambda_3(n_1g_2 + n_2g_1) - n_{3c}(\lambda_1g_2 + \lambda_2g_1) \\ &\quad + n_{3d}[\lambda_3(q_1g_2 + q_2g_1) - q_3(\lambda_1g_2 + \lambda_2g_1)] \end{aligned} \quad (12.41)$$

$$\mathcal{N}_{22}(\xi) = -(n_1g_2 + n_2g_1) + n_{3c}(g_1 + g_2) + n_{3d}[q_3(g_2 + g_1) - (q_1g_2 + q_2g_1)] \quad (12.42)$$

and

$$m_1(\xi) = [(\kappa + 1)\lambda_1 - i\xi(3 - \kappa)\eta_1][1 + \ell^2(\xi^2 + i\beta\xi - \lambda_1^2)] \quad (12.43)$$

$$m_2(\xi) = [(\kappa + 1)\lambda_2 - i\xi(3 - \kappa)\eta_2][1 + \ell^2(\xi^2 + i\beta\xi - \lambda_2^2)] \quad (12.44)$$

$$q_1 = \frac{(i\xi - \lambda_1\eta_1)(\ell' - \ell^2\lambda_1)}{\lambda_3(\ell' - \ell^2\lambda_3)}, \quad q_2 = \frac{(i\xi - \lambda_2\eta_2)(\ell' - \ell^2\lambda_2)}{\lambda_3(\ell' - \ell^2\lambda_3)}, \quad q_3 = \frac{i\xi}{\lambda_3} \quad (12.45)$$

$$n_1 = (\ell^2\lambda_1 - \ell')[(\kappa + 1)\lambda_1 - i\xi(3 - \kappa)\eta_1] \quad (12.46)$$

$$n_2 = (\ell^2\lambda_2 - \ell')[(\kappa + 1)\lambda_2 - i\xi(3 - \kappa)\eta_2] \quad (12.47)$$

$$n_{3c} = (\kappa + 1)\lambda_3(\ell^2\lambda_3 - \ell'), \quad n_{3d} = i\xi(3 - \kappa)(\ell' - \ell^2\lambda_3) \quad (12.48)$$

Splitting the singularity from the four kernels  $\mathcal{K}_{ij}$  ( $i, j = 1, 2$ ) by performing the asymptotic analysis, one can reach the following system of hypersingular integral equations:

$$\begin{aligned} &\frac{1}{\pi} \int_{-a}^a \left[ \frac{-16\ell^2}{(\kappa + 2)(t - x)^3} - \frac{10\beta\ell^2(\kappa + 3)}{(\kappa + 2)^2(t - x)^2} + \frac{2(3\kappa + 7) - f_1}{(\kappa + 2)^2(t - x)} + \tilde{K}_{11}(x, t) \right] \phi(t) dt \\ &+ \frac{8\ell^2}{\kappa + 2} \psi'(x) + \frac{2\beta\ell^2(3\kappa + 11)}{(\kappa + 2)^2} \psi(x) + \frac{1}{\pi} \int_{-a}^a \tilde{K}_{12}(x, t) \psi(t) dt = \frac{p(x)}{G_0}, \quad |x| < a \end{aligned} \quad (12.49)$$

$$\begin{aligned} &\frac{1}{\pi} \int_{-a}^a \left[ \frac{2\ell'\kappa(\kappa - 3)}{(\kappa + 2)(\kappa - 1)t - x} + \tilde{K}_{21}(x, t) \right] \phi(t) dt + \frac{2\ell^2\kappa}{\kappa + 2} \phi'(x) + f_2\phi(x) \\ &+ \frac{1}{\pi} \int_{-a}^a \left[ \frac{2\ell^2(\kappa^2 + \kappa + 4)}{(\kappa + 2)(\kappa - 1)t - x} + \tilde{K}_{22}(x, t) \right] \psi(t) dt = 0, \quad |x| < a, \end{aligned} \quad (12.50)$$

with

$$f_1 = \frac{\beta^2 \ell^2 (\kappa^3 + 26\kappa^2 + 92\kappa + 63)}{2(\kappa + 1)(\kappa + 2)}$$

and

$$f_2 = \frac{\beta \ell^2 (\kappa^3 + 8\kappa^2 + 3\kappa + 12)}{2(\kappa - 1)(\kappa + 2)^2}.$$

Equations (12.49) and (12.50) are the final and main hypersingular integral equations that are solved together with the single-valuedness condition

$$\int_{-a}^a \phi(x) dx = 0 \quad , \quad \int_{-a}^a \psi(x) dx = 0. \quad (12.51)$$

### 12.3 Numerical Results

By choosing the dimensionless variables

$$r = x/a \quad , \quad s = t/a \quad , \quad \bar{\ell} = \ell/a \quad , \quad \text{and} \quad \bar{\ell}' = \ell'/a \quad ,$$

where  $a$  is the half crack length, the hypersingular integrodifferential equations (12.49) and (12.50) can be treated only on the normalized interval  $(-1, 1)$ . Denote the normalized  $\phi(x)$  and  $\psi(x)$  by  $\Phi(r)$  and  $\Psi(r)$ , respectively.

Based on the crack-tip asymptotics,  $\Phi$  and  $\Psi$  can be expanded by the Chebyshev polynomials of the second kind  $U_n(s)$ :

$$\Phi(s) = \sqrt{1-s^2} \sum_{n=0}^{\infty} A_n U_n(s) \quad , \quad \Psi(s) = \sqrt{1-s^2} \sum_{n=0}^{\infty} B_n U_n(s). \quad (12.52)$$

Notice that condition (12.51) implies that

$$A_0 = 0 \quad \text{and} \quad B_0 = 0.$$

Numerical solution procedures have been addressed in Chapter 8; formulas involving the Chebyshev polynomials  $T_n$  and  $U_n$  are detailed in Chapter 7. For instance,

$$\Psi(s) \approx \sqrt{1-s^2} \sum_{n=1}^N B_n U_n(s) \quad \Rightarrow \quad \Psi'(s) \approx \frac{-1}{2\sqrt{1-s^2}} \sum_{n=1}^N B_n (n+1) T_{n+1}(s)$$

is one of formulas needed in the numerical implementation. Numerical results that include SIFs and Mode I crack opening displacement (COD) profiles are given here.

Table 12.1: Normalized SIFs for a mode I crack under uniform loading,  $p(x) = -p_0$ . ( $\ell/a = 0.1$ ,  $\ell'/a = 0.01$ ,  $\nu = 0.3$ )

| $\beta a$ | $\frac{K_I(-a)}{p_0\sqrt{\pi a}}$ | $\frac{K_I(a)}{p_0\sqrt{\pi a}}$ |
|-----------|-----------------------------------|----------------------------------|
| 0.01      | 0.3166214                         | 1.0860864                        |
| 0.10      | 0.3077957                         | 1.1376156                        |
| 0.25      | 0.2863779                         | 1.2060054                        |
| 0.50      | 0.2534668                         | 1.3263192                        |
| 0.75      | 0.2245852                         | 1.4579430                        |
| 1.00      | 0.1996328                         | 1.6058326                        |

### 12.3.1 Stress Intensity Factors

SIFs are defined by:

$$\ell K_I(a) = \lim_{x \rightarrow a^+} 2\sqrt{2\pi(x-a)}(x-a) \sigma_{yy}(x, 0), \quad (12.53)$$

$$\ell K_I(-a) = \lim_{x \rightarrow -a^-} 2\sqrt{2\pi(-x-a)}(-x-a) \sigma_{yy}(x, 0). \quad (12.54)$$

Therefore, the following formulas for the mode I SIFs in the strain-gradient elasticity may be derived:

$$\begin{aligned} \ell K_I(a) &= \lim_{x \rightarrow a^+} 2\sqrt{2\pi(x-a)}(x-a) \sigma_{yz}(x, 0) \\ &= \lim_{r \rightarrow 1^+} 2\sqrt{2\pi(ar-a)}(ar-a) \sigma_{yz}(ar, 0) \\ &= \frac{2a\sqrt{2\pi a G_0}}{\kappa + 2} \lim_{r \rightarrow 1^+} e^{\beta ar} \sqrt{(r-1)}(r-1) \left(\frac{\ell}{a}\right)^2 \\ &\quad \times \left[ \frac{1}{\pi} \int_{-1}^1 \frac{-16\Phi(s)}{(s-r)^3} ds + 8\Psi'(r) \right] \end{aligned} \quad (12.55)$$



After cancellation of the common terms, equation (12.55) becomes:

$$K_I(a) = -\frac{8\sqrt{\pi a} G_0}{\kappa + 2} (\ell/a) e^{\beta a} \sum_{n=0}^N (n+1)(A_n - B_n). \quad (12.56)$$

Similarly,

$$K_I(-a) = \frac{8\sqrt{\pi a} G_0}{\kappa + 2} (\ell/a) e^{-\beta a} \sum_{n=0}^N (-1)^n (n+1)(A_n - B_n). \quad (12.57)$$

Formulas (12.56) and (12.57) are used to obtain the numerical results for SIFs in Table 12.1, in which  $N$  is the number of the collocation points.

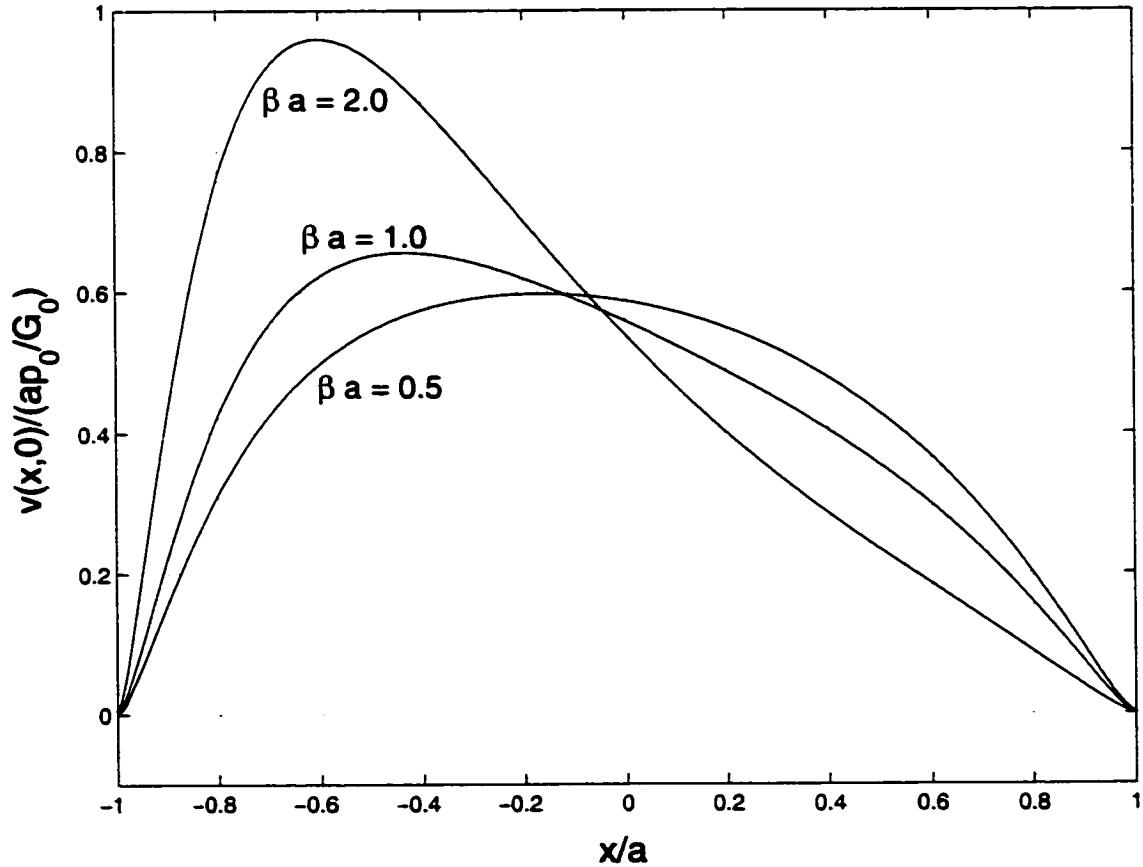


Figure 12.2: Normalized crack profiles at  $\beta a > 0$ ,  $\bar{\ell} = 0.10$ ,  $\bar{\ell}' = 0.01$ ;  $\nu = 0.3$ .

### 12.3.2 Crack Opening Displacement Profiles

The Mode I crack opening displacement (COD) profiles are given in Figures 12.2 – 12.5.

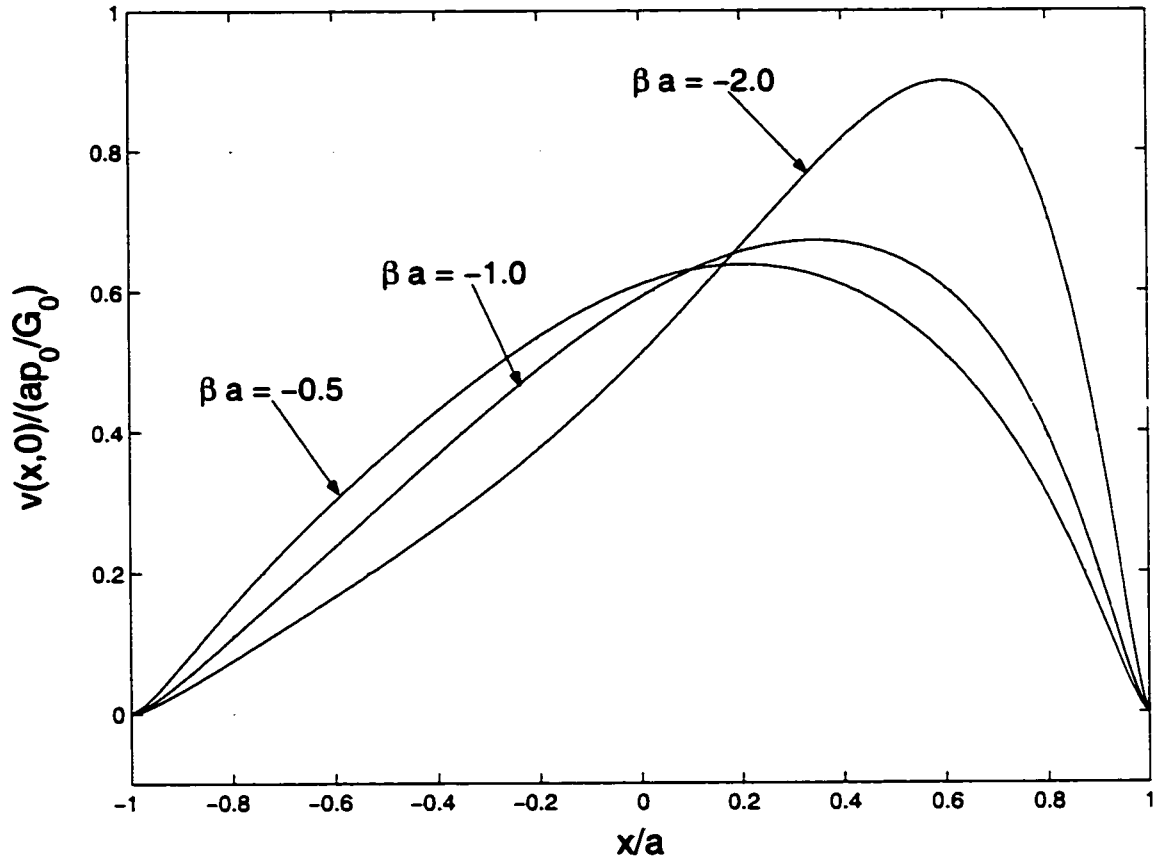


Figure 12.3: Normalized crack profiles at  $\beta a < 0$ ,  $\bar{\ell} = 0.10$ ,  $\bar{\ell}' = 0.01$ ;  $\nu = 0.3$ .

Figures 12.2 and 12.3 show the trend of the influence of the material nonhomogeneity (determined by the parameter  $\beta$ ) on the crack opening displacements. If  $\beta > 0$ , then the crack profiles tilt to the left; otherwise ( $\beta < 0$ ), the crack profiles tilt to the right. This trend is consistent with the classical results of Delale and Erdogan [21]. Figures 12.4 and 12.5 show the effect of the gradient parameters  $\ell$  and  $\ell'$  on the crack profiles, respectively. Figure 12.4 shows that the crack profiles increases as  $\ell$  decreases. An analogous effect for the parameter  $\ell'$  is shown in Figure 12.5. Notice that the negative

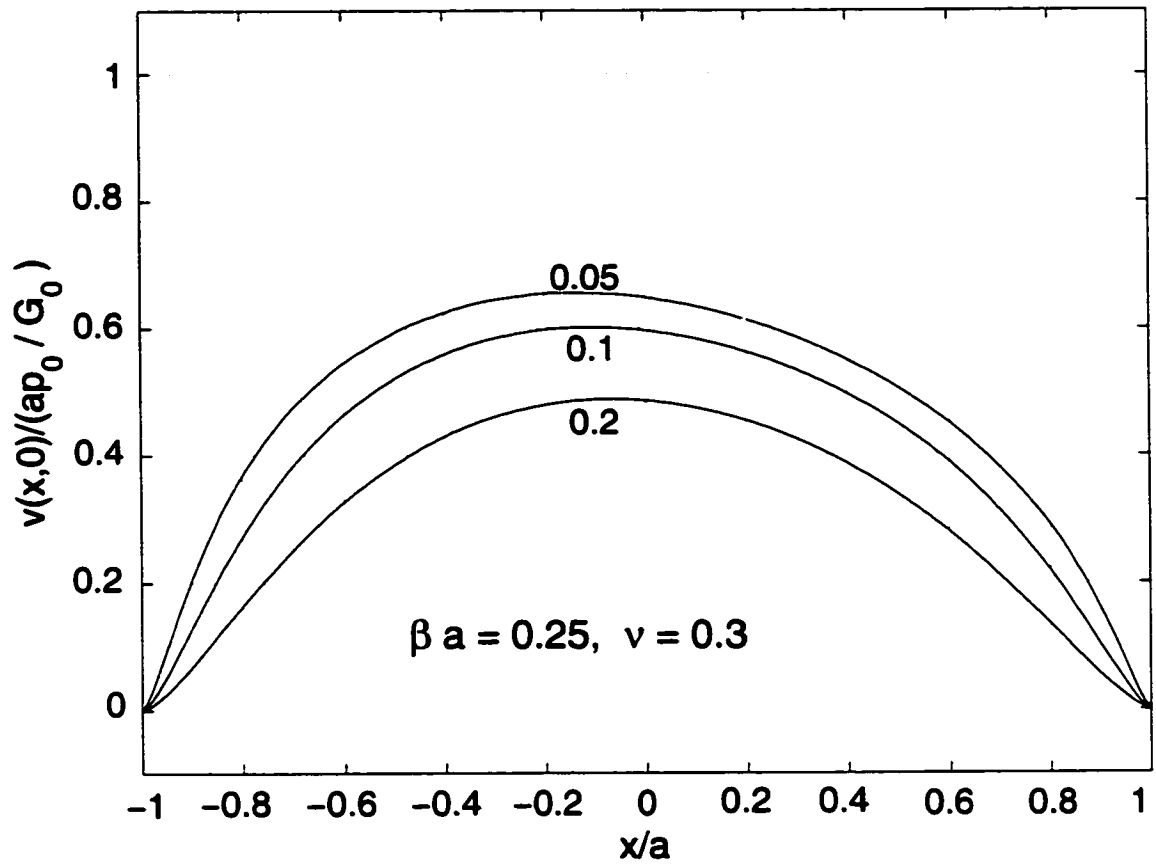


Figure 12.4: Normalized crack profiles at  $\beta a = 0.25$ ,  $\bar{\ell} = 0.05, 0.1, 0.2$ ,  $\bar{\ell}' = 0.01$ ;  $\nu = 0.3$ .

values of  $\ell'$  allow a more compliant fracture behavior than the positive ones. This is an important feature of the present gradient elasticity theory based on the Casal's continuum.

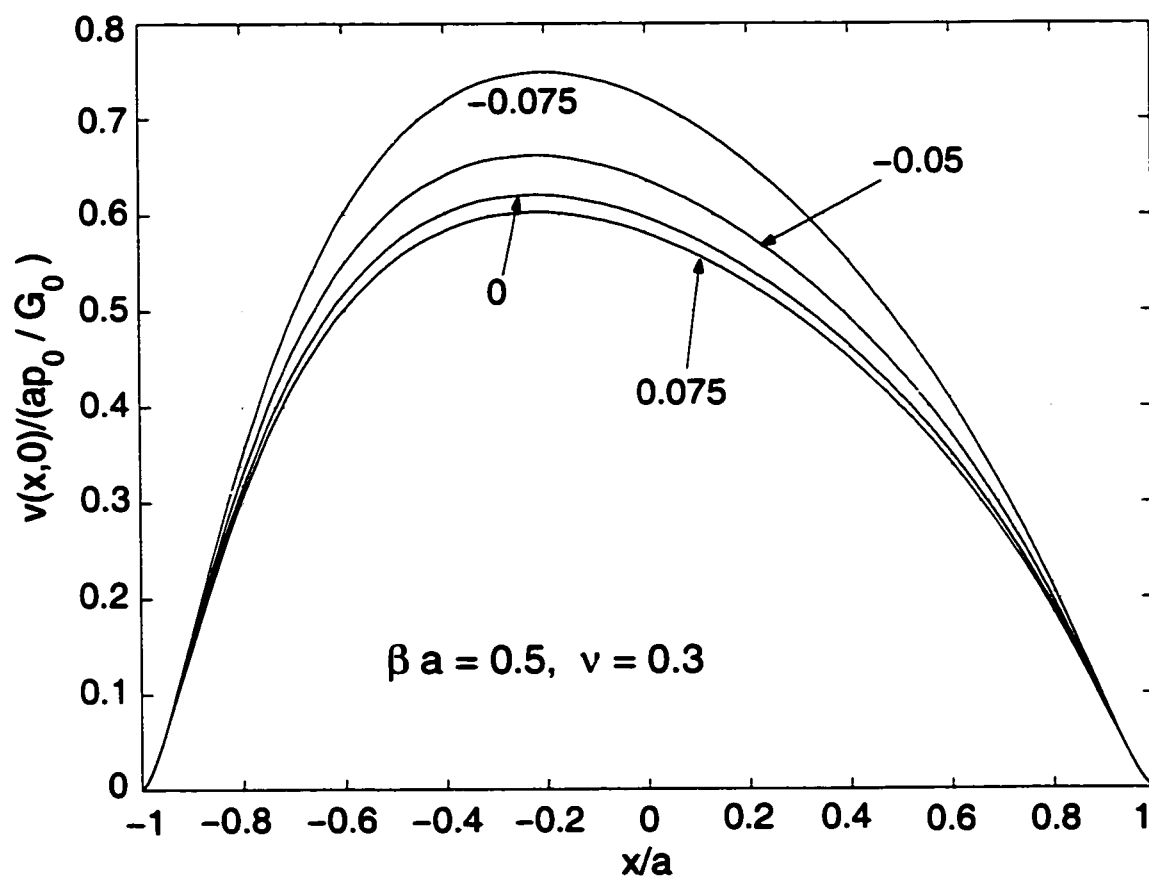


Figure 12.5: Normalized crack profiles at  $\beta a = 0.5$ ,  $\tilde{l} = 0.1$ ,  $\tilde{l} = 0.075, 0, -0.075$ ;  $\nu = 0.3$ .

## Chapter 13

# Conclusions and Future Work

### 13.1    Hypersingular Integrodifferential Equation Method

This thesis incorporates strain-gradient elasticity and graded materials within the framework of fracture mechanics. Thus, there are two elements that have revealed in the mathematical manipulation for solution:

1. Higher order strain-gradient elasticity theory.
2. Material gradation.

The first element gives rise to a higher order governing PDE, thus it leads to a higher order singularity of the derived integral equation. However, by using finite part integral, in some simple case, we can still find the closed form solution (see Chapter 9).

The second element, say materials with an exponential type of gradation, does not raise the order of the governing PDE; however, it always spoils the solvability for closed form solution (as we have seen in Chapters 2, 4, 10, 11, and 12). The remedy to this difficulty is to develop a reliable and efficient numerical scheme. For instance, the capability of exact evaluation of the hypersingular integrals (Chapter 7) offers a

contribution to this aspect.

Hypersingular integrodifferential equation method is like using one stone to kill two birds. The method combines the two merits together and resolves the complication. In this thesis, we have laid out the theoretical framework for the method and developed the corresponding computational implementation in detail.

## 13.2 Applicability of the Method

The applicability of the developed method has a wide spectrum. As we have demonstrated in the thesis, the method can be used to solve crack problems in

- both classical LEFM and strain-gradient elasticity,
- both homogeneous and nonhomogeneous (FGMs) materials,
- different geometric setting of crack location vs. material gradation.

In this study, we also learn that there is a non-trivial interaction between the material gradation and the strain-gradient effect (Chapter 3) . Again, the hypersingular integrodifferential equation approach provides a numerically tractable solution of the fracture problem and allows to find relevant fracture parameters:

- crack-tip asymptotics,
- crack displacement profiles,
- stress and strain fields, and
- (generalized) stress intensity factors (SIFs).

From the solution we know that material (with exponential) gradation will not affect the crack-tip asymptotics, while the strain-gradient theory gives different asymptotics from the conventional classical LEFM. For instance, the strain singularity is

eliminated from crack tips in strain-gradient elasticity. Here, we list the crack-tip asymptotics for the strain-gradient theory:

$$\text{Displacements} \sim r^{3/2}, \quad \text{Strains} \sim \sqrt{r}, \quad \text{Stresses} \sim r^{-3/2}. \quad (13.1)$$

### 13.3 Future Work

Some further work can be done in the future.

- Mixed mode problems.

We have solved both Mode I and Mode III crack problems in this thesis. As it has been pointed out on page 177, in Mode I fracture for FGMs, if the shear modulus  $G$  is a function of both  $x$  and  $y$  (e.g.  $G = G(x, y) = G_0 e^{\beta x + \gamma y}$ ), then it is a mixed mode problem to be solved. In terms of future work, this mixed mode problem with exponential gradation is probably the most doable one.

- Non-exponential material gradation.

We have assumed that materials possess exponential gradation. However, it would be more physically tenable if the crack problems can be solved for non-exponential material gradation. Especially, in the process of producing FGMs, the mediums are essentially made as two-phase particulate composites synthesized in a variation that the volume fractions of the constituents vary linearly in the thickness direction to a given predetermined composition profile.

- Three dimensional problems.

Sometimes, by the symmetry of the geometry, one can reduce the dimension to a lower one; however, it would be desirable if one can solve a general three dimensional crack problem. Most techniques in complex function theory may not be applicable in three dimension. Finite element and boundary element are two of major numerical methods in computational fracture mechanics.

- Thermal effect and time dependent problems.

One of the most important technological area of FGMs is the high temperature application. At high temperatures metals (and metal alloys) lose their strength and toughness. A variety of ceramic/metal composites and ceramic thermal barrier coating have become very effective in the high temperature designs. Also, transient problems attracts a lots more interest than the steady state ones if temperature is considered.

- Experimental corroboration.

Strain-gradient theory has been very controversial and generated a lot of debate mainly due to its physical meaning. However, recent investigations do show that size effects are widely observed in many experiments. Strain-gradient theory has been used to interpret for the size effects. Further experimental corroboration is needed; for instance, how to physically measure the characteristic lengths  $\ell$  and  $\ell'$ ?

As one can see, further works lead into a more interdisciplinary area and require a deeper and wider mathematical work.

At the end of this thesis, being an applied mathematician, I like to be always reminded by

*“It is in the nature of human endeavor that technology always looks forward and never waits for science to provide the fundamental solutions. Whether or not they have the necessary physically sound tools, the engineers have and will continue to design and build.”*,

said by Professor Erdogan at Lehigh University in his review paper [27] on fracture mechanics.



# Bibliography

- [1] J. D. Achenbach. *Wave Propagation in Elastic Solids*. North-Holland Publishing Company, Amsterdam, 1973.
- [2] E. Aifantis. On the role of gradients in the localization of deformation and fracture. *Int. J. Eng. Sci.*, 30:1279–1299, 1992.
- [3] G. I. Barenblatt. Mathematical theory of equilibrium cracks in brittle fracture. *Adv. Appl. Mech.*, 7:55–129, 1962.
- [4] N. Bleistein and R. A. Handelsman. *Asymptotic Expansions of Integrals*. Dover Publications, New York, 1986.
- [5] E. Cahen. Sur la fonction  $\zeta(s)$  de Riemann et sur des fonctions analogues. *Ann. de l'Éc. Norm.*, 11(3):75–164, 1894.
- [6] R. D. Carpenter, W. W. Liang, G. H. Paulino, J. C. Gibeling, and Z. A. Munir. Fracture testing and analysis of a layered functionally graded Ti/TiB beam in 3-point bending. *Materials Science Forum*, 837-842:971–976, 1999.
- [7] E. M. Carrillo-Heian, R. D. Carpenter, G. H. Paulino, J. C. Gibeling, and Z. A. Munir. Dense layered MoSi<sub>2</sub>/SiC functionally graded composites formed by field-activated synthesis. *J. Amer. Ceram. Soc.*, submitted, 2000.
- [8] P. Casal. La capillarite interne. Cahier du Groupe Francais d' Etudes de Rheologie C.N.R.S., 6(3):31–37, 1961.

- [9] P. Casal. Capillarite interne en mecanique. C.R. Acad. Sci., 256:3820–3822, 1963.
- [10] P. Casal. *La théorie du second gradient et la capillarité*. C.R. Acad. Sci. Paris Sér. A, 274:1571–1574, 1972.
- [11] Y.-S. Chan, A. C. Fannjiang, and G. H. Paulino. Integral equations with hypersingular kernels – theory and application to fracture mechanics. *Int. J. Eng. Sci.*, In Press, 2001.
- [12] Y.-S. Chan, G. H. Paulino, and A. C. Fannjiang. Gradient elasticity theory for a mode I crack in a homogeneous and nonhomogeneous materials. *The 20th Int. Congress of the Int. Union of Theoretical and Applied Mechanics (IUTAM)*, Accepted and Presented, 2000.
- [13] Y.-S. Chan, G. H. Paulino, and A. C. Fannjiang. Constitutive equations of strain-gradient elasticity theory for functionally graded materials. *J. Appl. Mech. Trans. ASME*, To be Submitted, 2001.
- [14] Y.-S. Chan, G. H. Paulino, and A. C. Fannjiang. The crack problem for non-homogeneous materials under antiplane shear loading – A displacement based formulation. *Int. J. Solids Struct.*, 38(17):2989–3005, 2001.
- [15] Y.-S. Chan, G. H. Paulino, and A. C. Fannjiang. Gradient elasticity theory for a mode I crack in functionally graded materials. *J. Amer. Ceram. Soc.*, In Press, 2001.
- [16] Y.-S. Chan, G. H. Paulino, and A. C. Fannjiang. Gradient elasticity theory for mode III fracture in functionally graded materials – Part II: crack parallel to the material gradation. *J. Appl. Mech. Trans. ASME*, Submitted, 2001.
- [17] D. L. Clements, J. Kusuma, and W. T. Ang. A note on antiplane deformations of inhomogeneous elastic materials. *Int. J. Eng. Sci.*, 35(6):593–601, 1997.

- [18] E. Cosserat and F. Cosserat. *Theories des Corps Deformables*. Hermann et Fils, Paris, 1909.
- [19] P. J. Davis and Rabinowitz. *Methods of Numerical Integration*. Academic Press, Inc., Orlando, Florida, 1984.
- [20] L. Debnath. *Integral Transforms and Their Applications*. CRC Press, Boca Raton, 1995.
- [21] F. Delale and F. Erdogan. The crack problem for a nonhomogeneous plane. *J. Appl. Mech. Trans. ASME*, 50(3):609–614, 1983.
- [22] J. Elliott. On some singular integral equations of the Cauchy type. *Ann. Math.*, 54(2):349–370, 1951.
- [23] A. Erdélyi, W. Magnus F., Oberhettinger, and F. G. Tricomi. *Tables of Integral Transforms*, volume 1. (Based, in part, on notes left by Harry Bateman, and compiled by the staff of the Bateman Manuscript Project.) McGraw-Hill, New York, 1954.
- [24] F. Erdogan. Mixed boundary value problems in mechanics. In S. Nemat-Nasser, editor, *Mechanics Today*, volume 4, pages 1–86. Pergamon Press Inc., New York, U.S.A., 1978.
- [25] F. Erdogan. The crack problem for bonded nonhomogeneous materials under antiplane shear loading. *J. Appl. Mech. Trans. ASME*, 52(4):823–828, 1985.
- [26] F. Erdogan. Fracture mechanics of functionally graded materials. *Composites Eng.*, 5(7):753–770, 1995.
- [27] F. Erdogan. Fracture mechanics. *Int. J. Solids Struct.*, 37:171–183, 2000.
- [28] F. Erdogan and G. D. Gupta. On the numerical solution of singular integral equations. *Quart. Appl. Math.*, 30:525–534, 1972.

- [29] F. Erdogan, G. D. Gupta, and T. S. Cook. Numerical solution of singular integral equations. In G. C. Sih, editor, *Mechanics of Fracture*, volume 1, chapter 7, pages 368–425. Noordhoff International Publishing, Leyden, The Netherlands, 1973.
- [30] F. Erdogan and M. Ozturk. Diffusion problems in bonded nonhomogeneous materials with an interface cut. *Int. J. Eng. Sci.*, 30(10):1507–1523, 1992.
- [31] A. C. Eringen. *Microcontinuum Field Theories I. Foundations and Solids*. Springer-Verlag, New York, 1999.
- [32] R. Estrada and R. P. Kanwal. *Singular Integral Equations*. Birkhäuser, Boston, 2000.
- [33] L. C. Evans. *Partial Differential Equations*. American Mathematical Society, Providence, R.I., 1998.
- [34] G. Exadaktylos. Gradient elasticity with surface energy: mode-I crack problem. *Int. J. Solids Struct.*, 35(5):421–456, 1998.
- [35] G. Exadaktylos, I. Vardoulakis, and E. Aifantis. Cracks in gradient elastic bodies with surface energy. *Int. J. Fract.*, 79(2):107–119, 1996.
- [36] A. C. Fannjiang, Y.-S. Chan, and G. H. Paulino. Mode III crack problem in strain-gradient elasticity: A hypersingular integrodifferential equation approach. *SIAM J. Appl. Math.*, In Press, 2001.
- [37] N. A. Fleck and J. W. Hutchinson. Strain gradient plasticity. In J. W. Hutchinson and T. Y. Wu, editors, *Advances in Applied Mechanics*, volume 33, pages 295–361. Academic Press, New York, N.Y., 1997.
- [38] G. B. Folland. *Fourier Analysis and its Applications*. Wadsworth & Brooks/Cole Advanced Books & Software, Pacific Grove, Calif., 1992.

- [39] E. E. Gdoutos. *Fracture Mechanics Criteria and Applications*. Kluwer Academic Publishers, Dordrecht, The Netherlands, 1990.
- [40] J. Hadamard. *Lectures on Cauchy's Problem in Linear Partial Differential Equations*. Dover, New York, N.Y. USA, 1952.
- [41] T. Hirai. Functionally gradient materials. In R. J. Brook, editor, *Materials Science and Technology*, volume 17B of *Processing of Ceramics, Part 2*, pages 292–341, Weinheim, Germany, 1993.
- [42] U. W. Hochstrasser. Orthogonal polynomials. In M. Abramowitz and I. A. Stegun, editors, *Handbook of Mathematical Functions*, chapter 22, pages 771–802. Dover Publications, Inc, New York, N.Y., 1972.
- [43] C.-Y. Hui and D. Shia. Evaluations of hypersingular integrals using Gaussian quadrature. *Int. J. Numer. Methods. Eng.*, 44(2):205–214, 1999.
- [44] J. W. Hutchison and A. G. Evans. Mechanics of materials: Top-down approaches to fracture. *Acta Mater.*, 48:125–135, 2000.
- [45] K. C. Hwang, T. F. Cuo, Y. Huang, and J.Y. Chen. Fracture in strain gradient elasticity. *Metals and Materials*, 4(4):593–600, 1998.
- [46] Z.-H. Jin and R. C. Batra. Some basic fracture mechanics concepts in functionally graded materials. *J. Mech. Phys. Solids*, 44(8):1221–1235, 1996c.
- [47] H. Kabir, E. Madenci, and A. Ortega. Numerical solution of integral equations with logarithmic-, Cauchy- and Hadamard-type singularities. *Int. J. Numer. Methods. Eng.*, 41(4):617–638, 1998.
- [48] R. P. Kanwal. *Linearr Integral Equations, Theory & Technique*. Birkhäuser, Boston, 1997.

- [49] A. C. Kaya. *Applications of Integral Equations with Strong Singularities in Fracture Mechanics*. PhD Thesis, Lehigh University, 1984.
- [50] A. C. Kaya and F. Erdogan. On the Solution of Integral Equations with Strongly Singular Kernels. *Quart. Appl. Math.*, 45(1):105–122, 1987.
- [51] N. Konda and F. Erdogan. The mixed mode crack problem in a nonhomogeneous elastic medium. *Eng. Fract. Mech.*, 47(4):533–545, 1994.
- [52] S. Krenk. On the use of interpolation polynomial for solutions of singular integral equations. *Quart. Appl. Math.*, 32(4):479–484, 1975a.
- [53] S. Krenk. On quadrature formulas for singular integral equations of the first and second kind. *Quart. Appl. Math.*, 33(3):225–232, 1975b.
- [54] H. R. Kutt. The numerical evaluation of principal value integrals by finite-part integration. *Numer. Math.*, 24:205–210, 1975.
- [55] R. S. Lakes. Size effects and micromechanics of a porous solid. *J. Mater. Sci.*, 18:2572–2580, 1983.
- [56] R. S. Lakes. Experimental microelasticity of two porous solids. *Int. J. Solids Struct.*, 22:55–63, 1986.
- [57] D. P. Linz. On the approximate computation of certain strongly singular integrals. *Computing*, 35:345–353, 1985.
- [58] A. I. Markushevich. *Theory of Functions of a Complex Variable (Volume I)*. Prentice-Hall, Inc., Englewood Cliffs, N.J., 1965.
- [59] A. J. Markworth, K. S. Ramesh, and W. P. Parks Jr. Review modelling studies applied to functionally graded materials. *J. Mater. Sci.*, 30:2183–2193, 1995.
- [60] P. A. Martin. End-point behaviour of solutions to hypersingular integral equations. *Proc. R. Soc. Lond. A*, 432(1885):301–320, 1991.

- [61] P. A. Martin and F. J. Rizzo. On boundary integral equations for crack problems. *Proc. R. Soc. Lond. A*, 421(1861):341–355, 1989.
- [62] S. A. Meguid and X. D. Wang. On the dynamic interaction between a microdefect and a main crack. *Proc. R. Soc. Lond. A*, 448(1934):449–464, 1995.
- [63] H. Mellin. Über den Zusammenhang zwischen den linearen Differential- und Differenzgleichungen. *Acta. Math.*, 25:139–164, 1902.
- [64] S. G. Mikhlin. *Integral Equations and their applications to certain problems in mechanics, mathematical physics and technology*. The MacMillan Company, New York, 1964.
- [65] R. D. Mindlin. Micro-structure in linear elasticity. *Arch. Ration. Mech. Anal.*, 16:51–78, 1964.
- [66] R. D. Mindlin. Second gradient of strain and surface-tension in linear elasticity. *Int. J. Solids Struct.*, 1:417–438, 1965.
- [67] G. Monegato. Numerical evaluation of hypersingular integrals. *J. Comput. Appl. Math.*, 50:9–31, 1994.
- [68] N. I. Muskhelishvili. *Singular Integral Equations*. Noordhoff International Publishing, Groningen, The Netherlands, 1953.
- [69] N. I. Muskhelishvili. *Some Basic Problems of the Mathematical Theory of Elasticity*. Noordhoff Ltd., Groningen, The Netherlands, 1963.
- [70] J. C. Nedelec. Integral equations with non-integrable kernels. *Integral Equations And Operator Theory*, 5(4):562–572, 1982.
- [71] F. Oberhettinger. *Tables of Mellin Transforms*. Springer-Verlag, Berlin and New York, 1974.

- [72] G. H. Paulino, Y.-S. Chan, and A. C. Fannjiang. Gradient elasticity theory for mode III fracture in functionally graded materials – Part I: crack perpendicular to the material gradation. *J. Appl. Mech. Trans. ASME*, In Press, 2001.
- [73] G. H. Paulino, A. C. Fannjiang, and Y.-S. Chan. Gradient elasticity theory for a mode III crack in a functionally graded material. *Materials Science Forum*, 308-311:971–976, 1999.
- [74] G. H. Paulino, M. T. A. Saif, and S. Mukherjee. A finite elastic body with a curved crack loaded in anti-plane shear. *Int. J. Solids Struct.*, 30(8):1015–1037, 1993.
- [75] A. S. Peters. A note on the integral equation of the first kind with a cauchy kernel. *Comm. Pure Appl. Math.*, 308-311:57–61, 1963.
- [76] A. C. Pipkin. *A Course on Integral Equations*. Springer-Verlag, New York, 1991.
- [77] B. Riemann. Ueber die Anzahl der Primzahlen unter einer gegebener Grösse. *Werke*, pages 136–144, 1876.
- [78] G. W. Schulze and F. Erdogan. Periodic cracking of elastic coatings. *Int. J. Solids Struct.*, 35(28-29):3615–3634, 1998.
- [79] H. Sölingen. Die Lösungen der Integralgleichungen  $g(x) = \frac{1}{2\pi} \int_{-a}^a \frac{f(\xi) d\xi}{x-\xi}$  und deren Anwendung in der Tragflügeltheorie. *Math. Z.*, 45:245–255, 1939.
- [80] A. Sellier. Hadamard's finite part concept in dimension  $n \geq 2$ , distributional definition, regularization forms and distributional derivatives. *Proc. R. Soc. Lond. A*, 445(1923):69–98, 1994.
- [81] A. Sellier. Asymptotic expansion of a general integral. *Proc. R. Soc. Lond. A*, 452(1955):2655–2690, 1996.



- [82] M. X. Shi, Y. Huang, and K. C. Hwang. Fracture in a higher-order elastic continuum. *J. Mech. Phys. Solids*, 48(12):2513–2538, 2000.
- [83] V. P. Smyshlyaev and N. A. Fleck. The role of strain gradients in the grain size effect for polycrystals. *J. Mech. Phys. Solids*, 44(4):465–495, 1996.
- [84] I. N. Sneddon. *Mixed boundary value problems in potential theory*. North-Holland Pub. Co. / Wiley, Amsterdam / New York, 1966.
- [85] I. N. Sneddon. *The Use of Integral Transforms*. McGraw-Hill, New York, 1972.
- [86] I. N. Sneddon and M. Lowengrub. *Crack problems in the classical theory of elasticity*. Series title: The SIAM series in applied mathematics. Wiley, New York, 1969.
- [87] A. H. Stroud and D. Secrest. *Gaussian Quadrature Formulas*. Prentice-Hall, New York, 1966.
- [88] S. Suresh and A. Mortensen. *Fundamentals of Functionally Gradient Materials*. The Institute of Materials, London, 1998.
- [89] C. Temperton. Self-sorting mixed-radix fast Fourier transforms. *J. Comput. Phys.*, 52:1–23, 1983.
- [90] R. A. Toupin. Elastic materials with couple stresses. *Arch. Rational Mech. Anal.*, 11:385–414, 1962.
- [91] F.G. Tricomi. *Integral Equations*. Interscience Publishers, Inc., New York, 1957.
- [92] I. Vardoulakis, G. Exadaktylos, and E. Aifantis. Gradient elasticity with surface energy: Mode-III crack problem. *Int. J. Solids Struct.*, 33(30):4531–4559, 1996.
- [93] I. Vardoulakis and J. Sulem. *Bifurcation Analysis in Geomechanics*. Blackie Academic and Professional, Glasgow, 1995.

- [94] M. R. A. Van Vliet and J. G. M. Van Mier. Effect of strain gradients on the size effect of concrete in uniaxial tension. *Int. J. Fract.*, 95:195–219, 1999.
- [95] J. Wang and B. L. Karihaloo. Mode II and mode III stress singularities and intensities at a crack tip terminating on a transversely isotropic-orthotropic bimaterial interface. *Proc. R. Soc. Lond. A*, 444(1922):447–460, 1994.
- [96] Waterloo Maple Inc. *The Maple Learning Guide*. Waterloo, 1995.
- [97] Waterloo Maple Inc. *The Maple Programming Guide*. Waterloo, 1995.
- [98] D. V. Widder. *An Introduction to Transform Theory*. Academic Press, New York and London, 1971.
- [99] C. H. Wu. Cohesive elasticity and surface phenomena. *Quart. Appl. Math.*, 50(1):73–103, 1992.
- [100] L. Zhang, Y. Huang, J. Y. Chen, and K. C. Hwang. The mode III full-field solution in elastic materials with strain gradient effects. *Int. J. Fract.*, 92(4):325–348, 1998.

1  
2  
3  
4  
5  
6  
7  
8  
9  
10  
11  
12  
13  
14  
15  
16  
17  
18  
19  
20  
21  
22  
23  
24  
25  
26  
27  
28